

# UC San Diego

## UC San Diego Electronic Theses and Dissertations

### Title

The Reactivity of Stable Metallacyclobutenes and Vinylcarbenes

### Permalink

<https://escholarship.org/uc/item/3dd9d5jq>

### Author

Holland, Ryan Lynn

### Publication Date

2016

Peer reviewed|Thesis/dissertation

UNIVERSITY OF CALIFORNIA, SAN DIEGO

**The Reactivity of Stable Metallacyclobutenes and Vinylcarbenes**

A dissertation submitted in partial satisfaction of the  
requirements for the degree of Doctor of Philosophy

in

Chemistry

by

Ryan Lynn Holland

Committee in charge:

Professor Joseph M. O'Connor, Chair  
Professor Joshua S. Figueroa  
Professor Ying S. Meng  
Professor Charles L. Perrin  
Professor Arnold L. Rheingold

2016

Copyright

Ryan Lynn Holland, 2016

All rights reserved.

The dissertation of Ryan Lynn Holland is approved, and it is acceptable in quality and form for publication on microfilm and electronically:

---

---

---

---

---

Chair

University of California, San Diego

2016

## DEDICATION

*This thesis is dedicated to my family,  
and to the friends that have become family,  
to Royce and Gloria Holland,  
to Dustin Holland,  
to Dave Martin,  
to Roy and Nelwynn Holland,  
to Matt and Julie Johnson,  
and to Oanh Phi Lam.*

## EPIGRAPH

“What is REAL?” asked the Rabbit one day, when they were lying side by side near the nursery fender, before Nana came to tidy the room. “Does it mean having things that buzz inside you and a stick-out handle?”

“Real isn’t how you are made,” said the Skin Horse. “It’s a thing that happens to you. When a child loves you for a long, long time, not just to play with, but REALLY loves you, then you become Real.”

“Does it hurt?” asked the Rabbit.

“Sometimes,” said the Skin Horse, for he was always truthful. “When you are Real you don’t mind being hurt.”

“Does it happen all at once, like being wound up,” he asked, “or bit by bit?”

“It doesn’t happen all at once,” said the Skin Horse. “You become. It takes a long time. That’s why it doesn’t happen often to people who break easily, or have sharp edges, or who have to be carefully kept. Generally, by the time you are Real, most of your hair has been loved off, and your eyes drop out and you get loose in the joints and very shabby. But these things don’t matter at all, because once you are Real you can’t be ugly, except to people who don’t understand.”

“I suppose you are real?” said the Rabbit. And then he wished he had not said it, for he thought the Skin Horse might be sensitive. But the Skin Horse only smiled.”

Margery Williams – The Velveteen Rabbit

## TABLE OF CONTENTS

SIGNATURE PAGE .....	iii
DEDICATION.....	iv
EPIGRAPH .....	v
TABLE OF CONTENTS.....	vi
LIST OF ABBREVIATIONS .....	viii
LIST OF FIGURES .....	xiv
LIST OF SCHEMES.....	xxii
LIST OF TABLES .....	xxvi
ACKNOWLEDGEMENTS.....	xxviii
VITA.....	xxxii
ABSTRACT OF THE DISSERTATION .....	xxxiv
<b>Chapter 1</b> Historical Development of Stable Metallacyclobutenes .....	37
References .....	96
<b>Chapter 2</b> Reactivity of Stable Metallacyclobutenes and Vinylcarbenes with Alkenes .....	103
References .....	153
Experimental.....	158
Calculations and Equations for the Geometric Analysis of $\eta^4$ -1,4-Pentadiene Complexes.....	181
Computational Methods.....	185

General Experimental for X-Ray Structure Determinations .....	186
<b>Chapter 3</b> Reactivity of Stable Metallacyclobutenes with	
C-Nitroso Reagents .....	242
References .....	267
Experimental.....	270
General Experimental for X-Ray Structure Determinations .....	277
<b>Chapter 4</b> The Isolation of a Large Cyclopentadienylcobaltsulfide Cluster –	
Synthesis and Crystal Structure of Octahedral <i>closo</i> -[( $\eta^5$ -C <sub>5</sub> H <sub>5</sub> )Co] <sub>5</sub> S .....	293
References .....	299
Experimental.....	301
Experimental for X-Ray Structure Determination.....	303



## LIST OF ABBREVIATIONS

$\angle$  = angle

Å = Angstrom ( $10^{-10}$  m)

a = unit cell axis a, direction number of the normal to a plane

acac = acetylacetonate ( $\text{H}_3\text{CC}(\text{O})\text{CH}_2\text{C}(\text{O})\text{CH}_3$ )

AIBN = azobisisobutyronitrile ( $\text{N}_2[(\text{CN})_2\text{C}(\text{CH}_3)_2]$ )

Anal. = combustion analysis (elemental)

atm = unit of pressure

Ar = aryl

$\alpha$  = unit cell angle, position one atom removed, bend-back parameter

b = unit cell axis b, direction number of the normal to a plane

$\beta$  = unit cell angle, position two atoms removed

bis = prefix indicating two identical coordinating ligands

bs = broad singlet

c = unit cell axis c, direction number of the normal to a plane

calcd. = calculated

C(n) = carbon number n

C<sub>4</sub> = butane or 4-carbon isomer

C<sub>5</sub> = pentane or 5-carbon isomer

CCDC = Cambridge Crystallographic Data Centre

CO = carbon monoxide, carbonyl

COD = 1,5-cyclooctadiene ( $C_8H_{12}$ )

Cp = cyclopentadienyl ( $C_5H_5$ )

Cy = cyclohexyl (*cyclo*- $C_6H_{11}$ )

$cm^{-1}$  = wavenumber

Cmpd. = compound

Cnt = centroid

$^{\circ}C$  = degrees Celsius

CSD = Cambridge Structural Database

f = atomic orbital

fac = facial arrangement of ligands

d = doublet, days, deuterated, atomic orbital

$d^n$  = d electron count

$\Delta G^{\circ}$  = Gibbs free energy

DFT = Density Functional Theory

$\delta$  = chemical shift, delta

$\delta^-$  = partial negative polarization

$\delta^+$  = partial positive polarization

DMAP = dimethylaminopyridine ( $(CH_3)_2NC_5H_4N$ )

$\eta^n$  = hapticity of a ligand with n contiguous atoms bound to a metal center

E = energy, main-group atom, functional group

*E* = denoting a trans geometry about a double bond

EI = electron impact

equiv. = equivalents

esd = estimated standard deviation

Et = ethyl

Et<sub>2</sub>O = diethyl ether

EtOAc = ethyl acetate (CH<sub>3</sub>CO<sub>2</sub>CH<sub>2</sub>CH<sub>3</sub>)

eV = electron volts

e.Å<sup>-3</sup> = electron per cubic angstrom (X-ray crystallography)

FTIR = Fourier Transform Infrared Spectroscopy

g = grams

γ = unit cell angle

HMBC = Heteronuclear Multiple Bond Quantum Correlation

HOMO = Highest Occupied Molecular Orbital

HRMS = High Resolution Mass Spectrometry

HSQC = Heteronuclear Single Quantum Coherence

Hz = Hertz (s<sup>-1</sup>)

h = hours, Miller indice

<sup>i</sup>Pr = isopropyl (CH(CH<sub>3</sub>)<sub>2</sub>)

IR = Infrared

*J* = NMR coupling constant, magnetic coupling constant

<sup>n</sup>*J* = nth bond NMR coupling constant

κ<sup>n</sup> = a chelating ligand to a metal center with n ligating atom attachments

k = Miller indice

K = degrees Kelvin

$K_{\text{eq}}$  = equilibrium constant

kcal = kilocalories

l = Miller indice

IR = infrared

L = ligand (neutral), liters

$L_n$  = ligand set of a metal complex

LUMO = Lowest Unoccupied Molecular Orbital

$\lambda$  = wavelength

m = meter, multiplet, mili- ( $10^{-3}$ )

*m* = *meta* position

M = transition metal, mega- ( $10^6$ ), molar (mol/L)

Me = methyl ( $\text{CH}_3$ )

MeCN = acetonitrile

mer = meridional arrangement of ligands

MO = Molecular Orbital

min = minutes

mol = moles

*m/z* = mass-to-charge ratio

$\mu$  = bridging ligands, absorption coefficient (X-ray crystallography), micro- ( $10^{-6}$ )

$n$  = normal vector defining equation of a plane

$\vec{n}_n$  = vector equation defining plane  $n$

NMR = Nuclear Magnetic Resonance

$\nu$  = infrared stretching frequency

OTf = triflate, trifluoromethylsulfonate ([OSO<sub>2</sub>CF<sub>3</sub>])

$o$  = *ortho* position

ORTEP = Oak Ridge Thermal Ellipsoid Plot

$p$  = atomic orbital

Ph = phenyl (C<sub>6</sub>H<sub>5</sub>)

$p$  = *para* position

ppm = parts per million

PPN = bis(triphenylphosphine)iminium chloride ([N(P(C<sub>6</sub>H<sub>5</sub>)<sub>3</sub>)<sub>2</sub>])

$\pi$  = pi

q = quartet

QM = quantum mechanical

R = alkyl group

$R$  = residual value (X-ray crystallography), denoting *rectus* stereocenter

refcode = reference code (X-ray crystallography)

r.b.f. = round bottom flask

r.t. = room temperature

s = singlet, seconds, atomic orbital

S = denoting *sinister* stereocenter

S<sub>N</sub>2 = substitution nucleophilic (bi-molecular)

σ = sigma, standard deviation

σ<sub>P</sub> = Hammett parameter for *para*-substituents

T = temperature, triplet electronic state

t = triplet

tetrakis = prefix indicating four identical coordinating ligands

THF = tetrahydrofuran

Tf = triflyl, trifluoromethanesulfonyl (SO<sub>2</sub>CF<sub>3</sub>)

TIPS = triisopropylsilyl (Si(CH(CH<sub>3</sub>)<sub>2</sub>)<sub>3</sub>)

Tol = toluene, tolyl (C<sub>7</sub>H<sub>8</sub>)

tolyl = toluene (C<sub>7</sub>H<sub>8</sub>)

triphos = 1,1,1-tris(diphenylphosphinomethyl)ethane (CH<sub>3</sub>[CH<sub>2</sub>PPh<sub>2</sub>]<sub>3</sub>)

tris = prefix indicating three identical coordinating ligands

TS = transition state

<sup>t</sup>Bu = tertiary-butyl (C(CH<sub>3</sub>)<sub>3</sub>)

TMS = trimethylsilyl (Si(CH<sub>3</sub>)<sub>3</sub>), tetramethylsilane (Si(CH<sub>3</sub>)<sub>4</sub>)

V = unit cell volume

X = halide or pseudo halide

Z = number of molecules in unit cell, denoting a *cis* geometry about a double bond

## LIST OF FIGURES

<b>Figure 1-1.</b> Proposed structures for the complex $[(\eta^5\text{-C}_5\text{H}_5)_2\text{Ti}(\text{C}_2\text{Ph})]_2$ ( <b>1</b> ). .....	40
<b>Figure 1-2.</b> Ball-and-Stick representation of titanacycle <b>2</b> . Hydrogen atom coordinates not included in crystallographic information file. CCDC Number 1210264; refcode MCPBTI. R = 5.2%, Space Group $P2_1/c$ . .....	41
<b>Figure 1-3.</b> Unsaturated four-membered ring bonding motifs. ....	42
<b>Figure 1-4.</b> Proposed structure of $(\eta^5\text{-C}_5\text{H}_5)_2\text{Ti}(\kappa^2\text{-}(C,C)\text{-CH}_2\text{AlMe}_2\text{Cl})$ ( <b>3</b> ) and a $\text{Me}_2\text{AlCl}$ -stabilized adduct of an intermediate titanium methylene species ( <b>4</b> ). ...	44
<b>Figure 1-5.</b> Ball-and-Stick representation of titanacyclobutene <b>5a</b> . CCDC Number 1131477; refcode CPTICB. R = 3.8%, Space Group $Pbca$ . ....	50
<b>Figure 1-6.</b> Ball-and-Stick representation of titanacyclobutene <b>5b</b> . Hydrogen atom coordinates not included in crystallographic information file. CCDC Number 1106414; refcode BATMUE. R = 4.4%, Space Group $P2_1/c$ . ....	53
<b>Figure 1-7.</b> Ball-and-Stick representation of titanacyclobutene <b>5d</b> . CCDC Number 1106415; refcode BATNAL. R = 2.9%, Space Group $Fdd2$ . ....	56
<b>Figure 1-8.</b> Ball-and-Stick representation of iridacyclobutene <b>8-fac</b> . CCDC Number 1126788; refcode CIYKAW. R = 3.1%, Space Group $P2_1/n$ . ....	59
<b>Figure 1-9.</b> Ball-and-Stick representation of rhodacyclobutene <b>9</b> . CCDC Number 1132547; refcode CUFTIG10. R = 6.0%, Space Group $P6_1$ . ....	64
<b>Figure 1-10.</b> Ball-and-Stick representation of rhodacyclobutene <b>11</b> . CCDC Number 1151053; refcode FABJUN. R = 6.1%, Space Group $P2_1/a$ . ....	66

<b>Figure 1-11.</b> Ball-and-Stick representation of platinacyclobutene <b>13a</b> . CCDC Number 1168435; refcode GIPZIO. R = 3.61%, Space Group $P2_1/n$ .	68
<b>Figure 1-12.</b> Ball-and-Stick representation of iridacyclobutene <b>15</b> . CCDC Number 1258895; refcode SIGKEY. R = 5.88%, Space Group $P-1$ .	72
<b>Figure 1-13.</b> Ball-and-Stick representation of rhenacyclobutene <b>19b</b> . CCDC Number 1219626; refcode NIDJOZ. R = 3.16%, Space Group $Cc$ .	77
<b>Figure 1-14.</b> Resonance contributors of rhenacyclobutadiene complexes <b>32</b> .	83
<b>Figure 1-15.</b> Ball-and-Stick representation of rhenacyclobutene <b>34a</b> . CCDC Number 1172859; refcode HAWTEE. R = 4.4%, Space Group $P2_1/c$ .	86
<b>Figure 1-16.</b> Ball-and-Stick representation of iridacyclobutene <b>42</b> . CCDC Number 1163802; refcode GAPQAP. R = 5.9%, Space Group $P-1$ .	91
<b>Figure 1-17.</b> Crystallographically characterized metallacyclobutene complexes.	94
<b>Figure 1-18.</b> Crystallographically characterized metallacyclobutene complexes.	95
<b>Figure 2-1.</b> Solid-state structure of <b>9-ZE</b> . For clarity, only three hydrogen atoms are shown. CCDC Number 703132; refcode JOGWIM. R = 4.58%, Space Group $Pca2_1$ .	109
<b>Figure 2-2.</b> Crystallographically characterized examples of $\eta^4$ -1,4-pentadiene complexes. Identified by CSD Refcode.	113
<b>Figure 2-3.</b> Metallacyclohexene conformers in the reaction of <b>2</b> with acyclic cis alkenes.	118



<b>Figure 2-4.</b> Solid-state structure of <b>13-<i>exo</i></b> . For clarity, only three hydrogen atoms are shown. CCDC Number 703137; reftype JOKXEN. R = 2.77%, Space Group <i>P2<sub>1</sub>/n</i> . .....	121
<b>Figure 2.5.</b> Barrelene-type structures formed from maleic anhydride. For clarity, the L <sub>n</sub> M ligand set is abbreviated as [M]. For <b>RIFCIS</b> , [Ir] = (PEt <sub>3</sub> ) <sub>3</sub> Ir; for <b>DACREE</b> , [Fe] = (P(OMe) <sub>3</sub> )(CO) <sub>2</sub> Fe; For <b>13-<i>exo</i></b> and <b>13-<i>endo</i></b> , [Co] = (η <sup>5</sup> -C <sub>5</sub> H <sub>5</sub> )Co. ....	123
<b>Figure 2-6.</b> (Left) QM-computed structure for <b>18</b> [Å]; (Right) HOMO of <b>18</b> , which has a primary contribution from the <i>d<sub>xy</sub></i> and <i>d<sub>yz</sub></i> orbitals.....	127
<b>Figure 2-7.</b> Possible transition state structures for reaction of maleic anhydride with intermediates <b>15-17</b> , accounting for all diastereomeric products. ....	129
<b>Figure 2-8.</b> Electrostatic potential map of model complex <b>18</b> . ....	133
<b>Figure 2-9.</b> Various binding modes and resonance forms for vinylcarbenes. ...	142
<b>Figure 2-10.</b> Generic numbering and geometric analysis schema for η <sup>4</sup> -1,4-pentadienes. ....	181
<b>Figure 2-11.</b> ORTEP of orthorhombic cobalt complex <b>9-ZE</b> . Ellipsoids shown at 50% probability. Most hydrogens are omitted for clarity. ....	187
<b>Figure 2-12.</b> ORTEP of monoclinic cobalt complex <b>9-ZZ</b> . Ellipsoids shown at 50% probability. Most hydrogens are omitted for clarity.....	189
<b>Figure 2-13.</b> ORTEP of monoclinic cobalt complex <b>10-ZZ</b> . Ellipsoids shown at 50% probability. Most hydrogens are omitted for clarity.....	191

<b>Figure 2-14.</b> ORTEP of monoclinic cobalt complex <b>11-ZE</b> . Ellipsoids shown at 50% probability. Most hydrogens are omitted for clarity.....	193
<b>Figure 2-15.</b> ORTEP of monoclinic cobalt complex <b>12-ZZ-ortho</b> . Ellipsoids shown at 50% probability. Most hydrogens are omitted for clarity.....	195
<b>Figure 2-16.</b> ORTEP of monoclinic cobalt complex <b>12-ZZ-para</b> . Ellipsoids shown at 50% probability. Most hydrogens are omitted for clarity.....	197
<b>Figure 2-17.</b> ORTEP of monoclinic cobalt complex <b>13-exo</b> . Ellipsoids shown at 20% probability. Most hydrogens are omitted for clarity.....	199
<b>Figure 2-18.</b> ORTEP of monoclinic cobalt complex <b>13-endo</b> . Ellipsoids shown at 30% probability. Most hydrogens are omitted for clarity.....	201
<b>Figure 2-19.</b> ORTEP of monoclinic cobalt complex <b>14-exo</b> . Ellipsoids shown at 20% probability. Most hydrogens are omitted for clarity.....	203
<b>Figure 2-20.</b> ORTEP of monoclinic cobalt complex <b>14-endo</b> . Ellipsoids shown at 20% probability. Most hydrogens are omitted for clarity.....	205
<b>Figure 2-21.</b> ORTEP of monoclinic cobalt complex <b>20-exo</b> . Ellipsoids shown at 20% probability. Most hydrogens are omitted for clarity.....	207
<b>Figure 2-22.</b> ORTEP of monoclinic cobalt complex <b>25a</b> . Ellipsoids shown at 20% probability. Most hydrogens are omitted for clarity. ....	209
<b>Figure 2-23.</b> <b>12-ZZ-ortho</b> $^1\text{H}$ (400.053 MHz, $\text{CDCl}_3$ ).....	217
<b>Figure 2-24.</b> <b>12-ZZ-ortho</b> $^{13}\text{C}$ (100.567 MHz, $\text{CDCl}_3$ ).....	218
<b>Figure 2-25.</b> <b>12-ZZ-para</b> $^1\text{H}$ (400.053 MHz, $\text{CDCl}_3$ ).....	219
<b>Figure 2-26.</b> <b>12-ZZ-para</b> $^{13}\text{C}$ (100.567 MHz, $\text{CDCl}_3$ ).....	220

<b>Figure 2-27.</b> 14- <i>exo</i> $^1\text{H}$ (400.053 MHz, $\text{CDCl}_3$ ).....	221
<b>Figure 2-28.</b> 14- <i>exo</i> $^{13}\text{C}$ (100.567 MHz, $\text{CDCl}_3$ ).....	222
<b>Figure 2-29.</b> 14- <i>endo</i> $^1\text{H}$ (400.053 MHz, $\text{CDCl}_3$ ).....	223
<b>Figure 2-30.</b> 14- <i>endo</i> $^{13}\text{C}$ (100.567 MHz, $\text{CDCl}_3$ ). ....	224
<b>Figure 2-31.</b> 20- <i>exo</i> $^1\text{H}$ (400.053 MHz, $\text{CDCl}_3$ ).....	225
<b>Figure 2-32.</b> 20- <i>exo</i> $^{13}\text{C}$ (100.567 MHz, $\text{CDCl}_3$ ).....	226
<b>Figure 2-33.</b> 21 $^1\text{H}$ (400.053 MHz, $\text{CDCl}_3$ ).....	227
<b>Figure 2-34.</b> 21 $^{13}\text{C}$ (100.567 MHz, $\text{CDCl}_3$ ).....	228
<b>Figure 2-35.</b> 22 $^1\text{H}$ (400.053 MHz, $\text{CDCl}_3$ ).....	229
<b>Figure 2-36.</b> Reaction of <b>25a</b> with maleic anhydride (initial) $^1\text{H}$ (400.053 MHz, $\text{CDCl}_3$ ).....	230
<b>Figure 2-37.</b> Reaction of <b>25a</b> with maleic anhydride (final) $^1\text{H}$ (400.053 MHz, $\text{CDCl}_3$ ).....	231
<b>Figure 2-38.</b> Reaction of <b>25a</b> with maleimide (initial) $^1\text{H}$ (400.053 MHz, $\text{CDCl}_3$ ).....	232
<b>Figure 2-39.</b> Reaction of <b>25a</b> with maleimide (final) $^1\text{H}$ (400.053 MHz, $\text{CDCl}_3$ ).....	233
<b>Figure 2-40.</b> Reaction of <b>13-<i>exo</i></b> with maleic anhydride (initial) $^1\text{H}$ (400.053 MHz, $\text{CDCl}_3$ ).....	234
<b>Figure 2-41.</b> Reaction of <b>13-<i>exo</i></b> with maleic anhydride (final) $^1\text{H}$ (400.053 MHz, $\text{CDCl}_3$ ).....	235
<b>Figure 2-42.</b> Reaction of <b>13-<i>endo</i></b> with maleic anhydride (initial) $^1\text{H}$ (400.053	

MHz, CDCl <sub>3</sub> ). .....	236
<b>Figure 2-43.</b> Reaction of <b>13-endo</b> with maleic anhydride (final) <sup>1</sup> H (400.053 MHz, CDCl <sub>3</sub> ). .....	237
<b>Figure 2-44.</b> Reaction of <b>13-exo</b> with dimethyl acetylenedicarboxylate (initial) <sup>1</sup> H (400.053 MHz, CDCl <sub>3</sub> ). .....	238
<b>Figure 2-45.</b> Reaction of <b>13-exo</b> with dimethyl acetylenedicarboxylate (final) <sup>1</sup> H (400.053 MHz, CDCl <sub>3</sub> ). .....	239
<b>Figure 2-46.</b> Reaction of <b>13-endo</b> with dimethyl acetylenedicarboxylate (initial) <sup>1</sup> H (400.053 MHz, CDCl <sub>3</sub> ). .....	240
<b>Figure 2-47.</b> Reaction of <b>13-endo</b> with dimethyl acetylenedicarboxylate (final) <sup>1</sup> H (400.053 MHz, CDCl <sub>3</sub> ). .....	241
<b>Figure 3-1.</b> $\eta^2$ -( <i>N,O</i> )- and $\kappa^1$ -( <i>O</i> )-hydroxylamido coordination. ....	243
<b>Figure 3-2.</b> Crystallographically characterized examples of dihapto [Nb(NMe <sub>2</sub> ) <sub>3</sub> ( $\eta^2$ -N(O)Me <sub>2</sub> ) <sub>2</sub> ] (GAJHEG), ambidentate [( <sup>t</sup> BuNC)Ni( $\eta^2$ -2,2,6,6-Me <sub>4</sub> -N(O)C <sub>5</sub> H <sub>3</sub> )( $\kappa^1$ -2,2,6,6-Me <sub>4</sub> -N(O)C <sub>5</sub> H <sub>3</sub> )] (IWUPUM), and monohapto [ $\eta^2$ -(1,3-(CF <sub>3</sub> ) <sub>2</sub> -acac) <sub>2</sub> Cu( $\eta^1$ -N(O)(CHPh <sub>2</sub> )( <sup>t</sup> Bu))] (YUBDII), binding modes. ....	244
<b>Figure 3-3.</b> Solid-state structure of <b>5-trans</b> . For clarity, only hydrogen H(3) is shown. CCDC Number 724840; refcode DOWDID. R = 3.13%, Space Group <i>P2</i> <sub>1</sub> / <i>n</i> . .....	250
<b>Figure 3-4.</b> Solid-state structure of <b>7-cis</b> . For clarity, H(3) is the only hydrogen atom shown. CCDC Number 724841; refcode DOWDOJ. R = 4.21%, Space Group <i>P2</i> <sub>1</sub> / <i>n</i> . .....	252

<b>Figure 3-5.</b> Possible transition state structures arising from intermediate <b>4</b> . ....	260
<b>Figure 3-6.</b> Ball-and-Stick and Spacefill representations of <b>5-trans</b> . An orientation with both the ethyl ester (in red; bottom) and the oxametallaziridine ring oxygen (in red, top) on the same face of the five-membered ring is likely inaccessible. ....	262
<b>Figure 3-7.</b> ORTEP of monoclinic cobalt complex <b>5-trans</b> . Ellipsoids shown at 50% probability. Most hydrogens removed for clarity. ....	278
<b>Figure 3-8.</b> ORTEP of monoclinic cobalt complex <b>7-cis</b> . Ellipsoids shown at 50% probability. Most hydrogens removed for clarity. ....	280
<b>Figure 3-9.</b> ORTEP of triclinic cobalt complex <b>8-cis</b> . Ellipsoids shown at 50% probability. Most hydrogens removed for clarity. ....	282
<b>Figure 3-10.</b> ORTEP of triclinic cobalt complex <b>9-cis</b> . Ellipsoids shown at 50% probability. Most hydrogens removed for clarity. ....	284
<b>Figure 3-11.</b> Compound <b>8-cis</b> <sup>1</sup> H NMR spectrum (400.053 MHz, CDCl <sub>3</sub> ). ....	288
<b>Figure 3-12.</b> <b>8-cis</b> <sup>13</sup> C NMR spectrum (100.567 MHz, CDCl <sub>3</sub> ). ....	289
<b>Figure 3-13.</b> Minor peaks in <b>8-cis</b> <sup>1</sup> H NMR spectrum (400.053 MHz, CDCl <sub>3</sub> ). ...	290
<b>Figure 3-14.</b> <b>9-cis</b> <sup>1</sup> H NMR spectrum (400.053 MHz, CDCl <sub>3</sub> ). ....	291
<b>Figure 3-15.</b> <b>9-cis</b> <sup>13</sup> C NMR spectrum (100.567 MHz, CDCl <sub>3</sub> ). ....	292
<b>Figure 4-1.</b> Solid-state structure of monoclinic cobalt cluster <i>closo</i> -[( $\eta^5$ -C <sub>5</sub> H <sub>5</sub> )Co] <sub>5</sub> S ( <b>1</b> ). CCDC Number 710868; refcode VUKNIZ. R = 3.43%, Space Group <i>P2<sub>1</sub>/c</i> . ....	296
<b>Figure 4-2.</b> Crystallographically characterized [( $\eta^5$ -C <sub>5</sub> H <sub>5</sub> )Co] <sub>m</sub> S <sub>n</sub> clusters. ....	296

**Figure 4-3.** ORTEP of monoclinic *closo*-[( $\eta^5$ -C<sub>5</sub>H<sub>5</sub>)Co]<sub>5</sub>S (**1**). Ellipsoids shown at 30% probability. Hydrogens removed for clarity. .... 304

## LIST OF SCHEMES

<b>Scheme 1-1.</b> Synthesis of titanacyclobutenes <b>5</b> from compound <b>3</b> . .....	45
<b>Scheme 1-2.</b> Proposed catalytic cycle for alkyne polymerization. ....	46
<b>Scheme 1-3.</b> Reaction of <b>5b</b> with 2-methylpropene-1- <sup>13</sup> C to give 2- methylpropene and <b>5b</b> - <sup>13</sup> C. ....	48
<b>Scheme 1-4.</b> Synthesis of titanacyclobutane <b>6</b> from Tebbe's reagent, <b>3</b> , and reaction of compound <b>6</b> with Me <sub>2</sub> AlCl, <i>trans</i> -neohexene-1- <i>d</i> <sub>1</sub> , and diphenylacetylene.....	52
<b>Scheme 1-5.</b> Synthesis of <b>8-fac</b> from proposed iridium methylene intermediate.....	57
<b>Scheme 1-6.</b> Formation of <b>8-mer</b> from <b>8-fac</b> through $\eta^3$ -vinylcarbene intermediates, possibly through an $\eta^1$ -vinylcarbene transition state.....	60
<b>Scheme 1-7.</b> Proposed mechanism of the ring-closing enyne metathesis reaction.....	61
<b>Scheme 1-8.</b> Reported examples of the enyne metathesis reaction. ....	62
<b>Scheme 1-9.</b> Stereochemistry of metallacyclobutene ring-opening.....	62
<b>Scheme 1-10.</b> Formation of rhodacyclobutene <b>9</b> from a 1,3-dithiol-2-ylidene intermediate.....	63
<b>Scheme 1-11.</b> Synthesis of platinacyclobutenes <b>13</b> from (PR <sub>3</sub> ) <sub>2</sub> Pt( $\eta^2$ -H <sub>2</sub> C=CH <sub>2</sub> ) and tetrafluorocyclopropene.....	67
<b>Scheme 1-12.</b> Formation of iridacyclobutene <b>15</b> from metallacyclopentadiene <b>14-Cl</b> .....	70

<b>Scheme 1-13.</b> Formation of $\eta^3$ -propargyl complex <b>17b</b> from $\eta^2$ -alkyne complex <b>16b</b> .....	73
<b>Scheme 1-14.</b> Nucleophilic addition to $\eta^3$ -allyl and $\eta^3$ -propargyl complexes.....	74
<b>Scheme 1-15.</b> Reactions of $\eta^3$ -propargyl complexes <b>17</b> to give metallacyclobutenes <b>19-27</b> .....	76
<b>Scheme 1-16.</b> Reactivity of rhenacyclobutene complexes with acid. ....	81
<b>Scheme 1-17.</b> Formation of rhenacyclobutadienes <b>32</b> from rhenacyclobutenone complexes <b>31</b> .....	82
<b>Scheme 1-18.</b> Reaction of rhenacyclobutadienes <b>32a-b</b> with phosphines to generate rhenacyclobutenes <b>33a-b</b> and <b>34a</b> .....	84
<b>Scheme 1-19.</b> Reaction of rhenacyclobutadiene <b>32b</b> with tri( <i>p</i> -tolyl)phosphine to generate rhenacyclobutadiene <b>35</b> , with possible intermediacy of rhenacyclobutene <b>34b</b> .....	85
<b>Scheme 1-20.</b> Reaction of rhenacyclobutene <b>33b</b> to give rhenacyclobutadiene <b>36</b> and subsequent reaction with $\text{PEt}_3$ to generate the bis(triethylphosphine) substituted rhenacyclobutene <b>37</b> .....	88
<b>Scheme 1-21.</b> Reaction of $[\text{Pt}(\text{PPh}_3)_2(\eta^3\text{-C}_3\text{H}_3)][\text{BF}_4]$ <b>38</b> with nucleophiles to give platinumacyclobutene complexes <b>39</b> .....	89
<b>Scheme 1-22.</b> Reaction of $[\text{Ir}(\text{Cl})(\text{CO})(\text{PPh}_3)_2(\text{OTf})(\kappa^1\text{-CH=C=CH}_2)]$ ( <b>41</b> ) with nucleophiles to give iridacyclobutene complex <b>42</b> .....	90
<b>Scheme 2-1.</b> Reaction of the isolated metallacyclobutene <b>1</b> with 2-methylpropene-1- $^{13}\text{C}$ to give <b>1-<math>^{13}\text{C}</math></b> .....	105



<b>Scheme 2-2.</b> Established reactions of the metallacyclobutene <b>2</b> .....	106
<b>Scheme 2-3.</b> Reaction of <b>2</b> with dimethyl maleate and dimethyl fumarate. ....	107
<b>Scheme 2-4.</b> Reaction of <b>2</b> with acyclic alkenes.....	111
<b>Scheme 2-5.</b> Proposed metallacyclohexene to 1,4-diene conversion of trans alkenes (top) and cis alkenes (bottom).....	117
<b>Scheme 2-6.</b> Reaction of <b>2</b> with maleic anhydride and maleimide. ....	120
<b>Scheme 2-7.</b> Potential vinylcarbene intermediates. Compounds <b>15</b> and <b>16</b> may involve either monohapto or trihapto coordination, but are depicted as the $\eta^1$ -vinylcarbene.....	125
<b>Scheme 2-8.</b> Regioselective formation of <b>11-ZE</b> . ....	135
<b>Scheme 2-9.</b> Thermolytic reaction of <b>2</b> to give furan and dinuclear complexes.....	136
<b>Scheme 2-10.</b> Reaction of <b>13-exo</b> with trimethylphosphine to give <b>20-exo</b> . ....	137
<b>Scheme 2-11.</b> Oxidative demetallation reactions of <b>9-ZZ</b> and <b>9-ZE</b> with iodine. ....	139
<b>Scheme 2-12.</b> Synthesis of $(\text{CO})_3\text{Fe}[\eta^3\text{-C}(\text{OMe})\text{C}(\text{R}_1)=\text{CH}(\text{R}_2)]$ vinylcarbene complexes ( <b>25</b> ). ....	143
<b>Scheme 2-13.</b> Reactions of $\eta^3$ -vinylcarbene $(\text{CO})_3\text{Fe}(\eta^3\text{-C}(\text{OMe})\text{C}(\text{CO}_2\text{Me})=\text{CH}_2)$ ( <b>25b</b> ).....	144
<b>Scheme 2-14.</b> Reaction of $\eta^3$ -vinylcarbene <b>25c</b> with ethoxyethyne to give $\eta^4$ -cyclopentadiene product <b>29</b> .....	146

<b>Scheme 2-15.</b> Formation of dinuclear complex <b>30</b> from reaction of $\eta^3$ -vinylcarbene <b>25a</b> with $\text{Fe}_2(\text{CO})_9$ , and its isolobal relationship to dinuclear <b>8</b> . ...	148
<b>Scheme 2-16.</b> Formation of $(\text{CO})_3\text{Fe}(\eta^4\text{-2-pyrone})$ complex <b>33</b> from reaction of $\eta^3$ -vinylcarbene <b>25a</b> with carbon monoxide, and its thermal isomerization to <b>34</b> .....	148
<b>Scheme 2-17.</b> Possible identities for species <b>31</b> and <b>32</b> from reaction of <b>25a</b> with maleic anhydride and maleimide, respectively. ....	150
<b>Scheme 2-18.</b> Contrasting behavior of metallacyclobutenes toward alkenes. ....	152
<b>Scheme 3-1.</b> Mechanistic speculation for the conversion of <b>1</b> and maleic anhydride to <b>2</b> . ....	245
<b>Scheme 3-2.</b> Formation of $\eta^2\text{-}(N,O)\text{-}N,N\text{-dialkylhydroxylamido}$ complexes from <b>1</b> and nitroso reagents. ....	247
<b>Scheme 3-3.</b> Reaction of an iridapyrylium with nitrosobenzene to give a bicyclic [3.3.0] metallacycle. ....	248
<b>Scheme 3-4.</b> Mechanistic speculation for the formation of <b>5-trans</b> from <b>1</b> and <i>C</i> -nitroso reagents. ....	259
<b>Scheme 3-5.</b> Possible mechanism for product selection and formation. <b>III-O</b> and <b>TS-O-top</b> are shown from two additional perspectives for clarity.....	264
<b>Scheme 4-1.</b> Synthesis of title cluster compound <b>1</b> . ....	294

## LIST OF TABLES

<b>Table 1-1.</b> Structural Parameters for Complexes <b>5a-5d</b> .....	54
<b>Table 1-2.</b> Spectral Parameters for Complexes <b>33-34</b> .....	87
<b>Table 1-3.</b> Selected bond distances [ $\text{\AA}$ ] for metallacyclobutenes.....	93
<b>Table 2-1.</b> Alkene bond distances [ $\text{\AA}$ ], bend-back parameters [ $^\circ$ ], and fold angles [ $^\circ$ ] for $\eta^4$ -1,4-pentadiene complexes. ....	123
<b>Table 2-2.</b> Hammett $\sigma_p$ parameter for various functional groups. ....	141
<b>Table 2-3.</b> Crystal data and structure refinement for <b>9-ZE</b> .....	188
<b>Table 2-4.</b> Crystal data and structure refinement for <b>9-ZZ</b> .....	190
<b>Table 2-5.</b> Crystal data and structure refinement for <b>10-ZZ</b> .....	192
<b>Table 2-6.</b> Crystal data and structure refinement for <b>11-ZE</b> .....	194
<b>Table 2-7.</b> Crystal data and structure refinement for <b>12-ZZ-ortho</b> .....	196
<b>Table 2-8.</b> Crystal data and structure refinement for <b>12-ZZ-para</b> .....	198
<b>Table 2-9.</b> Crystal data and structure refinement for <b>13-exo</b> .....	200
<b>Table 2-10.</b> Crystal data and structure refinement for <b>13-endo</b> .....	202
<b>Table 2-11.</b> Crystal data and structure refinement for <b>14-exo</b> .....	204
<b>Table 2-12.</b> Crystal data and structure refinement for <b>14-endo</b> .....	206
<b>Table 2-13.</b> Crystal data and structure refinement for <b>20-exo</b> .....	208
<b>Table 2-14.</b> Crystal data and structure refinement for <b>25a</b> .....	210
<b>Table 2-15.</b> Selected bond distances [ $\text{\AA}$ ] for complexes <b>9-ZZ</b> , <b>9-ZE</b> , <b>10-ZZ</b> , <b>10-ZE</b> , <b>11-ZE</b> , <b>12-ZZ-ortho</b> , and <b>12-ZZ-para</b> . ....	211

<b>Table 2-16.</b> Selected bond distances [ $\text{\AA}$ ] for complexes <b>13-<i>exo</i></b> , <b>13-<i>endo</i></b> , <b>14-<i>exo</i></b> , and <b>14-<i>endo</i></b> . .....	212
<b>Table 2-17.</b> Selected angles [ $^{\circ}$ ] for complexes <b>13-<i>exo</i></b> , <b>13-<i>endo</i></b> , <b>14-<i>exo</i></b> , and <b>14-<i>endo</i></b> . .....	213
<b>Table 2-18.</b> Selected spectroscopic data for $\eta^4$ -1,4-pentadiene complexes ( $\text{CDCl}_3$ ). .....	214-215
<b>Table 2-19.</b> Selected spectroscopic data for 2-oxa-1-metalla-(7,8)-dihydrobarrelene complexes ( $\text{CDCl}_3$ ). .....	216
<b>Table 3-1.</b> Selected bond distances [ $\text{\AA}$ ] for complexes <b>5-<i>trans</i></b> , <b>7-<i>cis</i></b> , <b>8-<i>cis</i></b> , and <b>9-<i>cis</i></b> . .....	253
<b>Table 3-2.</b> Selected angles [ $^{\circ}$ ] for complexes <b>5-<i>trans</i></b> , <b>7-<i>cis</i></b> , <b>8-<i>cis</i></b> , and <b>9-<i>cis</i></b> . ....	254
<b>Table 3-3.</b> Crystal data and structure refinement for <b>5-<i>trans</i></b> . .....	279
<b>Table 3-4.</b> Crystal data and structure refinement for <b>7-<i>cis</i></b> . .....	281
<b>Table 3-5.</b> Crystal data and structure refinement for <b>8-<i>cis</i></b> . .....	283
<b>Table 3-6.</b> Crystal data and structure refinement for <b>9-<i>cis</i></b> . .....	285
<b>Table 3-7.</b> Selected spectroscopic data for <i>N,N</i> -Dialkylhydroxylamido complexes ( $\text{CDCl}_3$ ). .....	286-287
<b>Table 4-1.</b> Selected bond distances [ $\text{\AA}$ ] and angles [ $^{\circ}$ ] for complex <b>1</b> . .....	298
<b>Table 4-2.</b> Crystal data and structure refinement for <b>1</b> . .....	305

## ACKNOWLEDGEMENTS

Perhaps the best way to start this acknowledgement is to thank my advisor, Professor Joseph O'Connor. Thank you very much for taking me into your lab Joe, and for keeping me in your lab the many times I struggled to make progress. I don't think I would have been able to finish graduate school without your help, and your patience, and without you going to bat for me. Thank you also, very much so, for being such a wonderful advisor. Your genuine and earnest enthusiasm for chemistry, and for teaching, is refreshing, and inspiring. Some of my favorite times in graduate school were discussions with you about our chemistry, and in contemplation about how our system might work. Thank you for being a great role model, both personally and professionally. Your integrity, thoroughness, and due diligence in the consideration and publication of our chemistry is a standard I will strive toward in my own career.

Professor Joshua Figueroa has been in many ways a second advisor to me during my time here. Thank you Josh for all of the time and effort you have invested in me. In particular, thank you for helping me to better understand the importance of electronic structure in describing the reactivity of transition metal complexes. Thank you also for the great wealth of advice you've given me in regard to my career in chemistry. I think it is very rare to find people in life who give as much thought to how and what and why things should be done, and are as willing to pass along those lessons as Josh. I think Josh may have given me

as much practical, actionable advice on the things I need to be doing in each step of my academic progress as anyone, and I am sincerely grateful.

I remember when I came down for recruitment to UCSD, so very long ago, and Professor Arnie Rheingold came to the table where I was sitting for lunch. Arnie had been tipped off by Prof. Bitterwolf at the U. of Idaho that I was on my way down, and he made a point to come by and say hello, and to introduce himself. Since that time, Arnie has always been both genial and gracious; I've always felt like I had someone I could go and talk to when I needed it, and Arnie has always kept his door open for me. I appreciate the times that you invited me to your home, and also, for always making me feel at home in your lab. I consider it an honor to have learned crystallography from you, and from your postdoctoral associates Curtis and Antonio, and it was a pleasure to work with you in reporting our lab's foray into cluster chemistry. Thank you Arnie.

Professor Perrin has been attending group meetings with the O'Connor lab since I have been here, and has seen as many of my presentations over the years as anyone except Joe. Thank you Professor Perrin for your many pertinent and thoughtful questions over the years, and for lending me your keen insight in the analysis of my research project. Thank you also for the many excellent suggestions you've given me in regards to my chemistry. It is a rare scientist that is able to offer insight into a field of science at such a fundamental level as Prof. Perrin, and it has been both an honor and a privilege to be given the opportunity to learn from you.

I would like to thank my doctoral committee members over the years, including Profs. Hendrickson and Magde, who both served on my committee in my early years, Prof. Gustaf Arrhenius from the Scripps Institute of Oceanography, and Prof. Shirley Meng from the Department of NanoEngineering. Thank you for serving on my doctoral committee, for asking me questions and helping to guide me in my research, and for your time and service. I would especially like to thank Dave Hendrickson, who gave me a great deal of advice during my tumultuous first year.

I would also like to thank Prof. Dr. Karsten Meyer, who was my advisor during my first year. I came down to UCSD to work for Karsten, and though it was a rocky time, I want to express my gratitude to Karsten for looking after me, and for his generosity.

Finally, I would like to thank Dr. Antonio DiPasquale and Dr. Curtis Moore for their assistance in the X-ray Crystallography facility, and for their time and friendship. Dr. Anthony Mrse in the NMR facility was a great help in the collection of more complicated NMR experiments, and was always a pleasure to talk to. Dr. Yongxuan Su has collected many mass spectra for me over the years, and I would like to express my appreciation. Teresa Abendroth was a tremendous help in keeping out lab running, and is one of the most efficient and expeditious people I've met. Thank you all very much.

Chapter 2 is adapted from **R. L. Holland**, K. D. Bunker, C. H. Chen, A. G. DiPasquale, A. L. Rheingold, K. K. Baldrige, J. M. O'Connor, "Reactions of a

Metallacyclobutene Complex with Alkenes" *J. Am. Chem. Soc.*, **2008**, *130*, 10093-10095. Copyright 2008 American Chemical Society. Permission to use copyrighted images and data in the manuscript was also obtained from K. D. Bunker, C. H. Chen, A. G. DiPasquale, A. L. Rheingold, K. K. Baldrige, and J. M. O'Connor.

Chapter 3 is adapted from **R. L. Holland**, J. M. O'Connor, "Nitroso Compounds Serve as Precursors to Late-Metal  $\eta^2$ -(*N,O*)-Hydroxylamido Complexes" *Organometallics*, **2009**, *28*, 394-396. Copyright 2009 American Chemical Society. Permission to use copyrighted images and data in the manuscript was also obtained from J. M. O'Connor. The dissertation author is the first author of this paper.

Chapter 4 is adapted from **R. L. Holland**, J. M. O'Connor, A. L. Rheingold "The Isolation of a Large Cyclopentadienylcobaltsulfide Cluster. The Synthesis and Crystal Structure of Octahedral *closo*-( $\eta^5$ -C<sub>5</sub>H<sub>5</sub>Co)<sub>5</sub>S" *J. Clust. Sci.*, **2009**, *20*, 261-265. Copyright 2009 The Author(s). Permission to use copyrighted images and data in the manuscript was obtained from J. M. O'Connor, and A. L. Rheingold. The dissertation author is the first author of this paper.



## VITA

- 2005 Bachelor of Science, University of Idaho
- 2006 Master of Science, University of California, San Diego
- 2016 Doctor of Philosophy, University of California, San Diego

## PUBLICATIONS

**R. L. Holland**, J. M. O'Connor, K. D. Bunker, P. Qin, S. K. Cope, K. K. Baldrige, J. S. Siegel, "Stereospecific Oxidative Demetallation of Highly Functionalized CpCo(1,3-Diene) Complexes: An Experimental and Computational Study" *Synlett*, **2015**, *26*, 2243-2246.

K. K. Baldrige, K. D. Bunker, C. L. Vélez, **R. L. Holland**, A. L. Rheingold, C. E. Moore, J. M. O'Connor, "Structural Characterization of (C<sub>5</sub>H<sub>5</sub>)Co(PPh<sub>3</sub>)( $\eta^2$ -alkyne) and (C<sub>5</sub>H<sub>5</sub>)Co( $\eta^2$ -alkyne) Complexes of Highly Polarized Alkynes" *Organometallics*, **2013**, *32*, 5471-5480.

J. M. O'Connor, M.-C. Chen, **R. L. Holland**, A. L. Rheingold, "Addition of Dissimilar Carbenes across an Unsymmetrically Substituted Alkyne: Regio- and Stereoselective Synthesis of Trisubstituted 1,3-Dienes" *Organometallics*, **2011**, *30*, 369-371.

J. M. O'Connor, K. K. Baldrige, B. L. Rodgers, M. Aubrey, **R. L. Holland**, S. W. Kassel, A. L. Rheingold, "A Photochemical Metallocene Route to Anionic Eneidyne: Synthesis, Solid-State Structures, and ab Initio Computations on Cyclopentadienoidenediynes" *J. Am. Chem. Soc.*, **2010**, *132*, 11030-11032.

C. L. Vélez, P. R. L. Markwick, **R. L. Holland**, A. G. DiPasquale, A. L. Rheingold, J. M. O'Connor, "Cobalt 1,3-Diisopropyl-1*H*-imidazol-2-ylidene Complexes: Synthesis, Solid-State Structures, and Quantum Chemistry Calculations" *Organometallics*, **2010**, *29*, 6695-6702.

J. M. O'Connor, M.-C. Chen, **R. L. Holland**, "Protonation of Cobalt-Allyl and Oxacobaltacyclopentadiene Complexes" *Organometallics*, **2010**, *29*, 6161-6164.

J. M. O'Connor, A. P. Closson, **R. L. Holland**, S. K. Cope, C. L. Vélez, C. E. Moore, A. L. Rheingold, "Synthesis and Solid-State Structures of (triphos)iridacyclopentadiene Complexes as Models for Vinylidene Intermediates in the [2 + 2 + 1] Cyclootrimerization of Alkynes" *Inorg. Chim. Acta*, **2010**, *364*, 220-225.

**R. L. Holland**, J. M. O'Connor, "Nitroso Compounds Serve as Precursors to Late-Metal  $\eta^2$ -(*N,O*)-Hydroxylamido Complexes" *Organometallics*, **2009**, *28*, 394-396.

**R. L. Holland**, J. M. O'Connor, A. L. Rheingold, "The Isolation of a Large Cyclopentadienylcobaltsulfide Cluster. The Synthesis and Crystal Structure of Octahedral *closo*-( $\eta^5$ -C<sub>5</sub>H<sub>5</sub>Co)<sub>5</sub>S" *J. Cluster. Sci.*, **2009**, *20*, 261-265.

**R. L. Holland**, K. D. Bunker, C. H. Chen, A. G. DiPasquale, A. L. Rheingold, K. K. Baldrige, J. M. O'Connor, "Reactions of a Metallacyclobutene Complex with Alkenes" *J. Am. Chem. Soc.*, **2008**, *130*, 10093-10095.

ABSTRACT OF THE DISSERTATION

**The Reactivity of Stable Metallacyclobutenes and Vinylcarbenes**

by

Ryan Lynn Holland

Doctor of Philosophy in Chemistry

University of California, San Diego, 2016

Professor Joseph M. O'Connor, Chair

## Chapter 1. Historical Development of Stable Metallacyclobutenes

Fred Tebbe and co-workers synthesized the first stable metallacyclobutene complexes in the late 1970's by treatment of an intermediate titanium methylene species – later popularized as the “Tebbe reagent” – with acetylenes. Robert Grubbs at Caltech further studied this system, using it to detail a degenerate metathesis reaction and to isolate a metallacyclobutane complex – which was implicated in the emerging field of alkene metathesis. Further development of stable metallacyclobutene complexes is explored chronologically, particularly with regard to systems developed by Thorn, Bianchini, Hughes, O'Connor, Casey, Wojcicki, and Chen.

## Chapter 2. Reactivity of Stable Metallacyclobutenes and Vinylcarbenes with Alkenes

Cobalt-metallacyclobutene complex  $(\eta^5\text{-C}_5\text{H}_5)(\text{PPh}_3)\text{Co}[\kappa^2\text{-(C,C)-C}(\text{SO}_2\text{Ph})=\text{C}(\text{TMS})\text{CH}(\text{CO}_2\text{Et})]$  is allowed to react with a variety of acyclic and cyclic alkenes to generate stable  $\eta^4$ -1,4-pentadienes (**9-12**) and  $\kappa^2$ -metallacyclohexenes (**13-14**), respectively. The reaction is thought to occur through a vinylcarbene intermediate such as **15-17**, and a model complex of an oxametallabenzene containing an internal vinylcarbene moiety is calculated (**18**). Complex **13-exo** reacts with trimethylphosphine to decomplex the ester carbonyl, generating a  $\text{PMe}_3$  complex, **20-exo**. Oxidative demetallation of complexes **9-ZZ** and **9-ZE** is effected with iodine to generate organic pentadienes **21-22**. Iron vinylcarbene complex  $(\text{CO})_3\text{Fe}(\eta^3\text{-C}(\text{OMe})\text{C}(\text{CO}_2\text{Me})=\text{CH}(\text{CO}_2\text{Me}))$  (**25a**) is

synthesized, and its reactivity with maleic anhydride and maleimide is found to generate dinuclear iron complex **30**, and new organic species **31** and **32**. Compounds **31-32** are formulated as the [4 + 2]-cycloaddition product of an intermediate furan or  $\alpha$ -pyrone.

### **Chapter 3. Reactivity of Stable Metallacyclobutenes with C-Nitroso Reagents**

Cobaltacyclobutene complex  $(\eta^5\text{-C}_5\text{H}_5)(\text{PPh}_3)\text{Co}[\kappa^2\text{-(C,C)-C(SO}_2\text{Ph)=C(TMS)CH(CO}_2\text{Et)}]$  is found to react with C-nitroso reagents to afford bicyclic  $[\kappa^2\text{-(C,O)-}\eta^1\text{-(N)-hydroxylamido}$  complexes **5-9**. Complexes **5-9** contain a [3.1.0] fused-ring framework, with the 3-membered oxametallaziridine moiety formed in either a cis or trans relationship to the ethyl ester. Formation of products **5-9** is proposed to occur through a [4 + 2]-cycloaddition mechanism from an oxametallabenzene, with stereo-selection via rapid epimerization of nitrogen from the post-cyclization intermediate.

### **Chapter 4. The Isolation of a Large Cyclopentadienylcobaltsulfide Cluster – Synthesis and Crystal Structure of Octahedral *closo*- $[(\eta^5\text{-C}_5\text{H}_5)\text{Co}]_5\text{S}$**

The metallacyclobutene complex  $(\eta^5\text{-C}_5\text{H}_5)(\text{PPh}_3)\text{Co}[\kappa^2\text{-(C,C)-C(SO}_2\text{Ph)=C(TMS)CH(CO}_2\text{Et)}]$  reacts with added  $(\eta^5\text{-C}_5\text{H}_5)\text{Co}(\text{PPh}_3)_2$  to give the cluster compound *closo*- $[(\eta^5\text{-C}_5\text{H}_5)\text{Co}]_5\text{S}$  (**1**), the largest  $(\eta^5\text{-C}_5\text{H}_5)\text{Co}$  cluster known.

## **Chapter 1**

### Historical Development of Stable Metallacyclobutenes

Organometallic complexes, due to their rich reactivity and tunable electronic structure, serve as versatile intermediates in the preparation and elaboration of complex organic molecules. A metal center and pendant ligand set can serve as a scaffold on which multiple carbon or heteroatom-containing chemical moieties can be assembled and released, both stoichiometrically and catalytically. Metallacycles, defined as carbocycles in which one of the ring carbons has been replaced by a metal, have been widely developed as key components in a variety of useful synthetic methodology. The study and characterization of stable metallacycles can offer the physical organometallic chemist insight into the role these compounds play in metal-catalyzed reactions.

The following is a critical précis regarding the historical development and synthesis of stable metallacyclobutenes, with brief notations regarding their proposed intermediacy in the metathesis reaction. Metallacyclobutene complexes are four-membered ring metallacycles that contain a pi-bond between two of the ring atoms. Metallacyclobutenes have been proposed as critical intermediates in a number of important synthetic processes, particularly in the reactions of metal carbenes with alkynes. The synthesis of long-lived metallacyclobutenes can shed light on the factors that control the stability of these molecules, with inherent implications regarding transient metallacyclobutene intermediates. This account reviews the synthesis, characterization, and reactivity of stable metallacyclobutene complexes – focusing particularly on crystallographically and spectroscopically characterized mononuclear metallacyclobutenes.

Historically, the first unsaturated four-membered ring metallacycle, although not initially recognized as such, was prepared in 1969 by Teuben and de Liefde Meijer and reported along with a series of  $(\eta^5\text{-C}_5\text{H}_5)_2\text{M}(\text{C}_2\text{Ph})_m$  (M = V(III), V(IV), and Ti(IV); m = 1 or 2) complexes.<sup>1</sup> The reaction of two equivalents of phenylethynylsodium with  $[(\eta^5\text{-C}_5\text{H}_5)_2\text{TiCl}]_2$  dimer gave the dark green compound  $[(\eta^5\text{-C}_5\text{H}_5)_2\text{Ti}(\text{C}_2\text{Ph})]_2$  (**1**), which in contrast to the accompanying  $(\eta^5\text{-C}_5\text{H}_5)_2\text{V(III)}(\kappa^1\text{-C}\equiv\text{CPh})$  mono-ethynyl and  $(\eta^5\text{-C}_5\text{H}_5)_2\text{V(IV)}(\kappa^1\text{-C}\equiv\text{CPh})_2$  and  $(\eta^5\text{-C}_5\text{H}_5)_2\text{Ti(IV)}(\kappa^1\text{-C}\equiv\text{CPh})_2$  diethynyl compounds, did not exhibit the expected alkynyl stretching band in the infrared spectrum (Figure 1-1). Mass spectrometry was consistent with a dimeric structure with a molecular mass corresponding to two titanocene units bridged by two phenylethynyl groups. The hydrolysis of **1** with an ethereal solution of HCl followed by aerobic oxidation gave  $(\eta^5\text{-C}_5\text{H}_5)\text{TiCl}_2$  and *trans*-1,4-diphenylbutenyne, which indicated that the bonding of phenylethynyl groups was not  $\kappa^1\text{-C}\equiv\text{CPh}$ . The diamagnetic nature of the compound led to the assumption of an antiferromagnetically coupled metal-metal bond with two bridging ethynyl units, and two different structures were proposed: a  $(\mu\text{-C}\equiv\text{CPh})_2$  bridged dimer and a  $(\kappa^1, \eta^2\text{-C}\equiv\text{CPh})_2$  dimer featuring two ethynyl groups with a  $\sigma$ -bond to one metal and a  $\pi$ -bond to the second.



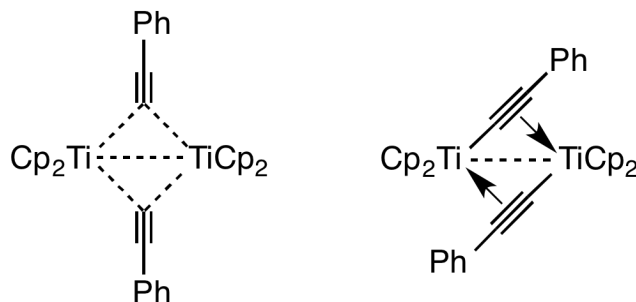


**Figure 1-1.** Proposed structures for the complex  $[(\eta^5\text{-C}_5\text{H}_5)_2\text{Ti}(\text{C}_2\text{Ph})]_2$  (**1**).<sup>1</sup>

An interest in the observed magnetic properties and reaction chemistry of **1** prompted a reinvestigation by Sekutowski and Stucky.<sup>2</sup> Preparation of the related compound  $[(\eta^5\text{-C}_5\text{H}_4\text{Me})_2\text{Ti}(\text{C}_2\text{Ph})]_2$  (**2**) was accomplished in an adapted protocol by reaction of the bis( $\eta^5$ -methylcyclopentadienyl)titanium(III) chloride monomer with the sodium phenylacetylide. Alternatively, synthesis was also accomplished by sodium-metal reduction of  $(\eta^5\text{-C}_5\text{H}_4\text{Me})_2\text{TiCl}$  in the presence of 1,4-diphenyl-1,3-butadiyne.

The methyl-substituted cyclopentadienyl variant was rationalized by the improved solubility of the resulting compound, as well as an observed tendency for the methyl substitution to “lock” the cyclopentadienyl rings in place, reducing the large thermal motions that hindered X-ray crystallographic analysis. Initial measurements of the magnetic properties, infrared spectrum, and mass spectrum were similar – indicating that bonding in compounds **1** and **2** was likely the same. X-ray diffraction analysis of **2** revealed a bicyclo[2.2.0]hexadiene structure with *pseudo*- $C_{2h}$  symmetry in which two metallacycle units are linked across two carbon atoms of a four-membered ring (Figure 1-2). The titanium

atoms and the C<sub>4</sub> unit are coplanar to within 0.20 Å, and the bond lengths are consistent with two Ti-C σ-bonds (Ti-C(1) and Ti-C(3) or Ti-C(1)' and Ti-C(3)'), one C-C σ-bond (C(3)-C(3)') and one C-C π-bond (C(1)-C(3)' or C(1)'-C(3)) on each half of the dimer. The phenyl groups are also coplanar with the fused four-membered rings, with the largest deviation from the best-fit plane of the sixteen carbon atoms being 0.03 Å. Notably, this is the first example of a four-membered metallacycle of an early transition metal.

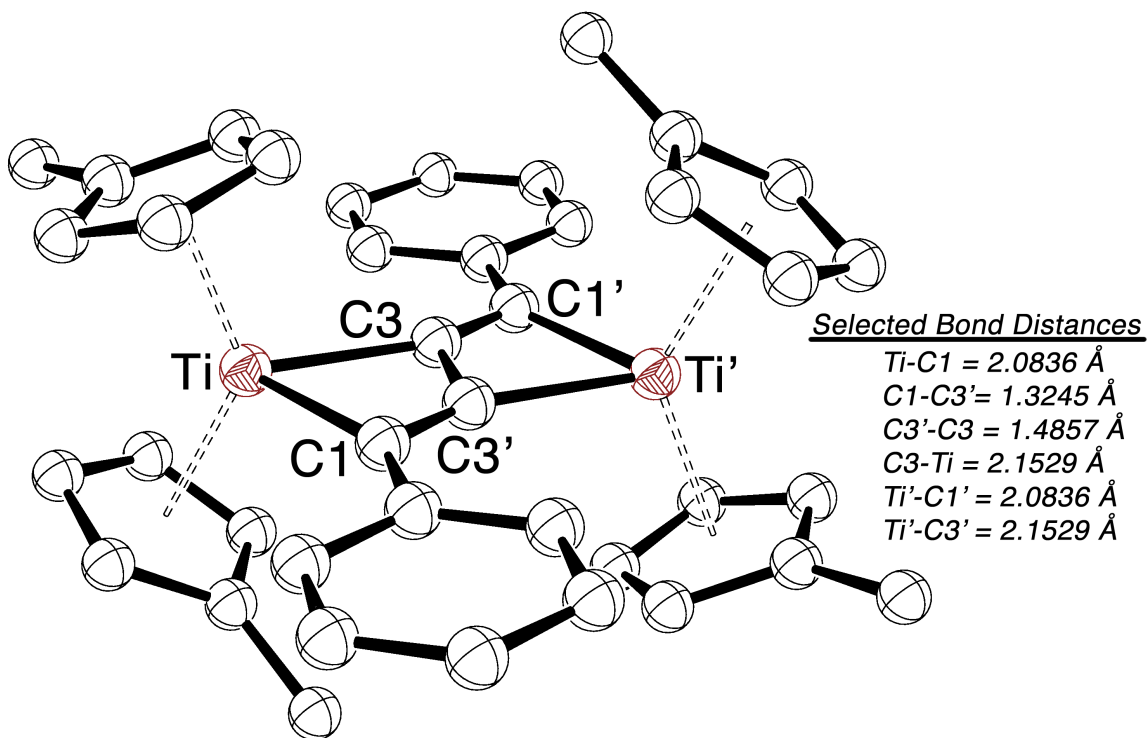


**Figure 1-2.** Ball-and-Stick representation of titanacycle **2**. Hydrogen atom coordinates not included in crystallographic information file. CCDC Number 1210264; refcode MCPBTI. R = 5.2%, Space Group  $P2_1/c$ .<sup>2</sup>

Unsaturated four-membered ring metallacycles are a class of compounds that can exist in a number of derivative forms. Metallacyclobutenes are most simply a cyclobutene ring containing a transition metal in place of a saturated

carbon and can thus feature a great deal of variation, most notably a ligand set that can be modified substantially, and which can play an important part in the reaction coordinates through which these complexes can traverse (Figure 1-3; **Type I**).<sup>3</sup> Additionally, the carbocyclic portion of a metallacyclobutene can be functionalized with an extensive array of chemical moieties to give metallacyclobutene derivatives, including exo-cyclic unsaturation at the C(3) carbon (Figure 1-3; **Type II**).<sup>4-6</sup> Titanacycle **2** is a bicyclic structure (Figure 1-3; **Type III**), and as such is closely related to **Type II** metallacyclobutene derivatives in which unsaturation is present at all three carbon atoms in the four-membered ring.<sup>7</sup> The parent metallacyclobutenes are a relatively rare class of compounds that can feature a variety of metals, ligand substitutions, functionalizations, and modes of reaction.

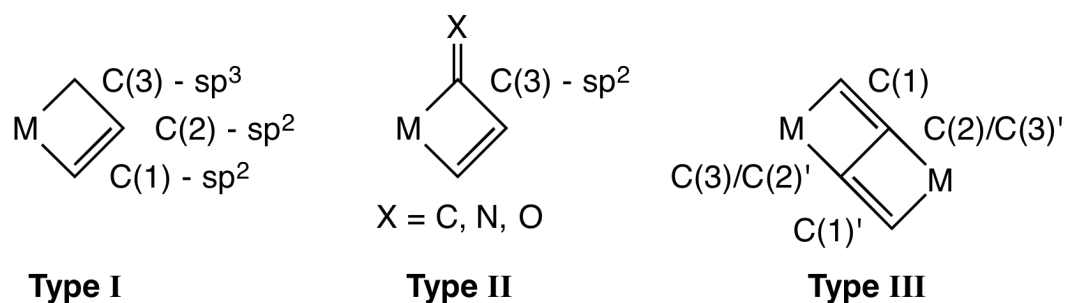


**Figure 1-3.** Unsaturation four-membered ring bonding motifs.

During the late 1960's and early 1970's, there was intense interest in the metathesis reaction of olefins catalyzed by transition metals, as well as in the formation of four-membered ring metallacycles that were thought to be involved as intermediates.<sup>8</sup> First reported in the 1960s by industrial chemists,<sup>9</sup> the

accepted mechanism of olefin metathesis was proposed in 1971 by Yves Chauvin and his student Jean-Louis Hérisson.<sup>10</sup> This mechanism was brought to mainstream attention in a communication by Casey<sup>11</sup> who proposed that an equilibrium between a metallacyclobutane and a metal complex containing both an alkene and carbene sufficiently explained the accumulated experimental evidence regarding metathesis. A report in 1975 by Masuda<sup>12</sup> and coworkers detailing the polymerization of phenylacetylene by  $WCl_6$  and  $MoCl_5$  suggested that metallacyclobutenes played a role in alkyne polymerization, predicting that just as “four-membered rings containing tungsten or molybdenum have been proposed as active species in the metathesis of olefins<sup>11</sup> and in the metathesis polymerization of cycloolefins,<sup>13</sup> it will be probable that the active species in the present polymerization is also a four-membered metallocycle (*sic*).”

In 1978, Tebbe and coworkers reported a titanocene system derived from  $(\eta^5-C_5H_5)_2TiCl_2$  for the homologation of olefins, such as propylene from ethylene, or isobutylene from propene.<sup>14</sup> Sinn and coworkers had previously reported the formation of methane from reactions of titanocene dichloride with trimethylaluminum, and had suggested several  $TiCH_2Al$  species as products.<sup>15</sup> Inspired by Schrock's report of tantalum alkylidene compounds (and also perhaps by working in lab with Schrock at the DuPont Experimental Station in Wilmington, Delaware)<sup>8h-8i</sup> and the role of tungsten methylene species in metathesis,<sup>16</sup> Tebbe set out to study and characterize the titanium-aluminum-methyl species. In a reaction of titanocene dichloride with two equivalents of

$\text{AlMe}_3$ , methane and  $\text{Me}_2\text{AlCl}$  were produced, as well as  $(\eta^5\text{-C}_5\text{H}_5)_2\text{Ti}(\kappa^2\text{-(C,C)}\text{-CH}_2\text{AlMe}_2\text{Cl})$  (**3**). Compound **3** was also produced from the reaction of  $(\eta^5\text{-C}_5\text{H}_5)_2\text{Ti}(\text{CH}_3)_2$  with  $\text{Me}_2\text{AlCl}$ .

Based on the spectral properties of **3** and related compounds, a cyclic structure was proposed. It was also suggested that **3** might exist in equilibrium with a  $\text{Me}_2\text{AlCl}$ -stabilized adduct of a titanocene-methylene species, **4** (Figure 1-4).

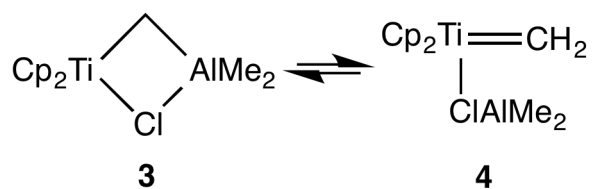
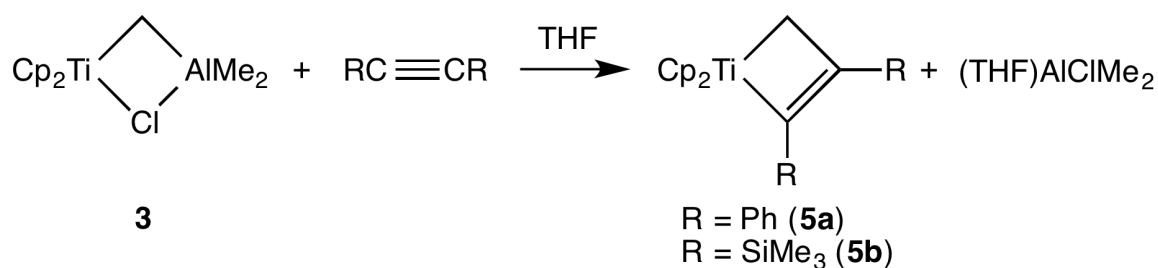


**Figure 1-4.** Proposed structure of  $(\eta^5\text{-C}_5\text{H}_5)_2\text{Ti}(\kappa^2\text{-(C,C)}\text{-CH}_2\text{AlMe}_2\text{Cl})$  (**3**) and a  $\text{Me}_2\text{AlCl}$ -stabilized adduct of an intermediate titanium methylene species (**4**).<sup>14</sup>

It was proposed that **3** should react with organic compounds through intermediate **4**, as well as with Lewis bases that could complex the aluminum, thereby enhancing reactivity. Indeed, compound **3** was found to react with alkenes to give homologated products: propylene from ethylene and isobutylene from propene (as well as trace amounts of other  $\text{C}_4$  products, including methylcyclopropane). Isobutylene was found to be mostly unreactive, though it did give small amounts of  $\text{C}_5$  products when THF or  $\text{NMe}_3$  were added. Additionally, a small amount of cyclopropane was detected from the reaction of ethylene in the presence of trimethylamine. In order to account for the observed homologation and cyclopropanation reactivity and to explain several isotopic

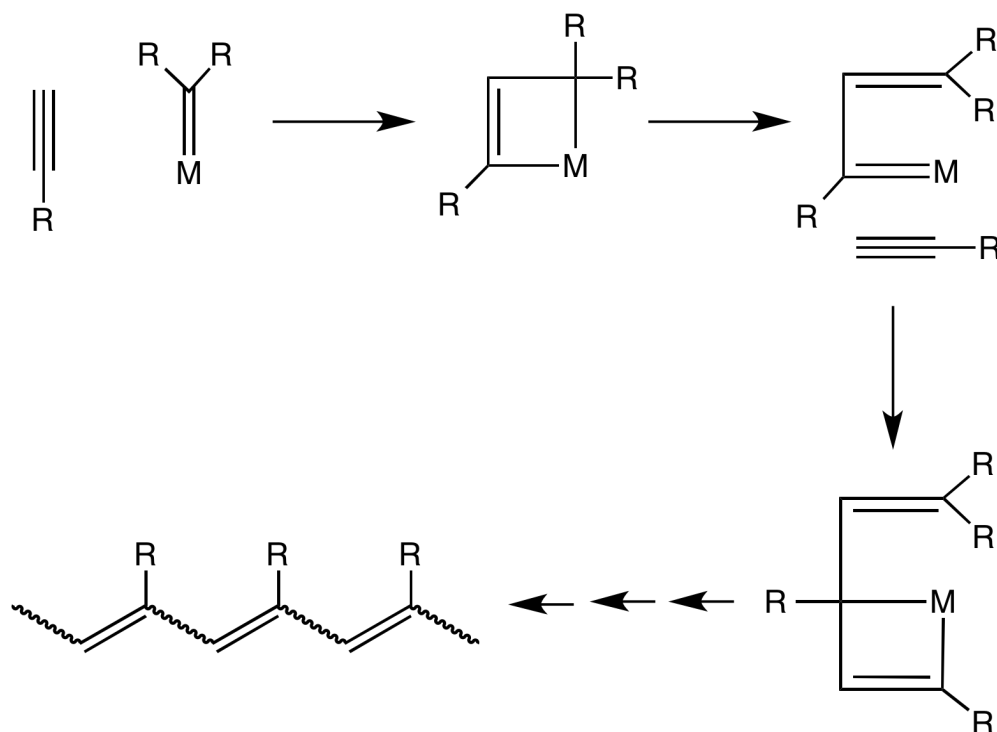
labeling studies, a metathesis-like metallacyclobutane intermediate was proposed. Though a metallacyclobutane intermediate was postulated – and several deuterated compounds consistent with a metathesis mechanism were produced – compound **3** was not thought to be a metathesis reagent, as of yet.

A second communication from the Tebbe group found that compound **3** did in fact react with isobutylene.<sup>17</sup> In a crossover experiment with  $^{13}\text{CH}_2=\text{CMe}_2$  and unlabeled methylenecyclohexane ( $\text{CH}_2=\text{C}_6\text{H}_{10}$ ) in the presence of unlabeled **3** ( $(\eta^5\text{-C}_5\text{H}_5)_2\text{Ti}(\kappa^2\text{-}(C,C)\text{-CH}_2\text{AlMe}_2\text{Cl})$ ), there was depletion of  $^{13}\text{CH}_2=\text{CMe}_2$  and concomitant enrichment of  $^{13}\text{CH}_2=\text{C}_6\text{H}_{10}$  and  $(\eta^5\text{-C}_5\text{H}_5)_2\text{Ti}(\kappa^2\text{-}(^{13}\text{C},C)\text{-}^{13}\text{CH}_2\text{AlMe}_2\text{Cl})$ . Reaction was extensive after 47 h at 51 °C and was limited solely to methylene exchange – thus demonstrating a “degenerate”<sup>18</sup> metathesis reaction. Of particular note with respect to the chemistry of metallacyclobutenes, reaction of **3** with diphenylacetylene in THF was very briefly described as giving a metallacyclobutene product ( $(\eta^5\text{-C}_5\text{H}_5)_2\text{Ti}[\kappa^2\text{-C(Ph)=C(Ph)CH}_2]$  (**5a**) as well as the  $\text{Me}_2\text{AlCl}\cdot\text{THF}$  adduct (Scheme 1-1). Metallacyclobutene **5a** was also briefly mentioned in an article comparing the similar reactivity of **3** with alkylidene-phosphoranes, such as in the Wittig reaction.<sup>19</sup>



**Scheme 1-1.** Synthesis of titanacyclobutenes **5** from compound **3**.<sup>25a</sup>

Since metal carbenes were thought to combine with olefins through a metallacyclobutane intermediate to propagate the metal-catalyzed metathesis of alkenes, Katz proposed<sup>20a</sup> that metal carbenes could similarly combine with acetylenes through an analogous metallacyclobutene intermediate to propagate the metal-catalyzed polymerization of alkynes (Scheme 1-2).



**Scheme 1-2.** Proposed catalytic cycle for alkyne polymerization.<sup>20a</sup>

The metal carbenes pentacarbonyl(phenylmethoxycarbene)tungsten(0)<sup>21</sup> and pentacarbonyl(diphenylcarbene)tungsten(0)<sup>11,22</sup> – species used previously to mediate olefin metathesis<sup>23</sup> – were shown to facilitate acetylene polymerization, *quod erat demonstrandum*. Subsequent communications further demonstrate

and elaborate this principle, and also detail the use of alkynes in the ring-opening alkene metathesis polymerization reaction.<sup>24</sup>

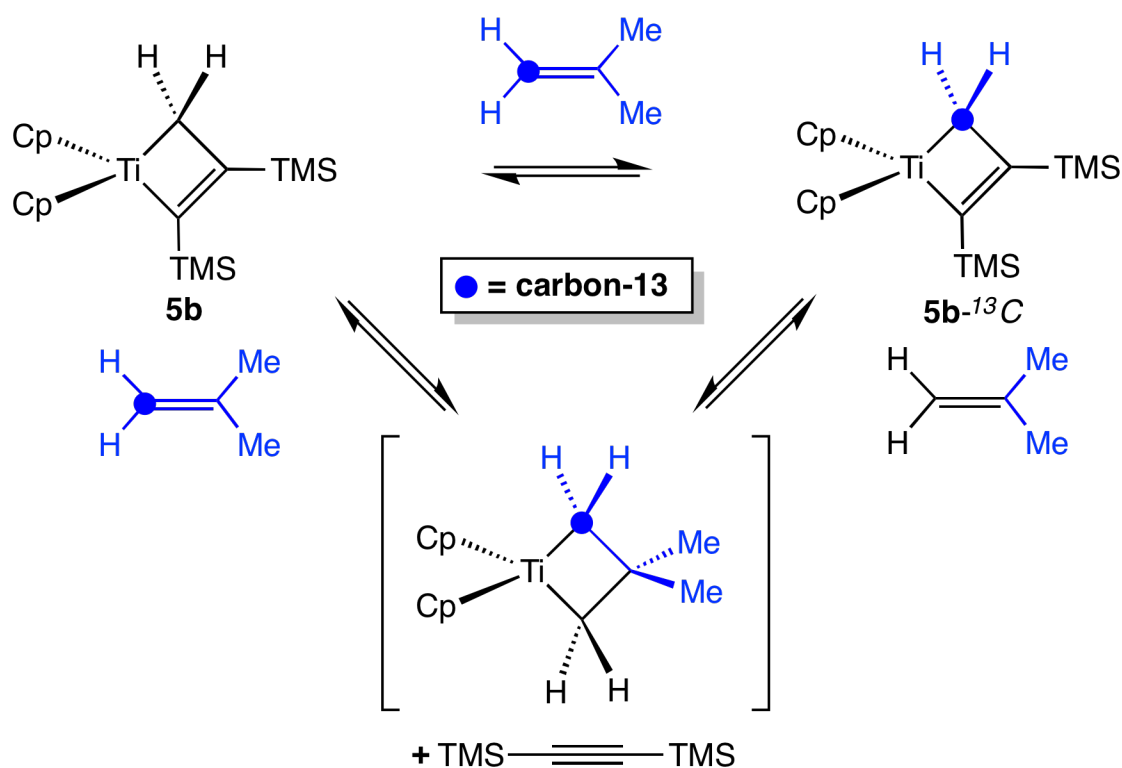
It is worth noting that later calculations by Peter Hofmann and co-workers call into question the role of metallacyclobutenes in alkyne polymerization and other reactions.<sup>20b-20c</sup> Molecular orbital studies for metallacyclobutenes – particularly in regard to chromacyclobutene intermediates suggested for the Dötz benzannulation reaction<sup>20d-20g</sup> – suggest that the intermediates in these reactions are more likely to be  $\eta^3$ -vinylcarbenes.

In 1980 a third report by Tebbe and coworkers gave greater detail on the synthesis and reactivity of metallacyclobutenes from **3**.<sup>25a</sup> Reaction of **3** with acetylenes in THF gave titanacyclobutenes **5** (Scheme 1-2). In contrast, reaction with acetylenes in toluene was sluggish, and significant byproduct was formed. Conditions that favor the syntheses of **5** also significantly enhanced the rate of olefin metathesis catalyzed by **3**, i.e., basic reagents or electron-pair donating solvents appeared to complex the aluminum, shifting the equilibrium toward the chemically active titanium methylene species. In the absence of electron-pair donors, the aluminum serves as an electron-sink for the titanium methylene species, preserving it in solution and rendering it mostly unreactive.

The phenyl-substituted titanacyclobutene **5a** underwent reaction with water to give  $\alpha$ -methyl-*cis*-stilbene, or with D<sub>2</sub>O to give the  $\alpha$ -methyl-*d*<sub>2</sub>-*cis*-stilbene. The TMS-substituted titanacyclobutene,  $(\eta^5\text{-C}_5\text{H}_5)_2\text{Ti}(\kappa^2\text{-C}(\text{TMS})=\text{C}(\text{TMS})\text{CH}_2)$  (**5b**), was found to react with diphenylacetylene at elevated



temperatures to give **5a** (36% yield; 6 h at 85 °C); however, the reverse was found to be insignificant, even with prolonged heating. When heated, **5b** also underwent reaction with 2-methylpropene-1-<sup>13</sup>C to give **5b-<sup>13</sup>C** with enrichment at the sp<sup>3</sup>-carbon C(3) of the metallacyclobutene ring (Scheme 1-3). Though not detected, this exchange was proposed to occur through a metallacyclobutane intermediate. This metallacyclobutane intermediate could return a <sup>13</sup>C-enriched titanium methylene species that would react with liberated bis(trimethylsilyl)acetylene to give the ( $\eta^5$ -C<sub>5</sub>H<sub>5</sub>)<sub>2</sub>Ti( $\kappa^2$ -C(TMS)=C(TMS)<sup>13</sup>CH<sub>2</sub>) metallacycle **5b-<sup>13</sup>C**.



**Scheme 1-3.** Reaction of **5b** with 2-methylpropene-1-<sup>13</sup>C to give 2-methylpropene and **5b-<sup>13</sup>C**.<sup>25a-b</sup>

In contrast to the elevated temperatures required for the reaction of **5b** with acetylenes and olefins, it was found that  $\text{Me}_2\text{AlCl}$  would react with **5b** at room temperature when supplied in the absence of THF. THF-complexed  $\text{Me}_2\text{AlCl}$  was not competitive with bis(trimethylsilyl)acetylene for reaction with the putative titanium methylene. Intriguingly, metallacycle **3** and metallacyclobutene **5b** could serve as pro-catalysts for the metathesis-capable carbene synthon ( $\eta^5\text{-C}_5\text{H}_5$ )<sub>2</sub>Ti=CH<sub>2</sub>, similar to an analogous metallacyclobutane proposal discussed by Grubbs.<sup>26</sup>

The crystal structure of titanacycle **5a** was reported, which showed a planar metallacyclobutene unit bisected by the plane formed by titanium and the two cyclopentadienyl centroids, with the cyclopentadienyl rings and carbons C(1) and C(3) arranged in a *pseudo*-tetrahedral fashion about the metal (Figure 1-5). The phenyl substituents were found to be nearly orthogonal at C(1) (87.87°) and near coplanar at C(2) (6.54°). This was the first reported crystal structure of a mononuclear metallacyclobutene.

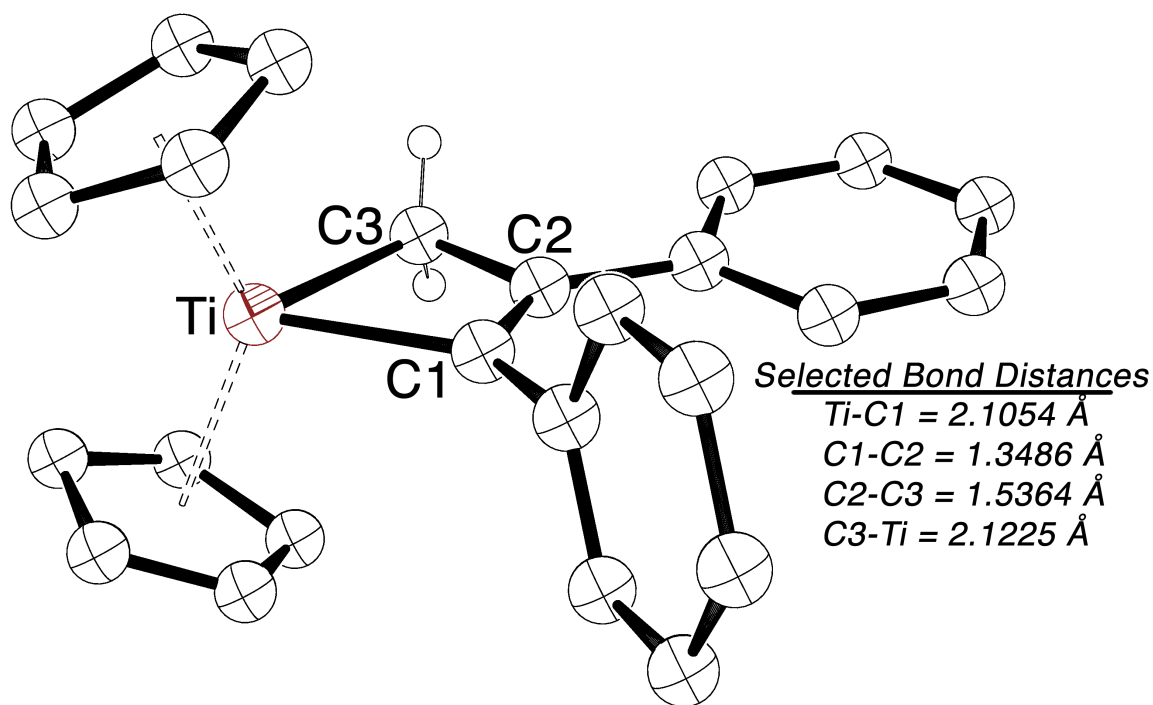
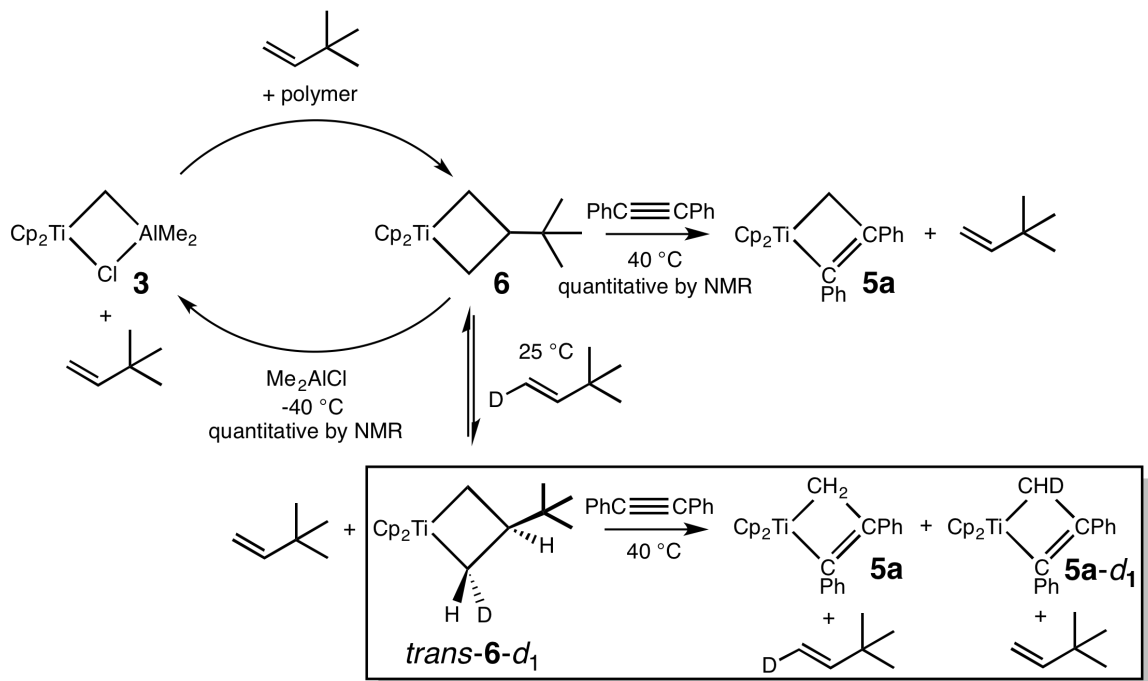


**Figure 1-5.** Ball-and-Stick representation of titanacyclobutene **5a**. CCDC Number 1131477; refile CPTICB. R = 3.8%, Space Group *Pbca*.<sup>25a</sup>

An effort to elucidate the factors controlling the stereochemistry of olefin metathesis led Grubbs and coworkers to attempt the synthesis of cyclopentadienyl-substituted analogues to the “Tebbe” reagent, **3**. As part of that effort, a reinvestigation of the reactivity of **3** was undertaken.<sup>27</sup> Compound **3** was found to react with neohexene in THF to give an intractable mixture of products. However, when the same reaction was run in benzene with one equivalent of pyridine, a near-quantitative yield of a single metallocene product was obtained, as well as the Me<sub>2</sub>AlCl-pyridine adduct. Once the role of pyridine in the reactivity of **3** was realized, a more convenient Lewis base was utilized. A 4-vinylpyridine-styrene copolymer (1:1) was prepared from 4-vinylpyridine and styrene in THF with AIBN as initiator, and used as a filterable reagent in the reactions of **3**. In the

reaction of **3** with neohexene,  $^1\text{H}$  and  $^{13}\text{C}$  NMR spectroscopy were used to elucidate the nature of the metallocene product as the metallacyclobutane,  $(\eta^5\text{-C}_5\text{H}_5)_2\text{Ti}(\kappa^2\text{-CH}_2\text{CH}(\text{tBu})\text{CH}_2)$  (**6**) – an isolable example of the proposed metallacyclobutane intermediate in Tebbe's metathesis reactions. Isolated **6** was found to react with  $\text{Me}_2\text{AlCl}$  to return **3** and neohexene, thus closing the metathesis catalytic cycle (Scheme 1-4). Reaction of **6** with *trans*-neohexene-1- $d_1$  gave *trans*-**6**- $d_1$  and neohexene – demonstrating a lack of isomerization in the course of the reaction, while reaction of **6** with diphenylacetylene gave neohexene and the previously reported titanacyclobutene **5a** – establishing degeneracy. Reaction of isolated *trans*-**6**- $d_1$  with diphenylacetylene gave a 1:1 mixture of the titanacyclobutenes **5a** and **5a**- $d_1$ , as well as the deuterated olefin (50%) as pure *trans*-neohexene-1- $d_1$  (Scheme 1-4 inset), thus validating that the active catalytic species could be formed from either side of the metallacyclobutane ring as the isotopologues  $\text{Ti}=\text{CH}_2$  or  $\text{Ti}=\text{CHD}$ .



**Scheme 1-4.** Synthesis of titanacyclobutane **6** from Tebbe's reagent, **3**, and reaction of compound **6** with  $\text{Me}_2\text{AlCl}$ , *trans*-neohexene-1- $d_1$ , and diphenylacetylene. Inset: Reaction of *trans-6-}d\_1* with diphenylacetylene.<sup>27</sup>

In 1981, Tebbe reported the crystal structure of **5b** (Figure 1-6).<sup>28</sup> This bis-trimethylsilyl substituted titanacyclobutene had several notable differences as compared to its diphenyl congener.<sup>25a</sup> While both structures contain bond lengths consistent with a metallacyclobutene formulation, **5b** has a much longer C(2)-C(3) bond, as well as slightly shorter C(1)-C(2) and Ti-C(3) bonds (though not statistically significant; i.e.,  $\geq 3\sigma$ ), as shown in Table 1-1.

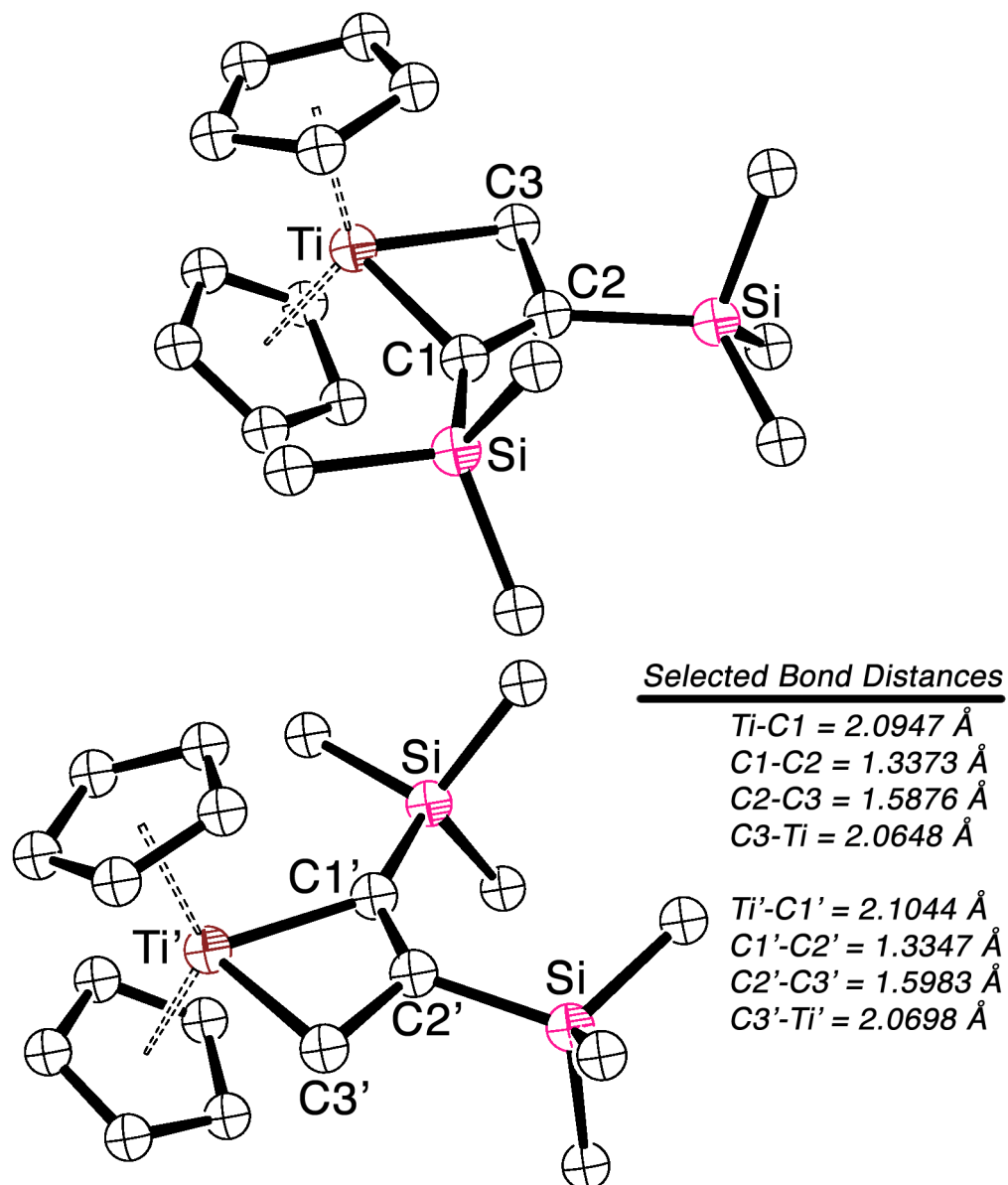


**Figure 1-6.** Ball-and-Stick representation of titanacyclobutene **5b**. Hydrogen atom coordinates not included in crystallographic information file. CCDC Number 1106414; refcode BATMUE. R = 4.4%, Space Group  $P2_1/c$ .<sup>28</sup>

These structural differences suggested a substantial contribution from a metallacyclobutene valence isomer, i.e., an acetylene adduct of a titanium-methylene species. Recall that the di(trimethylsilyl)-substituted titanacyclobutene **5b** featured a labile bis(trimethylsilyl)acetylene unit that could be substituted by

diphenylacetylene, 2-methylpropene, and the chloroaluminum reagent **3**, while the diphenyl-substituted titanacyclobutene **5a** was only found to be reactive with water, and inert to the former substrates. Structurally, **5b** appears to feature a partial fragmentation of the metallacyclobutene ring with incipient formation of new titanium-methylene and titanium-acetylene bonds, thus, the difference in reactivity might be ascribed to that which might occur between a metallacyclobutene, and a metal species at the alkyne-carbene intersection – an important and recurring motif in metallacyclobutene chemistry.<sup>29-37,39,45,47</sup>

In an effort to elaborate the electronic differences between structures **5a** and **5b**, molecular orbital calculations were performed on a model titanacyclobutene structure ( $\eta^5\text{-C}_5\text{H}_5$ )<sub>2</sub>Ti( $\kappa^2\text{-CH=CHCH}_2$ ) (**5c**), which was found to contain bond lengths most similar to the bis(trimethylsilyl) titanacyclobutene **5b** (Table 1-1).

**Table 1-1.** Structural Parameters for Complexes **5a-5d**.

A-B	<b>5a</b>	<b>5b<sup>a</sup></b>	<b>5c</b>	<b>5d</b>
Bond Length [Å]				
Ti-C(1)	2.104(4)	2.099(3)	2.11	2.050(4)
Ti-C(2)	2.533(5)	2.355(3)	2.38	2.348(4)
Ti-C(3)	2.122(5)	2.064(4)		2.083(5)
C(1)-C(2)	1.344(6)	1.335(5)		1.340(5)
C(2)-C(3)	1.537(6)	1.598(5)	1.65	1.556(5)

(a) ave. of two independent data; esd shown is higher of two calc. values.

Additionally, a Walsh diagram was constructed by translating from left to right along the axis of the acetylene unit, which showed that complexes **5b** and

**5c** were shifted toward the carbene-acetylene description and that **5a** was closer to an idealized metallacyclobutene structure. It was also found that the mutually orthogonal phenyl substituents at C(1) and C(2) polarized the acetylenic  $\pi$  system, which had the effect of enhancing overlap between C(2) and C(3) (an effect of the C(1) substituent), as well as increasing the C(1)-Ti overlap and decreasing C(2)-C(3) repulsions (an effect of the C(2) substituent). An asymmetric alkyne, phenyl(trimethylsilyl)acetylene, was used with **3** to prepare the titanacyclobutene  $(\eta^5\text{-C}_5\text{H}_5)_2\text{Ti}(\kappa^2\text{-C(Ph)=C(TMS)CH}_2)$  (**5d**). This titanacyclobutene was isolated as a single regioisomer, with the phenyl group positioned at C(1) and the trimethylsilyl group at C(2) (Figure 1-7). This titanacycle was found to be structurally intermediate between **5a** and **5b** in most respects, albeit with a shorter Ti-C(1) bond. The phenyl substituent was found to be oriented perpendicular to the metallacyclobutene plane, as in **5a** (83.31°). The orientation of the phenyl group in **5d** was taken to suggest that the substituent effect at C(1) was of more importance to metallacyclobutene stability than that of the substituent at C(2), relative to the alkyne-carbene adduct.



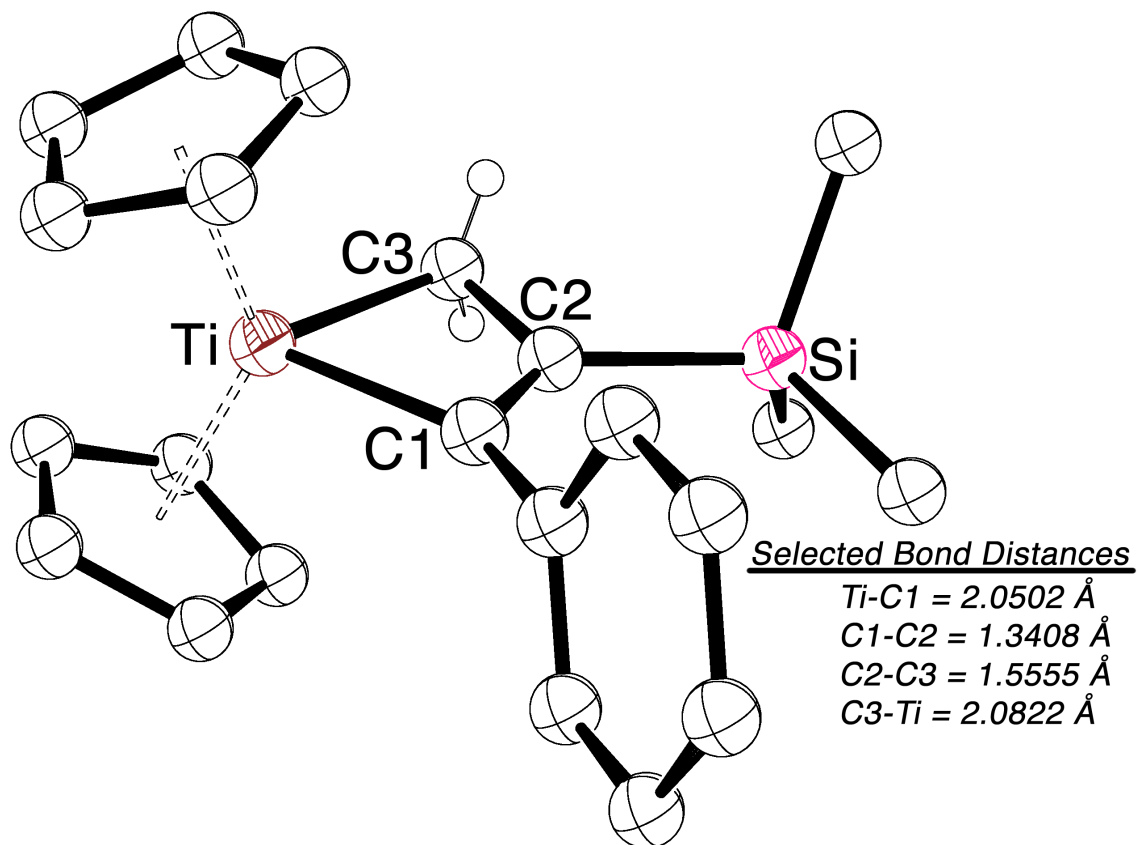
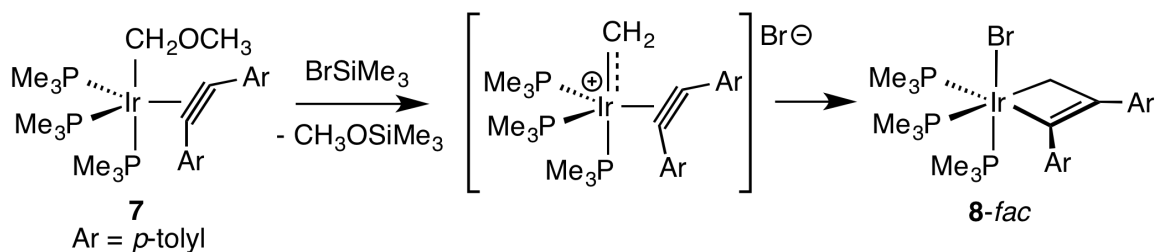


**Figure 1-7.** Ball-and-Stick representation of titanacyclobutene **5d**. CCDC Number 1106415; refcode BATNAL. R = 2.9%, Space Group *Fdd2*.<sup>28</sup>

Interest in the role of carbenes and alkylidenes in the formation of new C-H and C-C bonds led the Thorn group to study electrophilic methylene complexes of iridium, particularly “incipient methylene” species derived from (methoxymethyl)- and (hydroxymethyl)iridium complexes.<sup>38</sup> Thorn reported in 1984 the conversion of a (methoxymethyl)iridium acetylene complex to a new iridacyclobutene complex, as well as a metallacyclobutene isomerization reaction.<sup>39</sup> Preparation of the (methoxymethyl)iridium complex  $(\text{PMe}_3)_4\text{IrCH}_2\text{OCH}_3$  could be accomplished by reaction of  $(\text{PMe}_3)_4\text{IrH}$  with

bromomethyl methyl ether to give the cationic (methylmethoxy)(hydrido)iridium complex, followed by reductive deprotonation with potassium *tert*-butoxide. Treatment of  $(\text{PMe}_3)_4\text{IrCH}_2\text{OCH}_3$  with di-*p*-tolylacetylene gave the (methylmethoxy)iridium acetylene complex  $(\text{PMe}_3)_3\text{Ir}(\text{CH}_2\text{OCH}_3)[(p\text{-C}_6\text{H}_4\text{Me})\text{C}\equiv\text{C}(p\text{-C}_6\text{H}_4\text{Me})]$  (**7**; Scheme 1-5). Crystallographic characterization of this complex was reported, which showed that while the Ir-C bond of the methylmethoxy group was not particularly short (2.136(7) Å), the vicinal C-O bond was especially long (1.449(9) Å), consistent with some contribution from a “carbenoid” resonance structure.<sup>40,38c</sup> This bond proved amenable to cleavage in the presence of electrophilic reagents. Specifically, reaction of **7** with bromotrimethylsilane gave *fac*-( $\text{PMe}_3$ )<sub>3</sub>(Br)Ir( $\kappa^2$ -C(*p*-C<sub>6</sub>H<sub>4</sub>Me)=C(*p*-C<sub>6</sub>H<sub>4</sub>Me)CH<sub>2</sub>) (**8-fac**) as the sole kinetic product through a proposed cationic (di-*p*-tolylacetylene)iridium methylene intermediate (Scheme 1-5). It is also possible that **8-fac** forms through alkyne insertion into the metal-alkyl bond, however, **7** is indefinitely stable in the absence of electrophiles, and reaction through a *tetra*-substituted metal vinyl intermediate should give meridional isomer **8-mer**.



**Scheme 1-5.** Synthesis of **8-fac** from proposed iridium methylene intermediate.<sup>39</sup>

Analysis by X-ray diffraction of single crystals of **8-fac** indicated a planar metallacyclobutene with a maximum deviation from the ring plane of only 0.032 Å (Figure 1-8). Compounds **8-fac** and **5a** show remarkably consistent bond lengths, with only slightly longer M-C bonds in the iridium metallacycle.<sup>25a</sup> The iridacyclobutene also shows a similar conformation in regard to the substituents at C(1) and C(2): the plane of the *p*-tolyl ring at C(1) is tilted toward perpendicular at 74.14° while the ring at C(2) is tilted only 11.42° from the plane of the metallacycle. Both aryl rings of **8-fac** freely rotate in solution, which was unclear from the reported <sup>1</sup>H NMR data for titanacyclobutene **5a**, and unremarked upon by Tebbe. The equatorial PMe<sub>3</sub> ligands have slightly different bond lengths with the PMe<sub>3</sub> trans to the sp<sup>2</sup>-C(1) carbon being 2.339(2) Å versus 2.360(2) Å for the PMe<sub>3</sub> trans to the sp<sup>3</sup>-C(3) carbon, suggesting that the saturated C(3) carbon has a greater trans influence. The axial PMe<sub>3</sub> ligand is much shorter than both at 2.245(2) Å.

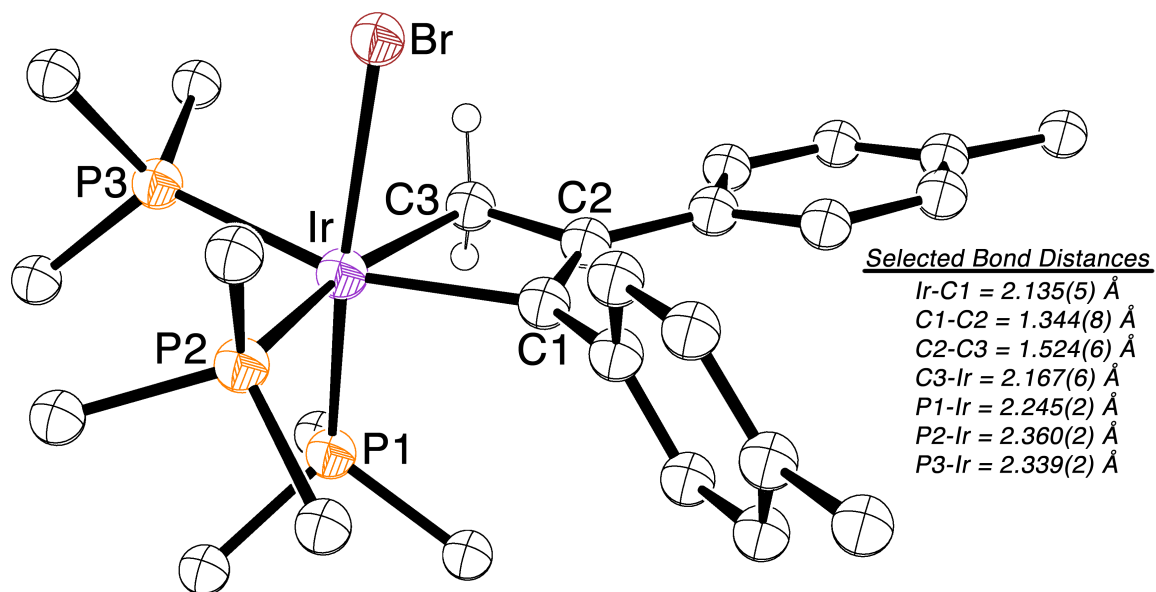
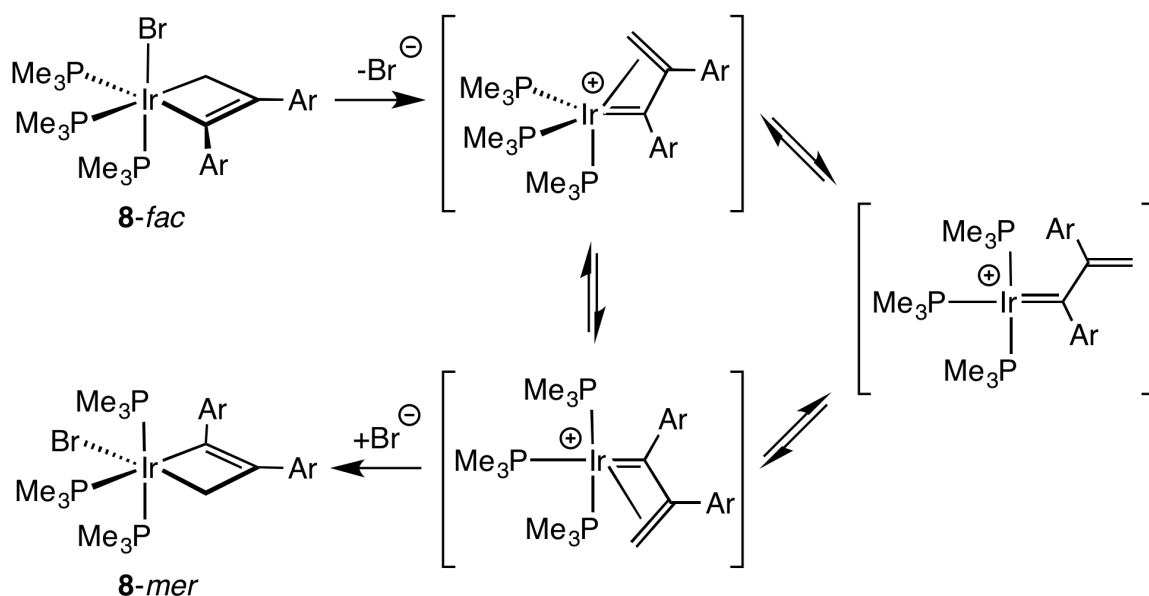


**Figure 1-8.** Ball-and-Stick representation of iridacyclobutene **8-fac**. CCDC Number 1126788; refcode CIYKAW. R = 3.1%, Space Group  $P2_1/n$ .<sup>39</sup>

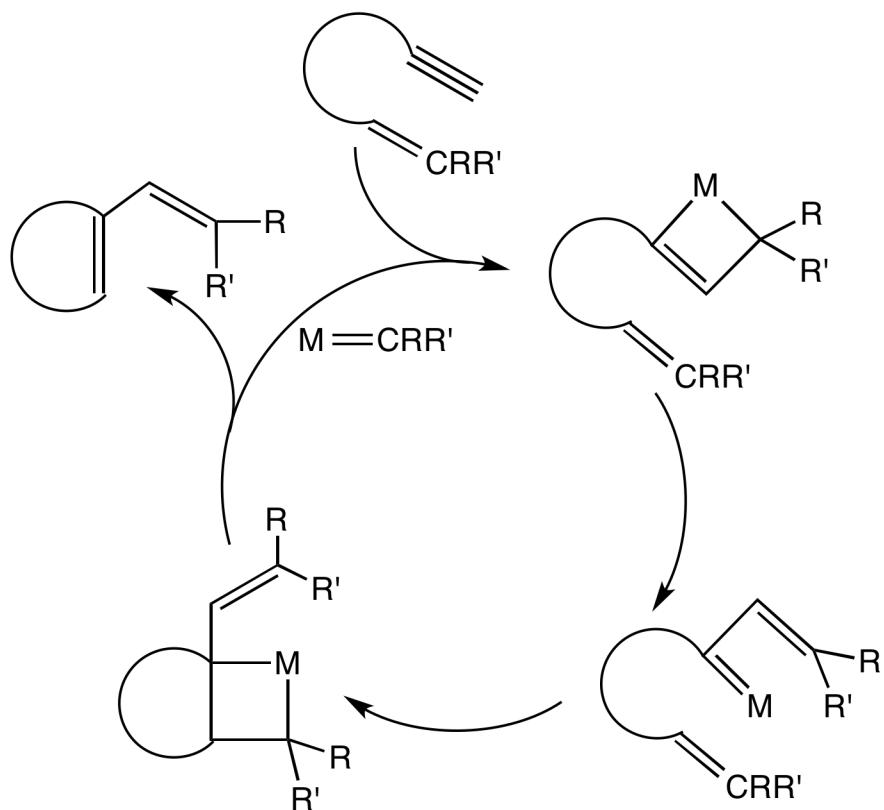
When left in a  $CD_2Cl_2$  solution, **8-fac** slowly rearranged ( $35 \pm 5\%$ ; 4 d at r.t.,  $80 \pm 5\%$ ; 12 h at  $40^\circ C$ ) to give the isomeric species **8-mer**, identified by its  $^1H$  and  $^{13}C$  NMR spectra. The bromide ligand was thought to be relatively labile, as shown by rapid precipitation of AgBr when compound **8-fac** is treated with  $AgPF_6$ . The isomerization likely occurs by loss of bromide to give a coordinatively unsaturated cationic metal species, which rearranges with subsequent re-addition of bromide to form **8-mer**. Since **8-fac** is directly formed from **7**, any rearrangement of ligands to give **8-mer** must occur after the C-C bond-forming step. Assuming that the mechanism for formation of **8-fac** proceeds through a carbene-alkyne intermediate, two possibilities were considered for the bond-forming transition state: a non-planar TS<sup>41</sup> with direct formation of the C-C bond across the orthogonal carbene and alkyne, perhaps involving stabilization by an

$\eta^3$ -vinylcarbene resonance structure, or by a sequential acetylene rotation and bond formation through a planar TS, perhaps accompanied by a pseudorotation<sup>42</sup> at the metal center. A third possibility is that the isomerization occurs after bond formation through equilibrating  $\eta^3$ -vinylcarbene intermediates with possible evolution through an  $\eta^1$ -vinylcarbene transition state, thus initially forming **8-fac** as the product of kinetic addition, and ultimately forming **8-mer** as the thermodynamic product (Scheme 1-6).



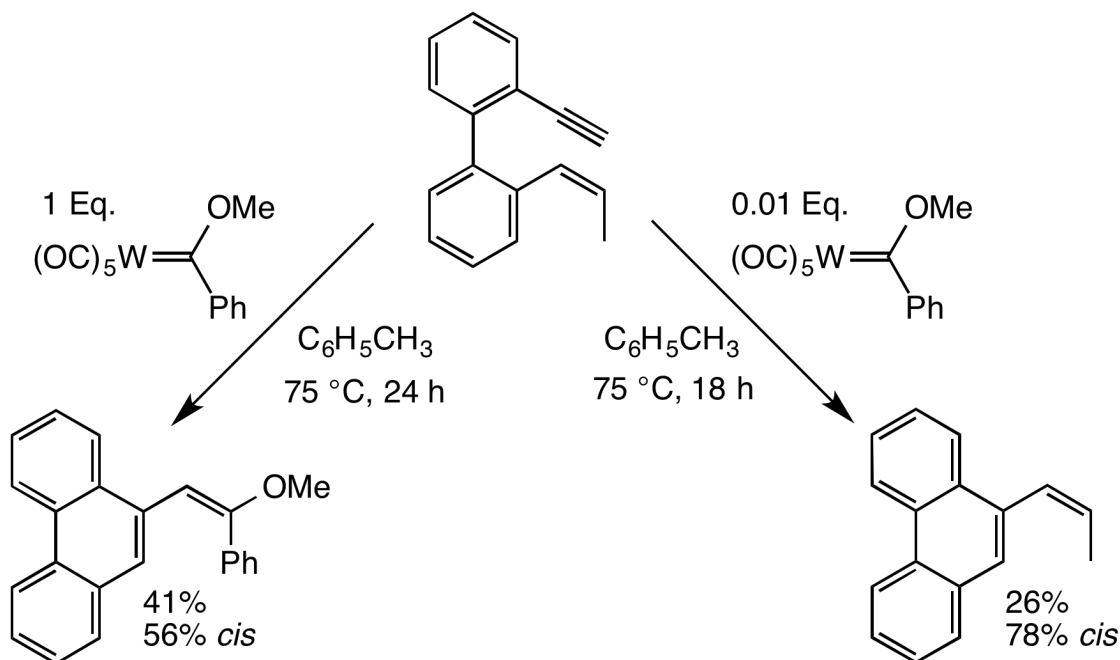
**Scheme 1-6.** Formation of **8-mer** from **8-fac** through  $\eta^3$ -vinylcarbene intermediates, possibly through an  $\eta^1$ -vinylcarbene transition state.

In 1985, Katz and Sivavec reported a new and important variation of the metathesis reaction that also may involve a metallacyclobutene intermediate – the “enyne metathesis” reaction (Scheme 1-7).<sup>43</sup>



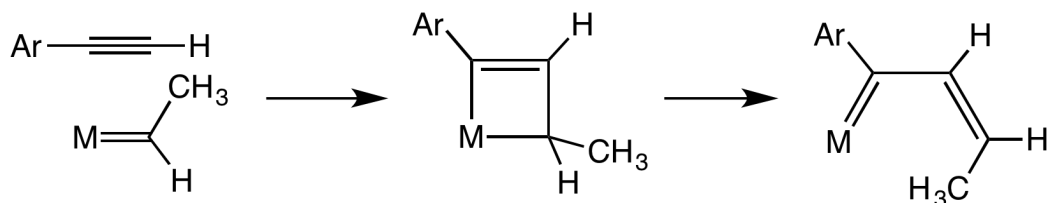
**Scheme 1-7.** Proposed mechanism of the ring-closing enyne metathesis reaction.<sup>43</sup>

Although Katz and coworkers had previously investigated the metathesis reactions of alkenes and alkynes, their work focused mostly on the initiation of carbene catalysts with acetylenes to affect the subsequent polymerization of cyclic olefins.<sup>24</sup> In their 1985 communication, they reported the use of a metal carbene to catalyze the ring-closing metathesis of an enyne (Scheme 1-8).



**Scheme 1-8.** Reported examples of the enyne metathesis reaction.<sup>43</sup>

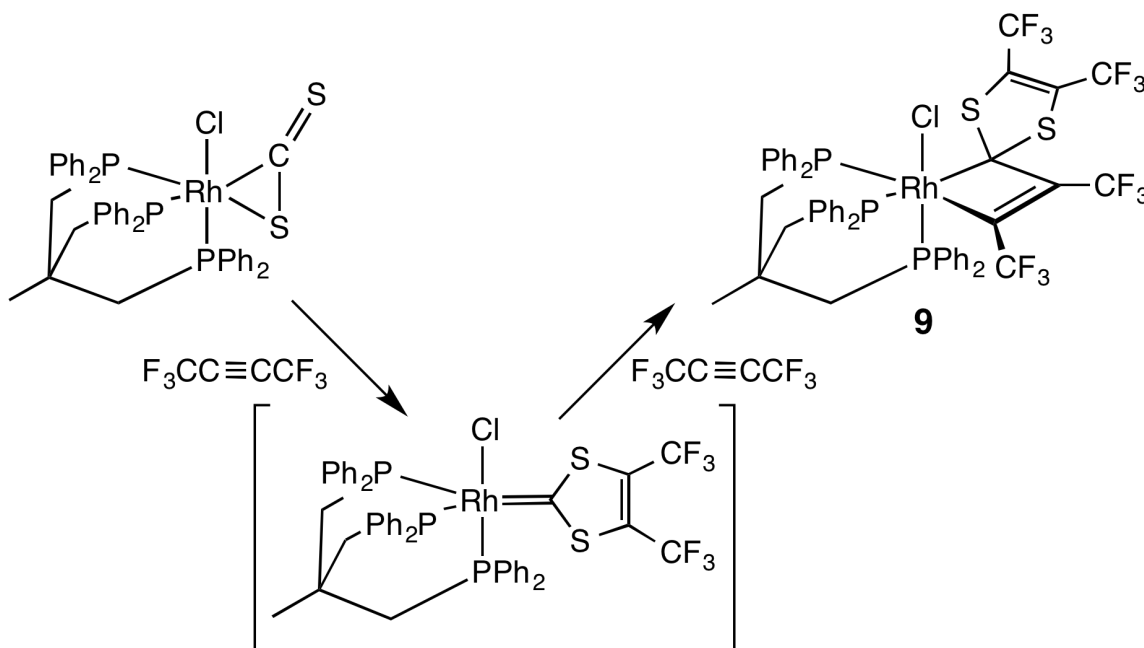
They also reported on the stereoselectivity of metallacyclobutene ring-opening to give acyclic metallabutadienes, finding it to be highly selective towards the *cis* stereoisomer, at least in the case of a methyl substituent (Scheme 1-9). This was rationalized on the basis of a possible intramolecular agostic interaction.<sup>44</sup>



**Scheme 1-9.** Stereochemistry of metallacyclobutene ring-opening.<sup>43</sup>

That same year, researchers at the Institute for the Study of Stereochemistry and Energy of Coordination Compounds in Firenze, Italy reported the synthesis of a rhodacyclobutene (**9**) from the reaction of an  $\eta^2-CS_2$

rhodium(triphos) complex and two equivalents of hexafluoro-2-butyne (Scheme 1-10).<sup>45</sup> The reaction was thought to proceed through a 1,3-dithiol-2-ylidene intermediate, for which there were two reported nickel dithiocarbene precedents.<sup>46</sup> Attempts to isolate such a dithiocarbene intermediate in the present case were unsuccessful.



**Scheme 1-10.** Formation of rhodacyclobutene **9** from a 1,3-dithiol-2-ylidene intermediate.<sup>45</sup>

The rhodacyclobutene **9** adopts a formal 5,8-dithia-1-rhodaspiro[3.4]octa-2,6-diene structure, with the C(3) carbon bridging a four- and five-membered ring. The crystal structure of **9** showed a *pseudo*-octahedral coordination environment about rhodium, with two phosphine donors and the metallacyclobutene moiety in the equatorial plane, while the chloride ligand and one of the three phosphines of the triphos ligand were in axial positions (Figure 1-9). Notably, the phosphorus



atoms trans to the  $sp^2$  and  $sp^3$  carbons of the metallacyclobutene ring were of the same length, suggesting a lack of appreciable trans influence in the present case – likely as a result of the tridentate triphos ligand.

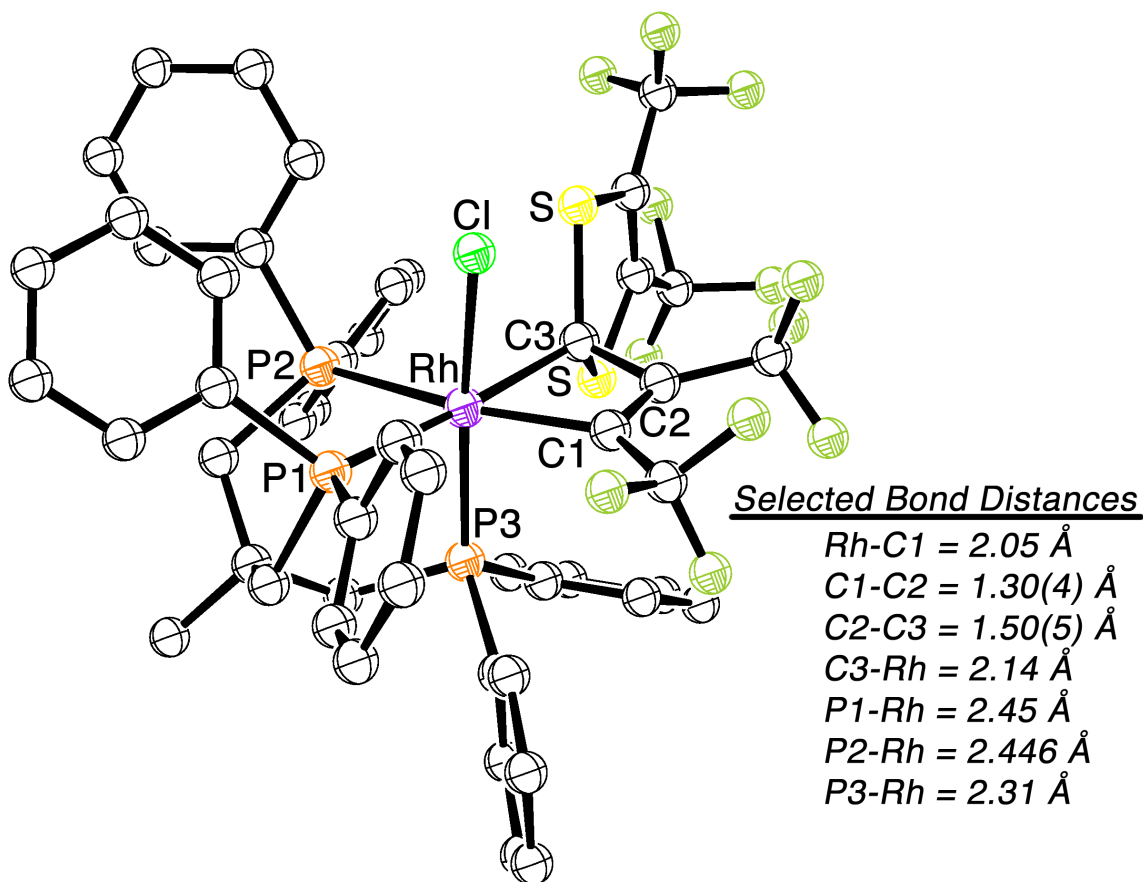


**Figure 1-9.** Ball-and-Stick representation of rhodacyclobutene **9**. CCDC Number 1132547; refcode CUFTIG10. R = 6.0%, Space Group  $P6_1$ .<sup>45,47</sup>

Bianchini, Hoffmann, and coworkers reported further details the following year regarding this metallacyclobutene and its formation, as well as the heavier chalcogenide rhodacyclobutene congener formed from  $CSe_2$ .<sup>47</sup> Formation of **9** as well as its diselenide congener **10** were accomplished in ~ 90% yield from the  $\eta^2$ - $CS_2$  and  $\eta^2$ - $CSe_2$  rhodium(triphos) complexes when treated at room temperature

with a two-fold excess of hexafluoro-2-butyne in  $\text{CH}_2\text{Cl}_2$  solution. Reaction of the  $\eta^2$ -heteroallene  $\text{CS}_2$  and  $\text{CSe}_2$  complexes with one equivalent of the alkyne yielded compounds **9** and **10** in  $\sim 40\%$  yield, with equal amounts of the starting  $\eta^2$ -heteroallene complex. Formation of the proposed intermediate in this reaction was not observed.

A second crystal structure of **9** was reported, with improved data which allowed for a better structural refinement as compared to that previously communicated.<sup>45</sup> The phosphine donors of triphos trans to the  $\text{sp}^3$ -C(3) and  $\text{sp}^2$ -C(1) carbons were nearly identical at 2.446 and 2.45 Å, respectively, while the axial phosphine was much shorter at 2.31 Å. The metallacyclobutene unit had bond lengths: Rh-C(1) 2.05 Å, C(1)-C(2) 1.30(4) Å, C(2)-C(3) 1.50(5) Å, and C(3)-Rh 2.14 Å.

Attempts to substitute the chloride ligand in **9** and **10** with other anions such as  $\text{BPh}_4^-$ ,  $\text{PF}_6^-$ ,  $\text{BF}_4^-$ ,  $\text{Br}^-$ , and  $\text{I}^-$  did not lead to replacement. However, treatment with  $\text{Ag}^+$  or  $\text{Tl}^+$  allowed for chloride abstraction and isolation as the red crystalline  $\text{BPh}_4$  salts **11** and **12**, respectively. It was also shown that addition of a chloride anion in the form of bis(triphenylphosphine)iminium chloride allows for the regeneration of compounds **9** and **10** from their cationic precursors.

Single-crystal X-ray diffraction analysis of **11** showed that chloride abstraction did not rupture the metallacyclobutene ring; rather, the chloride ligand is replaced by coordination of a sulfur atom (Figure 1-10). Compound **11** is also spirocyclic with three-, four-, and five-membered rings forming across the

spiro[2.3.4] sp<sup>3</sup>-C(3) carbon. The geometric distortion necessary for thioether coordination renders the metallacyclobutene fragment slightly non-planar (deviations as large as 0.10(7) Å), as compared to the essentially planar **9** (largest deviations < 0.01 Å).

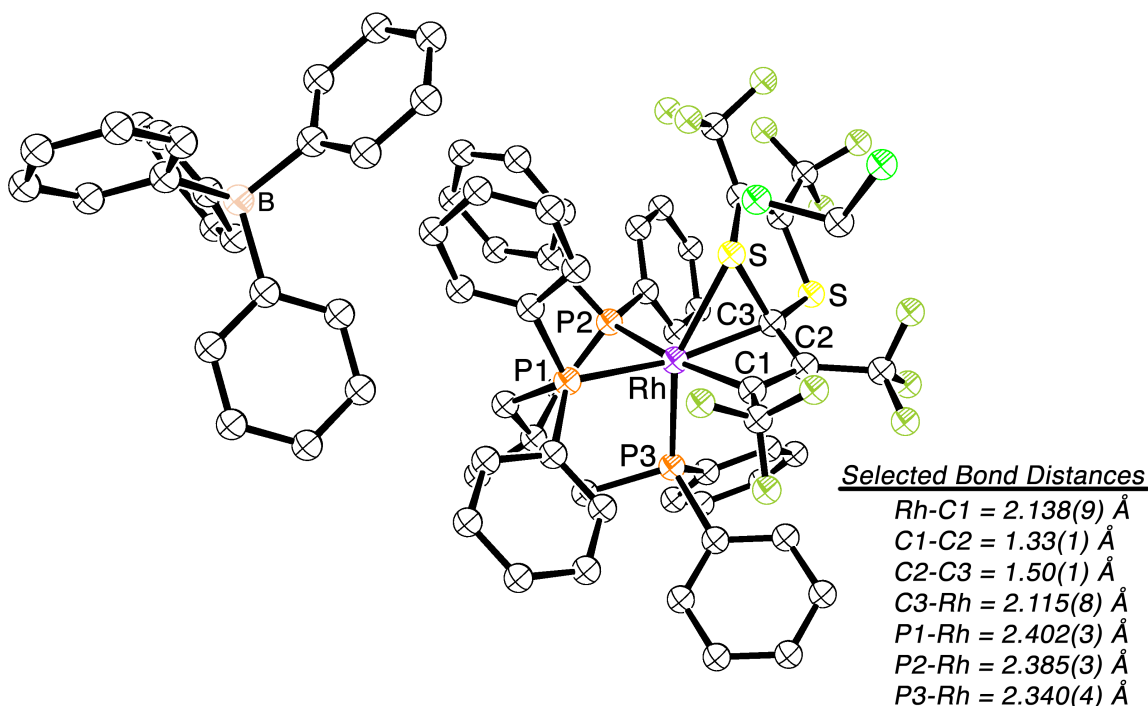
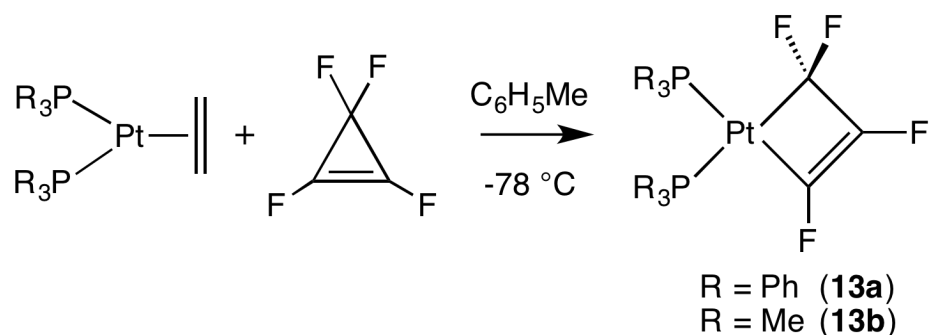


**Figure 1-10.** Ball-and-Stick representation of rhodacyclobutene **11**. CCDC Number 1151053; refcode FABJUN. R = 6.1%, Space Group  $P2_1/a$ .<sup>47</sup>

The key step in the formation of metallacyclobutenes **9** and **10** is thought to be the addition of an alkyne across a Rh-carbene intermediate. The (triphos)Rh(Cl) fragment could be considered as a d<sup>8</sup>-ML<sub>4</sub> species with C<sub>2v</sub> symmetry, hence isolobal with a methylene fragment.<sup>48</sup> The addition of an alkyne across a Rh=C double bond to give a metallacyclobutene could thus be considered as analogous to the symmetry-forbidden [2 + 2] cycloaddition of an alkene and an alkyne to give a cyclobutene.<sup>49</sup>

Russell Hughes and colleagues at Dartmouth reported in 1988 the formation of platinacyclobutenes from the reaction of  $\text{Pt}(\text{C}_2\text{H}_4)(\text{PR}_3)_2$  ( $\text{R} = \text{Ph}, \text{Me}$ ) with tetrafluorocyclopropene.<sup>50</sup> The perfluoro-cyclopropene was prepared by an ultrasonically-assisted vicinal dechlorination<sup>51</sup> of 1,2-dichloro-1,2,3,3-tetrafluorocyclopropane with Zn dust in a modification of the literature method.<sup>52</sup> Reaction of a dilute toluene solution of the cyclopropene with the platinum ethylene complexes at  $-78\text{ }^\circ\text{C}$  gave the platinacyclobutenes  $(\text{PR}_3)_2\text{Pt}(\kappa^2\text{-CF}=\text{CFCF}_2)$  (**13**) smoothly (Scheme 1-11). The trimethylphosphine-substituted platinacyclobutene complex **13b** could also be synthesized by treatment of **13a** with an excess of  $\text{PMe}_3$ . Observation of the formation of platinacycles **13** by  $^{19}\text{F}$  spectroscopy at  $-78\text{ }^\circ\text{C}$  showed formation of the metallacycle with concomitant depletion of the cyclopropene without formation of any observable intermediate. Single crystals of **13a** were subjected to an X-ray diffraction study by the Rheingold lab at Delaware, which confirmed the platinacyclobutene structure (Figure 1-11).



**Scheme 1-11.** Synthesis of platinacyclobutenes **13** from  $(\text{PR}_3)_2\text{Pt}(\eta^2\text{-H}_2\text{C}=\text{CH}_2)$  and tetrafluorocyclopropene.<sup>50</sup>

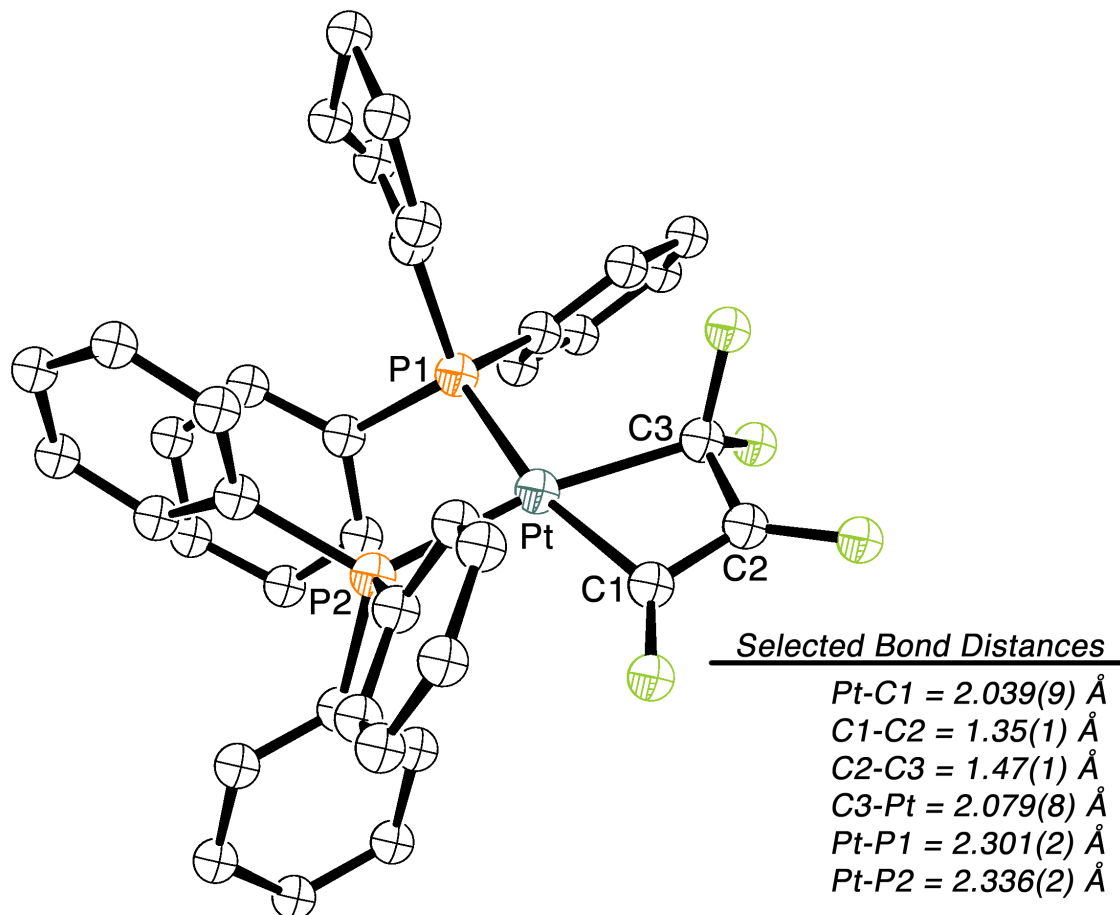


**Figure 1-11.** Ball-and-Stick representation of platinacyclobutene **13a**. CCDC Number 1168435; refcode GIPZIO. R = 3.61%, Space Group  $P2_1/n$ .<sup>50</sup>

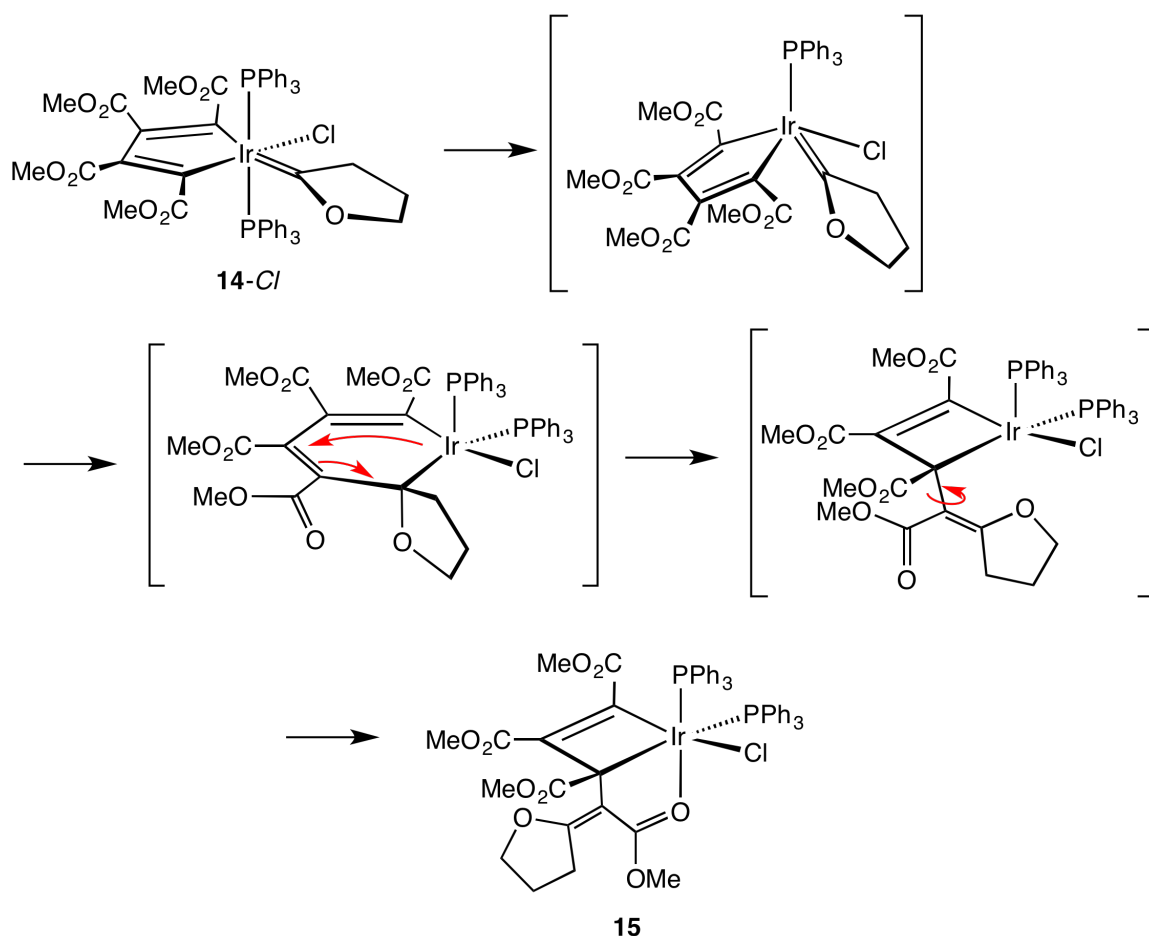
The metallacyclobutene ring in platinacyclobutene **13a** is planar, with no atom deviating more than 0.015 Å. The complex is *pseudo*-square planar, with the plane of the metallacycle canted 7.6° from the plane defined by P-Pt-P, however, <sup>19</sup>F NMR spectroscopy indicated only three fluorine resonances in a 2:1:1 ratio down to -78 °C. The phosphorus atom trans to the sp<sup>3</sup>-C(3) has a longer Pt-P distance (2.336(2) Å) as compared to the phosphorus atom trans to sp<sup>2</sup>-C(1) (2.302(2) Å), thus demonstrating again a larger trans influence for the saturated carbon in the metallacyclobutene. Additionally, the Pt-P coupling

constants in the  $^{31}\text{P}\{^1\text{H}\}$  spectra of complexes **13a** and **13b** are much larger for the phosphines trans to the  $\text{sp}^3$  carbon (**13a**: 2710 vs. 2019 Hz; **13b**: 2504 vs. 1989 Hz), also indicative of a stronger trans influence. The metallacyclobutene ring has distances of Pt-C(1) 2.039(9) Å, C(1)-C(2) 1.351(12) Å, C(2)-C(3) 1.474(12) Å, and C(3)-Pt 2.079(8) Å. Metallacyclobutenes **13** are formally the result of an oxidative addition of a C-C bond in tetrafluorocyclopropene, in contrast to the usual method of coupling a metal carbene across an alkyne.

Thus far, many of the metallacyclobutenes reported were formed from coupling of a metal carbene to an alkyne. In regard to the Dewar-Chatt-Duncanson model explaining the bonding in metal-alkene and metal-alkyne species,<sup>53</sup> such reactivity could be considered as the formal coupling of a carbene moiety to the vinylic carbon of a resonance metallacyclopropene. O'Connor *et alia* reported in 1990 the coupling of an iridium carbene species to a metallacyclopentadiene,<sup>54</sup> which forms an iridium metallacyclobutene upon rearrangement from the intermediate metallacyclohexene.<sup>55</sup>

When a solution of the mononuclear metallacycle-carbene complex **14-CI** was heated at 72 °C in chloroform- $d_1$ , the proton resonances of **14-CI** were gradually and quantitatively replaced by new resonances corresponding to iridacyclobutene **15** (Scheme 1-12). The formation of **15** was proposed to occur by loss of phosphine ligand from **14-CI** to generate a coordinatively unsaturated metal complex, which could rearrange to affect a carbene-vinyl coupling. A subsequent 1,3-shift of iridium forms the metallacyclobutene ring, and

coordination of the ester carbonyl generates the octahedral iridacyclobutene complex **15**. Interestingly, similar complexes **14-F**, and cationic **14-CO** and **14-H<sub>2</sub>O** – in which the chloride ligand was substituted – did not undergo clean reactions to give metallacyclobutene compounds, and instead decomposed under similar conditions (for the fluoride and aqua complexes), while proving to be thermally stable for the carbonyl complex.



**Scheme 1-12.** Formation of iridacyclobutene **15** from metallacyclopentadiene **14-Cl**.<sup>55</sup>

Crystallographic characterization confirmed the structural assignment of iridacyclobutene **15** (Figure 1-12), which shows a similarity to previous characterized

metallacyclobutene complexes with regard to having a longer metal-carbon bond to the  $sp^3$  carbon (2.187(11) Å) vs. the  $sp^2$  carbon (2.045(16) Å). The metallacyclobutene ring is nearly planar, with the largest deviation being 0.0231 Å at C(2). A chloride ligand is trans to the  $sp^2$  carbon with a bond length of 2.451(4) Å, while a phosphine ligand occupies the fourth equatorial site opposite the  $sp^3$  carbon with an iridium-phosphorus bond distance of 2.410(3) Å, in contrast to the much shorter phosphorus-metal distance of the axial triphenylphosphine ligand (2.289(4) Å). The carbon-carbon bond lengths of the metallacyclobutene ring are 1.326(17) Å for the double bond, and 1.536(21) Å for the single bond. The carbonyl oxygen of the coordinating methyl ester features a bond length of 2.162(9) Å.



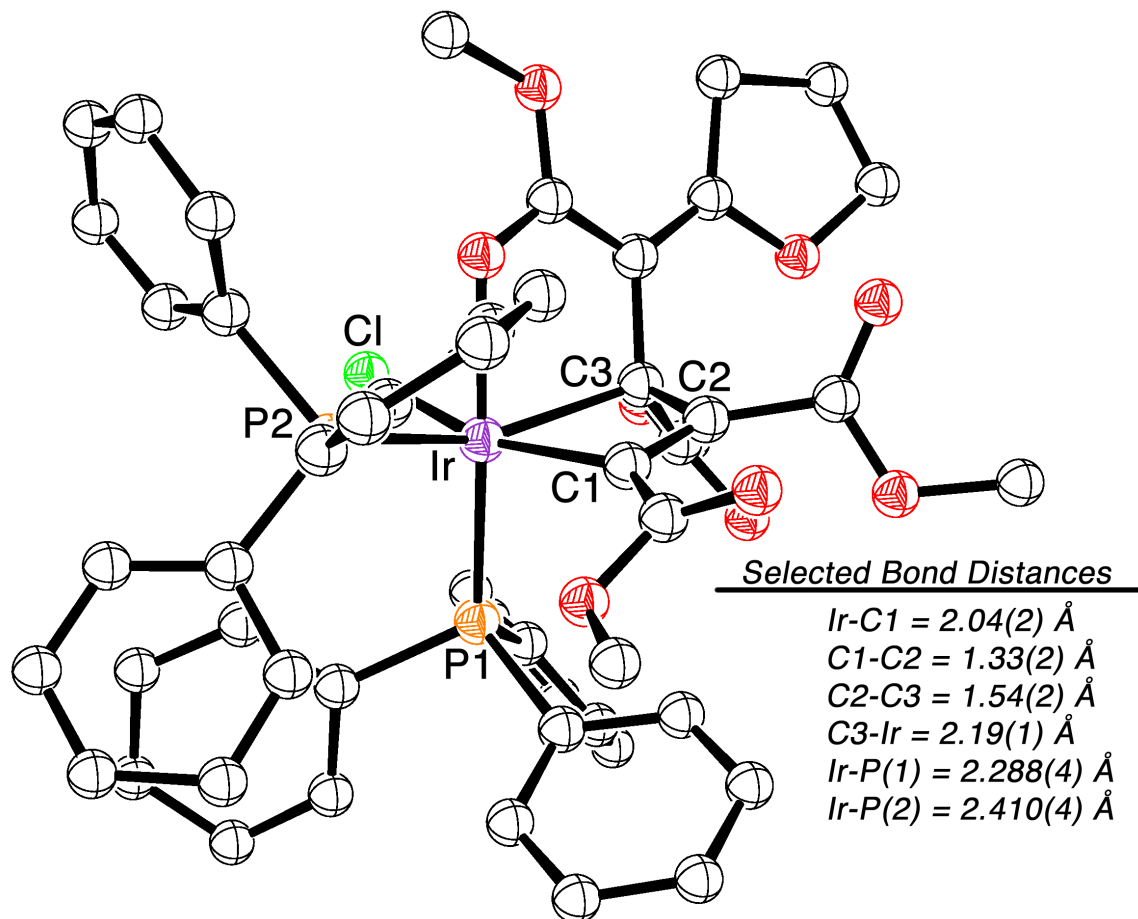
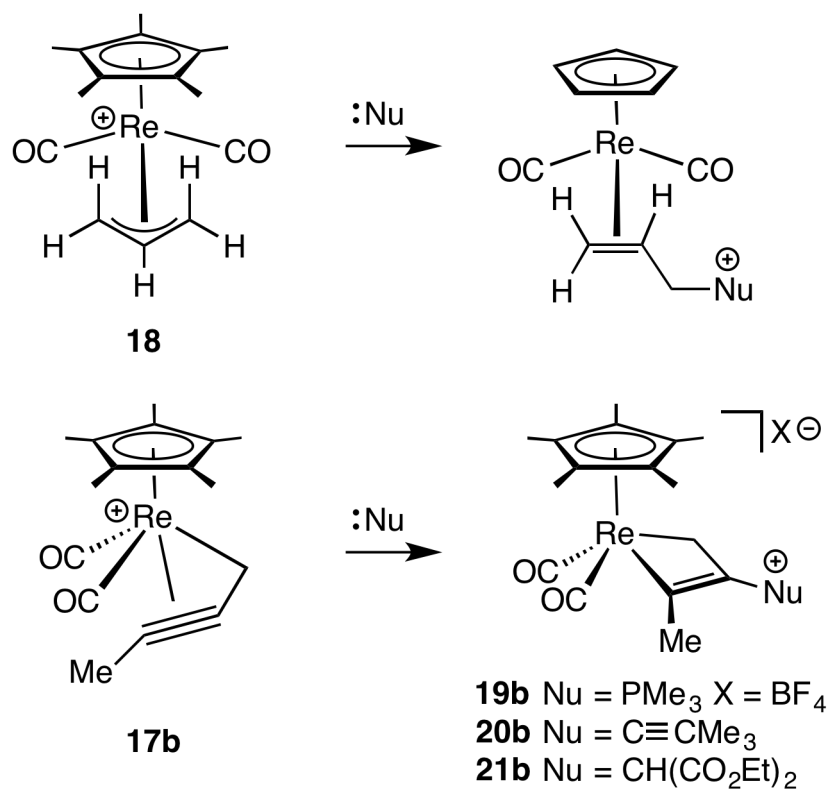


**Figure 1-12.** Ball-and-Stick representation of iridacyclobutene **15**. CCDC Number 1258895; refcode SIGKEY. R = 5.88%, Space Group *P*-1.<sup>55</sup>

In 1992, Casey and Yi reported a novel method of metallacyclobutene formation from nucleophilic addition to the central carbon of an  $\eta^3$ -propargyl complex.<sup>56</sup> Previous work in the Casey lab had demonstrated efficient synthesis of an  $\eta^3$ -allyl complex from the hydride-abstraction of a rhenium-propene complex; extension of this same methodology to a rhenium-alkyne complex **16b** formed from  $(\eta^5\text{-C}_5\text{Me}_5)(\text{CO})_2\text{Re}(\text{THF})$  and 2-butyne gave access to the cationic propargyl complex  $[(\eta^5\text{-C}_5\text{Me}_5)(\text{CO})_2\text{Re}(\eta^3\text{-H}_2\text{CC}=\text{CCH}_3)][\text{PF}_6]$  (**17b**) from reaction with triphenylmethyl hexafluorophosphate (Scheme 1-13).<sup>57</sup>





**Scheme 1-14.** Nucleophilic addition to  $\eta^3$ -allyl and  $\eta^3$ -propargyl complexes.<sup>57</sup>

Treatment of propargyl complex **17b** with trimethylphosphine gave the cationic metallacyclobutene complex  $[(\eta^5\text{-C}_5\text{Me}_5)(\text{CO})_2\text{Re}(\kappa^2\text{-C}(\text{CH}_3)=\text{C}(\text{PMe}_3)\text{CH}_2)]\text{[PF}_6\text{]}$  (**19b**) in 72% yield. Correspondingly, treatment of **17b** with the lithium salt of *tert*-butyl acetylide or the sodium salt of diethyl malonate gave the neutral metallacyclobutene complexes  $(\eta^5\text{-C}_5\text{Me}_5)(\text{CO})_2\text{Re}(\kappa^2\text{-C}(\text{CH}_3)=\text{C}(\text{C}\equiv\text{C}(\text{CH}_3)_3)\text{CH}_2)$  (**20b**) and  $(\eta^5\text{-C}_5\text{Me}_5)(\text{CO})_2\text{Re}(\kappa^2\text{-C}(\text{CH}_3)=\text{C}(\text{CH}(\text{CO}_2\text{Et})_2)\text{CH}_2)$  (**21b**) in 47% and 55% yield, respectively.

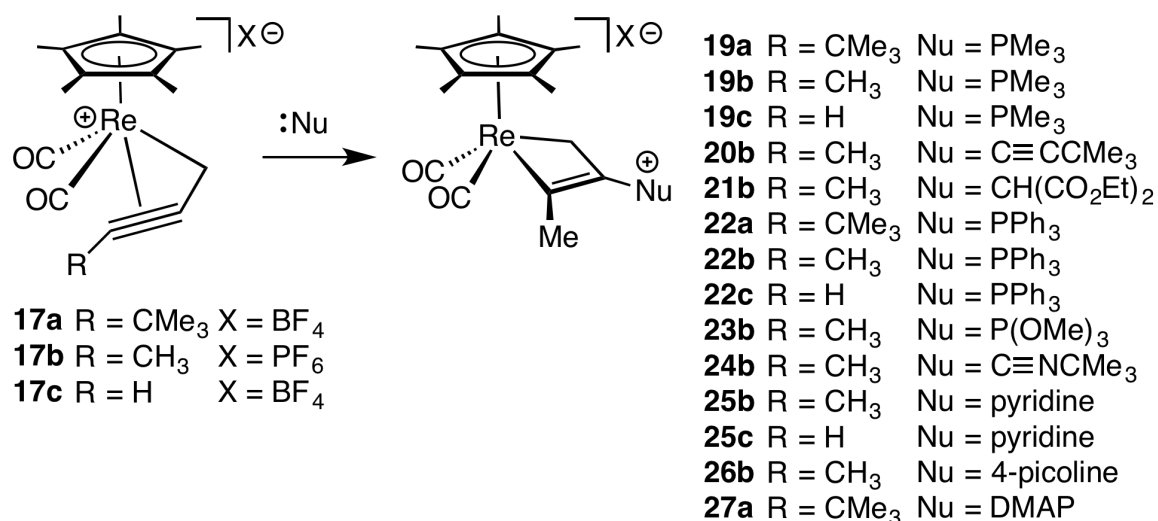
The structures of the rhenacyclobutene complexes **19b**, **20b**, and **21b** were established spectroscopically, on the basis of an upfield chemical shift of the proton and carbon resonances at the  $\text{sp}^3\text{-C}(3)$  carbon, in similar fashion to

that observed by Thorn and co-workers for **8-mer**.<sup>39</sup> In particular, **8-mer** gave resonances at  $\delta$  1.16 in the  $^1\text{H}$  spectrum and  $\delta$  -18.0 in the  $^{13}\text{C}$  spectrum, while complex **19b** gave similar shift values of  $\delta$  0.3 and  $\delta$  1.45 in the  $^1\text{H}$  NMR spectrum for the inequivalent hydrogens at C(3), as well a peak at  $\delta$  -31.7 in the  $^{13}\text{C}$  NMR spectrum. Coupling patterns helped establish the spectral assignments unambiguously, including a geminal coupling of 11.5 Hz between the two inequivalent protons at C(3), as well as a  $^5J_{\text{HH}}$  coupling of 2.3 Hz from the same C(3) hydrogens to the methyl group at the  $\text{sp}^2$ -C(1) carbon. A triplet splitting in the proton-coupled  $^{13}\text{C}$  NMR spectrum gave definitive assignment to the C(3) carbon in the carbon spectrum.

Following the initial communication reporting formation of rhenacyclobutenes from  $\eta^3$ -propargyl complexes,<sup>56</sup> Casey *et alia* further elaborated on the scope and regiochemistry of this reactivity in a detailed 1998 article.<sup>58</sup> A small family of  $\eta^3$ -propargyl complexes were synthesized from the previously reported hydride abstraction of  $\eta^2$ -alkyne complexes,<sup>56,59</sup> as well as from the protonation of  $\eta^2$ -propargyl complexes.<sup>59</sup> The reactivity of these  $\eta^3$ -propargyl complexes with carbon, nitrogen, and phosphorus-based nucleophiles was explored in depth.

The reactions of  $\eta^3$ -propargyl complexes **17** with phosphine nucleophiles gave exclusively addition to the central carbon of the propargyl moiety to form C(2)-phosphine substituted metallacyclobutenes **19a-c** and **22a-c** in good yield

(Scheme 1-15). Additionally, reaction of trimethylphosphite with **17b** also gave the corresponding metallacyclobutene **23b** in 55% yield.



**Scheme 1-15.** Reactions of  $\eta^3$ -propargyl complexes **17** to give metallacyclobutenes **19-27**.

Previously reported rhenacyclobutene complex **19b** was characterized crystallographically (Figure 1-13). The crystal structure of **19b** shows two metallacyclobutene complexes in the asymmetric unit, with substantial differences in bond length and angles for each. Close inspection of the crystal structure shows that these differences in bond length and angles are a result of irregular thermal ellipsoids at both rhenium and the C(2) carbon in the second metallacyclobutene molecule, though the overall quality of the structure is high (R-Factor = 3.16%) and no anomalies are present in the first metallacyclobutene molecule. The non-deviant rhenacyclobutene moiety in the crystal structure of **19b** shows bond metrics that are consistent with other metallacyclobutenes (*vide*

*supra*), whereas the carbon-carbon bond lengths for the second molecule are intermediate between those typically seen.

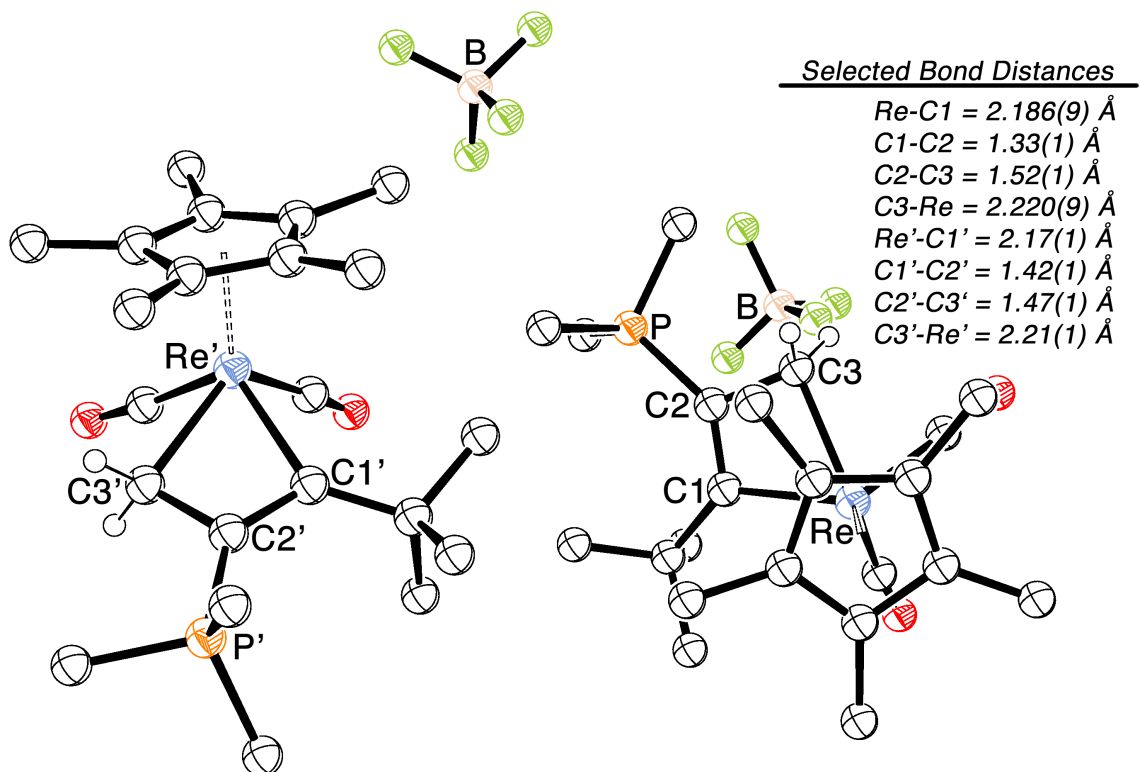


**Figure 1-13.** Ball-and-Stick representation of rhenacyclobutene **19b**. CCDC Number 1219626; refcode NIDJOZ. R = 3.16%, Space Group *Cc*.<sup>58</sup>

As was previously noted, the methyl-substituted rhenacyclobutene complex **17b** reacted with the carbanions of *tert*-butyl acetylene and diethyl malonate to generate the neutral rhenacyclobutene complexes **20b** and **21b**, respectively. Reaction of **17b** with an excess of *tert*-butyl isocyanide at -78 °C generated a meta-stable rhenacyclobutene **24b** whose proton NMR spectrum at -55 °C was consistent with the diagnostic spectral features for this family of compounds. Allowing a solution of **24b** to warm above 5 °C gave further reaction with isocyanide, leading to an uncharacterized mixture of products, though

complex **24b** could be isolated by evaporation of volatile material under high vacuum at 0 °C. Upon exposure to sodium diethyl malonate or the lithium salt of *tert*-butyl acetylide, the unsubstituted rhenium propargyl complex **17c** decomposed upon warming to give uncharacterized products, whereas the *tert*-butyl substituted rhenium complex **17a** failed to react with either of these two carbanions.

The reactions of rhenium  $\eta^3$ -propargyl complexes **17** with nitrogen-based nucleophiles were, in general, more complicated, and the meta-stable kinetic metallacyclobutene products derived therefrom tended to rearrange upon warming. Addition of pyridine to a -78 °C solution of **17b** followed by warming to -40 °C resulted in the rapid formation of rhenacyclobutene **25b**. When warmed to room temperature, this solution gave kinetic and thermodynamic  $\eta^2$ -allene complexes by migration of pyridine from C(2) to either C(1) or C(3). An NMR experiment was conducted to help determine whether the conversion of **25b** to give allene products proceeded through an intra- or intermolecular mechanism. Thus, excess 4-picoline was added to a solution of **25b** in CD<sub>2</sub>Cl<sub>2</sub> at -78 °C, warmed to -40 °C and inspected by proton NMR spectroscopy. The resonances for **25b** were gone, and spectral features consistent with the formation of a new picoline-substituted rhenacyclobutene **26b** were observed – which suggested a dissociative mechanism for exchange of the two nitrogen-containing rings at the metallacyclobutene stage. Warming of this solution gave a complicated mixture of  $\eta^2$ -allenyl complexes incorporating either pyridine or 4-picoline. A second

experiment in which 4-picoline was added to a solution of the allenyl complexes formed from **25b** was conducted, in which no observable 4-picoline products were formed upon warming – which suggested that the formation of allene complexes from **25b** was intramolecular and irreversible.

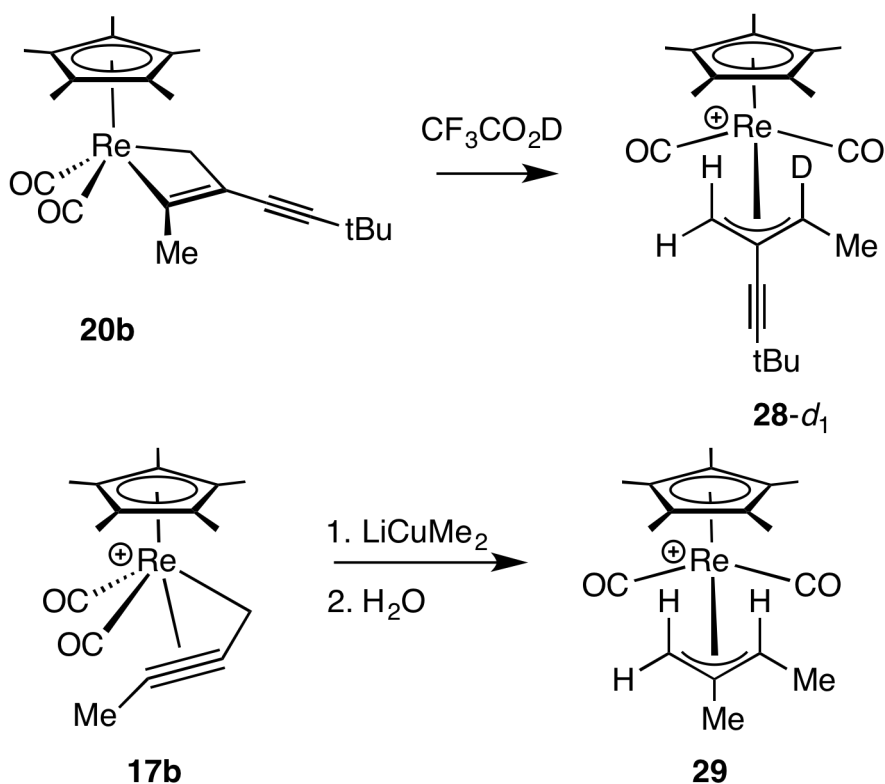
When pyridine was added to a solution of the unsubstituted  $\eta^3$ -propargyl complex **17c** below  $-43\text{ }^\circ\text{C}$ , formation of the rhenacyclobutene complex  $[(\eta^5\text{-C}_5\text{Me}_5)(\text{CO})_2\text{Re}(\kappa^2\text{-CH=C}(\text{NC}_5\text{H}_5)\text{CH}_2)][\text{BF}_4]$  (**25c**) as the sole product occurred, though this complex decomposed above  $-20\text{ }^\circ\text{C}$  to give a mixture of more than ten pentamethylcyclopentadienyl-containing products. Reactions of  $\text{NEt}_3$  with the methyl-substituted propargyl complex **17b** at room temperature gave a single isomer of an  $\eta^2$ -allene complex  $[(\eta^5\text{-C}_5\text{Me}_5)(\text{CO})_2\text{Re}(\eta^2\text{-H}_2\text{C=C=C}(\text{NEt}_3)\text{CH}_3)][\text{PF}_6]$ ; likewise halide attack at **17b** with either  $\text{PPh}_4\text{PBr}$  or  $\text{PPh}_4\text{Cl}$  gave the allene complexes  $[(\eta^5\text{-C}_5\text{Me}_5)(\text{CO})_2\text{Re}(\eta^2\text{-H}_2\text{C=C=C}(\text{Br})\text{CH}_3)][\text{PF}_6]$  and  $[(\eta^5\text{-C}_5\text{Me}_5)(\text{CO})_2\text{Re}(\eta^2\text{-H}_2\text{C=C=C}(\text{Cl})\text{CH}_3)][\text{PF}_6]$  in 60% and 58% yield, respectively.

The *tert*-butyl substituted  $\eta^3$ -propargyl complex **17a** underwent reaction at the central carbon with 4-(dimethylamino) pyridine (DMAP) to give rhenacyclobutene **27a** below  $-38\text{ }^\circ\text{C}$ . When warmed to  $-20\text{ }^\circ\text{C}$ , rhenacyclobutene complex **27a** did not give an allene complex, and instead rearranged to give an  $\eta^2$ -alkyne complex  $[\eta^5\text{-(C}_5\text{Me}_5)(\text{CO})_2\text{Re}(\eta^2\text{-(CH}_3)_3\text{CC}\equiv\text{CCH}_2(\text{DMAP}))][\text{BF}_4]$  from addition to the methylene termini of **17a**. Apparently, attack at the sterically encumbering *tert*-butyl substituted-carbon in **17a** to give an allene complex is



unfavored, and it was suggested that metallacyclobutene **27a** instead dissociated DMAP to reform the propargyl complex **17a**, and then added at the  $\kappa^1$ -CH<sub>2</sub> termini to form the resultant alkyne complex. In similar fashion to that observed for the nitrogen-substituted rhenacyclobutenes, the sterically bulky rhenacyclobutenes **19a** and **22a** – which feature a *tert*-butyl substituent at the C(3) position and phosphine substitution at the C(2) position – also rearranged over 2 days at room temperature in solution to give alkyne complexes in excellent yield.

The rhenacyclobutene complex **20b** formed from the reaction of propargyl complex **17b** and LiC≡CC(CH<sub>3</sub>)<sub>3</sub>, showed thermal instability. This instability was traced in part to side reactions that could occur by protonation with acid. When complex **20b** was isolated and then treated with five equivalents of CF<sub>3</sub>CO<sub>2</sub>H at room temperature an  $\eta^3$ -allyl complex [( $\eta^5$ -C<sub>5</sub>Me<sub>5</sub>)(CO)<sub>2</sub>Re( $\eta^3$ -H<sub>2</sub>CC(C≡CC(CH<sub>3</sub>)<sub>3</sub>)CHCH<sub>3</sub>)[CF<sub>3</sub>CO<sub>2</sub>] (**28**) was immediately observed to form by <sup>1</sup>H and <sup>13</sup>C spectroscopy. The deuterium-labeled isotopologue formed by protonation of **20b** with CF<sub>3</sub>CO<sub>2</sub>D gave deuterium only in the methyl-substituted allylic position of **28-d**<sub>1</sub> (Scheme 1-16). Complex **28** could also be formed in 45% yield by treatment of the propargyl complex **17b** with lithium *tert*-butyl acetylide followed by water and trifluoroacetic acid. A similar  $\eta^3$ -allyl complex [( $\eta^5$ -C<sub>5</sub>Me<sub>5</sub>)(CO)<sub>2</sub>Re( $\eta^3$ -H<sub>2</sub>CC(CH<sub>3</sub>)CHCH<sub>3</sub>)[PF<sub>6</sub>] (**29**) could be formed by addition of the Gilman Reagent LiCu(CH<sub>3</sub>)<sub>2</sub> to **17b** at -78 °C followed by treatment with wet ether – presumably through the formation of an intermediate metallacyclobutene.

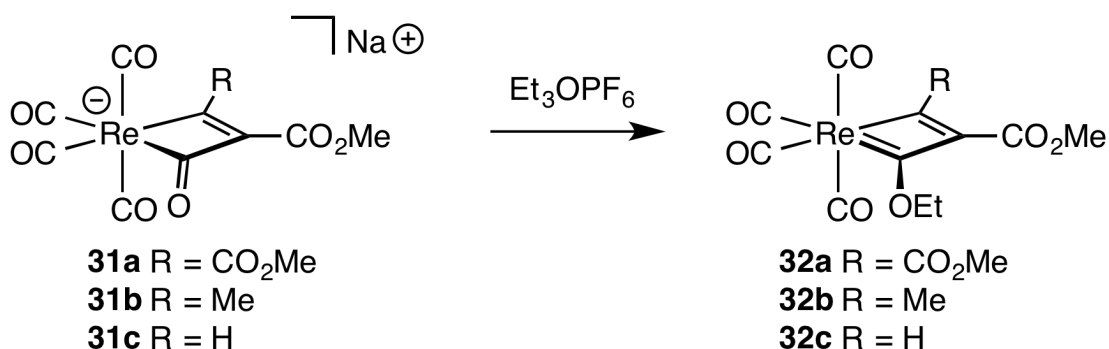


**Scheme 1-16.** Reactivity of rhenacyclobutene complexes with acid.<sup>59</sup>

The reactions of  $\eta^3$ -propargyl complexes with water or alcohols did not form metallacyclobutene complexes, and instead formed  $\eta^3$ -allyl complexes – presumably through an unobserved metallacyclobutene intermediate from addition of the oxygen-based nucleophile to the central carbon of the propargyl species. Thus, addition of water to a solution of propargyl complex **17c** gave the  $\eta^3$ -hydroxyallyl species  $[(\eta^5\text{-C}_5\text{Me}_5)(\text{CO})_2\text{Re}(\eta^3\text{-H}_2\text{CC}(\text{OH})\text{CH}_2)[\text{BF}_4]]$  (**30**) in 35% yield. Monitoring a reaction of **17c** with water in  $\text{CD}_2\text{Cl}_2$  at  $-20^\circ\text{C}$  did not show evidence for an intermediate metallacyclobutene species. The stereochemistry of this addition was probed by monitoring a reaction of **17c** with  $\text{D}_2\text{O}$  in  $\text{CD}_2\text{Cl}_2$ , which showed clean formation of the deuterium-labeled allyl product  $[(\eta^5\text{-$

$C_5Me_5)(CO)_2Re(\eta^3-HDCC(OD)CH_2)[BF_4]$  (**30-d<sub>2</sub>**) in 30% yield. In similar fashion, treatment of **17c** with acid in the presence of methanol gave the  $\eta^3$ -methoxyallyl species  $[(\eta^5-C_5Me_5)(CO)_2Re(\eta^3-H_2CC(OCH_3)CH_2)][BF_4]$  in 73% yield.

Padolik, Gallucci, and Wojcicki reported in 1993 the synthesis of a family of Fischer-type metallacyclobutadiene complexes as well as their reactivity with nucleophiles to give metallacyclobutenes.<sup>60</sup> Sodium pentacarbonylrhenate underwent reaction with both terminal and internal alkynes to give rhenate metallacyclobutenone complexes (**31**), which were alkylated upon exposure to triethyloxonium hexafluorophosphate to give the title metallacyclobutadienes (**32**; Scheme 1-17).



**Scheme 1-17.** Formation of rhenacyclobutadienes **32** from rhenacyclobutenone complexes **31**.<sup>60</sup>

Rhenacyclobutadienes **32a-c** represent interesting examples of metal complexes in which resonance forms can be drawn describing two ambifunctional metal vinylcarbene moieties (Figure 1-14). Furthermore, the two possible metal carbenes are quite different in character; the carbon stabilized by an oxygen heteroatom might be described as a Fischer-type carbene, whereas

the second possible metal carbene is an example of a metal alkylidene species.<sup>2h,61a</sup> Crystallographic characterization of rhenacyclobutadiene **32b** supports the Fischer vinylcarbene resonance form, with a shorter Re-C bond to the ethoxy-substituted carbon (Re-C 2.13(1) vs. 2.18(1) Å). Additionally, the carbon-oxygen bond displays some double-bond character (1.30(1) Å) as compared to the carbon-oxygen bond of the ethoxy group (1.46(1) Å), thus supporting the Fischer and zwitterionic resonance descriptions of this complex.

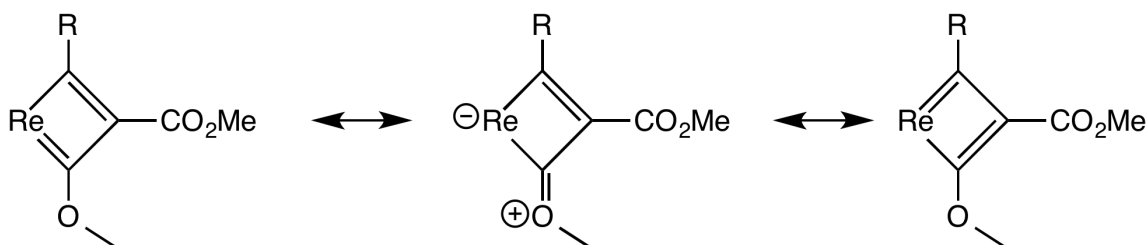
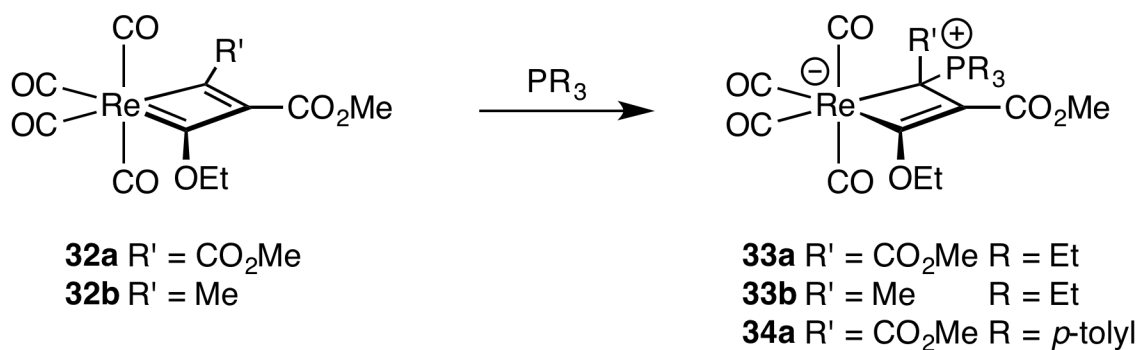


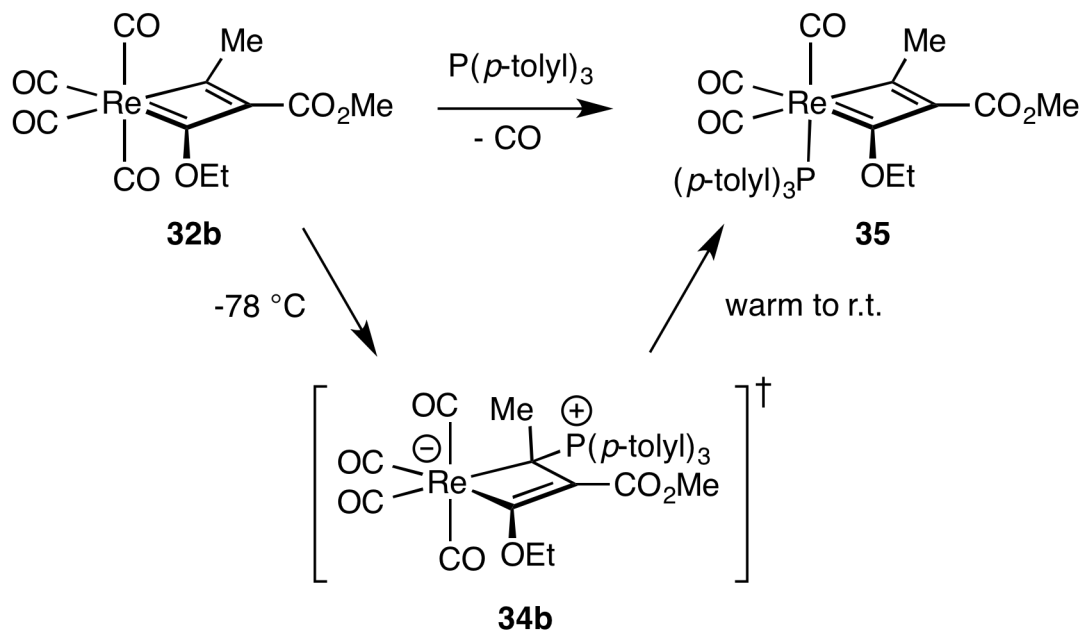
**Figure 1-14.** Resonance contributors of rhenacyclobutadiene complexes **32**.

Fischer carbenes are typically electrophilic, and thus display reactivity toward nucleophiles at the carbon of the metal-carbon double bond.<sup>61b</sup> When rhenacyclobutadienes **32** were treated with a soft nucleophile such as a phosphine however, exclusive addition to the latent metal alkylidene was observed to give rhenacyclobutenes **33** and **34** (Scheme 1-18). When treated with triethylphosphine, complexes **32a** and **32b** gave rhenacyclobutenes **33a** and **33b**, respectively.



**Scheme 1-18.** Reaction of rhenacyclobutadienes **32a-b** with phosphines to generate rhenacyclobutenes **33a-b** and **34a**.<sup>60</sup>

In the case of **32a**, addition of a relatively bulky phosphine such as P(*p*-tolyl)<sub>3</sub> generated rhenacyclobutene **34a**, however, addition of tri(*p*-tolyl)phosphine to rhenacyclobutadiene **32b** produced a new rhenacyclobutadiene **35**, with phosphine coordination to the metal and loss of carbonyl (Scheme 1-19). When a reaction of **32b** with P(*p*-tolyl)<sub>3</sub> was undertaken at -78 °C, and then allowed to warm to room temperature, <sup>31</sup>P NMR spectroscopy initially indicated the formation of two complexes including the rhenacyclobutadiene **35**, and an uncharacterized complex having a similar chemical shift value to characterized rhenacyclobutenes **33** and **34**, thus suggesting the intermediacy of a meta-stable metallacyclobutene compound **34b** in the formation of **35**. Attempts to isolate **34b** were unsuccessful however, as the reaction mixture eventually proceeded to **35** exclusively.



**Scheme 1-19.** Reaction of rhenacyclobutadiene **32b** with tri(*p*-tolyl)phosphine to generate rhenacyclobutadiene **35**, with possible intermediacy of rhenacyclobutene **34b**.<sup>60</sup>

Rhenacyclobutene complex **34a** was characterized in the solid-state by X-ray diffraction analysis, which showed an octahedral coordination environment about rhenium, with two axial carbon monoxide ligands, and two equatorial carbon monoxide ligands in the plane of the four-membered rhenacycle (Figure 1-15). The four-membered metallacycle is puckered, with a fold angle of 6.17° between the planes formed by atoms Re-C(1)-C(2) and Re-C(3)-C(2). The metal-carbon bond to the sp<sup>3</sup>-hybridized carbon is longer than to the sp<sup>2</sup>-hybridized carbon (2.377(6) Å vs. 2.153(9) Å), while the carbonyl ligands trans to the sp<sup>3</sup> and sp<sup>2</sup> carbons measures 1.916(8) Å and 1.95(1) Å, respectively. The C(1)-C(2) bond is 1.35(1) Å, indicative of a carbon-carbon double bond, while the C(2)-C(3) bond length is typical of a carbon-carbon single bond at 1.50(1) Å. Complexes

**33a-b** were identified as rhenacyclobutenes on the basis of a pronounced upfield shift in the  $^{13}\text{C}$  NMR spectra for the C(1) resonances, as previously noted by Thorn<sup>39</sup> and Casey,<sup>56</sup> as well as the similar chemical shift values to the crystallographically-characterized complex **34b** (Table 1-2).

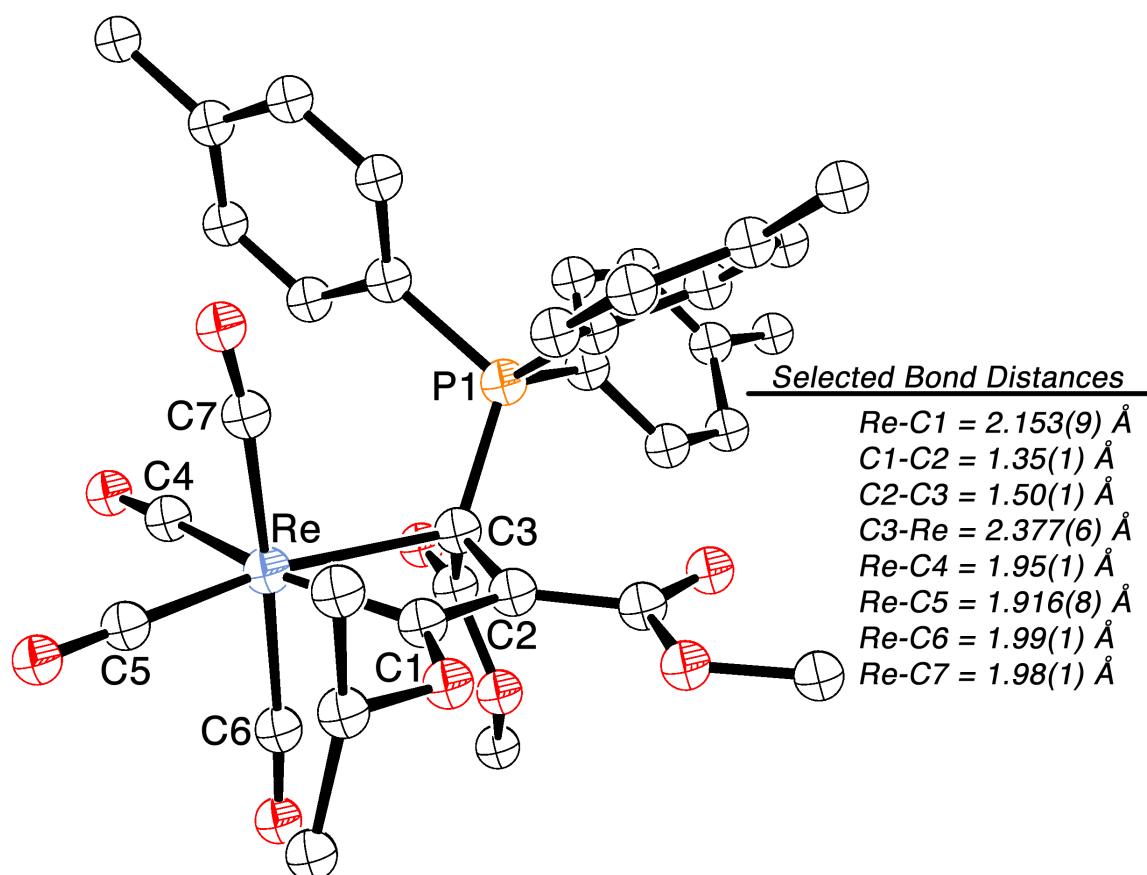


**Figure 1-15.** Ball-and-Stick representation of rhenacyclobutene **34a**. CCDC Number 1172859; refcode HAWTEE. R = 4.4%, Space Group  $P2_1/c$ .<sup>60</sup>

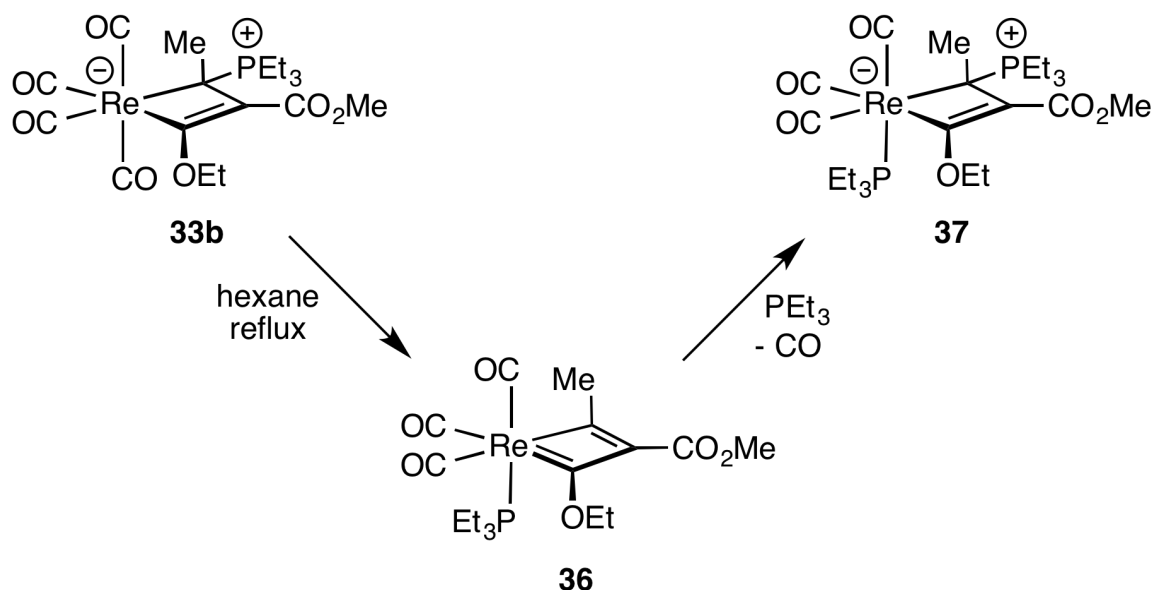
**Table 1-2.** Spectral Parameters for Complexes **33-34**.

	<b>33a</b>	<b>33b</b>	<b>34a</b>	<b>34b</b>
Chemical Shift and Coupling ( $\delta$ [ppm]; multiplicity, $J_{CP}$ [Hz])				
C(1) $^{13}\text{C}\{^1\text{H}\}$	12.09 <sup>a</sup> (d), 55.15	-2.58 <sup>a</sup> (d), 28.07	122.50 <sup>a</sup> (d br), 81.45	
P(1) $^{31}\text{P}\{^1\text{H}\}$	38.6 <sup>a</sup>	41.9 <sup>b</sup>	35.3 <sup>b</sup>	27.7 <sup>a</sup>

(a)  $\text{CD}_2\text{Cl}_2$ . (b)  $(\text{CD}_3)_2\text{CO}$ .

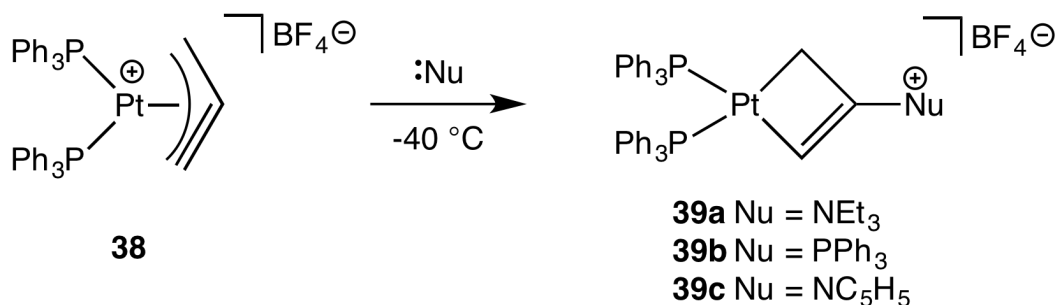
In the case of rhenacyclobutene **33b**, refluxing in hexane solvent gave rise to a new rhenacyclobutadiene analogous to **35**, thus loss of one equivalent of CO and phosphine rearrangement gave a quantitative yield of the Re-substituted phosphine complex **36**. Isolation of complex **36** and further treatment with triethylphosphine gave a new zwitterionic metallacyclobutene **37** with phosphine substitution at both the metal and the C(3) carbon (Scheme 1-20). Attempts to prepare the related rhenacyclobutadiene complexes from **33a** and **34a** failed. Specifically, heating of **33a** in refluxing hexane for 40 h gave no reaction, while heating **34a** in refluxing toluene or treatment with carbonyl-scavenging  $\text{Me}_3\text{NO}$  gave only uncharacterized decomposition products.





**Scheme 1-20.** Reaction of rhenacyclobutene **33b** to give rhenacyclobutadiene **36** and subsequent reaction with PEt<sub>3</sub> to generate the bis(triethylphosphine) substituted rhenacyclobutene **37**.

Chen and co-workers at the National Taiwan University in Taipei reported similar reactivity to that observed by Casey, and noted nucleophilic addition to the central carbon of  $\eta^3$ -allenyl/propargyl complexes of platinum and  $\kappa^1$ -allenyl complexes of iridium to give platina- and iridacyclobutenes, respectively.<sup>62</sup> The ( $\eta^3$ -allenyl/propargyl) platinum complex [Pt(PPh<sub>3</sub>)<sub>2</sub>( $\eta^3$ -C<sub>3</sub>H<sub>3</sub>)] [BF<sub>4</sub>] (**38**) underwent reaction with nucleophiles such as triethylamine, pyridine, or triphenylphosphine by addition to the central carbon to give metastable cationic platinacyclobutene complexes (**39**) (Scheme 1-21). Reaction of **38** with NEt<sub>3</sub> at -40 °C gave metastable complex [Pt(PPh<sub>3</sub>)<sub>2</sub>( $\kappa^2$ -CH=C(NEt<sub>3</sub>)CH<sub>2</sub>)] [BF<sub>4</sub>] (**39a**), which decomposes under vacuum, likely due to loss of triethylamine. Reaction with triphenylphosphine gave a similar complex **39b**, which was isolated by crystallization below 0 °C.

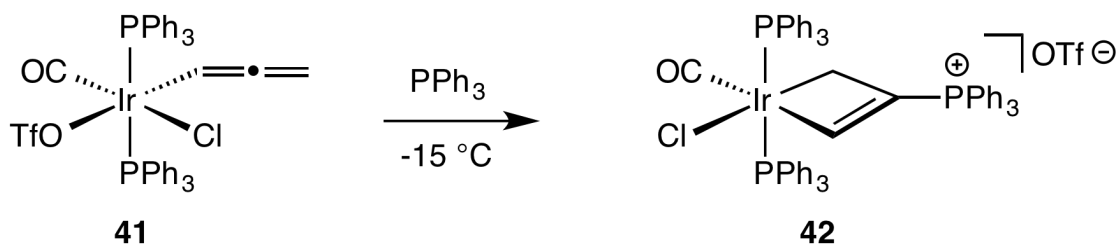


**Scheme 1-21.** Reaction of [Pt(PPh<sub>3</sub>)<sub>2</sub>(η<sup>3</sup>-C<sub>3</sub>H<sub>3</sub>)] [BF<sub>4</sub>] **38** with nucleophiles to give platinacyclobutene complexes **39**.<sup>62</sup>

The reaction of **38** with pyridine at -40 °C gave the related platinacyclobutene complex **39c** in 91% yield, based on NMR spectral data. When **39c** was allowed to warm to -20 °C, further reaction ensued resulting in the formation of a κ<sup>1</sup>-allenyl complex [Pt(PPh<sub>3</sub>)<sub>2</sub>(NC<sub>5</sub>H<sub>5</sub>)(κ<sup>1</sup>-HC=C=CH<sub>2</sub>)] [BF<sub>4</sub>] (**40**) – identified by its characteristic NMR spectral signature – which existed in solution in addition to **38** and **39c**. Raising the temperature of the solution to 0 °C favored the formation of allenyl complex **40** which integrated to 85% of the starting material **38**. Further increase in temperature to 25 °C resulted in the formation of several new platinum complexes, including η<sup>3</sup>-2-hydroxyallyl, η<sup>3</sup>-oxatrimethylenemethane, and diplatina-η<sup>6</sup>-diallyl ether complexes. The oxygen-containing platinum species were attributed to reaction of **40** with trace water present in the reaction mixture.

Platinum κ<sup>1</sup>-allenyl species such as **40** did not react with triphenylphosphine to form metallacyclobutene species, however stirring a mixture of PPh<sub>3</sub> with the iridium allenyl species Ir(Cl)(CO)(PPh<sub>3</sub>)<sub>2</sub>(OTf)(κ<sup>1</sup>-HC=C=CH<sub>2</sub>) (**41**) at -15 °C for 30 minutes resulted in a color change from

reddish-brown to yellow, and formation of the iridacyclobutene complex  $[(\text{Cl})(\text{CO})(\text{PPh}_3)_2\text{Ir}(\kappa^2\text{-CH=C}(\text{PPh}_3)\text{CH}_2)][\text{OTf}]$  (**42**) (Scheme 1-22). Reaction of **41** with pyridine did not result in nucleophilic addition to the central allenyl carbon to yield a metallacyclobutene, and instead resulted in displacement of the triflate ligand to give  $[(\text{Cl})(\text{CO})(\text{PPh}_3)_2(\text{NC}_5\text{H}_5)\text{Ir}(\kappa^1\text{-CH=C=CH}_2)][\text{OTf}]$ .<sup>63</sup>



**Scheme 1-22.** Reaction of  $[\text{Ir}(\text{Cl})(\text{CO})(\text{PPh}_3)_2(\text{OTf})(\kappa^1\text{-CH=C=CH}_2)]$  (**41**) with nucleophiles to give iridacyclobutene complex **42**.<sup>62</sup>

Single crystals of iridacyclobutene complex **42** were obtained from a solution of methylene chloride and diethyl ether (Figure 1-16). The metallacyclobutene moiety is largely planar, with the largest deviation occurring at the middle carbon C(2) (0.04 Å). The structural parameters for **42** are largely consistent with the iridacyclobutenes **8-fac** and **15** reported by Thorn<sup>39</sup> and O'Connor,<sup>55</sup> respectively.

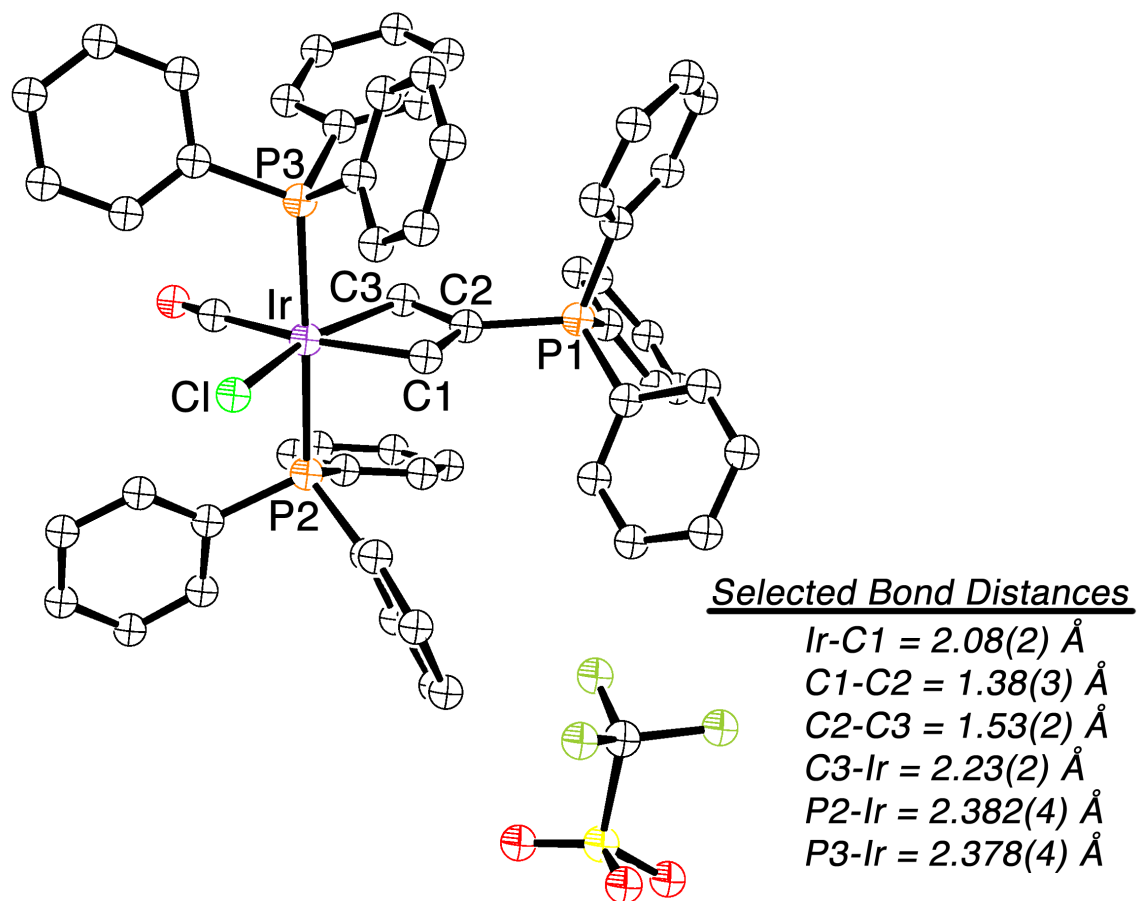


**Figure 1-16.** Ball-and-Stick representation of iridacyclobutene **42**. CCDC Number 1163802; refcode GAPQAP. R = 5.9%, Space Group *P*-1.<sup>62</sup>

Stable metallacyclobutenes are a relatively rare chemical species, with just twenty-two crystallographically characterized, C(1)/C(2) unsaturated, mononuclear examples.<sup>64</sup> As discussed in this account, metallacyclobutene complexes are most typically formed from the reaction of a transient metal carbene with an alkyne.<sup>3b-3d,3j,3k,25a,28,39,45,47,55</sup> Metallacyclobutenes are also formed from structural rearrangements,<sup>3g-3i,47,55</sup> oxidative addition of cyclopropenes,<sup>3e,50</sup> nucleophilic addition to  $\eta^3$ -propargyl<sup>56,58</sup> or  $\eta^3$ -propargyl/allenyl species,<sup>63</sup> as well as  $\kappa^1$ -allenes,<sup>63</sup> and metallacyclobutadienes.<sup>60</sup>

There is also one example of a metallacyclobutene species synthesized from the trapping of an alkyl halide radical with an *in situ* generated  $\eta^3$ -propargyl complex.<sup>3a</sup>

Structurally, metallacyclobutenes usually display a shorter metal-carbon bond to the C(1)  $sp^2$ -hybridized carbon, a result of attachment to the more electronegative vinyl group as compared to the alkyl C(3) carbon. In addition, for systems in which  $d^n$  ( $n \neq 0$ ),  $\pi$ -back-bonding can also strengthen this metal-carbon interaction. The metal-vinyl and metal-alkyl bonds differ in their relative trans influence, or structural trans effect, with the ligand trans to the metal-vinyl bond having a longer distance compared to the trans ligand of the metal-alkyl bond of the metallacyclobutene ring – for cases in which two identical ligands occupy these positions. Metallacyclobutenes can be described as existing along a continuum between an idealized four-membered ring with a carbon-carbon double-bond, and a metal-carbene species with a coordinate alkyne, in which the  $sp^3$ -carbon-metal bond and the  $sp^2$ -carbon-carbon bonds would both be relatively shorter.<sup>28</sup> Examples of the latter typically display a relatively labile alkyne group, which can be displaced to give reactions between the incipient metal carbene and a second species. Additionally for metallacyclobutenes, non-systematic effects of metal, oxidation state,  $d^n$  electron count, ligand set, and crystal packing forces contribute to the structural features of these complexes, as summarized in Table 1-3.

**Table 1-3.** Selected bond distances [ $\text{\AA}$ ] for metallacyclobutenes.

CSD Refcode, Cmpd No., [M]:	M-C(1)	C(1)-C(2)	C(2)-C(3)	M-C(3)
CPTICB, <sup>25a</sup> ( <b>5a</b> ), Ti, Tebbe	2.104(4)	1.344(6)	1.537(6)	2.122(5)
BATMUE, <sup>28</sup> ( <b>5b</b> ), Ti, Tebbe	2.099(3) <sup>a</sup>	1.335(5) <sup>a</sup>	1.598(5) <sup>a</sup>	2.064(4) <sup>a</sup>
BATNAL, <sup>28</sup> ( <b>5d</b> ), Ti, Tebbe	2.050(4)	1.340(5)	1.556(5)	2.083(5)
GABPEE, <sup>3a</sup> Ti, Stryker	2.088(6)	1.32(1)	1.50(1)	2.152(6)
IFODEN, <sup>3d</sup> Ti, Takeda	2.100(3)	1.339(4)	1.543(4)	2.130(3)
IBACIZ, <sup>3b</sup> Co, O'Connor	1.940(8)	1.336(10)	1.542(12)	2.061(7)
IFARUE, <sup>3c</sup> Co, O'Connor	1.938(3)	1.345(5)	1.514(3)	2.055(4)
IFASAL, <sup>3c</sup> Co, O'Connor	1.934(3)	1.342(4)	1.530(4)	2.055(2)
SOMTOD, <sup>3e</sup> Zr, Binger	2.306(5)	1.344(8)	1.483(8)	2.386(6)
CUFTIG, <sup>45</sup> ( <b>9</b> ), Rh, Bianchini	2.09(3)	1.30(4)	1.50(4)	2.15(3)
CUFTIG10, <sup>47</sup> ( <b>9</b> ), Rh, Bianchini	2.05(3)	1.30(4)	1.50(4)	2.14(3)
FABJUN, <sup>47</sup> ( <b>11</b> ), Rh, Bianchini	2.137(9)	1.33(1)	1.50(1)	2.115(9)
PEMSEF, <sup>3j</sup> W, Rothwell	2.041(4)	1.376(5)	1.454(5)	2.297(4)
SASHUP, <sup>3k</sup> W, Muir	2.242(2)	1.322(5)	1.509(5)	2.195(4)
NIDJOZ, <sup>58</sup> ( <b>19b</b> ), Re, Casey	2.19(1)	1.33(1)	1.52(1)	2.22(1)
	2.17(1) <sup>b</sup>	1.42(1) <sup>b</sup>	1.47(1) <sup>b</sup>	2.21(1) <sup>b</sup>
HAWTEE, <sup>60</sup> ( <b>34a</b> ), Re, Wojcicki	2.153(8)	1.352(10)	1.497(9)	2.377(7)
ASODER, <sup>3g</sup> Ir, Paneque	2.025(2)	1.337(3)	1.524(3)	2.136(2)
GOGHIV, <sup>3i</sup> Ir, Paneque	2.017(4)	1.353(5)	1.541(5)	2.081(3)
CIYKAW, <sup>39</sup> ( <b>8-fac</b> ), Ir, Thorn	2.134(5)	1.344(8)	1.525(7)	2.166(6)
GAPQAP, <sup>63</sup> ( <b>42</b> ), Ir, Chen	2.08(2)	1.39(2)	1.53(3)	2.23(2)
SIGKEY, <sup>55</sup> ( <b>15</b> ), Ir, O'Connor	2.04(2)	1.33(2)	1.54(2)	2.19(1)
GIPZIO, <sup>50</sup> ( <b>13a</b> ), Pt, Hughes	2.039(9)	1.351(12)	1.474(12)	2.079(8)

(a) ave. of two independent data; esd shown is higher of two calc. values.

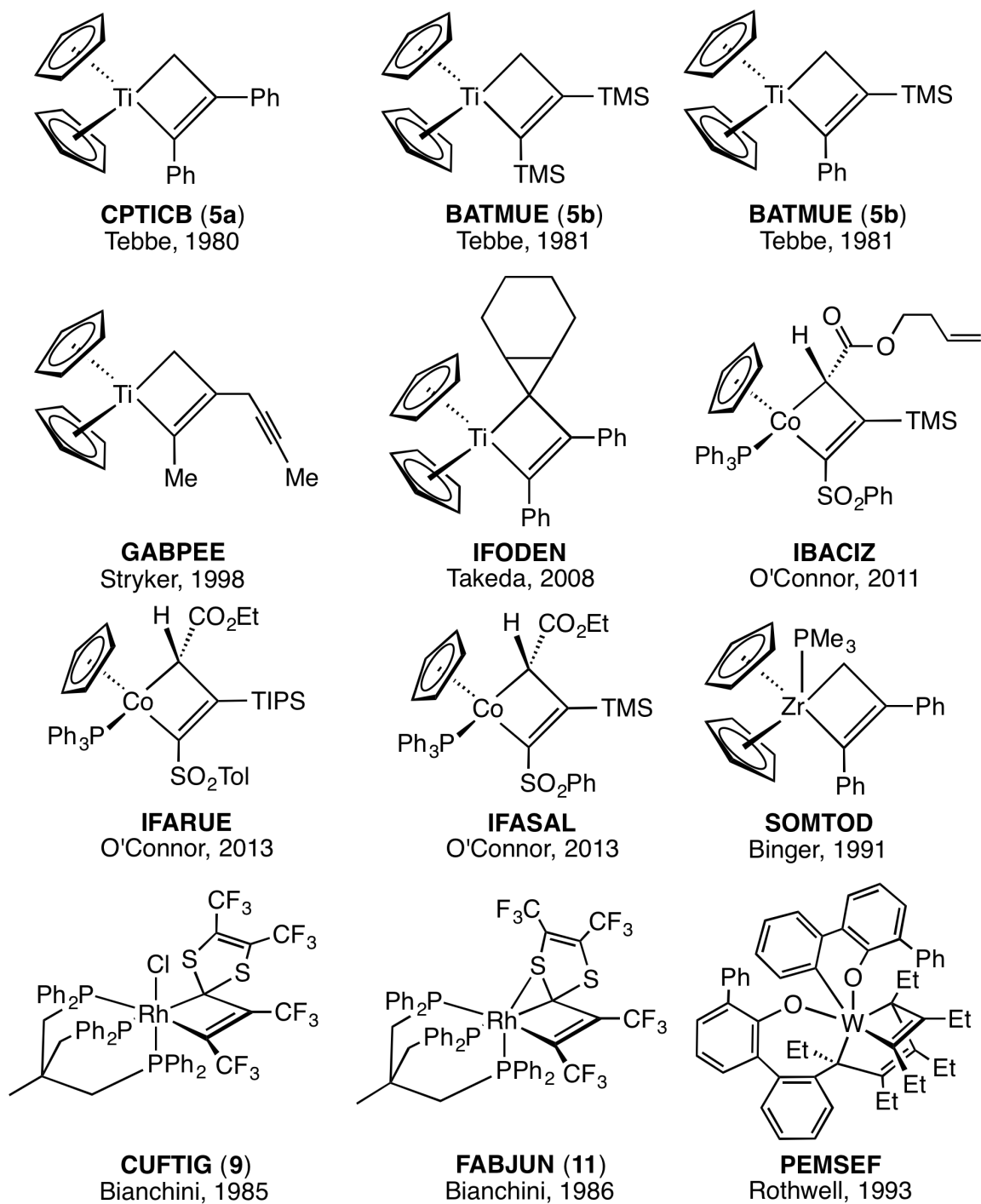


**Figure 1-17.** Crystallographically characterized metallacyclobutene complexes.

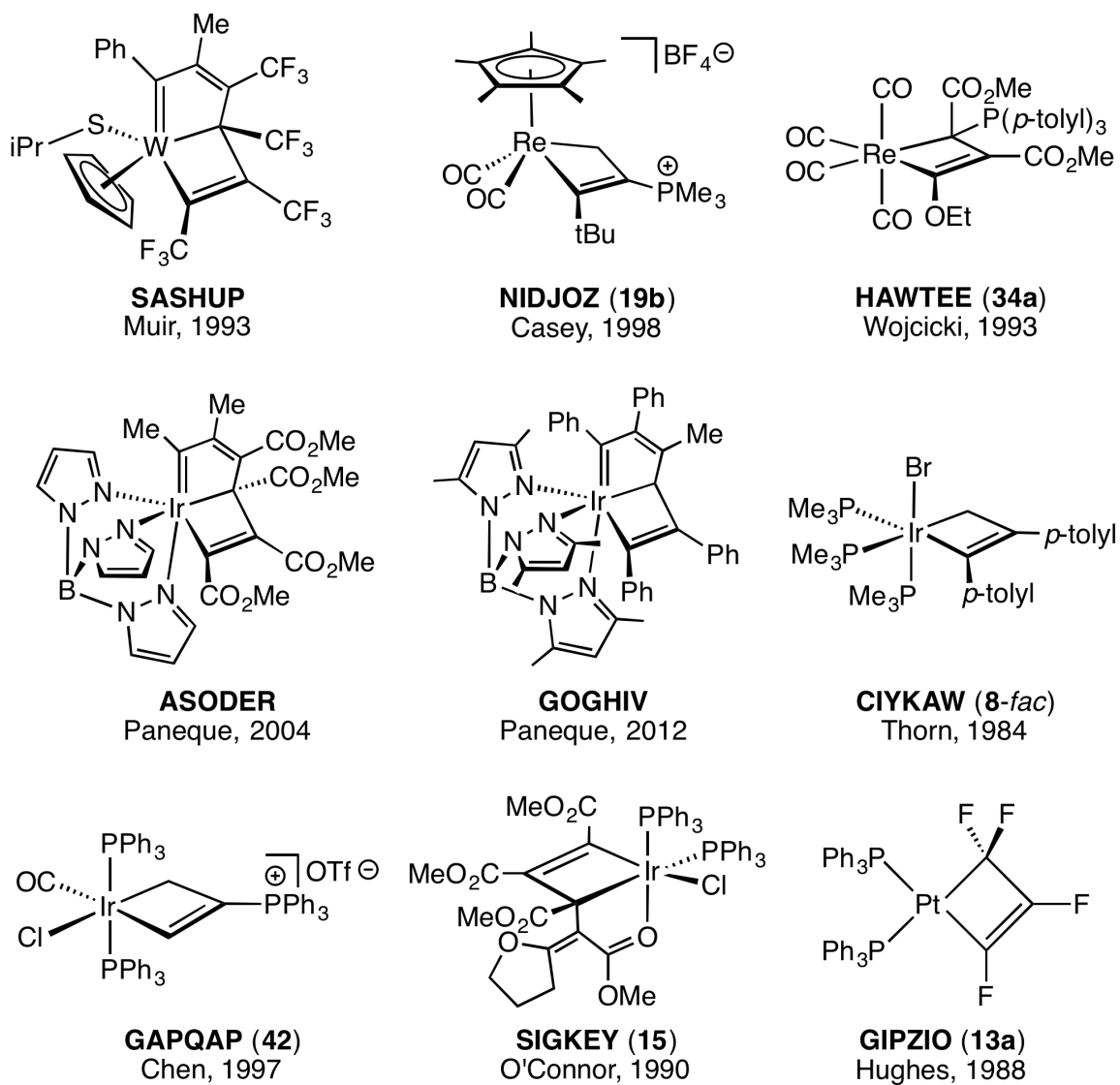


**Figure 1-18.** Crystallographically characterized metallacyclobutene complexes.



## References.

1. Teuben, J. H.; de Liefde Meijer, H. J. *J. Organomet. Chem.* **1969**, *17*, 87.
2. Sekutowski, D. G.; Stucky, G. D. *J. Am. Chem. Soc.* **1976**, *98*, 1376.
3. For examples of crystallographically characterized metallacyclobutenes, see: (a) CSD Refcode: GABPEE; CCDC No. 1162340 (Ti). Ogoshi, S.; Stryker, J. M. *J. Am. Chem. Soc.*, **1998**, *120*, 3514. (b) CSD Refcode: IBACIZ; CCDC No. 847556 (Co). O'Connor, J. M.; Chen, M.-C.; Holland, R. L.; Rheingold, A. L. *Organometallics*, **2011**, *30*, 369. (c) CSD Refcode: IFARUE; CCDC No. 954622 (Co); CSD Refcode: IFASAL; CCDC No. 954623 (Co), O'Connor, J. M.; Baldrige, K. K.; Vélez, C. L.; Rheingold, A. L.; Moore, C. E. *J. Am. Chem. Soc.* **2013**, *135*, 8826. (d) CSD Refcode: IFODEN; CCDC No. 678446 (Ti). Shono, T.; Nagasawa, T.; Tsubouchi, A.; Nogucki, K.; Takeda, T. *Chem. Commun.* **2008**, 3537. (e) CSD Refcode: SOMTOD; CCDC No. 1261904 (Zr). Binger, P.; Müller, P.; Herrmann, A. T.; Philipps, P.; Gabor, B.; Langhauser, F.; Krüger, C. *Chem. Ber.* **1991**, *124*, 2165. (f) CSD Refcode: WAFWEF; CCDC No. 1289364 (Co). O'Connor, J. M.; Ji, H.; Iranpour, M.; Rheingold, A. L. *J. Am. Chem. Soc.* **1993**, *115*, 1586. (g) CSD Refcode: ASODER; CCDC No. 232727 (Ir). Paneque, M.; Poveda, M. L.; Rendón, N.; Mereiter, K. *J. Am. Chem. Soc.* **2004**, *126*, 1610. (h) CSD Refcode: ASODER01; CCDC No. 232727 (Ir). Paneque, M.; Poveda, M. L.; Rendón, N.; Mereiter, K. *Organometallics*, **2009**, *28*, 172. (i) Rendón, N.; Paneque, M.; Poveda, M. L.; Mereiter, K. *Private Communication*, **2012**. (j) Kriley, C. E.; Kerschner, J. L.; Fanwick, P. E.; Rothwell, I. P. *Organometallics*, **1993**, *12*, 2051. (k) Agh-Atabay, N. M.; Davidson, J. L.; Douglas, G.; Muir, K. W. *J. Chem. Soc., Chem. Commun.* **1989**, 549.
4. For examples of crystallographically characterized exo-methylene metallacyclobutenes, see: (a) CSD Refcode: DCMPTB; CCDC No. 1137491 (Pt); CSD Refcode: PCYMBP; CCDC No. 1229537 (Pt). Lenarda, M.; Pahor, N. B.; Calligaris, M.; Graziani, M.; Randaccio, L. *Inorg. Chim. Acta.* **1978**, *26*, L19. (b) CSD Refcode: RAQXIQ; CCDC No. 1246725 (Ti). Beckhaus, R.; Sang, J.; Englert, U.; Bohme, U. *Organometallics*, **1996**, *15*, 4731. (c) CSD Refcode: RUBYET; CCDC No. 710365 (Ru); CSD Refcode: RUBYIX; CCDC No. 710366 (Ru). Yamaguchi, M.; Arikawa, Y.; Nishimura, Y.; Umakoshi, K.; Onishi, M. *Chem. Commun.* **2009**, 2911. (d) CSD Refcode: ZUXHEF; CCDC No. 1317401 (Ti); CSD Refcode: ZUXHIJ; CCDC No. 1317402 (Ti). Beckhaus, R.; Sang, J.; Wagner, T.; Ganter, B. *Organometallics*, **1996**, *15*, 1176.
5. For examples of crystallographically characterized imino metallacyclobutenes, see: (a) CSD Refcode: CORLUQ; CCDC No. 1129869 (Co); CSD Refcode: CORMAX; CCDC No. 1129871 (Co); CSD Refcode: CORMEB; CCDC No.

1129873 (Co). Wakatsuki, Y.; Miya, S.-Y. Ikuta, S.; Yamazaki, H. *Chem. Commun.* **1985**, 35. (b) CSD Refcode: CORLUQ10; CCDC No. 1129870 (Co); CSD Refcode: CORMAX10; CCDC No. 1129872 (Co); CSD Refcode: CORMEB10; CCDC No. 1129874 (Co), Wakatsuki, Y.; Miya, S.-Y.; Yamazaki, H. *J. Chem. Soc., Dalton Trans.* **1986**, 1207. (c) CSD Refcode: QOKPUB; CCDC No. 155029 (Mo). Adams, C. J.; Anderson, K. M.; Bartlett, I. M.; Connelly, N. G.; Orpen, A. G.; Paget, T. J.; Phetmung, H.; Smith, D. W. *J. Chem. Soc., Dalton Trans.* **2001**, 1284. (d) CSD Refcode: TODYIU; CCDC No. 1273154 (Rh). Werner, H.; Heinemann, A.; Windmüller, B.; Steinert, P. *Chem. Ber.* **1996**, *129*, 903.

6. For examples of crystallographically characterized metallacyclobutenones, see: (a) CSD Refcode: PBUOPT; CCDC No. 1229324 (Pt). Wong, W.; Singer, S. J.; Pitts, W. D.; Watkins, S. F.; Baddley, W. H. *Chem. Commun.* **1972**, 672. (b) CSD Refcode: SENTUA; CCDC No. 1257283 (Re). Padolik, L. L.; Gallucci, J.; Wojcicki, A. *J. Organomet. Chem.* **1990**, *383*, C1. (c) CSD Refcode: SENTUA10; CCDC No. 1257284 (Re). Padolik, L. L.; Gallucci, J. C.; Wojcicki, A. *J. Am. Chem. Soc.* **1993**, *115*, 9986. (d) CSD Refcode: WEDXOS; CCDC No. 137406 (Co). Foerstner, J.; Kakoschke, A.; Wartchow, R.; Butenschon, H. *Organometallics*, **2000**, *19*, 2108.

7. For examples of crystallographically characterized dinuclear metallacyclobutenes, see: (a) CSD Refcode: CIBWAN; CCDC No. 911895 (Ti). Altenburger, K.; Semmler, J.; Arndt, P.; Spannenberg, A.; Meel, M. J.; Villinger, A.; Seidel, W. W.; Rosenthal, U. *Eur. J. Inorg. Chem.* **2013**, 4258. (b) CSD Refcode: WOFGED; CCDC No. 114272 (Ti). Pellny, P.-M.; Burlakov, V. V.; Baumann, W.; Spannenberg, A.; Kempe, R.; Rosenthal, U. *Organometallics*, **1999**, *18*, 2906.

8. (a) Mol, J. C.; Moulijn, J. A.; Boelhouwer, C. *Chem. Commun. (London)* **1968**, 633. (b) Lewandos, G. S.; Pettit, R. *Tetrahedron Lett.* **1971**, *11*, 789. (c) Lewandos, G. S.; Pettit, R. *J. Am. Chem. Soc.* **1971**, *93*, 7087. (d) Grubbs, R. H.; Brunck, T. K. *J. Am. Chem. Soc.* **1972**, *94*, 2538. (e) Cardin, D. J.; Doyle, M. J.; Lappert, M. F. *J. Chem. Soc., Chem. Commun.* **1972**, 927. (f) Cardin, D. J.; Çetinkaya, B.; Doyle, M. J.; Lappert, M. F. *Chem. Soc. Rev.* **1973**, *2*, 99. (g) Biefeld, C. G.; Eick, H. A.; Grubbs, R. H. *Inorg. Chem.* **1973**, *12*, 2166. (h) Schrock, R. R. *J. Am. Chem. Soc.* **1974**, *96*, 6796. (i) Nobel Media AB 2014 Richard R. Schrock – Biographical. *Nobelprize.org* [online] [http://www.nobelprize.org/nobel\\_prizes/chemistry/laureates/2005/schrock-bio.html](http://www.nobelprize.org/nobel_prizes/chemistry/laureates/2005/schrock-bio.html) (accessed May 31, 2016).

9. (a) Peters, E. F.; Evering, B. L. (Standard Oil Co.). U.S. Patent 2,963,447, Dec. 6, 1960; *Chem. Abstr.* **1961**, *55*, 29435. (b) Banks, R. L.; Bailey, G. C. *Ind. Eng.*

*Chem. Prod. Res. Dev.* **1964**, *3*, 170. (c) Calderon, N.; Chen, H. Y.; Scott, K. W. *Tetrahedron Lett.* **1967**, *8*, 3327. (d) Calderon, N.; Ofstead, E. A.; Ward, J. P.; Judy, W. A.; Scott, K. W. *J. Am. Chem. Soc.* **1968**, *90*, 4133.

10. Hérisson, J.-L.; Chauvin, Y. *Makromol. Chem.* **1971**, *141*, 161.

11. Casey, C. P.; Burkhardt, T. J. *J. Am. Chem. Soc.* **1974**, *96*, 7808.

12. Masuda, T.; Sasaki, N.; Higashimura, T. *Macromolecules*, **1975**, *8*, 717.

13. Katz, T. J.; McGinnis, J. *J. Am. Chem. Soc.* **1975**, *97*, 1592.

14. Tebbe, F. N.; Parshall, G. W.; Reddy, G. S. *J. Am. Chem. Soc.* **1978**, *100*, 3611.

15. Heins, E.; Hinck H.; Kaminsky, W.; Oppermann, G.; Raulinat, P.; Sinn, H. *Makromol. Chem.* **1970**, *134*, 1.

16. Calderon, N.; Ofstead, E. A.; Judy, W. A. *Angew. Chem. Int. Ed. Engl.* **1976**, *15*, 401.

17. Tebbe, F. N.; Parshall, G. W.; Ovenall, D. W. *J. Am. Chem. Soc.* **1979**, *101*, 5074.

18. (a) Muetterties, E. L. *Inorg. Chem.* **1975**, *14*, 951. (b) Mocella, M. T.; Busch, M. A.; Muetterties, E. L. *J. Am. Chem. Soc.*, **1976**, *98*, 1283. (c) Kelly, W. J.; Calderon, N. *J. Macromol. Sci. Chem., Part A*, **1975**, *9*, 911.

19. Klabunde, U.; Tebbe, F. N.; Parshall, G. W.; Harlow, R. L. *J. Mol. Catal.* **1980**, *8*, 37.

20. (a) Katz, T. J.; Lee, S. J. *J. Am. Chem. Soc.* **1980**, *102*, 422. (b) Hofmann, P.; Hämmerle, M. *Angew. Chem. Int. Ed. Engl.* **1989**, *28*, 908. (c) Hofmann, P.; Hämmerle, M.; Unfried, G. *New. J. Chem.* **1991**, *15*, 769. (d) Dötz, K. H. *Naturwissenschaften*, **1975**, *62*, 365. (e) Dötz, K. H. *Angew. Chem. Int. Ed. Engl.* **1975**, *14*, 644. (f) Dötz, K. H.; Dietz, R.; von Imhof, A.; Lorenz, H.; Huttner, G. *Chem. Ber.* **1976**, *109*, 2033. (g) Dötz, K. H.; Dietz, R. *Chem. Ber.* **1977**, *110*, 1555.

21. (a) Fischer, E. O.; Maasböl, A. *Chem. Ber.* **1967**, *100*, 2445. (b) Aumann, R.; Fischer, E. O. *Angew. Chem. Int. Ed.* **1967**, *6*, 878. (c) Darensbourg, D. J. *Inorg. Chem.* **1970**, *9*, 32.

22. Casey, C. P.; Burkhardt, T. J. *J. Am. Chem. Soc.* **1973**, *95*, 5833.

23. (a) Katz, T. J.; Lee, S. J.; Acton, N. *Tetrahedron Lett.* **1976**, 4247. (b) Katz, T. J.; Acton, N. *Tetrahedron Lett.* **1976**, 4251. (c) Katz, T. J.; Hersh, W. H. *Tetrahedron Lett.* **1977**, 585. (d) McGinnis, J.; Katz, T. J.; Hurwitz, S. *J. Am. Chem. Soc.* **1976**, *98*, 605. (e) Katz, T. J.; McGinnis, J.; Altus, C. *J. Am. Chem. Soc.* **1976**, *98*, 606. (f) Lee, S. J.; McGinnis, J.; Katz, T. J. *J. Am. Chem. Soc.* **1976**, *98*, 7818.
24. (a) Katz, T. J.; Lee, S. J.; Nair, M.; Savage, E. B. *J. Am. Chem. Soc.* **1980**, *102*, 7940. (b) Katz, T. J.; Savage, E. B.; Lee, S. J.; Nair, M. *J. Am. Chem. Soc.* **1980**, *102*, 7942.
25. (a) Tebbe, F. N.; Harlow, R. L. *J. Am. Chem. Soc.* **1980**, *102*, 6149. (b) Holland, R. L.; Bunker, K. D.; Chen, C. H.; DiPasquale, A. G.; Rheingold, A. L.; Baldridge, K. K.; O'Connor, J. M. *J. Am. Chem. Soc.* **1998**, *130*, 10093.
26. Grubbs, R. H. *Prog. Inorg. Chem.* **1978**, *24*, 1.
27. Howard, T. R.; Lee, J. B.; Grubbs, R. H. *J. Am. Chem. Soc.* **1980**, *102*, 6876.
28. McKinney, R. J.; Tulip, T. H.; Thorn, D. L.; Coolbaugh, T. S.; Tebbe, F. N. *J. Am. Chem. Soc.* **1981**, *103*, 5584.
29. Casey, C. P.; Polichnowski, S. W.; Shusterman, A. J.; Jones, C. R. *J. Am. Chem. Soc.* **1979**, *101*, 7282.
30. (a) Dötz, K. H. *J. Organomet. Chem.* **1977**, *140*, 177. (b) Casey, C. P. In *Reactive Intermediates*; Jones Jr., M.; Moss, R. A., Eds.; Wiley: New York, **1981**; Vol. 2, p 155. (c) Fischer, H.; Mühlemeier, J.; Märkl, R.; Dötz, K. H. *Chem. Ber.* **1982**, *115*, 1355. (d) Dötz, K. H. *Pure Appl. Chem.* **1983**, *55*, 1689. (e) Reissig, H. U. *Nachr. Chem. Tech. Lab.* **1986**, *34*, 22.
31. (a) McCallum, J. S.; Kunng, F.-A.; Gilbertson, S. R.; Wulff, W. D. *Organometallics*, **1988**, *7*, 2346. (b) Semmelhack, M. F.; Ho, S.; Cohen, D.; Steigerwald, M.; Lee, M. C.; Lee, G.; Gilbert, A. M.; Wulff, W. D.; Ball, R. G. *J. Am. Chem. Soc.* **1994**, *116*, 7108. (c) Hughes, R. P.; Trujillo, H. A.; Gauri, A. J. *Organometallics*, **1995**, *14*, 4319.
32. Foley, H. C.; Strubinger, L. M.; Targos, T. S.; Geoffroy, G. L. *J. Am. Chem. Soc.* **1983**, *105*, 3064.
33. Semmelhack, M. F.; Tamura, R.; Schnatter, W.; Springer, J. *J. Am. Chem. Soc.* **1984**, *106*, 5363.

34. Wulff, W. D.; Gilbertson, S. R.; Springer, J. P. *J. Am. Chem. Soc.* **1986**, *108*, 520.
35. Harvey, D. F.; Brown, M. F. *J. Am. Chem. Soc.* **1990**, *112*, 7806.
36. Hoye, T. R.; Dinsmore, C. J. *J. Am. Chem. Soc.* **1991**, *113*, 4343.
37. Padwa, A.; Krumpe, K. E.; Kassir, J. M. *J. Org. Chem.* **1992**, *57*, 4940.
38. (a) Thorn, D. L. *J. Am. Chem. Soc.* **1980**, *102*, 7109. (b) Thorn, D. L. *Organometallics*, **1982**, *1*, 197. (c) Thorn, D. L.; Tulip, T. H. *Organometallics*, **1982**, *1*, 1580. (d) Thorn, D. L.; Tulip, T. H. *J. Am. Chem. Soc.* **1981**, *103*, 5584. (e) Parshall, G. W.; Thorn, D. L.; Tulip, T. H. *ChemTech*, **1982**, 571. (f) Thorn, D. L. *J. Mol. Catal.* **1982**, *17*, 279. (g) Thorn, D. L. *Organometallics*, **1982**, *1*, 879.
39. Calabrese, J. C.; Roe, D. C.; Thorn, D. L.; Tulip, T. H. *Organometallics*, **1984**, *3*, 1223.
40. Chou, C.-K.; Miles, D. L.; Bau, R.; Flood, T. C. *J. Am. Chem. Soc.* **1978**, *100*, 7271.
41. Nakamura, A.; Otsuka, S. *J. Mol. Catal.* **1975**, *1*, 285.
42. Albright, T. A.; Hoffmann, R.; Thibeault, J. C.; Thorn, D. L. *J. Am. Chem. Soc.* **1979**, *101*, 3801.
43. Katz, T. J.; Sivavec, T. M. *J. Am. Chem. Soc.* **1985**, *107*, 737.
44. Brookhart, M.; Green, M. L. H. *J. Organomet. Chem.* **1983**, *250*, 395.
45. Bianchini, C.; Mealli, C.; Meli, A.; Sabat, M. *Organometallics*, **1985**, *4*, 421.
46. (a) Bianchini, C.; Meli, A. *J. Chem. Soc., Chem Commun.* **1983**, 1309. (b) Bianchini, C.; Meli, A.; Scapacci, G. *Organometallics*, **1985**, *4*, 264.
47. Bianchini, C.; Mealli, C.; Mell, A.; Sabat, M.; Silvestre, J.; Hoffmann, R. *Organometallics*, **1986**, *5*, 1733.
48. Hoffmann, R. *Angew. Chem. Int. Ed.* **1982**, *21*, 711.
49. Woodward, R. B.; Hoffmann, R. *The Conservation of Orbital Symmetry*; Verlag Chemie: Weinheim/Bergstr. **1970**.

50. Hemond, R. C.; Hughes, R. P.; Robinson, D. J.; Rheingold, A. L. *Organometallics*, **1988**, *7*, 2239.
51. Waldron, R. F.; Lemal, D. M.; Barefoot, A. C., III. *J. Am. Chem. Soc.* **1984**, *106*, 8301.
52. Sargeant, P. B.; Krespan, C. G. *J. Am. Chem. Soc.* **1969**, *91*, 415.
53. (a) Dewar, M. *Bull. Soc. Chim. Fr.* **1951**, *18*, C71-C79. (b) Dewar, M. *Ann. Rep. Prog. Chem.* **1951**, *48*, 112. (c) Chatt, J.; Duncanson, L. A. *J. Chem. Soc.* **1953**, 2939. (d) Chatt, J.; Duncanson, L. A. *J. Chem. Soc.* **1955**, 4456.
54. (a) O'Connor, J. M.; Pu, L.; Rheingold, A. L. *J. Am. Chem. Soc.* **1987**, *109*, 7578. (b) O'Connor, J. M.; Pu, L.; Rheingold, A. L. *J. Am. Chem. Soc.* **1990**, *112*, 6232.
55. O'Connor, J. M.; Pu, L.; Woolard, S.; Chadha, R. K. *J. Am. Chem. Soc.* **1990**, *112*, 6731.
56. Casey, C. P.; Yi, C. S. *J. Am. Chem. Soc.* **1992**, *114*, 6597.
57. Casey, C. P.; Yi, C. S. *Organometallics*, **1990**, *9*, 2413.
58. Casey, C. P.; Nash, J. R.; Yi, C. S.; Selmeczy, A. D.; Chung, S.; Powell, D. R.; Hayashi, R. K. *J. Am. Chem. Soc.* **1998**, *120*, 722.
59. Casey, C. P.; Selmeczy, A. D.; Nash, J. R.; Yi, C. S.; Powell, D. R.; Hayashi, R. K. *J. Am. Chem. Soc.* **1996**, *118*, 6698.
60. Padolik, L. J.; Gallucci, J. C.; Wojcicki, A. *J. Am. Chem. Soc.* **1993**, *115*, 9986.
61. (a) Fischer, E. O. *Adv. Organomet. Chem.* **1976**, *14*, 1. (b) Crabtree, R. H. *The Organometallic Chemistry of the Transition Metals* (6<sup>th</sup> Ed.); Wiley: New Jersey, **2014**.
62. Cheng, Y.-C.; Chen, Y.-K.; Huang, T.-M.; Yu, C.-I.; Lee, G.-H.; Wang, Y.; Chen, J.-T. *Organometallics*, **1998**, *17*, 2953.
63. Chen, J.-T.; Chen, Y.-K.; Chu, J.-B.; Lee, G.-H.; Wang, Y. *Organometallics*, **1997**, *16*, 1476.

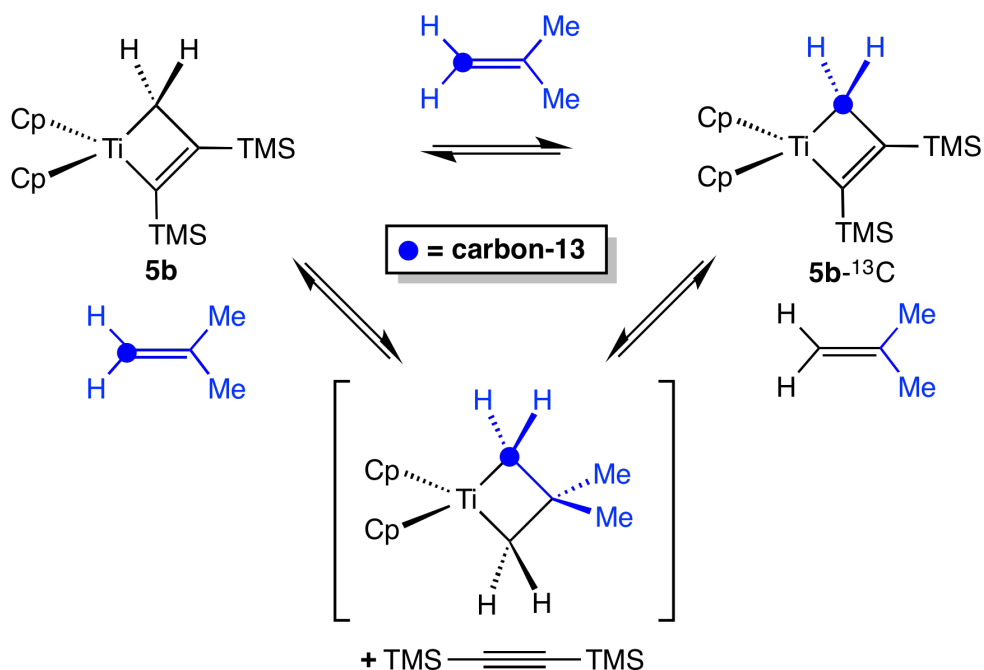
64. (a) Bruno, I. J.; Cole, J. C.; Edgington, P. R.; Kessler, M.; Macrae, C. F.; McCabe, P.; Pearson, J.; Taylor, R. *Acta. Cryst.*, **2002**, B58, 389. (b) Allen, F. H. *Acta. Cryst.*, **2002**, B58, 380.

## **Chapter 2**

Reactivity of Stable Metallacyclobutenes and Vinylcarbenes with Alkenes



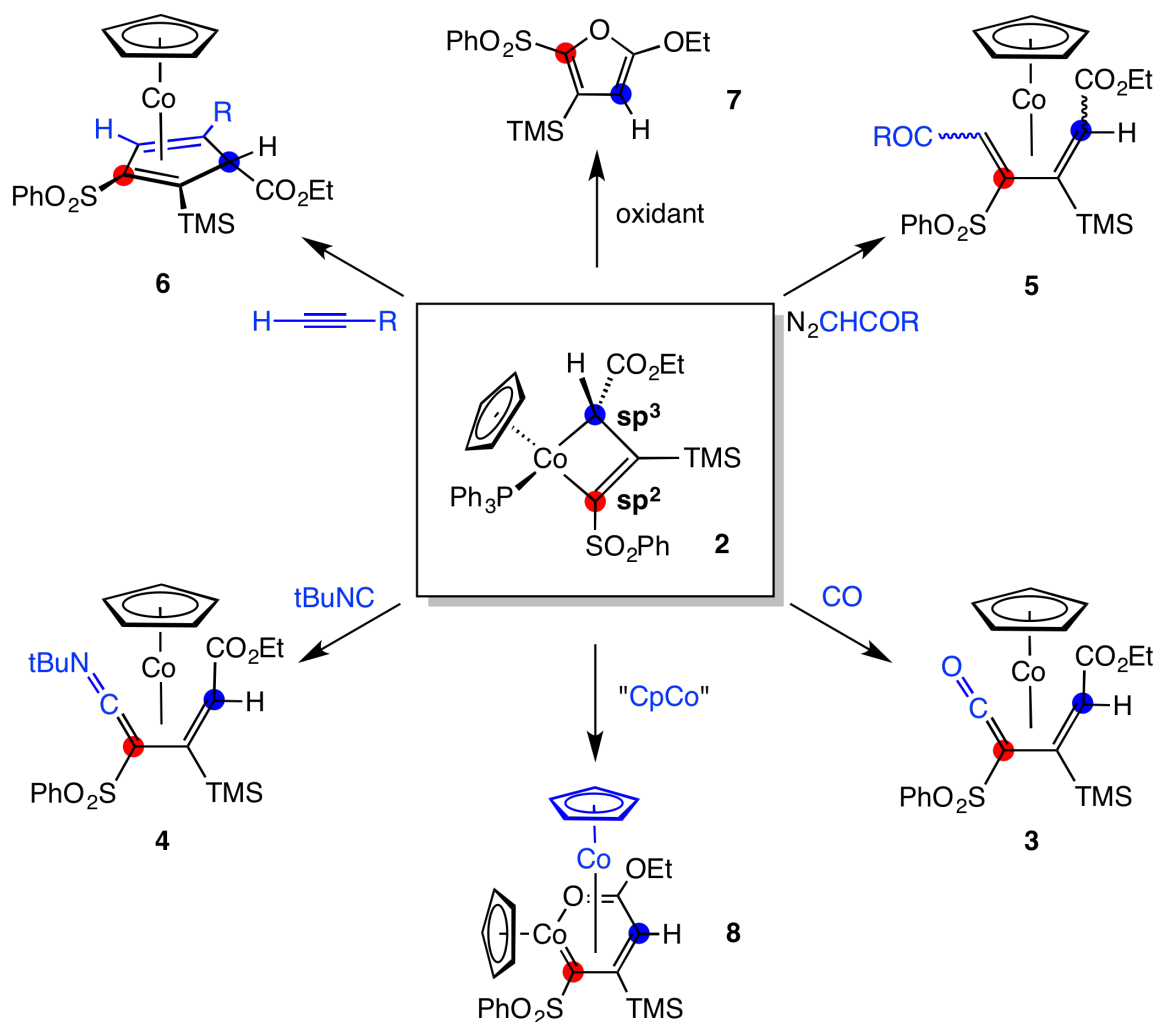
The reactions of alkenes with metallacyclopentadienes and metallacyclobutanes have been widely developed as synthetic methodology.<sup>1</sup> In contrast, metallacyclobutene-alkene chemistry remains largely unexplored.<sup>2,3</sup> Metallacyclobutenes have been proposed as unobserved intermediates in numerous metal-catalyzed reactions, including alkyne polymerization and enyne metathesis;<sup>4</sup> however, the only alkene reaction previously reported for a characterized metallacyclobutene is the Tebbe and Harlow 1980 observation that titanacyclobutene **1** reacts with 2-methylpropene-1-<sup>13</sup>C at 85 °C to give **1**-<sup>13</sup>C (Scheme 2-1).<sup>5</sup> When heated, compound **1** reacts to lose bis(trimethylsilyl)acetylene and generate a titanocene methylene species - which can undergo formal electrocyclozation with the labeled alkene to form an intermediate metallacyclobutane complex. This metallacyclobutane intermediate can undergo degenerate retro-electrocyclozation to regenerate alkene and either of two titanocene methylene species: the <sup>13</sup>C-labeled titanocene methylene with concomitant formation of the unlabeled alkene, or the unlabeled titanocene isotopomer and the <sup>13</sup>C-labeled alkene. Both titanocene methylene compounds react with liberated alkyne to give the labeled and unlabeled complexes **1** and **1**-<sup>13</sup>C. Here we report the first productive reactions of a metallacyclobutene complex with alkenes, to give 1,4-diene complexes with excellent regio- and stereochemical control. The results are consistent with a mechanism that involves conversion of the metallacyclobutene to a vinylcarbene intermediate, which then undergoes a [4 + 2]-cycloaddition reaction with the activated alkene.<sup>6</sup>



**Scheme 2-1.** Reaction of the isolated metallacyclobutene **1** with 2-methylpropene-1- $^{13}\text{C}$  to give **1- $^{13}\text{C}$** .

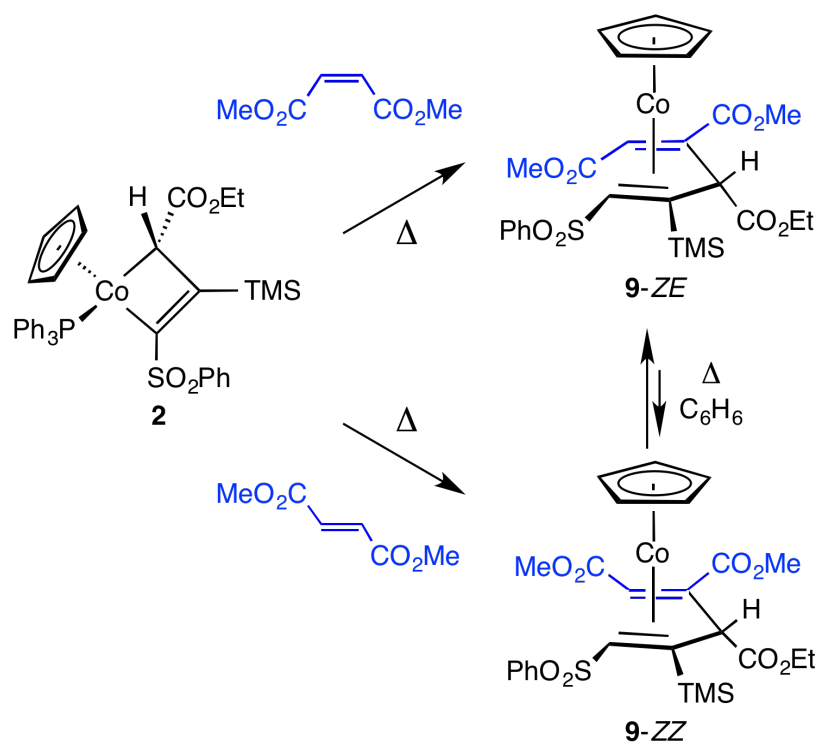
Access to the stable cobaltacyclobutene complex  $(\eta^5\text{-C}_5\text{H}_5)(\text{PPh}_3)\text{Co}[\kappa^2\text{-}(C,C)\text{-C}(\text{SO}_2\text{Ph})=\text{C}(\text{TMS})\text{CH}(\text{CO}_2\text{Et})]$  (**2**)<sup>3c</sup> has permitted the first systematic investigations into the reactivity of late-metal metallacyclobutenes. Cobaltacyclobutene **2** undergoes reaction with one-carbon addends such as carbon monoxide, tert-butyl isocyanide, and diazocarbonyls to give vinylketene **3**,<sup>3d</sup> vinylketenimine **4**,<sup>3d</sup> and 1,3-dienes **5**,<sup>3f</sup> with selective carbon-carbon bond formation at the  $\alpha$ -( $\text{sp}^2$ )-carbon of the metallacycle ring in **2** (Scheme 2-2). In contrast, metallacyclobutene **2** reacts with alkynes to give coupling at both the  $\alpha$ -( $\text{sp}^2$ )-carbon and the  $\gamma$ -( $\text{sp}^3$ )-carbon to yield cyclopentadienes **6**.<sup>3e</sup> Metallacyclobutene **2** undergoes a 2-electron oxidation under electrochemical conditions, or in the presence of silver tetrafluoroborate or diacetylferrocenium to

give furan product **7**.<sup>39</sup> Finally, metallacyclobutene **2** can also form dinuclear complex **8** at elevated temperatures via ring-expansion by coordination to the ester carbonyl at the  $\gamma$ -( $sp^3$ )-carbon, with subsequent trapping by a ( $\eta^5$ -C<sub>5</sub>H<sub>5</sub>)Co moiety; the trapping ( $\eta^5$ -C<sub>5</sub>H<sub>5</sub>)Co fragment is generated by disproportionation of **2** with concomitant formation of furan species **7**.<sup>7</sup> Heating **2** in the presence of ( $\eta^5$ -C<sub>5</sub>H<sub>5</sub>)Co(PPh<sub>3</sub>)<sub>2</sub> generates **8** without formation of furan.



**Scheme 2-2.** Established reactions of the metallacyclobutene **2**.

When a benzene solution of metallacyclobutene **2** (228 mg, 12.8 mM) and dimethyl fumarate (63 mM) was heated at 70 °C for 96 h, followed by chromatographic workup in air, the 1,4-diene complex, **9-ZE**, was isolated as an orange, air-stable solid in 87% yield (Scheme 2-3).<sup>8,9</sup> The <sup>1</sup>H NMR spectrum (CDCl<sub>3</sub>) of **9-ZE** exhibits two upfield singlets at  $\delta$  2.87 (H<sup>anti</sup>, CHSO<sub>2</sub>Ph) and 3.76 (H<sup>syn</sup>, CHCO<sub>2</sub>Me), suggestive of a cobalt-diene structure. For comparison, the vinyl hydrogens in the 1,3-diene complex, **5-ZE** (R = CO<sub>2</sub>Et), are observed at  $\delta$  1.09 (H<sup>anti</sup>) and 3.73 (H<sup>syn</sup>).<sup>3f</sup> The observation of a third singlet in the <sup>1</sup>H NMR spectrum of **9-ZE** at  $\delta$  4.80 (1H, CHCO<sub>2</sub>Et) is inconsistent with a 1,3-diene structure, which could have resulted from alkene coupling at the cobalt- $\alpha$ -(sp<sup>2</sup>)-carbon bond of **2**.<sup>3f</sup>



**Scheme 2-3.** Reaction of **2** with dimethyl maleate and dimethyl fumarate.

When the reaction of **2** and dimethyl fumarate was monitored by  $^1\text{H}$  NMR spectroscopy, the formation of **9-ZZ** was observed in addition to **9-ZE**; however, during the course of reaction the resonances for **9-ZZ** were gradually replaced by those of **9-ZE**. Complex **9-ZZ** was isolated in 58% yield by terminating a reaction of **2** and dimethyl fumarate after 2.5 h at 70 °C. In the  $^1\text{H}$  NMR spectrum ( $\text{CDCl}_3$ ) of **9-ZZ**, the three singlets assigned to the hydrogens of the pentadiene skeleton ( $\delta$  2.32, 2.58, and 4.16) resonate upfield of the corresponding resonances for **9-ZE**.

The observation that **9-ZZ** was formed during the course of the reaction between **2** and dimethyl fumarate suggested that the *ZZ*-isomer was thermally converted to the *ZE*-isomer under the reaction conditions. Heating a benzene- $d_6$  solution of isolated **9-ZZ** and monitoring the sample by  $^1\text{H}$  NMR spectroscopy confirmed thermal isomerization. Equilibrium was established after 116 h at 70 °C, with  $K_{\text{eq}} = [\text{9-ZE}]/[\text{9-ZZ}] = 38$  ( $\Delta G^\circ = 2.5$  kcal/mol).<sup>10,11</sup> The initial formation of **9-ZZ** from the trans alkene, dimethyl fumarate, over short periods of heating suggested that the reaction of **2** with a cis alkene such as dimethyl maleate should give the trans product **9-ZE** directly. Thus, a reaction of **2** with dimethyl maleate in benzene- $d_6$  at 70 °C was also monitored by  $^1\text{H}$  NMR spectroscopy and conversion to **9-ZE** (62% yield) was observed over the course of 70 h (Scheme 2-3). Only a trace amount of **9-ZZ** was observed during the reaction, consistent with the isolated thermal isomerization experiment.

X-ray crystallographic analysis of **9-ZE** and **9-ZZ** unambiguously established the anti relationship of cobalt and the ethyl ester substituent on C(3) of the  $\eta^4$ -1,4-pentadiene ligand (Figure 2-1).<sup>12</sup> For both complexes, the five-carbon pentadiene ligand exhibits a pronounced fold, with 57.2(2)° (**9-ZE**) and 61.27(7)° (**9-ZZ**) dihedral angles between the mean diene plane, C(1)-C(2)-C(4)-C(5), and the C(2)-C(3)-C(4) plane (Table 2-1). For comparison, the fold angle observed for the ( $\eta^5$ -C<sub>5</sub>H<sub>5</sub>)Co( $\eta^4$ -cyclopentadiene) complex, **6** (R = CO<sub>2</sub>Me), is 34.1(6)°. <sup>3e</sup> The C(1)-C(5) distance in **9-ZE** (2.880(4) Å) is longer than in **9-ZZ** (2.829(2) Å), and the O(7)-H(1) distance of 2.04 Å in **9-ZE** is well below the sum of the van der Waals radii of hydrogen and oxygen (2.6 Å; Table 2-15).<sup>13</sup>

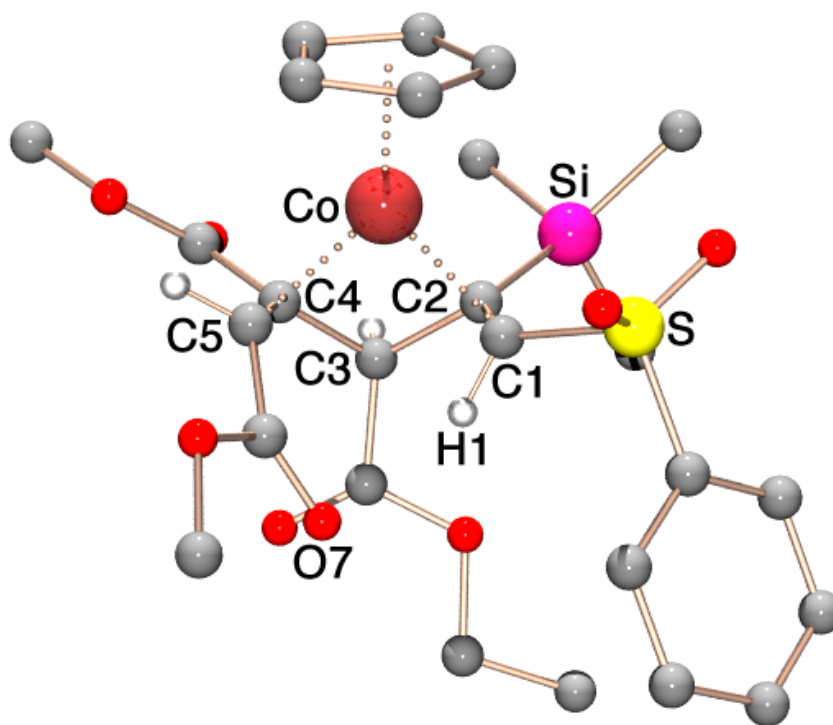
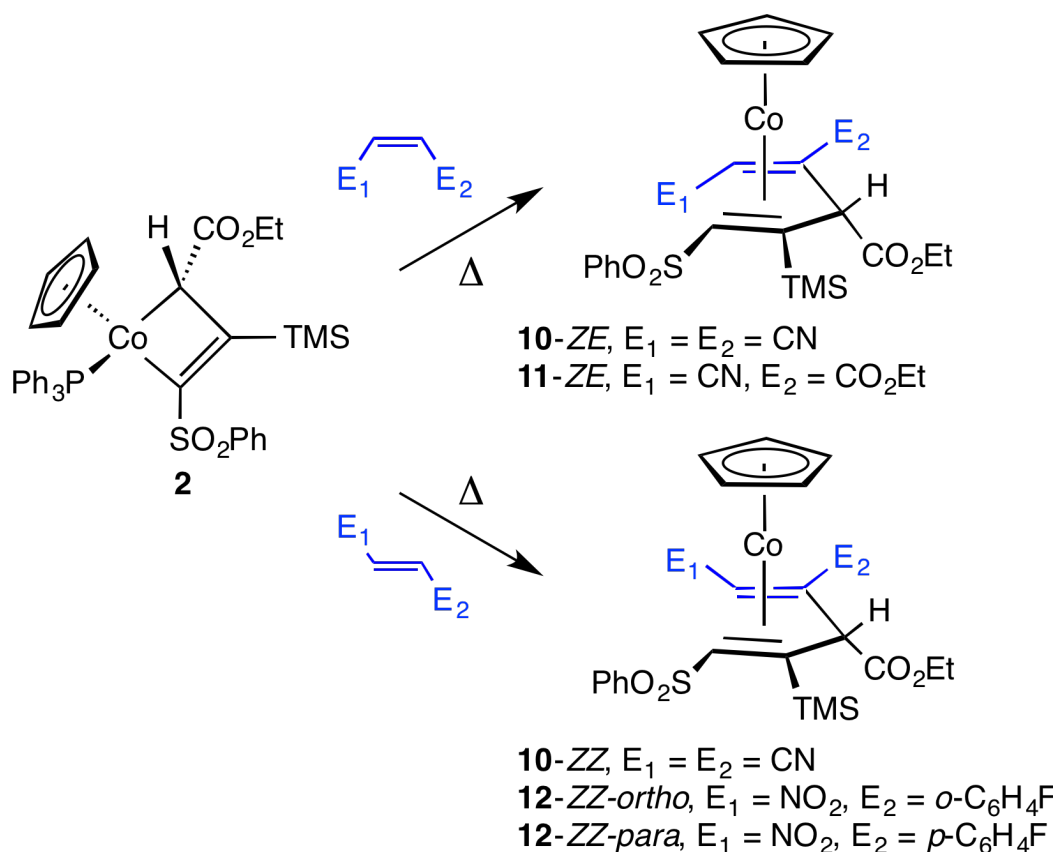


**Figure 2-1.** Solid-state structure of **9-ZE**. For clarity, only three hydrogen atoms are shown. CCDC Number 703132; refcode JOGWIM. R = 4.58%, Space Group *Pca2*<sub>1</sub>.

The formation of a *ZZ*-pentadiene product from the trans alkene dimethyl fumarate and a *ZE*-pentadiene product from the cis alkene dimethyl maleate suggested that a comparable study utilizing cis and trans isomers of a different alkene would yield similar isomerized products. In addition, it was thought that the further isomerization of **9-ZZ** to give **9-ZE** might result from a hydrogen-bonding interaction between the ester carbonyl O(7) to H(1) across the back of the 1,4-pentadiene skeleton. An alkene bearing linear substituents such as a nitrile might form products that lack the ability to engage in such secondary interactions. Heating a benzene-*d*<sub>6</sub> solution of **2** (12.7 mM) and fumaronitrile (101 mM) led to a 92% yield of **10-ZZ** after 11 h at 70 °C (Scheme 2-4). Prolonged heating of an analytically pure sample of **10-ZZ** at 70 °C led to slow decomposition, with no evidence for formation of **10-ZE**. Preparation of the (*Z*)-1,2-dicyanoethylene maleonitrile was accomplished by the base-catalyzed isomerization of fumaronitrile in acetonitrile.<sup>14</sup> The un-optimized reaction of **2** with an excess of maleonitrile gave **10-ZE** in low yield, and chromatographic purification and recrystallization of the NMR-scale reaction gave a small sample suitable for X-ray diffraction analysis, which confirmed the connectivity and relative stereochemistry.



**Scheme 2-4.** Reaction of **2** with acyclic alkenes.

To test regioselectivity with respect to the alkene, a dichloromethane solution of **2** (159 mg, 8.9 mM) and excess ethyl-*cis*- $\beta$ -cyanoacrylate (60 mM) was heated at 70 °C for 11 h. Chromatographic workup gave a mixture of **11-ZE** and a second minor product in combined 92% yield. Recrystallization of this sample led to isolation of **11-ZE** as analytically pure orange-red crystals in 81% yield (Scheme 2-4). X-ray diffraction analysis of **11-ZE** showed a similar  $\eta^4$ -1,4-pentadiene structure, with the ethyl ester substituent at the C(4) position and the nitrile at C(5). Analysis of the exploratory NMR-scale reaction of the same reaction indicated that trace amounts of a minor product were also formed in low



yield, which was tentatively identified as the  $ZE$ -C(4)<sub>CN</sub>-C(5)<sub>CO<sub>2</sub>Et</sub> regioisomer on the basis of similar NMR chemical shift values.

In an expansion of scope for the reaction of **2** with alkenes, as well as a further test of the regioselectivity, the reactions of 2- and 4-fluoro- $\beta$ -nitrostyrenes were tested. Heating a toluene solution of **2** (202.6, 7.3 mM) in the presence of 2-fluoro- $\beta$ -nitrostyrene (28 mM) for 26 h at 70 °C, followed by chromatographic workup gave **12-ZZ-ortho** in 54% yield. Similarly, the reaction of **2** (203.2 mg, 7.3 mM) in toluene with 4-fluoro- $\beta$ -nitrostyrene (28 mM) at 70 °C for 26 h gave **12-ZZ-para** in 53% yield. Observation of an NMR-scale reaction for the two substrates indicated that minor products were also formed in the course of the reaction, likely the  $ZE$  stereoisomers from thermal isomerization of the  $ZZ$  products. The nitro functionality of the nitrostyrenes was well-tolerated, although formation of 1,4-diene products occurred in reduced yield in comparison to that observed for the reaction of **2** with other acyclic alkenes, perhaps as a result of employing an alkene with only one major electron-withdrawing substituent.

The 1,4-pentadiene bonding motif is not uncommon for organometallic species, however, the vast majority of these complexes are in the form of simple metal-bound hydrocarbon ring structures such as  $\eta^4$ -norbornadiene,  $\eta^4$ -bicyclo[2.2.2]octa-2,5-diene (klovosene),  $\eta^4$ -benzoquinone,  $\eta^4$ -fulvene, and  $\eta^4$ -cyclohexa-, hepta-, and octa-1,4-diene. An acyclic  $\eta^4$ -1,4-pentadiene structure is exceedingly rare, with only five other structurally characterized examples, including  $[(Cl)_2Pt(\eta^5-H_2C=CHCH_2CH=CH_2)]$  (**CLPPTA**),<sup>15a</sup>  $[\eta^2-(1,3-(tBu)_2-$

$\text{acac}_2\text{Rh}(\eta^5\text{-CH}(\text{CF}_3)\text{=C}(\text{CF}_3)\text{C}(\text{=CMe}_2)\text{CH=CH}_2)]$  (**PVMFRI**),<sup>15b</sup>  $[(\text{CO})_3\text{Fe}(\eta^5\text{-H}_2\text{C=C}(\text{-C}(\text{=O})\text{OCH}_2)\text{-CHCH=CH}_2)]$  (**MVHFUI10**),<sup>12b</sup>  $[(\eta^5\text{-C}_5\text{Me}_5)\text{Rh}(\eta^5\text{-CH}(\text{Ph})\text{=CHC}(\text{=O})\text{CH=CH}(\text{Ph}))]$  (**BZAMCR10**),<sup>15c</sup> and  $[(\eta^5\text{-C}_5\text{Me}_5)(\text{Cl})\text{Rh}(\eta^5\text{-CH}(\text{Ph})\text{=CHCH}(\text{OTMS})\text{CH=CH}_2)]$  (**PONFED**) (Figure 2-2).<sup>12a</sup>

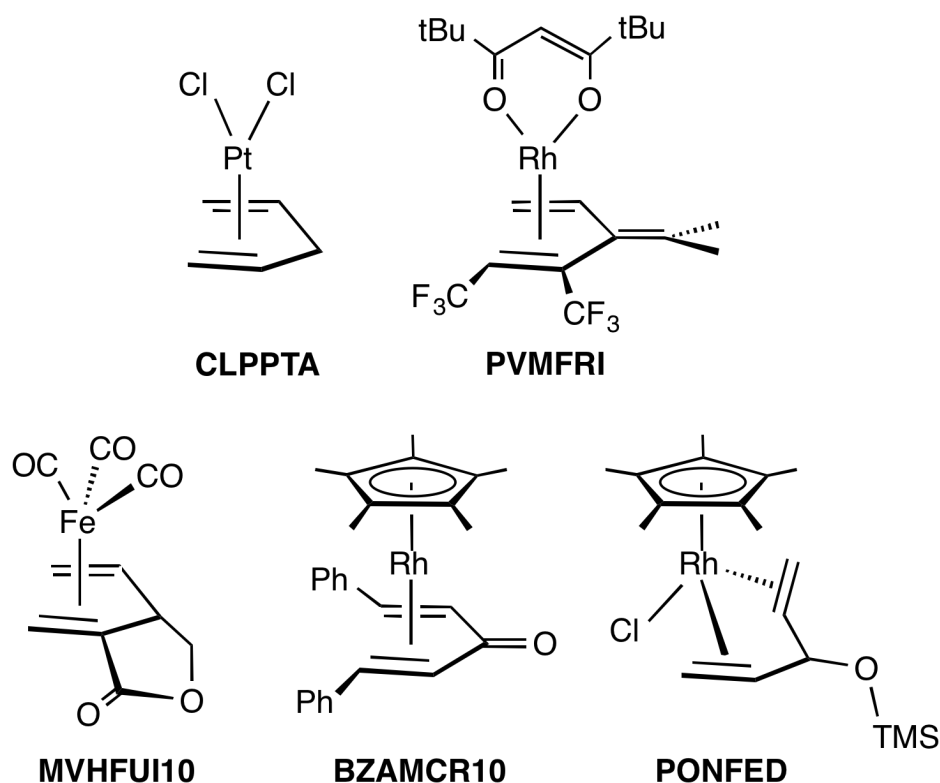


**Figure 2-2.** Crystallographically characterized examples of  $\eta^4$ -1,4-pentadiene complexes. Identified by CSD Refcode.

Typical alkene-metal binding will result in an elongation of the carbon-carbon bond length of the coordinated alkene due to back-bonding of electron density from the metal into the  $\pi^*$  orbitals, the extent of which is dependent on orbital overlap, as well as the nature of substituents on the alkene. Electron-withdrawing alkene substituents typically increase  $\pi$  back-bonding by introducing

a partial positive charge and an increased electrophilic character. The  $\eta^4$ -1,4-pentadienes formed from reaction of **2** with acyclic alkenes results in a significant elongation of the alkene carbon-carbon bond, but to a lesser extent than with other similar complexes, as summarized in Table 2-1. A second consequence of this back-bonding interaction is a partial rehybridization of the alkene carbons from purely  $sp^2$  to more  $sp^3$ -like, resulting in a bend-back angle of the alkene substituents away from the formerly planar alkene. A measure of this interaction is the bend-back parameter  $\alpha$ , which is the angle formed by the two normal vectors describing the planes containing each alkene carbon and its two substituents.<sup>16</sup> Complexes **9-12** feature a relatively substantial bend-back angle, resulting in a range of bend-back parameters between 42.6-54.0°, much greater than that found for  $(\eta^5\text{-C}_5\text{Me}_5)\text{Rh}(\eta^4\text{-CH(Ph)=CHC(=O)CH=CH(Ph)})$ , with an  $\alpha$  value of 27.2° and 28.3°. The complex  $(\eta^5\text{-C}_5\text{Me}_5)\text{Rh}(\eta^4\text{-CH(Ph)=CHCH(OTMS)CH=CH}_2)$  has similar bend-back parameter values, but is only indirectly comparable as it contains two nearly orthogonal alkene ligands ( $\alpha$  values of 54.4° and 52.0°), in comparison to the nearly planar alkene ligands in complexes **9-12**. The lack of structural data for other 1,4-pentadiene complexes doesn't allow for the calculation of this parameter. A third pertinent geometric feature of these complexes is the fold angle formed between the four planar alkene carbons and the three-carbon inner flap comprised by the two inner alkene carbons and the bridging  $sp^3$ -carbon. This fold angle is quite substantial for complexes **9-12**, with angles between 58.1(3)° and 61.7(4)°, which is much

larger in comparison to the fold angle of other structurally characterized  $\eta^4$ -1,4-pentadienes. This fold angle is particularly large in comparison to  $\eta^4$ -1,3-cyclopentadienes such as those formed by the reaction of **2** with alkynes, which typically feature a fold angle in the range (33.5-36.4°).<sup>3e,7,17</sup>

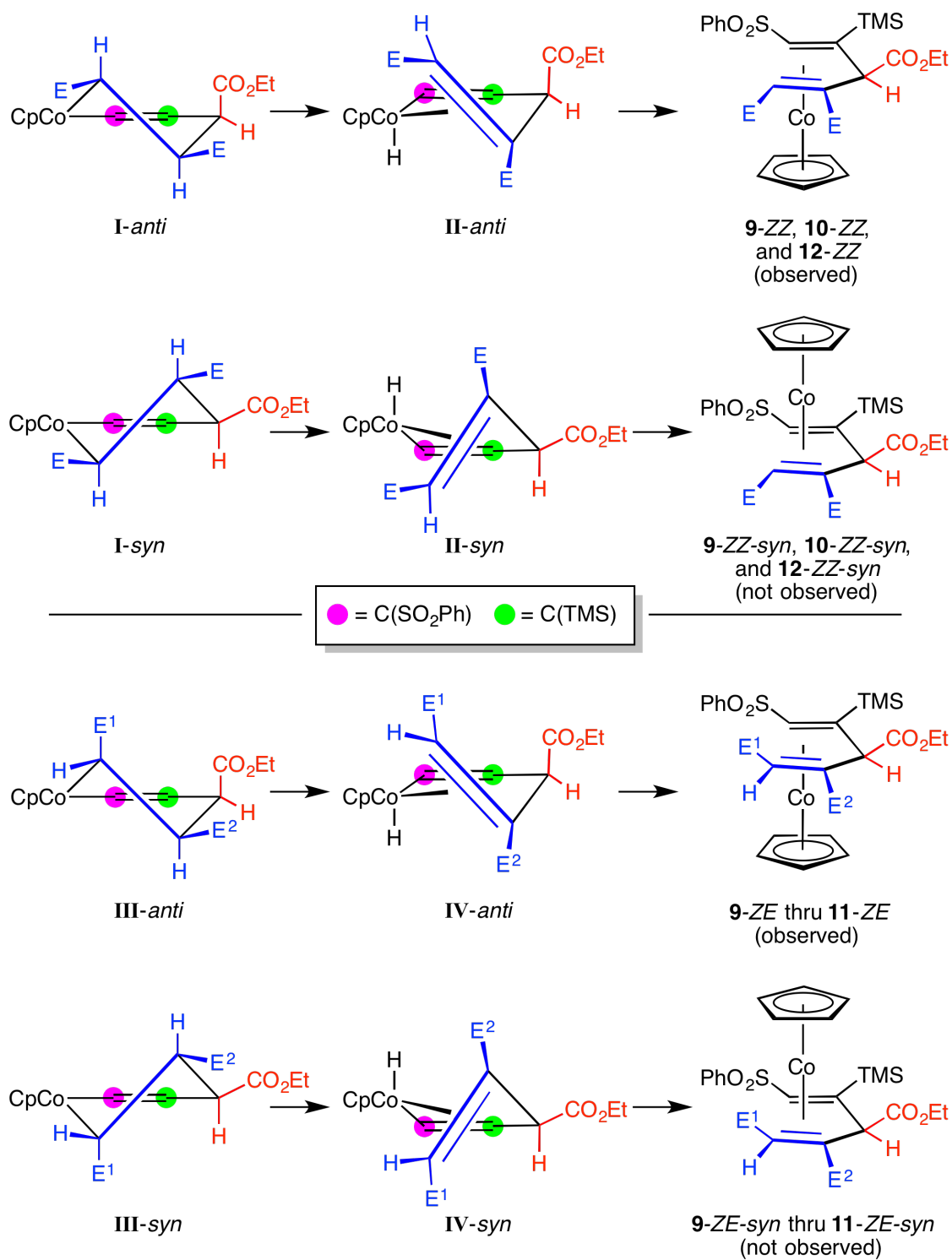
**Table 2-1.** Alkene bond distances [Å], bend-back parameters [°], and fold angles [°] for  $\eta^4$ -1,4-pentadiene complexes.<sup>a,b</sup>

<b>Cmpd No.:</b>	C(1)-C(2)	$\alpha(\vec{n}_1, \vec{n}_2)$	C(4)-C(5)	$\alpha(\vec{n}_4, \vec{n}_5)$	Fold angle
<b>BZAMCR10</b> <sup>15c</sup>	1.405	27.22	1.416	28.32	27.47
<b>MVHFUI10</b> <sup>12b</sup>	1.4027		1.3697		52.42
<b>PONFED</b> <sup>12a</sup>	1.40(1)	54.41	1.33(1)	52.03	45.28
<b>9-ZZ</b> JOGWIM <sup>6</sup>	1.4298(16)	44.16	1.4208(16)	54.00	61.26(10)
<b>9-ZE</b> JOKXAJ <sup>6</sup>	1.433(4)	44.98	1.423(5)	42.61	58.1(3)
<b>10-ZZ</b> JOGWOS <sup>6</sup>	1.428(3)	49.43	1.437(3)	45.88	60.24
<b>10-ZE</b>	1.417(6)	47.47	1.436(6)	45.19	61.7(4)
<b>11-ZE</b> JOGWUY <sup>6</sup>	1.430(2)	47.56	1.428(2)	42.85	59.96(14)
<b>12-ZZ-ortho</b>	1.449(9)	50.83	1.414(10)	53.01	61.4(5)
<b>12-ZZ-para</b>	1.431(3)	51.07	1.425(3)	51.06	60.97(18)

(a) calculation details and formulae included in Experimental Section. (b) see Figure 2-2 for **BZAMCR10**, **MCVHFUI10**, and **PONFED** structures.

The observation that cis alkenes form *ZE*-dienes, whereas trans alkenes generate *ZZ*-dienes, is consistent with a mechanism that involves the formation of metallacyclohexene intermediates from coupling of the alkene with the  $sp^3$ -

carbon of the metallacyclobutene ring (Scheme 2-5). Subsequent  $\beta$ -hydride elimination and reductive elimination would then generate the observed products. For trans alkenes, two metallacyclohexene diastereomers are possible: **I-anti**, from addition to the *re,re*-face of the alkene; and **I-syn**, from addition to the *si,si*-face (Scheme 2-5, top).  $\beta$ -Hydride elimination from **I-anti** leads to cobalt-hydride **II-anti**, followed by reductive elimination to the observed anti products (**9-ZZ**, **10-ZZ**, **12-ZZ-ortho**, and **12-ZZ-para**) – with cobalt and CO<sub>2</sub>Et on opposite faces of the diene ligand. Alternatively, the formation of **I-syn** would sequentially lead to **II-syn** and syn diene complexes – with cobalt and the ethyl ester on the same face of the diene. The  $\beta$ -hydride elimination pathway is prevented in the syn pathway by preferential coordination to the ester carbonyl. A similar analysis applies to the reaction of **2** with cis alkenes (Scheme 2-5, bottom).



**Scheme 2-5.** Proposed metallacyclohexene to 1,4-diene conversion of trans alkenes (top) and cis alkenes (bottom).

Formally, metallacyclohexene intermediates **I** and **III** are electronically unsaturated 16-electron species, but can attain electronic saturation by either coordinating the ester carbonyl, or by  $\beta$ -hydride elimination and progression to 1,4-diene product. A Newman projection of these intermediates clearly establishes the relationship between the  $\beta$ -hydrogen and the ethyl ester necessary to accommodate the  $\beta$ -hydride elimination (Figure 2-3). For example, intermediate **III-syn** contains the ester and the  $\beta$ -hydrogen in a gauche conformation; oxidative addition of the C-H bond is prevented by coordination of the ester carbonyl, which lies on the same side of the ring as the metal and  $\beta$ -hydrogen. In intermediate **III-anti**, however, the ester and  $\beta$ -hydrogen are in a 1,2-diaxial conformation, and cobalt can bend toward the  $\beta$ -hydrogen without coordination of the ester carbonyl, ultimately affecting conversion to product.

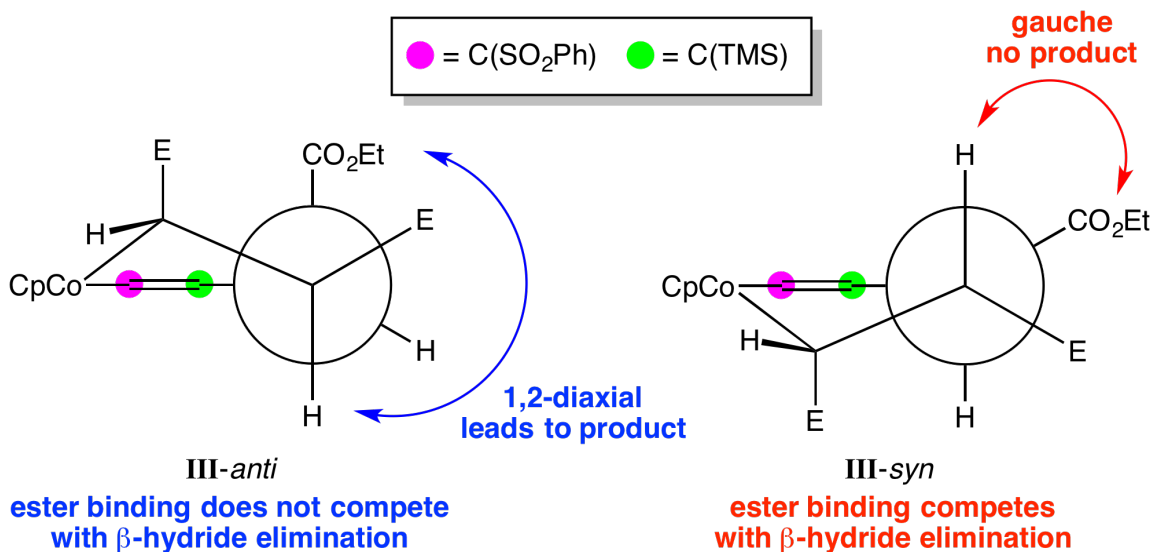
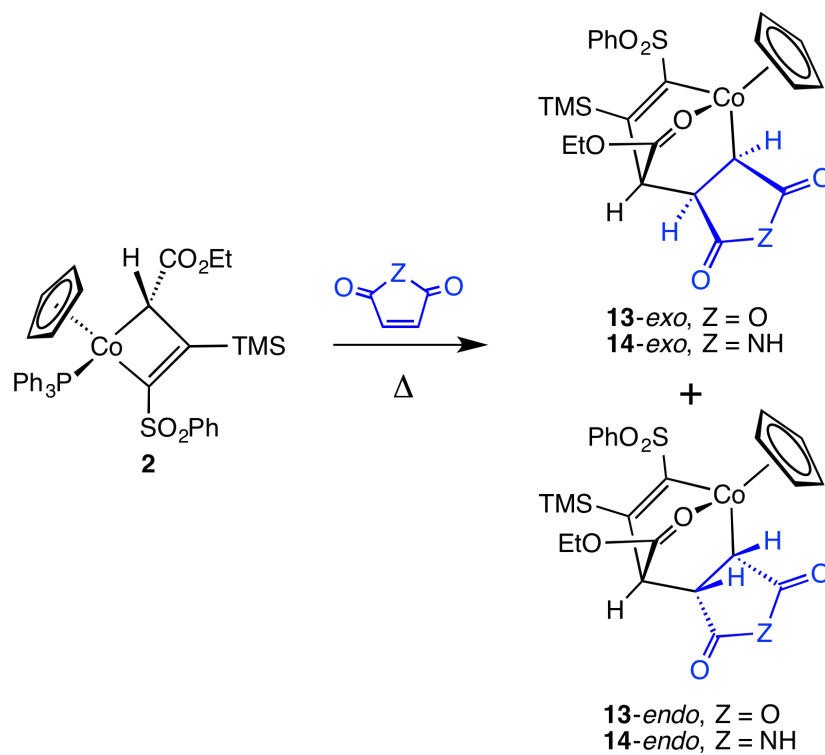


**Figure 2-3.** Metallacyclohexene conformers in the reaction of **2** with acyclic cis alkenes.

The conformational requirement that the ethyl ester and  $\beta$ -hydrogen are trans across the newly formed carbon-carbon bond precludes the possibility of 1,4-diene products arising from the **I-syn** and **III-syn** pathways. Additionally, this mechanism readily accounts for the observation that trans alkenes give *ZZ*-products and cis alkenes give *ZE*-products – the syn-periplanar arrangement of cobalt and the  $\beta$ -hydrogen requires torsion of the metallacyclohexene ring that isomerizes the arrangement of substituents during the  $\beta$ -hydride elimination. Finally, this mechanism suggests that the metallacyclohexene intermediate formed from the reaction of **2** with a small-ring cyclic alkene will not undergo  $\beta$ -hydride elimination due to ring constraints, thereby permitting observation of metallacyclohexenes related to **I** and **III**.

The possibility that metallacyclohexene intermediates were involved in the formation of products **9-12** led us to explore the reactions of **2** with cyclic alkenes in the hopes of isolating these putative species as stable products. Heating a toluene solution of **2** (12.8 mM) and excess maleic anhydride (62 mM) led to the isolation of both **13-exo** (50% yield) and **13-endo** (42%) as air-stable solids (Scheme 2-6, Figure 2-4). Similarly, heating a solution of **2** (5.8 mM) in toluene in the presence of maleimide (25 mM) gave **14-exo** and **14-endo** in 42% and 60% yield, respectively.





**Scheme 2-6.** Reaction of **2** with maleic anhydride and maleimide.

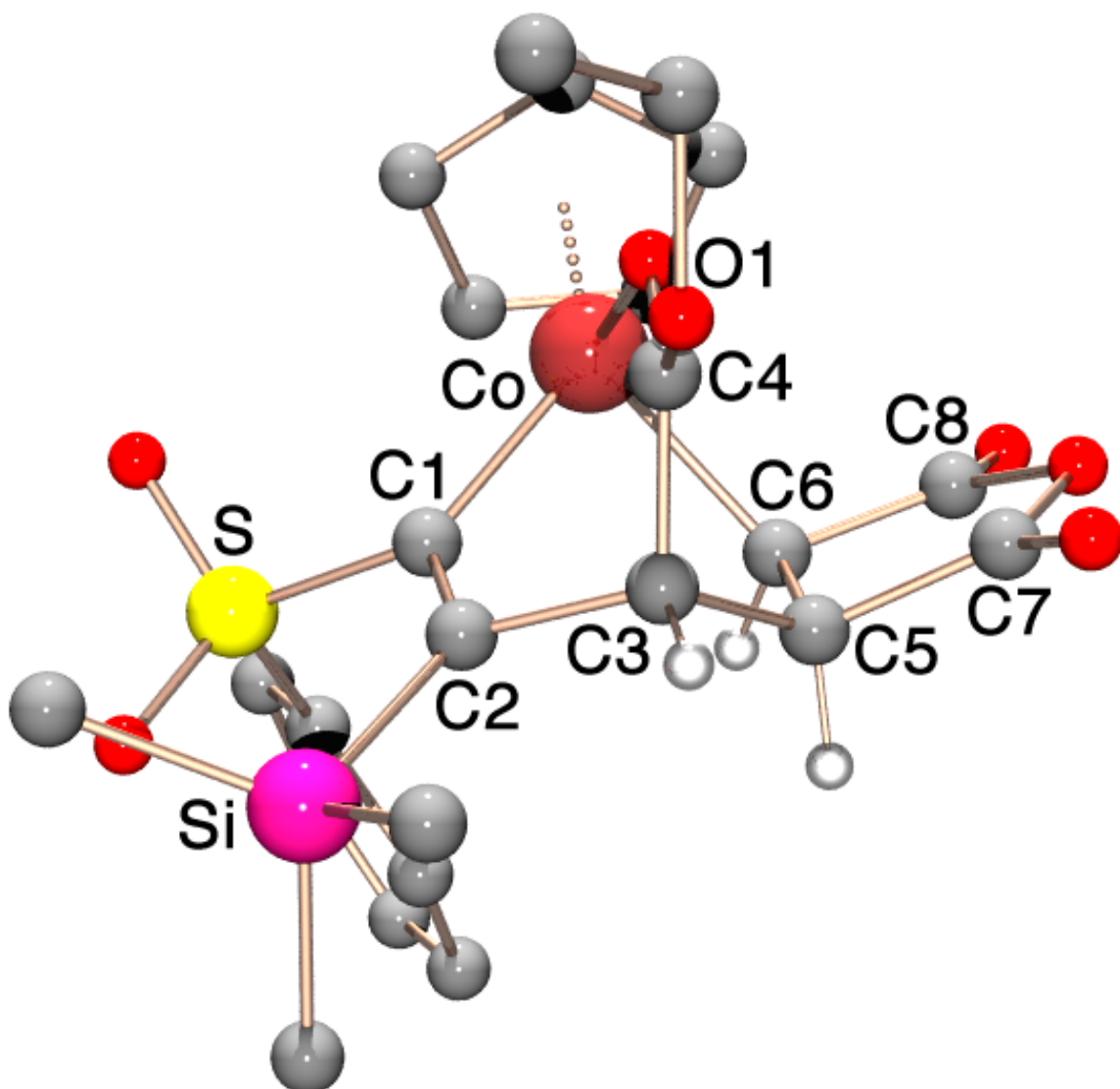


**Figure 2-4.** Solid-state structure of **13-exo**. For clarity, only three hydrogen atoms are shown. CCDC Number 703137; refcode JOKXEN. R = 2.77%, Space Group  $P2_1/n$ .

Crystallographic analysis of the products from reaction of **2** with maleic anhydride and maleimide showed a unique and highly-substituted 2-oxa-1-metalla-(7,8)-dihydrobarrelene structure, with the newly incorporated ring from the cyclic alkene in either an endo or exo configuration with respect to the bicyclo[2.2.2]octa-2,5,7-triene fragment (Figure 2-4).<sup>18a</sup> Organometallic species

with a transition metal incorporated into a barrelene-like ring structure are rare. One pertinent example is work by Bleeke and co-workers, who demonstrated the cycloaddition reactions of a tris(triethylphosphine)-substituted "iridabenzene" with a number of substrates, including with maleic anhydride (**RIFCIS**; Figure 2-5).<sup>18b</sup> Dioxygen and carbon disulfide also react with this same iridabenzene to give similar barrelene-type structures, the latter of which can lose phosphine to form dimeric and trimeric SO<sub>2</sub>-containing barrelene oligomers.<sup>18c</sup> Haley reports a comparable iridabenzene system to Bleeke, which can also react with atmospheric oxygen to give a similar endoperoxide-bridged iridabarrelene complex.<sup>18d</sup> Finally, Frühauf has reported on the reactions of  $\alpha$ -diimine iron and ruthenium(tricarbonyl) complexes which can undergo 1,3-dipolar cycloadditions with alkynes with subsequent CO-migration to give iron species with imine and amide moieties incorporated into the barrelene ring structure (**DACREE**; Figure 2-5).<sup>18-g</sup>

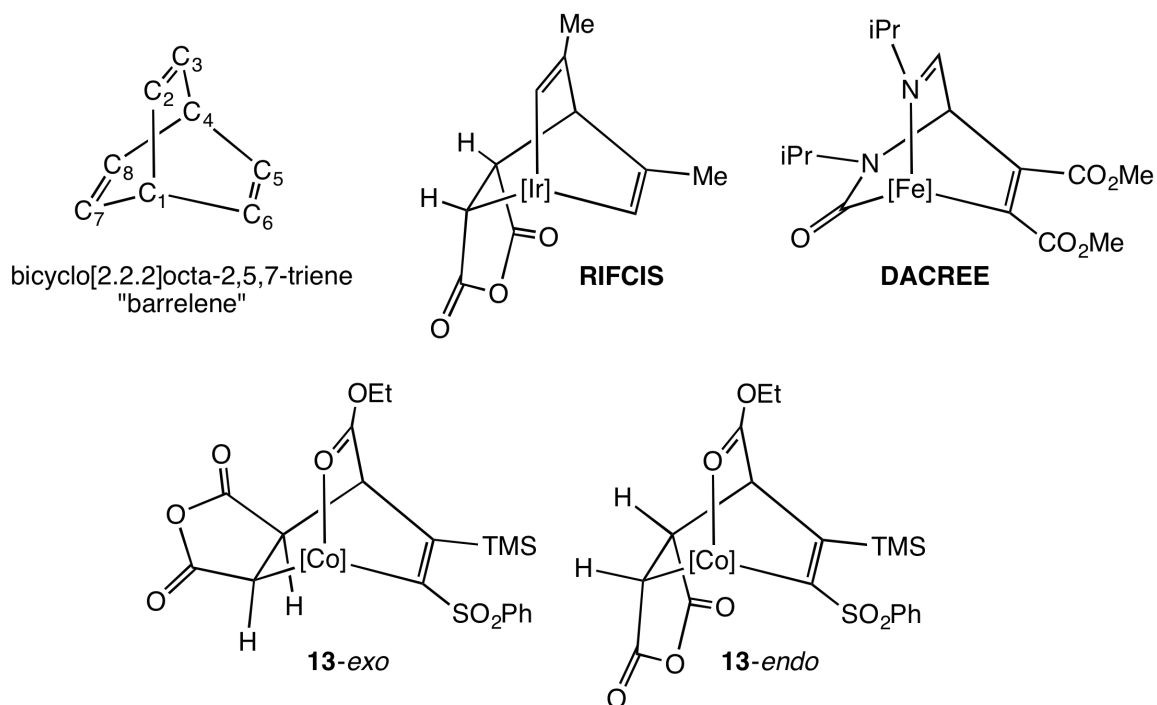
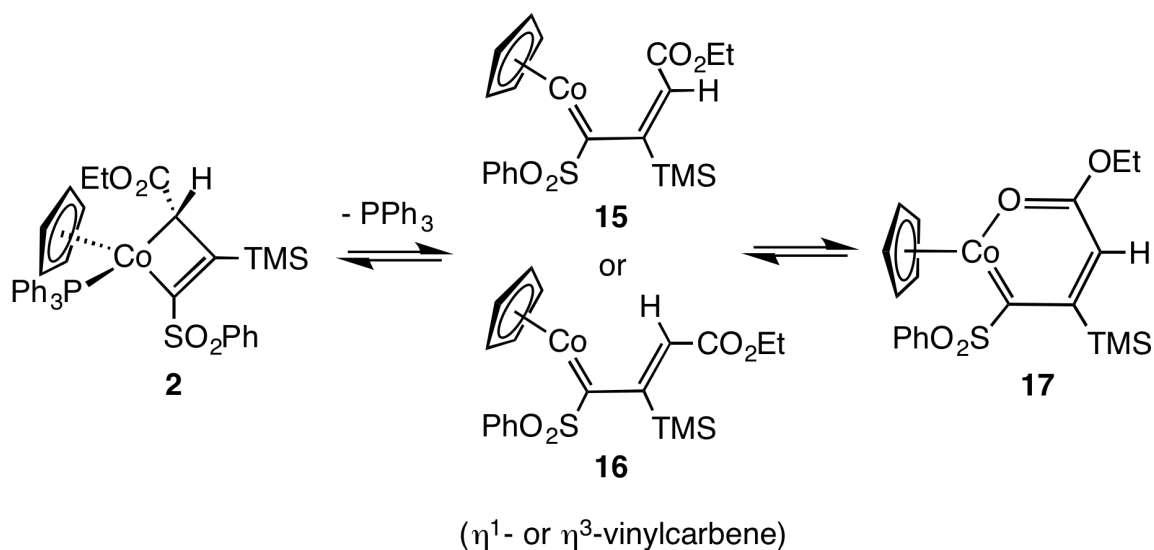


**Figure 2.5.** Barrelene-type structures formed from maleic anhydride. For clarity, the  $L_nM$  ligand set is abbreviated as [M]. For **RIFCIS**, [Ir] =  $(PEt_3)_3Ir$ ; for **DACREE**, [Fe] =  $(P(OMe)_3)(CO)_2Fe$ ; For **13-exo** and **13-endo**, [Co] =  $(\eta^5-C_5H_5)Co$ .

Products **13-exo** and **14-exo** have the appropriate relationship between the  $\beta$ -hydrogen and the ethyl ester to proceed to *anti*-1,4-pentadiene products – the reaction progression is arrested however, due to the ring constraints of the cyclic alkene employed. Furthermore, these exo products account for only half of the product formed in the reactions of **2** with maleic anhydride and maleimide; nearly equal amounts of **13-endo** and **14-endo** are also formed, respectively. In the case of acyclic alkenes however, it appears as though the reaction is completely selective to give the anti product, which would form from intermediates similar to products **13-exo** and **14-exo**. There is no evidence for the formation of metallacyclohexene products similar to **13-endo** and **14-endo**. The

complete absence of these products suggests the possibility that there is a measure of reversibility to the reactions of **2** with alkenes, although the reactivity of **2** with cyclic and acyclic alkenes could proceed through different mechanisms. Alternatively, the reactions of **2** with acyclic alkenes could be selective due to steric arguments, whereas the cyclic alkenes successfully employed were sufficiently tied back to reduce steric pressure, and allow for a mixture of diastereomers.

Two fundamentally distinct mechanisms for the key carbon-carbon bond-forming step in the conversion of **2** to metallacyclohexene intermediates are (1) alkene coordination and insertion into the cobalt-(sp<sup>3</sup>)-carbon bond of the metallacycle ring, and (2) ring-opening of the metallacyclobutene to a vinylcarbene (**15-17**, Scheme 2-7), which then undergoes a [4 + 2]-cycloaddition reaction with the alkene to form **I/III**. We believe the former mechanism to be unlikely since it requires that CO and carbenes insert into the cobalt-(sp<sup>2</sup>)-carbon bond of the metallacycle, but that alkenes insert into the cobalt-(sp<sup>3</sup>)-carbon bond. Alternatively, a vinylcarbene mechanism provides a reasonable explanation for the selectivity observed with CO, carbenes, and alkenes. Additionally, a [4 + 2] cycloaddition mechanism may more readily facilitate reversibility in the course of these reactions, which would otherwise require a  $\beta$ -carbon elimination if the reaction proceeded through an insertion mechanism.



**Scheme 2-7.** Potential vinylcarbene intermediates. Compounds **15** and **16** may involve either monohapto or trihapto coordination, but are depicted as the η<sup>1</sup>-vinylcarbene.

To test the possibility that the reactions of **2** with alkenes are reversible, a CDCl<sub>3</sub> solution (0.6 mL) of isolated, crystalline **13-*exo*** (4.3 mg, 13 mM) and excess maleic anhydride (110 mM) was heated under nitrogen at 70 °C. After 3 h of heating, analysis by <sup>1</sup>H NMR spectroscopy indicated the formation of a trace amount of **13-*endo*** (Figure 2-41). A similar experiment conducted with crystalline **13-*endo*** (3.4 mg, 10 mM) and maleic anhydride (116 mM) in CDCl<sub>3</sub> (4h, 70 °C) did not, however, exhibit any formation of the **13-*exo*** isomer (Figure 2-43). As the formation of **13-*endo*** from **13-*exo*** was relatively minor in the former, and the formation of **13-*exo*** from **13-*endo*** completely absent in the latter, these results suggest that the reaction of metallacyclobutene **2** with maleic anhydride gave a kinetic mixture of products, with the product ratio ultimately unaffected by thermodynamic selection through a reversible process. These results do suggest

that the reaction may include reversible processes, although to a very limited extent.

As a further test of possible reversibility for the reactions of **2**, a set of experiments were conducted whereby metallacyclohexenes **13-*exo*** and **13-*endo*** were heated in the presence of the alkyne dimethyl acetylenedicarboxylate (DMAD). Alkynes were previously demonstrated to form ( $\eta^5\text{-C}_5\text{H}_5$ )Co( $\eta^4$ -1,3-cyclopentadiene) complexes from reaction with **2**, and it was thought that these  $\eta^4$ -cyclopentadiene products would be less likely to exhibit reversibility than products **13**.<sup>3e,7,17</sup> Additionally, it was expected that alkynes were likely to react more quickly with metallacyclobutene **2** than their alkene counterparts. Finally, the methyl diester-substituted acetylene DMAD was the most reactive alkyne substrate evaluated with metallacyclobutene **2**, and gave a single diastereomer in near quantitative yield; thus, it was anticipated that this substrate might serve as an effective, irreversible trap for the putative reactive intermediate formed on the reaction coordinate between **2** and either **13-*exo*** or **13-*endo***. When a solution ( $\text{CDCl}_3$ ) of **13-*exo*** (4.5 mg, 14 mM) was heated in the presence of DMAD (271 mM) for 4 h at 70 °C, a small amount of the expected ( $\eta^5\text{-C}_5\text{H}_5$ )Co( $\eta^4$ -1,3-[ $\text{C}(\text{SO}_2\text{Ph})=\text{C}(\text{TMS})\text{CH}(\text{CO}_2\text{Et})\text{C}(\text{CO}_2\text{Me})=\text{CO}_2\text{Me}$ ]-]) complex was observed to form (Figure 2-45). Similarly, when a  $\text{CDCl}_3$  solution of **13-*endo*** (4.4 mg, 13 mM) was heated (4 h, 70 °C) in the presence of DMAD (271 mM), a trace amount of the  $\eta^4$ -1,3-cyclopentadiene was also observed to form, further demonstrating that

the reactions of **2** with cyclic alkenes may display some small measure of reversibility (Figure 2-47).

The tricyclic structures observed for **13-14** raise the intriguing possibility that the cyclic vinylcarbene intermediate **17** may play an important role in this novel alkene chemistry. We therefore examined the structure of a model complex,  $(\eta^5\text{-C}_5\text{H}_5)\text{Co}[\kappa^2\text{-(C,O)-C(SO}_2\text{Me)C(SiH}_3\text{)CH(CO}_2\text{Me)}]$  **18**, using quantum mechanical (QM) methods (Figure 2-6).<sup>19-26</sup> Comparisons of the bond distances in **18** with those in **13-exo** and **14-exo** indicate a significant degree of Co-C(1) and C(2)-C(3) double-bond character in **18** (Co-C(1) = 1.965(1) and 1.968(2) Å, C(2)-C(3) = 1.541(2) and 1.545(2) Å, for **13-exo** and **14-exo**, respectively). The orbital coefficient on cobalt in the HOMO of **18** (Figure 2-6, right structure) and the planar six-membered ring structure are ideally disposed for participation in a [4 + 2]-cycloaddition reaction.<sup>27-29</sup>

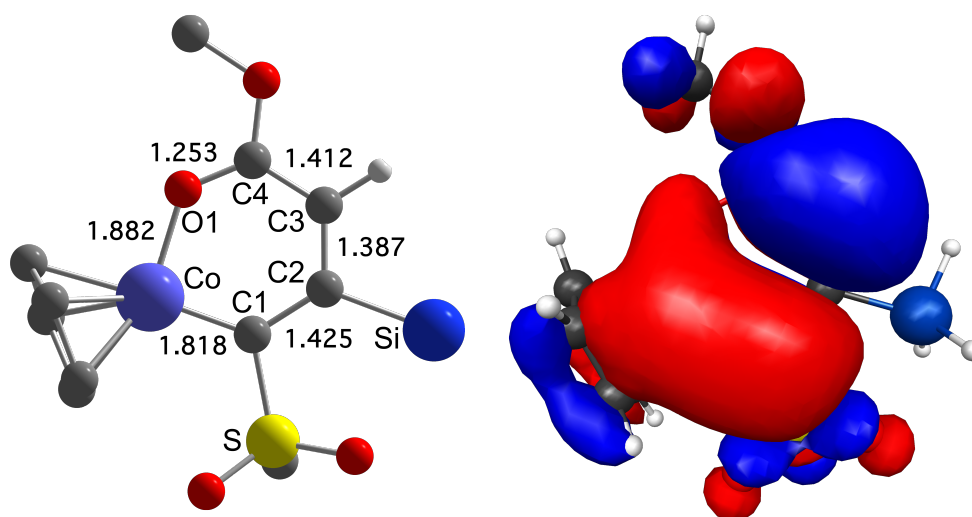


**Figure 2-6.** (Left) QM-computed structure for **18** [Å]; (Right) HOMO of **18**, which has a primary contribution from the  $d_{xy}$  and  $d_{yz}$  orbitals.



In principle, reactions of **2** with alkenes could proceed via a cyclization reaction from vinylcarbenes **15** or **16**, or from an oxametallabenzene such as **17**, which has an internal vinylcarbene fragment. The metallacyclohexene products or intermediates that arise from a cyclization reaction have four contiguous stereocenters, including Co, C(3), C(5), and C(6). The metallacyclobutene starting material is racemic, with an  $R^{Co}S^{C3}/S^{Co}R^{C3}$  configuration, and thus the products that arise from reaction with an achiral alkene are racemic. Additionally, the possibility of either an endo or exo approach of the alkene prior to reaction results in diastereomeric endo and exo isomers. For example, the reaction of **2** with maleic anhydride gives **13-exo** with relative stereochemistry  $S^{Co}S^{C6}S^{C5}R^{C3}/R^{Co}R^{C6}R^{C5}S^{C3}$ , and the diastereomeric set of **13-endo** enantiomers, with relative stereochemistry  $S^{Co}R^{C6}R^{C5}R^{C3}/R^{Co}S^{C6}S^{C5}S^{C3}$ . A careful analysis of the transition state structures arising from reaction of maleic anhydride with acyclic “metallabutadienes” **15-17** demonstrates that intermediates **15** and **17** can both proceed to give identical products with the appropriate relative stereochemistry (as confirmed by X-ray diffraction analysis), whereas intermediate **16** would give rise to four diastereomers with the incorrect stereochemical configurations (Figure 2-7).

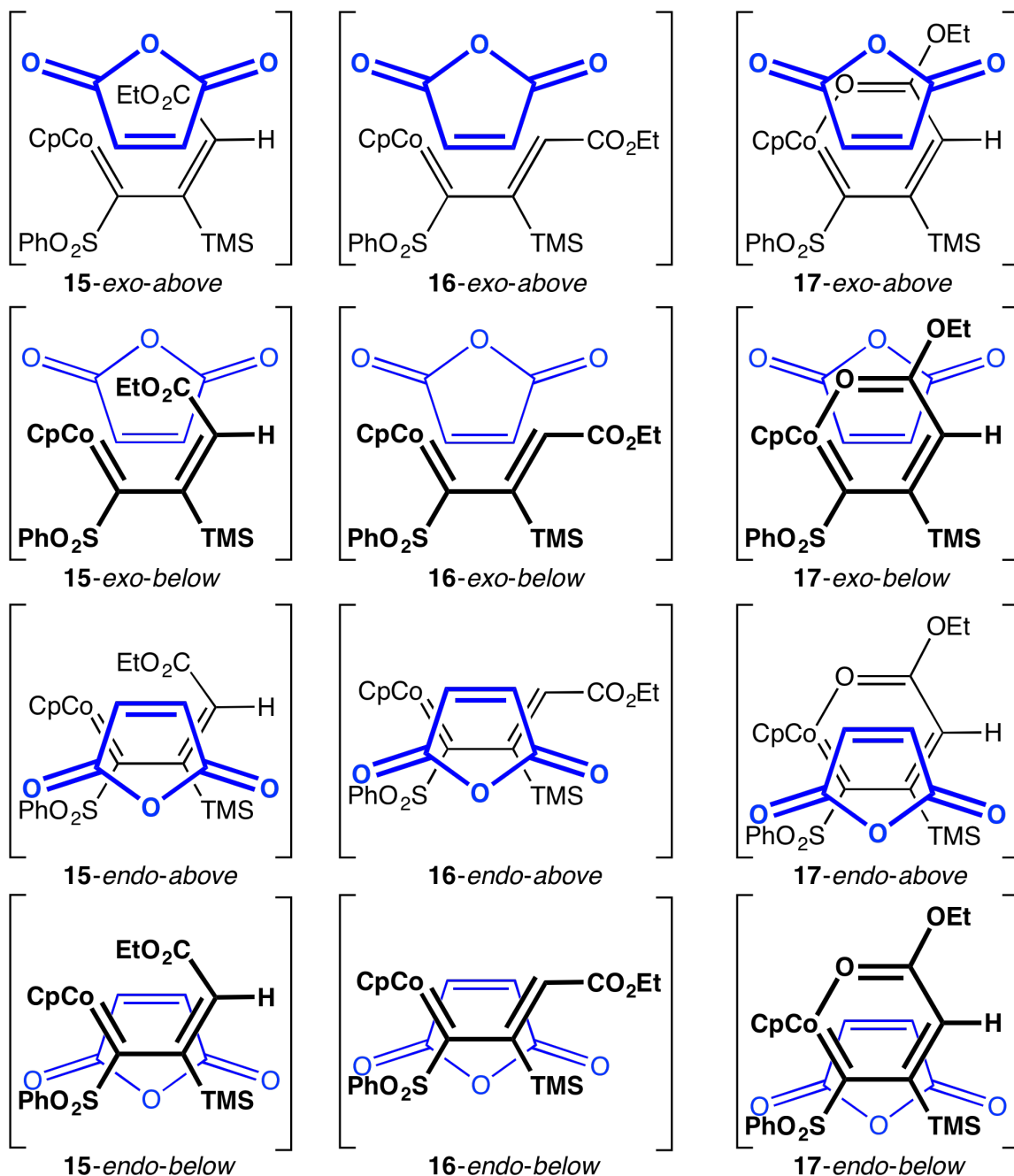


**Figure 2-7.** Possible transition state structures for reaction of maleic anhydride with intermediates 15-17, accounting for all diastereomeric products.

For a [4 + 2]-cycloaddition reaction to proceed to product, the frontier molecular orbitals of the butadiene and alkene fragments must be sufficiently matched in terms of orbital symmetry as well as energy. For a 'normal' electron

demand Diels-Alder reaction, the HOMO of the butadiene fragment – in this case a “metallabutadiene” such as **15-17** – interacts with the LUMO of an alkene. Intermediates such as **15-17** contain a metal in place of a carbon, and therefore might be expected to be particularly electron-rich as compared to a normal hydrocarbon-based butadiene fragment. Typical Diels-Alder reactions often make use of an “electronically activated” alkene which has electron-withdrawing substituents such as a cyano or carbonyl adjacent to one or both of the alkene carbons, and which has the effect of lowering the energy of the alkene LUMO. This activation creates a better energy match between the HOMO of the butadiene, and the LUMO of the alkene, and results in a significant increase in the speed of reaction.<sup>30</sup> For reactions of **2** with alkenes, it appears necessary for the alkene moiety to possess electron-withdrawing groups in order for the reaction to proceed. Reactions with cyclic alkenes bearing a carbonyl immediately adjacent to the alkene carbons proceeded most quickly, as was demonstrated with maleic anhydride and maleimide; the speed of this reaction can be rationalized by both the presence of electron-withdrawing groups, as well as the relief of ring-strain in the resultant products.<sup>31</sup> Reactions with acyclic trans alkenes proceeded more quickly than alkenes with a cis arrangement of functional groups. For both cis and trans alkenes, reactions with **2** proceeded more quickly with cyano substituents in comparison to esters. Alkenes with just one major electron-withdrawing group give product in their reaction with **2**, as was demonstrated with the alkenes 2- and 4-fluoro- $\beta$ -nitrostyrene – though these

reactions proceeded more slowly and gave lower yield. For alkenes without any electron-withdrawing group, such as styrene, metallacyclobutene **2** failed to react. Initial studies analyzed by  $^1\text{H}$  NMR spectroscopy suggest that benzoquinone and Super Glue<sup>TM</sup> (methyl-2-cyanoacrylate) both react with **2**, though the former analysis was plagued by solubility issues, while the latter presented difficulties due to polymerization of substrate. The long reaction times required and low yields obtained from reaction of **2** with alkenes such as the fluoro-substituted nitrostyrenes, or dimethyl maleate or fumarate, suggest that there may be a minimum electronic activation required to ensure reactivity. The Hammett  $\sigma_{\text{P}}$  parameter is a useful gauge for describing the relative electron-withdrawing abilities for various substituents, and values for relevant functional groups in the alkenes employed are tabulated in Table 2-2.<sup>32,33</sup> The minimal electronic activation needed to ensure reactivity of an alkene with metallacyclobutene **2** appears to be the presence of two electron-withdrawing groups having a minimum  $\sigma_{\text{P}}$  value of  $\sim 0.3$ - $0.45$ , or at least one major electron-withdrawing group such as a nitro moiety, though further experimentation would be required to ascertain this value conclusively. Furthermore, the reactivity of metallacyclobutene **2** with electron-rich alkenes remains predominantly unexplored.

**Table 2-2.** Hammett  $\sigma_P$  parameter for various functional groups.

<b>Substituent</b>	$\sigma_P$	<b>Substituent</b>	$\sigma_P$
H	0.000	NO <sub>2</sub>	0.778
C <sub>6</sub> H <sub>5</sub>	-0.01	F	0.062
CO <sub>2</sub> Et	0.45	SO <sub>2</sub> Ph	0.71 <sup>33</sup>
CN	0.660	SiMe <sub>3</sub>	-0.070

In addition to calculating the molecular orbitals for the model complex **18**, which include a HOMO ideally disposed to participate in a [4 + 2]-cycloaddition reaction, an electrostatic potential energy map was generated which shows the three-dimensional charge distribution for this molecule (Figure 2-8). This map shows a molecule with partial positive charge buildup at the cobalt metal center, the C(2) position functionalized with the silyl substituent, and at the C(4) carbonyl carbon of the methyl ester. Additionally, the C(3) position shows a buildup of partial negative charge. The charge distribution of model complex **18** is in many ways similar to that of the popularly known Danishefsky diene (or Kitahara diene), a very electron-rich and regioselective butadiene often employed as a reagent in Diels-Alder reactions.<sup>34</sup>

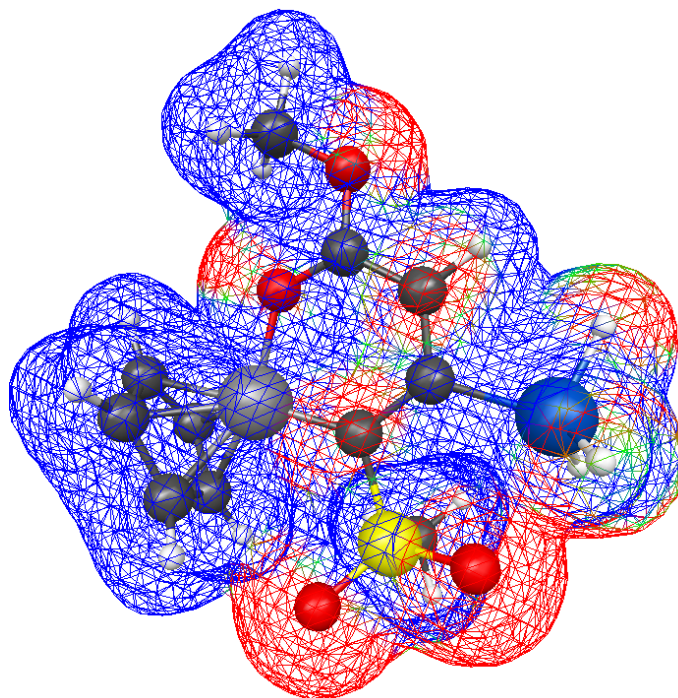
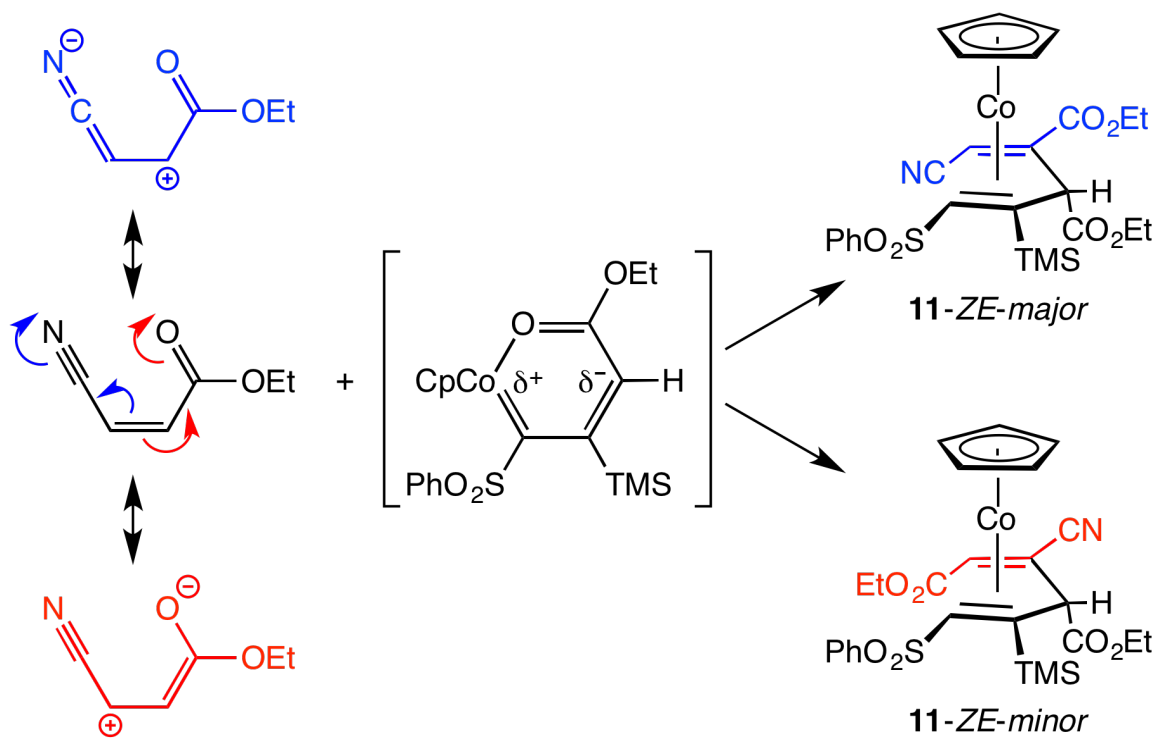


**Figure 2-8.** Electrostatic potential map of model complex **18**.

In its reactions with alkenes, metallacyclobutene **2** appears to function as a synthon for a vinylcarbene – or “metallabutadiene” moiety – and as with the Danishefsky diene, exhibits a high degree of regioselectivity. In the reaction of **2** with ethyl-*cis*- $\beta$ -cyanoacrylate – an alkene with a moderate difference in electron-withdrawing ability between the two alkene substituents – the major product **11-ZE** forms in greater than 11:1 ratio with a second minor product. The major product forms with C(4)<sub>CO<sub>2</sub>Et</sub>-C(5)<sub>CN</sub> regiochemistry, with the carbon containing the more electron-withdrawing substituent attached to the metal in the intermediates of product formation. Product **11-ZE** can be easily rationalized on the basis of resonance forms and the electrostatic potential of the two reactants (Scheme 2-8). In a reaction with a similar dienophile, Danishefsky’s diene reacts

with 4-cyanocoumarin with complete regioselectivity to give a 2:1 mixture of endo and exo stereoisomers.<sup>35</sup> The reaction of **2** with the *ortho*- and *para*- $\beta$ -nitrostyrenes also appears to be regioselective, although this designation is preliminary as there are minor products formed in these two reactions. The minor products formed are expected to be the thermally isomerized products, where the major **12-ZZ-ortho** and **12-ZZ-para** complexes formed are driven to a *ZE* stereochemistry, likely as a result of a hydrogen-bond stabilization interaction across the back of the pentadiene skeleton. The formation of just one regioisomer with the nitrostyrenes is probable, since a nitro moiety is substantially more electron-withdrawing than a fluoro-substituted arene. Node and co-workers report on the reactions of Danishefsky's diene with ten different  $\beta$ -nitroolefins to give complete regioselectivity, and exo-selectivity ranging from 2:1 to 10:1.<sup>36</sup>

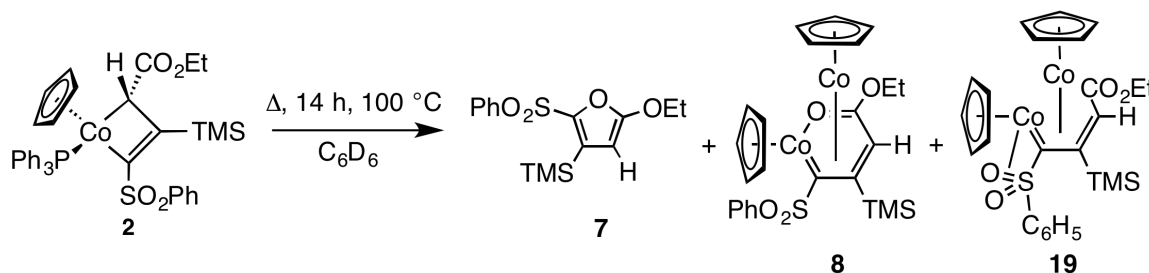


**Scheme 2-8.** Regioselective formation of **11-ZE**.

The thermolytic reactions of metallacyclobutene **2** demonstrate further evidence to corroborate the oxametallabenzene intermediate **17**. When a benzene-*d*<sub>6</sub> solution of **2** is heated under nitrogen at 100 °C for 14 h, analysis by <sup>1</sup>H NMR spectroscopy indicates formation of a previously characterized furan **7** (35% yield),<sup>39</sup> as well as two dinuclear complexes **8** and **19** in 31% and 35% yield, respectively (Scheme 2-9).<sup>7</sup> Product **8** was characterized by X-ray diffraction analysis, which showed an ( $\eta^5$ -C<sub>5</sub>H<sub>5</sub>)Co moiety bound  $\eta^4$  to an oxametallabenzene species ( $\eta^5$ -C<sub>5</sub>H<sub>5</sub>)Co[ $\kappa^2$ -(C,O)-C(SO<sub>2</sub>Me)C(TMS)CH(CO<sub>2</sub>Et)]. The second dinuclear species **19** remains structurally uncharacterized, but exists in equilibrium with **8** (**19/8** // 1.34:1 ratio,  $\Delta G^\circ = 0.2$  kcal/mol). Formation of an oxametallabenzene intermediate from **2** could lead to furan **7** and release of an



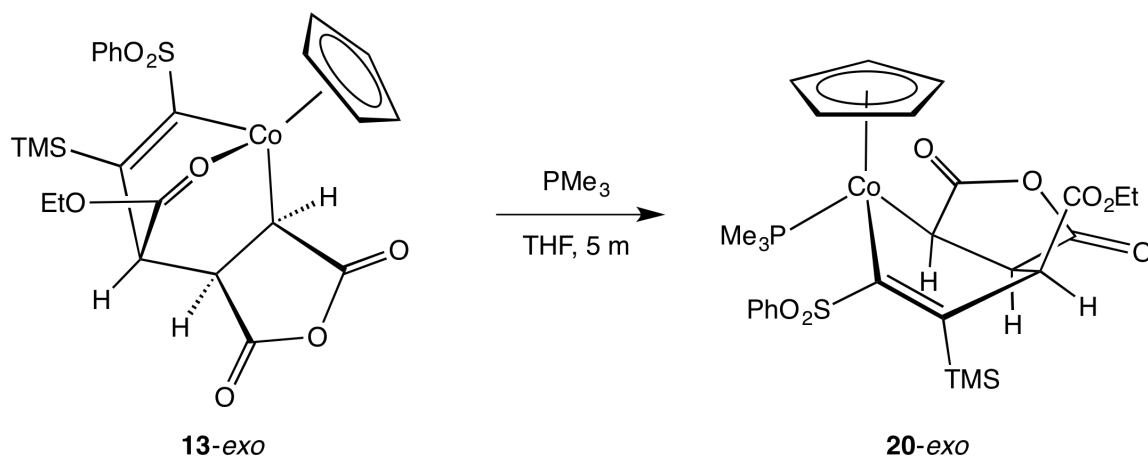
( $\eta^5\text{-C}_5\text{H}_5$ )Co fragment, which could then coordinate and stabilize further oxametallabenzene intermediates formed from **2**. The structure of **19** may feature an unusual sulfone metal coordination, as suggested by spectroscopic differences between **8** and **19**.<sup>7</sup> Ritter and co-workers propose a similar sulfonyl coordination in a sulfonamide ligand, and notice a shift of the *ipso*-carbon of the phenyl sulfone of 6.9 ppm by  $^{13}\text{C}$  NMR spectroscopy, as compared to a related solvate complex; complex **19** features a similar shift of the arenesulfonyl *ipso*-carbon of 6.2 ppm, as compared to complex **8**.<sup>38</sup>



**Scheme 2-9.** Thermolytic reaction of **2** to give furan and dinuclear complexes.

The polycyclic compounds **13-*exo*** and **13-*endo*** formed from reaction of **2** with maleic anhydride feature a *pseudo*-tetrahedral ( $\eta^5\text{-C}_5\text{H}_5$ )Co[ $\eta^1\text{-}(O),\kappa^2\text{-}(C(\text{sp}^2),C(\text{sp}^3))$ ] coordination environment about the cobalt metal. In principle, the alkyl and vinyl ligands could potentially be coupled through a reductive elimination to generate a bicyclic organic compound with two fused, unsaturated five-membered rings. The reactions of **2** with alkynes generate ( $\eta^5\text{-C}_5\text{H}_5$ )Co[ $\eta^4\text{-cyclopentadienes}$ ], presumably through an intermediate in which a new carbon-carbon bond is formed between two vinyl ligands. It was thought that treatment with an excess of trimethylphosphine might displace the coordination of

the ester carbonyl in **13**, and trigger a reductive elimination with concomitant formation of  $(\eta^5\text{-C}_5\text{H}_5)\text{Co}(\text{PMe}_3)_2$ . At a minimum, it was thought that disrupting the tris-chelate by displacing the carbonyl should assist in eventual decomplexation of the organic fragment. In an inert-atmosphere dry box, freshly prepared **13-*exo*** (247 mg, 45 mM) was dissolved in THF (10 mL) and treated dropwise with an excess of trimethylphosphine (ca. 400 mg). A color change from dark green to red-orange was observed during the phosphine addition. The reaction was stirred for 5 m, and then layered with hexanes to afford **20-*exo*** as crystalline material suitable for X-ray diffraction analysis (Scheme 2-10, Figure 2-31, and Figure 2-32).



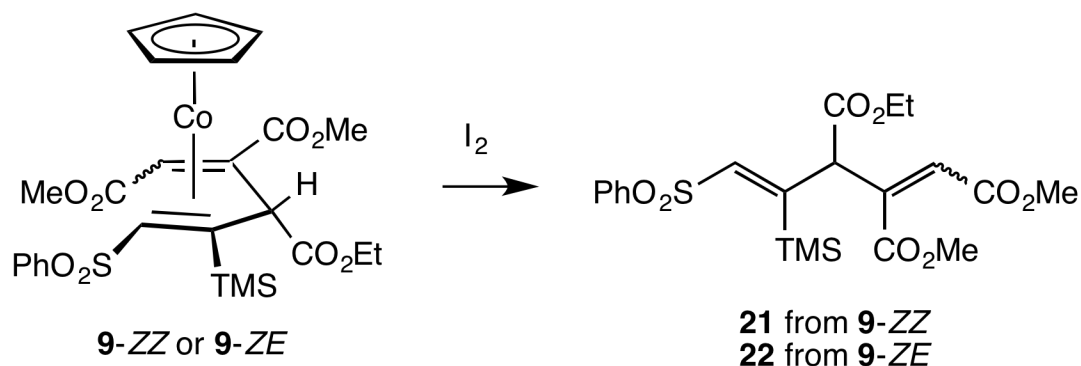
**Scheme 2-10.** Reaction of **13-*exo*** with trimethylphosphine to give **20-*exo***.

Solid-state analysis of **20-*exo*** confirmed the coordination of a trimethylphosphine ligand to displace the carbonyl of the ethyl ester from cobalt. This displacement could ostensibly occur by either step-wise or concerted substitution at the metal. The chirality at cobalt was inverted and thus racemic

**13-*exo*** with relative stereochemistry  $S^{Co}S^{C6}S^{C5}R^{C3}/R^{Co}R^{C6}R^{C5}S^{C3}$  gave **20-*exo*** product with  $R^{Co}S^{C6}S^{C5}R^{C3}/S^{Co}R^{C6}R^{C5}S^{C3}$  stereochemistry; the relative stereochemistry confirms a metal-centered inversion. This decomplexation afforded a bidentate metallacyclohexene, which assumed the same *pseudo*-boat conformation as **13-*exo*** in the solid-state, despite the absence of ester coordination. The cyclopentadienyl resonance in the  $^1H$  NMR spectrum was shifted upfield from  $\delta$  5.02 to 4.51 as a result of the more electron-rich metal center. Additionally, the CH proton at C(6) was shifted upfield from  $\delta$  3.53 to 1.97 ppm, and displayed a  $^3J_{PH}$  coupling from phosphine of 10.8 Hz.

The reactions of metallacyclobutene **2** with alkenes present a potentially useful route toward the synthesis of highly-functionalized 1,4-pentadiene skeletons. The demetallation of the  $(\eta^5-C_5H_5)Co$  fragment would liberate an organic species containing two alkene moieties, functional groups off each of the five carbons, as well as a doubly-allylic CH proton. Such a highly substituted organic molecule would likely be very difficult to synthesize in a typical organic approach. An oxidative demetallation strategy can be employed to remove the  $(\eta^5-C_5H_5)Co$  from the diene fragment to yield organic species of general formula  $CH(SO_2Ph)=C(TMS)CH(CO_2Et)C(R)=CH(R)$ . When a J-Young style NMR tube charged with a  $C_6D_6$  solution of **9-ZZ** (15.2 mg, 50 mM) and iodine (167 mM) was monitored by  $^1H$  NMR spectroscopy, resonances for **9-ZZ** gradually disappeared over the course of 12 h, and quantitative formation of a new product consistent with a 1,4-pentadiene skeleton appeared (by comparison to residual solvent).

Treatment with an excess of  $S_2O_3 \cdot 5H_2O$  and subsequent purification by chromatography gave **21** as colorless oil in excellent purity (Scheme 2-11, Figure 2-33, and Figure 2-34). In a similar preparative-scale reaction, **9-ZE** (132.8 mg, 1.1 mM) and iodine (4.7 mM) were dissolved in 200 mL benzene, and stirred for 17 h in an inert-atmosphere dry box. The reaction was filtered, treated with  $S_2O_3 \cdot 5H_2O$  to remove excess iodine, and then purified by chromatography to give **22** in 98% yield and high purity (Figure 2-35).



**Scheme 2-11.** Oxidative demetallation reactions of **9-ZZ** and **9-ZE** with iodine.

Spectral analysis of **21** and **22** ( $^1H$  NMR spectroscopy,  $C_6D_6$ ) indicated that **9-ZZ** and **9-ZE** each gave a unique compound with the resonances expected for the 1,4-pentadiene framework, however it is unclear whether the reaction of these two complexes with iodine proceeded by simple decomplexation or decomplexation/isomerization.<sup>39</sup> The resonances for the three CH protons in **21** and **22** are shifted substantially downfield as compared to their position in **9-ZZ** and **9-ZE**, respectively. Resonances for the  $CH(CO_2Me)$ ,  $CH(CO_2Et)$ , and  $CH(SO_2Ph)$  protons range from  $\delta$  2.30-4.80 for the metal complexes, with the proton next to the ethyl ester resonating farthest downfield, whereas in the pure

organics **21** and **22**, they are located at  $\delta$  5.92 and 5.90 ( $CHCO_2Me$ ),  $\delta$  6.68 ( $CHCO_2Et$ ), and  $\delta$  6.89 and 6.88 ( $CHSO_2Ph$ ), respectively. The protons being removed from the shielding environment of the cobalt metal center can readily explain this shift to lower field. Additionally, the two CH resonances at low field show a very small allylic  $^4J$  coupling constant of 0.50 Hz for **21** and 0.80 Hz for **22**. High-resolution mass spectrometry (EI) of **22** confirmed the expected spectral mass for a pentadiene with molecular formula  $C_{21}H_{28}O_8SiS$ . While the spectral analysis gathered for these two compounds confirms the likely structures, more evidence is necessary to unambiguously determine the stereochemistry about each of the carbon-carbon double bonds. Such characterization might be readily accomplished by binding to a metal fragment, perhaps  $(\eta^5-C_5H_5)Co(PPh_3)_2$ , or by deprotonation and crystallization as the pentadienyl anion.

The reactions of metallacyclobutene **2** with alkenes can be rationalized by invoking a vinylcarbene intermediate. Indeed, vinylcarbene intermediates such as **15** or **17** can readily explain the product regioselectivity, and stereochemistry. Vinylcarbene intermediates in the chemistry of metallacyclobutene **2** can also offer a ready explanation for the formation of  $\eta^4$ -ketenes,  $\eta^4$ -ketenimines, and  $\eta^4$ -1,3-butadienes, which would form from reaction of the respective substrate at the C(1) position of either **16** or **17**. Concurrent efforts in the O'Connor laboratory demonstrated the first experimental observation of a  $\kappa^2$ -metallacyclobutene- $\eta^3$ -vinylcarbene equilibration.<sup>40</sup> The synthesis and preparation of the sterically congested metallacyclobutene  $(\eta^5-C_5H_5)Co[\kappa^2-C(SO_2Tol)=C(TIPS)CH(CO_2Et)]$

(**23**) was accomplished in a similar preparative scheme to that of **2**, by treatment of the  $(\eta^5\text{-C}_5\text{H}_5)\text{Co}[\eta^2\text{-C}(\text{SO}_2\text{Tol})\equiv\text{C}(\text{TIPS})]$  alkyne complex with ethyl diazoacetate. Metallacyclobutene **23** was shown to equilibrate over the course of 4 days with a second species **24** (**23/24** // 3:1 ratio,  $\Delta G^\circ = 4.1$  kcal/mol). Addition of excess phosphine increased the concentration of **23** relative to **24**, while conversely, addition of a phosphine scavenger such as CuCl, AuCl(PPh<sub>3</sub>), or preferably Ir(PPh<sub>3</sub>)<sub>2</sub>(Cl)(N<sub>2</sub>) allowed for near quantitative conversion of **23** to **24**. Characterization by NMR spectroscopy and HRMS in combination with *ab initio* quantum chemical computations allowed formulation of complex **24** as the  $\eta^3$ -vinylcarbene  $(\eta^5\text{-C}_5\text{H}_5)\text{Co}[\eta^3\text{-C}(\text{SO}_2\text{Tol})\text{C}(\text{TIPS})=\text{CH}(\text{CO}_2\text{Et})]$ . In contrast to the chemistry of **2** which requires heating to at least 60-70 °C, reactions of metallacyclobutene **23** proceeded at room temperature. Treatment of **24** with ethyl diazoacetate proceeded in analogous fashion to metallacyclobutene **2** to afford the  $\eta^4$ -1,3-butadiene  $(\eta^5\text{-C}_5\text{H}_5)\text{Co}[\eta^4\text{-CH}(\text{CO}_2\text{Et})=\text{C}(\text{SO}_2\text{Tol})=\text{C}(\text{TIPS})\text{CH}(\text{CO}_2\text{Et})]$  by addition to the C(1) carbon. The reaction of **24** with maleic anhydride, however, gave only exo product, a result that can be understood by the increased steric bulk of a triisopropylsilyl group relative to the trimethylsilyl substituent at C(2), which precludes the formation of an endo transition state. Computational analysis suggested that the chemistry of metallacyclobutene **23** likely proceeded by conversion to the  $\eta^3$ -vinylcarbene product **24**.

Vinylcarbenes are well known in organometallic chemistry,<sup>41</sup> albeit somewhat rare, and their coordination about a metal center can involve a number of different ambidentate modes and conformations (Figure 2-9). Additionally, the bonding from the C(2)-C(3) double bond to the metal center can be described as either  $\eta^2$ -hapto or  $\kappa^2$ -diyl, in accordance with the Dewar-Chatt-Duncanson model of alkene bonding.<sup>42</sup>

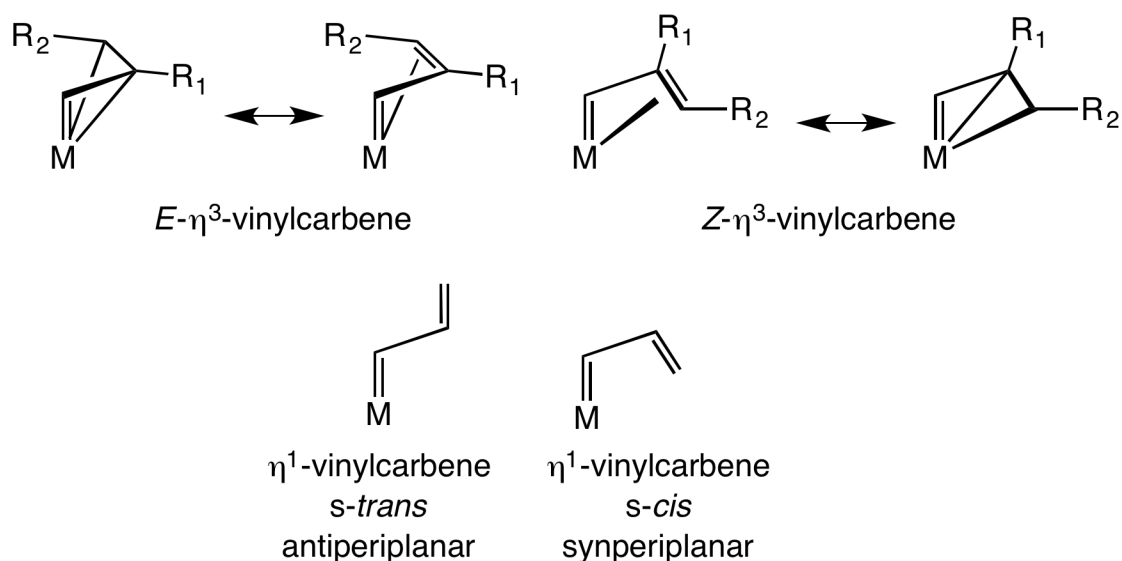
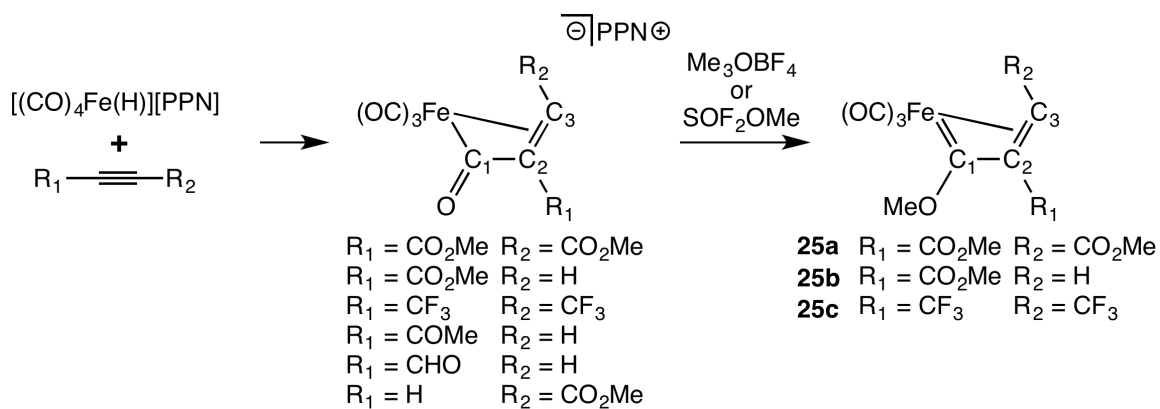


**Figure 2-9.** Various binding modes and resonance forms for vinylcarbenes.

The first  $\eta^3$ -vinylcarbene was reported by Mitsudo and co-workers in 1976, and synthesized by alkylation of an ( $\eta^3$ -acryloyl)iron(tricarbonyl) species to give  $(\text{CO})_3\text{Fe}(\eta^3\text{-C}(\text{OMe})\text{C}(\text{CO}_2\text{Me})=\text{CH}(\text{CO}_2\text{Me}))$  (**25a**; Scheme 2-12).<sup>43</sup> The  $\eta^3$ -vinylcarbene complex **25a** displays a typical carbene resonance in the  $^{13}\text{C}$  NMR spectrum at  $\delta$  270.9 ( $\text{CD}_2\text{Cl}_2$ ), and the C(3) proton appears at  $\delta$  4.30 in the  $^1\text{H}$  NMR spectrum ( $\text{CD}_2\text{Cl}_2$ ). The crystal structure obtained from X-ray diffraction analysis was reported in 1977 and confirms an  $E$ - $\eta^3$ -vinylcarbene coordination

environment about the C(2)-C(3) double bond, with a short Fe-C(1) bond of 1.819(3) – which at the time was the shortest metal-carbene bond reported.<sup>44</sup> Iron complex **25a** represents the first of a small family of  $\eta^3$ -vinylcarbenes derived in similar fashion. The synthesis of ( $\eta^3$ -acryloyl)iron(tricarbonyl) species  $[(\text{CO})_3\text{Fe}(\eta^3\text{-C(=O)C(R)=CH(R))][\text{PPN}]$  from  $[(\text{CO})_4\text{Fe(H)}][\text{PPN}]$  and alkyne precursors is general, and can accommodate different functionalities at the C(2) and C(3) position.<sup>45</sup> Formation of the metal carbene is accomplished by methylation of the C(1) carbonyl, and is facilitated by either trimethyloxonium or methyl fluorosulfonate (“Magic Methyl”). Ethylation of the C(1) carbonyl was also demonstrated to give an  $\eta^3$ -vinylcarbene, though this alkylation resulted in an oil, and thus this particular avenue of substitution was not well-explored.

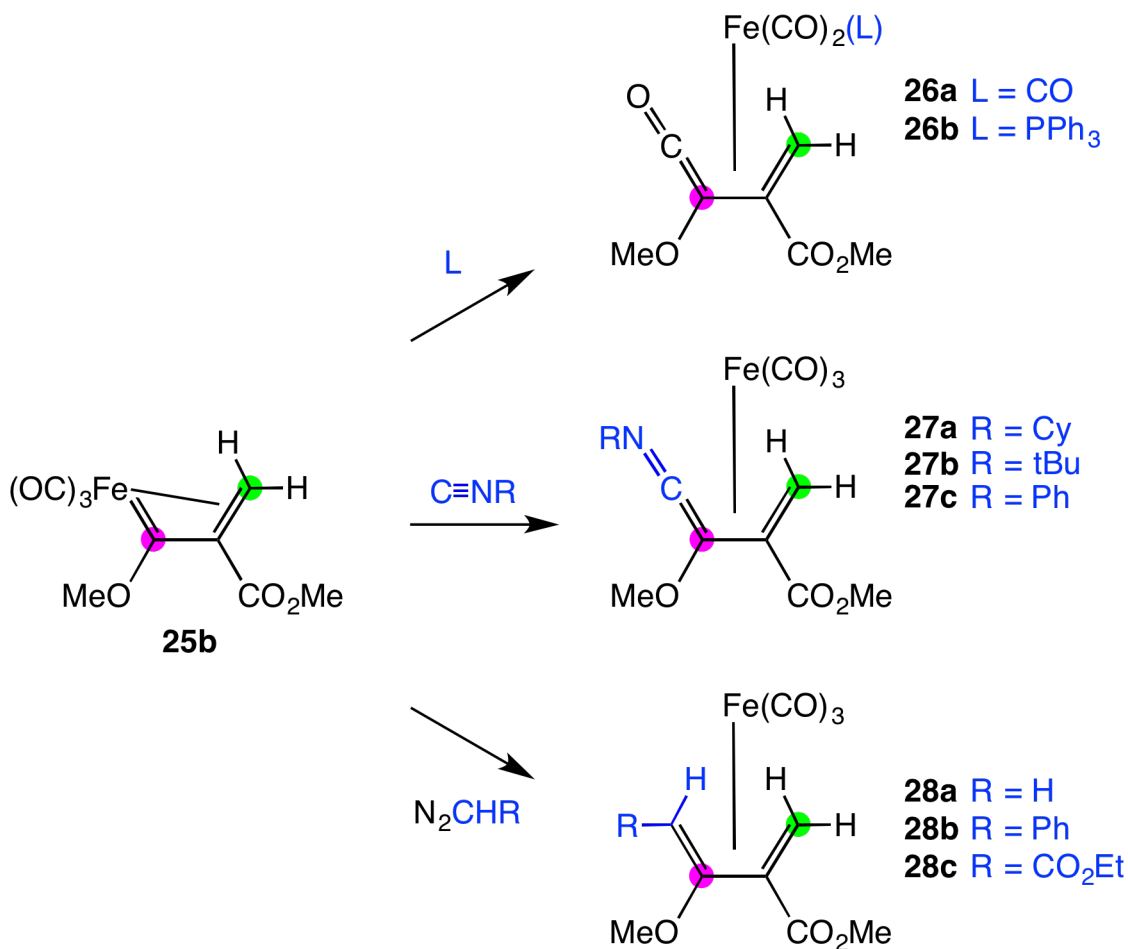


**Scheme 2-12.** Synthesis of  $(\text{CO})_3\text{Fe}[(\eta^3\text{-C(OMe)C(R}_1\text{)=CH(R}_2\text{)})]$  (**25**) vinylcarbene complexes.

The chemistry of  $\eta^3$ -vinylcarbenes **25** display a remarkable similarity to the known reactions of metallacyclobutene **2**. The  $\eta^3$ -vinylcarbene **25b** can react with additional ligand such as carbon monoxide or triphenylphosphine to give  $\eta^4$ -

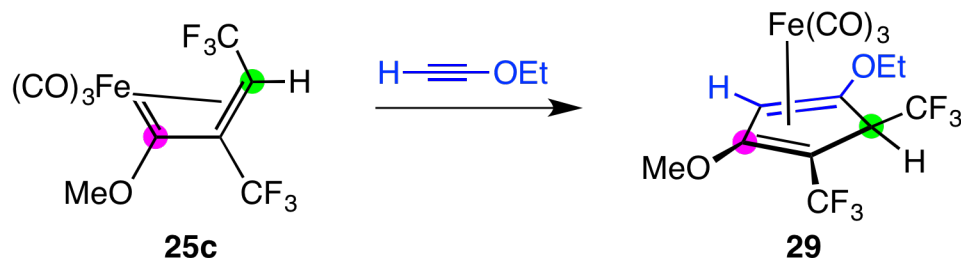


vinylketene products **26a-b** (Scheme 2-13),<sup>46</sup> with isonitriles to give the first examples of an  $\eta^4$ -vinylketenimine **27a-c**,<sup>47</sup> and with diazo reagents to give  $\eta^4$ -1,3-butadienes **28a-c**.<sup>48</sup> In each case, coupling to the C(1) carbon was observed. A more detailed report on the reactions of vinylcarbenes **25** with carbon monoxide and mixed alkyl/aryl phosphines also demonstrated the formation of ferracyclo-pent-2-en-5-ones and 2-pyrones ( $\alpha$ -pyrones), depending on the reaction conditions and ligands employed.<sup>49</sup>



**Scheme 2-13.** Reactions of  $\eta^3$ -vinylcarbene  $(CO)_3Fe(\eta^3-C(OMe)C(CO_2Me)=CH_2)$  (**25b**).

In 1995, Mitsudo and co-workers reported the synthesis of  $\eta^3$ -vinylcarbene  $(\text{CO})_3\text{Fe}(\eta^3\text{-C}(\text{OMe})\text{C}(\text{CF}_3)=\text{CH}(\text{CF}_3))$  (**25c**) from hexafluoro-2-butyne, utilizing the synthetic strategy outlined in Scheme 2-12.<sup>50</sup> Complex **25c** also reacts with triphenylphosphine to give an  $\eta^4$ -vinylketene, similar to vinylcarbene **25b**. The reaction of **25c** with the alkyne ethoxyethyne was shown to give an  $\eta^4$ -cyclopentadiene complex **29** analogous to complexes **6** derived from the reactions of metallacyclobutene **2** with acetylenes (Scheme 2-14). The reaction of **25c** with ethoxyethyne was endo-selective, giving just one product in which the trifluoromethyl group at the C(3) methylene carbon was on the same face of the  $\eta^4$ -cyclopentadiene ring as the iron(tricarbonyl) fragment. The formation of compound **29** was suggested to occur through insertion between the iron and carbene carbon to give a ferracyclohexadiene intermediate, followed by reductive elimination to give product. The regioselectivity was rationalized as nucleophilic attack of the acetylenic carbon at the carbene carbon, while the stereoselectivity was thought to be a result of subsequent reactivity by any exo-products formed, likely by hydrogen abstraction of the methylene proton (formation of **29** occurred in 50% yield). Other alkynes such as dimethyl acetylenedicarboxylate, phenylacetylene, diphenylacetylene, and hexafluoro-2-butyne did not give reaction with **25c** under similar conditions.

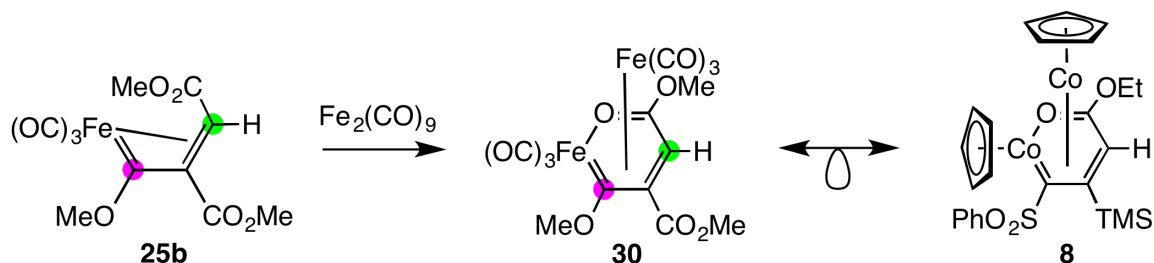


**Scheme 2-14.** Reaction of  $\eta^3$ -vinylcarbene **25c** with ethoxyethyne to give  $\eta^4$ -cyclopentadiene product **29**.

The similarity in chemistry between the Mitsudo vinylcarbene system and the O'Connor metallacyclobutene system further corroborate the proposal that the chemistry of **2** may involve vinylcarbene intermediates. Somewhat surprisingly, Mitsudo does not report on the chemistry of vinylcarbenes **25** with alkenes. The resemblance in product scope between the two systems prompted an exploration of this reactivity, particularly in regard to  $\eta^3$ -vinylcarbene **25a**, in which the C(3) substituent was a methyl ester – analogous to the ethyl ester substituent at the same position in metallacyclobutene **2**. When a solution of **25a** (1.3 mg, 8.0 mM) in  $C_6D_6$  (500  $\mu$ L) was heated at 70 °C in the presence of maleic anhydride (11 mM) and analyzed by  $^1H$  NMR spectroscopy, resonances appeared in a 1:1 ratio consistent with a known dinuclear iron complex **30**, as well as a new set of resonances for unknown species **31**. Compound **31** exhibited resonances in the  $^1H$  NMR spectrum corresponding to three methyl groups ( $\delta$  3.46, 3.28, and 2.79), an isolated hydrogen resonance at  $\delta$  4.64, and two 1H doublets at  $\delta$  3.85 and 3.32 ( $J_{HH} = 8.0$  Hz). A similar reaction of **25a** (1.0 mg, 5.9 mM) in  $C_6D_6$  (500  $\mu$ L) with maleimide (13 mM) also gave dinuclear

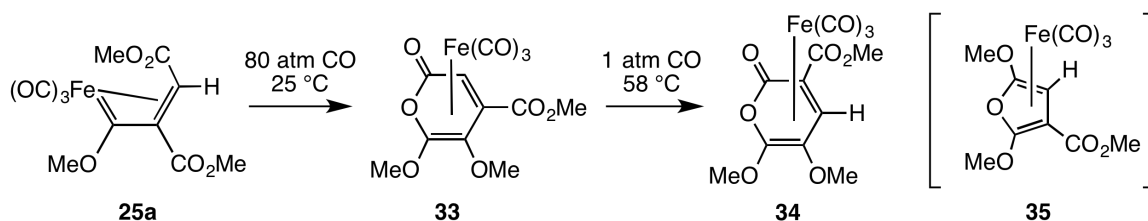
complex **30**, as well as a new compound **32** having a spectral profile similar to that of **31**: three methyl groups ( $\delta$  3.57, 3.32, and 2.93), an isolated hydrogen resonance at  $\delta$  4.72, two 1H doublets at  $\delta$  3.92 and 3.28 ( $J_{\text{HH}} = 7.6$  Hz), and a broad resonance corresponding to the NH proton at  $\delta$  6.58. These spectral features are inconsistent with either the  $\eta^4$ -1,4-pentadienes or the cyclohexadienes that arise from the reactions of **2** with alkenes.

Compound **30** was previously reported by Mitsudo in the reaction of **25a** with  $\text{Fe}_2(\text{CO})_9$  to give a dinuclear species, in which  $\text{Fe}(\text{CO})_3$  binds to an oxametallabenzene (Scheme 2-15).<sup>51</sup> Complex **30** is very similar to the dinuclear species **8** formed by thermolysis of **2**, in which the isolobal fragments  $\text{Fe}(\text{CO})_3$  and  $(\eta^5\text{-C}_5\text{H}_5)\text{Co}$  bind and stabilize an  $\eta^4$ -oxametallabenzene. The formation of the dinuclear cobalt complex **8** was accompanied by the liberation of a furan species **7**, and is consistent with an overall mechanism in which the organic moiety of one molecule of metallacyclobutene **2** was lost to generate furan and uncomplexed  $(\eta^5\text{-C}_5\text{H}_5)\text{Co}$  – the liberated cobalt fragment can then bind a second rearranged molecule of **2** to give **8**. Likewise, the formation of dinuclear species **30** in the reactions of **25a** with maleic anhydride and maleimide suggests that the organic fragment from **25a** might have been liberated to generate a free  $\text{Fe}(\text{CO})_3$  species in solution, which binds to a second molecule of **25a**. The organic species liberated from **25a** might then react with maleic anhydride or maleimide to give a new organic product with desymmetrized proton resonances corresponding to the former alkene hydrogens.



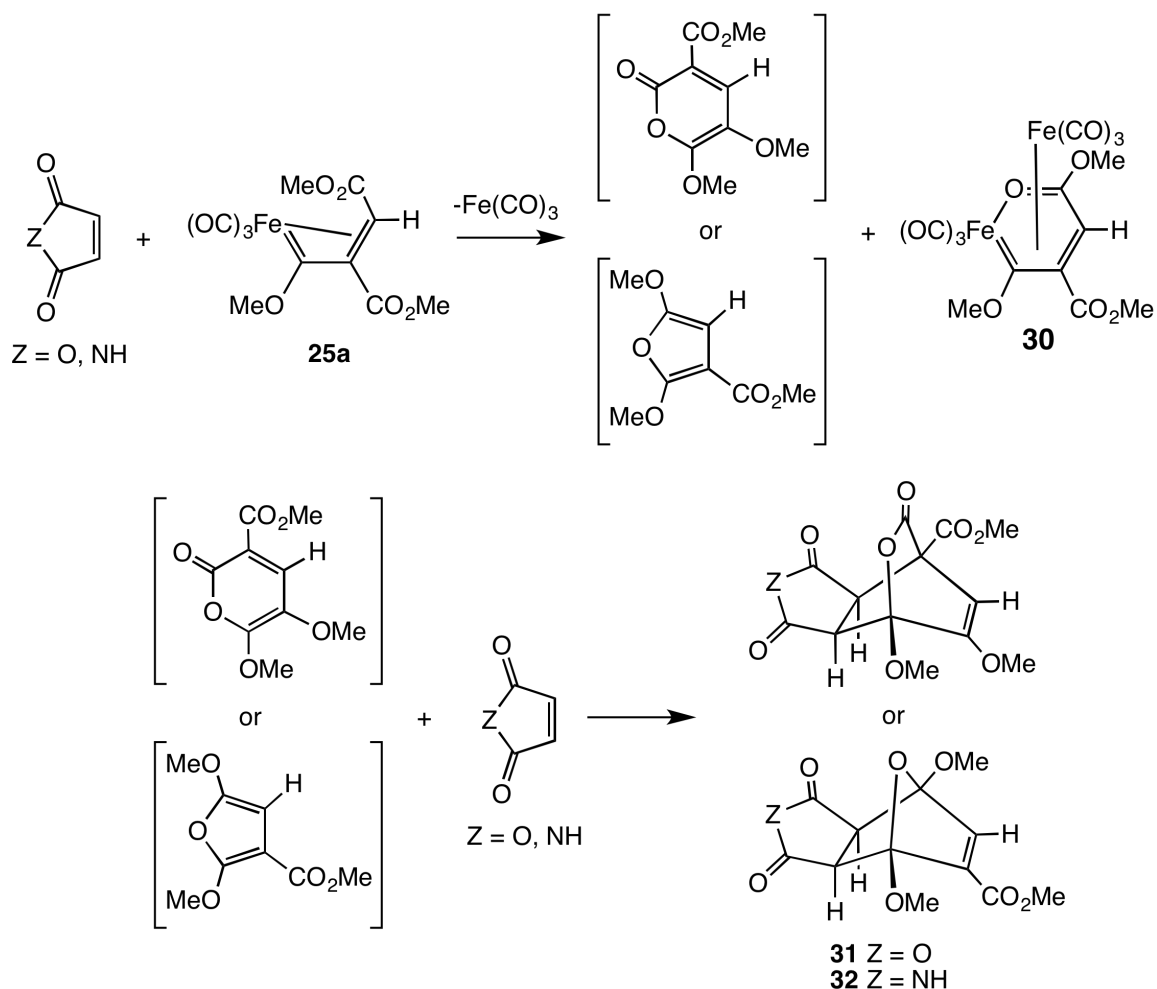
**Scheme 2-15.** Formation of dinuclear complex **30** from reaction of  $\eta^3$ -vinylcarbene **25a** with  $\text{Fe}_2(\text{CO})_9$ , and its isolobal relationship to dinuclear **8**.

The literature regarding iron vinylcarbene **25a** suggests several possibilities for the identity of unknown organics **31** and **32** from the reactions with maleic anhydride and maleimide. Vinylcarbene **25a** reacts with carbon monoxide (80 atm) at room temperature to give an  $(\text{CO})_3\text{Fe}(\eta^4\text{-2-pyrone})$  species **33**, which was the first crystallographically characterized 2-pyrone complex (Scheme 2-16).<sup>52</sup> When isolated **33** is heated at 58 °C for 12 hours under an atmosphere of carbon monoxide, isomerization occurred to generate a new  $\eta^4\text{-2-pyrone}$  complex, **34**. It was suggested that furan complex **35** might play a role in this isomerization process, which was supported by the observation that 2-methoxyfuran reacts with  $\text{Fe}_2(\text{CO})_9$  to give  $(\text{CO})_3\text{Fe}(\eta^4\text{-6-methoxy-2-pyrone})$ .<sup>49</sup>



**Scheme 2-16.** Formation of  $(\text{CO})_3\text{Fe}(\eta^4\text{-2-pyrone})$  complex **33** from reaction of  $\eta^3$ -vinylcarbene **25a** with carbon monoxide, and its thermal isomerization to **34**.

The liberation of the organic portion from any of the iron complexes **33-35** would yield an  $\text{Fe}(\text{CO})_3$  fragment which could then generate the dinuclear complex **30** from a second equivalent of **25a**, as well an organic moiety which could participate in subsequent reactivity with the cyclic alkenes. In particular, the 2-pyrones derived from **33** and **34** or the furan derived from **35** should readily participate in a Diels-Alder reaction with either maleic anhydride or maleimide, especially at the slightly elevated temperatures at which the reaction was conducted.<sup>29,53</sup> A Diels-Alder adduct of the cyclic alkene and either the 2-pyrone from **34** or the furan from **35** would give products consistent with the spectral signature observed for species **31** and **32** (Scheme 2-17); the  $^1\text{H}$  NMR characteristics of **31** and **32** are, however, inconsistent with the product that would arise from reaction with the 2-pyrone derived from **33**. This observation is consistent with the literature result in which **33** is thermally isomerized to complex **34**.



**Scheme 2-17.** Possible identities for species **31** and **32** from reaction of **25a** with maleic anhydride and maleimide, respectively.

Products **31** and **32**, depicted as the bicyclo-adduct as shown in Scheme 2-17, are consistent with the spectral signature observed by <sup>1</sup>H NMR. However, the formation of products **31-32** could occur as either or both of the exo and endo stereoisomers. Typically, exo products arising from a Diels-Alder reaction are the more stable thermodynamic product, whereas the endo stereoisomer is preferred kinetically. Analysis of the <sup>1</sup>H NMR during the reaction of **25a** with maleic anhydride or maleimide indicates the formation of just one product, even at short

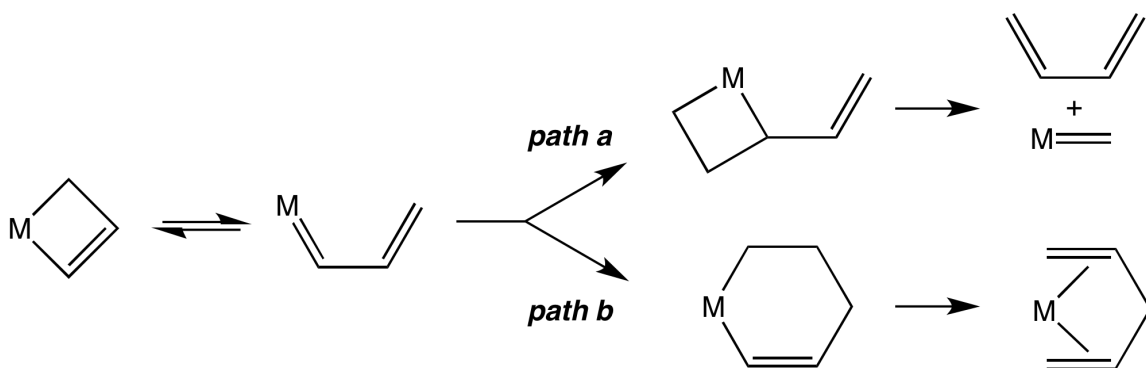
reaction times, thus **31** and **32** are formulated as the exo isomer. Additionally, if a 2-pyrone intermediate is involved in the formation of **31** and **32**, CO<sub>2</sub>-extrusion could occur as the result of a retro-hetero-Diels-Alder reaction, resulting in either a tri-substituted dihydrophthalic anhydride or dihydrophthalimide – which would also readily explain the formation of a single product.<sup>54</sup>

The reactions of vinylcarbene **25a** with cyclic alkenes are divergent from that of the metallacyclobutene **2**, though they do appear to feature several similarities. In particular, the formation of dinuclear product **30** suggests that both **25a** and **2** may involve similar oxametallabenzene intermediates, as well as (possibly) the liberation of a furan. Further studies involving this particular vinylcarbene should focus on elucidation of the auto-thermolytic decomposition of **25a**, which likely includes the formation of **30** and either a 2-pyrone or furan byproduct. Additionally, treatment of **25a** with a suitable oxidant – perhaps AgBF<sub>4</sub>, might facilitate oxidation and liberation of the organic fragment from this complex. Reactions with electron-rich alkenes could serve to differentiate the iron and cobalt  $\eta^4$ -oxametallabenzene chemistry, for which the metallacyclobutene **2** appears to be unreactive. Of particular interest would be the alkene dicyclopentadiene, which could form a very stable tri-substituted indene after CO<sub>2</sub> and cyclopentadiene extrusion, in the case of 2-pyrone intermediates.<sup>54</sup> The reactions of **25a** with alkynes are also currently unexplored, and might serve as an interesting example of a benzannulation reaction, comparable to the Dötz benzannulation with a chromium carbene.<sup>55</sup> Surprisingly, none of these four



avenues of chemistry are currently reported in the literature regarding this complex, though their elucidation would be of interest, especially in comparison to the metallacyclobutene chemistry of **2**.

To the best of our knowledge, the reactions reported herein are the first productive reactions of a characterized metallacyclobutene complex with alkenes. Reactions of metallacyclobutenes with alkenes have been widely proposed as a key step in metal-catalyzed enyne metathesis reactions, as shown in Scheme 2-18 (*path a*).<sup>4,56</sup> The reactions of **2** with alkenes take a much different and unexpected course, to ultimately form 1,4-diene complexes (*path b*). Future work will aim towards the elucidation and characterization of reaction mechanism, focusing particularly on the role vinylcarbenes play in the reactivity of metallacyclobutene **2** and related metallacyclobutene complexes.



**Scheme 2-18.** Contrasting behavior of metallacyclobutenes toward alkenes.

## References.

1. For leading references: (a) Stewart, I. C.; Douglas, C. J.; Grubbs, R. H. *Org. Lett.* **2008**, *10*, 441. (b) Geny, A.; Lebœuf, D.; Rouquié, G.; Vollhardt, K. P. C.; Malacria, M.; Gandon, V.; Aubert, C. *Chem.-Eur. J.* **2007**, *13*, 5408.
2. For early-metal metallacyclobutene reactivity: (a) Petasis, N. A.; Staszewski, J. P.; Fu, D.-K. *Tetrahedron Lett.* **1995**, *36*, 3619. (b) Binger, P.; Müller, P.; Langhauser, F.; Sandmeyer, F.; Philipps, P.; Gabor, B.; Mynott, R. *Chem. Ber.* **1993**, *126*, 1541. (c) Doxsee, K. M.; Mouser, J. K. M.; Farahi, J. B. *Synlett* **1992**, 13. (d) Meinhart, J. D.; Grubbs, R. H. *Bull. Chem. Soc. Jpn.* **1988**, *61*, 171.
3. For late-metal metallacyclobutene reactivity: (a) Casey, C. P.; Nash, J. R.; Yi, C. S.; Selmeczy, A. D.; Chung, S.; Powell, D. R.; Hayashi, R. K. *J. Am. Chem. Soc.* **1998**, *120*, 722. (b) Cheng, Y.-C.; Chen, Y.-K.; Huang, T.-M.; Yu, C.-I.; Lee, G.-H.; Wang, Y.; Chen, J.-T. *Organometallics* **1998**, *17*, 2953. (c) O'Connor, J. M.; Ji, H.; Iranpour, M.; Rheingold, A. L. *J. Am. Chem. Soc.* **1993**, *115*, 1586. (d) O'Connor, J. M.; Ji, H.-L.; Rheingold, A. L. *J. Am. Chem. Soc.* **1993**, *115*, 9846. (e) O'Connor, J. M.; Fong, B. S.; Ji, H.-L.; Hiibner, K.; Rheingold, A. L. *J. Am. Chem. Soc.* **1995**, *117*, 8029. (f) O'Connor, J. M.; Chen, M.-C. *Tetrahedron Lett.* **1997**, *38*, 5241. (g) Donovan-Merkert, B. T.; Malik, J.; Gray, L. V.; O'Connor, J. M.; Fong, B. S.; Chen, M.-C. *Organometallics*, **1998**, *17*, 1007.
4. (a) Singh, R.; Schrock, R. R.; Müller, P.; Hoveyda, A. H. *J. Am. Chem. Soc.* **2007**, *129*, 12654. (b) Diver, S. T. *J. Mol. Catal.* **2006**, *254*, 29. (c) Hansen, E. C.; Lee, D. *Acc. Chem. Res.* **2006**, *39*, 509. (d) Katz, T. J. *Angew. Chem., Int. Ed.* **2005**, *44*, 3010. (e) Kim, S.-H.; Bowden, N.; Grubbs, R. H. *J. Am. Chem. Soc.* **1994**, *116*, 10801.
5. Tebbe, F. N.; Harlow, R. L. *J. Am. Chem. Soc.* **1980**, *102*, 6149.
6. Portions of this chapter were previously communicated: Holland, R. L.; Bunker, K. D.; Chen, C. H.; DiPasquale, A. G.; Rheingold, A. L. Baldrige, K. K.; O'Connor, J. M. *J. Am. Chem. Soc.*, **2008**, *130*, 10093.
7. Bunker, K. D.; Ph.D. Dissertation, University of California, San Diego, CA, **2003**.
8. The first stereochemical designator in the compound numbers (e.g., #-ZZ) refers to the alkene bearing the sulfone.

9. Complexes **9-ZZ**, **9-ZE**, **10-ZZ**, **10-ZE**, **11-ZE**, **12-ZZ-ortho**, **12-ZZ-para**, **13-exo**, **14-exo**, **13-endo**, and **14-endo** were characterized in the solid-state by X-ray crystallography.

10. The mild conditions for isomerization of **6-ZZ** to the *ZE*-stereoisomer contrast with the behavior of  $(\eta^5\text{-C}_5\text{H}_5)\text{Co}(\eta^4\text{-(Z,Z)-1,4-dideuterio-1,3-butadiene})$  and related complexes, which are much less prone to isomerization: (a) Eaton, B.; King, J. A.; Vollhardt, K. P. C. *J. Am. Chem. Soc.* **1986**, *108*, 1359. (b) Baldrige, K. K.; O'Connor, J. M.; Chen, M.-C.; Siegel, J. S. *J. Phys. Chem. A* **1999**, *103*, 10126.

11. Thermal isomerization of  $(\eta^5\text{-C}_5\text{H}_5)\text{Co}(\eta^4\text{-1,4-pentadiene})$  to the 1,3-pentadiene isomer occurs in benzene at 50 °C: (a) King, J. A., Jr.; Vollhardt, K. P. C. *J. Organomet. Chem.* **1993**, *460*, 91.

12. Structurally characterized  $\eta^4$ -complexes of acyclic 1,4-pentadienes are exceedingly rare. As described in ref. 10a, the 1,4-pentadiene ligand in  $(\eta^5\text{-C}_5\text{Me}_5)\text{Ru}[\text{CH}_2=\text{CHCH}(\text{OTMS})\text{CH}=\text{CH}_2]\text{Cl}$  adopts a "sickle"-shaped structure with a 3.64 Å distance between the diene termini. (a) Trakarnpruk, W.; Rheingold, A. L.; Haggerty, B. S.; Ernst, R. D. *Organometallics* **1994**, *13*, 3914. (b) For a ring-fused 1,4-pentadiene ligand, see: Chisnall, B. M.; Green, M.; Hughes, R. P.; Welch, A. J. *J. Chem. Soc., Dalton Trans.* **1976**, 1899.

13. Desiraju, G. R. *Acc. Chem. Res.* **1996**, *29*, 441.

14. Young, Jr., H. W. (Dow Chemical Co.). U.S. Patent 4,814,481, Mar. 21, 1989; *Chem. Abstr.* **1989**, *110*, 231131.

15. (a) Kopp, M.; Krauth, L. R.; Ratka, R.; Weidenhammer, K.; Ziegler, M. L. *Z. Naturforsch. B* **1980**, *35*, 802. (b) Dean, C. E.; Kemmitt, R. D. W.; Russell, D. R.; Schilling, M. D. *J. Organomet. Chem.* **1980**, *187*, C1. (c) Ibers, J. A.; *J. Organomet. Chem.* **1974**, *73*, 389.

16. (a) Stalick, J. K.; Ibers, J. A. *J. Am. Chem. Soc.* **1970**, *90*, 5333. (b) Love, R. A.; Koetzle, T. F.; Williams, G. J. B.; Andrews, L. C.; Bau, R. *Inorg. Chem.* **1975**, *14*, 2653.

17. Cenzano-Fong, B. S.; Ph.D. Dissertation, University of California, San Diego, CA, **1997**.

18. (a) Zimmerman, H. E.; Paufler, R. M. *J. Am. Chem. Soc.* **1960**, *82*, 1514. (b) Bleeke, J. R.; Behm, R.; Xie, Y.-F.; Chiang, M. Y.; Robinson, K. D.; Beatty, A. M. *Organometallics*, **1997**, *16*, 606. (c) Bleeke, J. R.; Behm, R.; Beatty, A. M.

*Organometallics*, **1997**, *16*, 1103. (d) Gilbertson, R. D.; Lau, T. L. S.; Lanza, S.; Wu, H.-P.; Weakley, T. J. R.; Haley, M. M. *Organometallics*, **2003**, *22*, 3279. (e) Frühauf, H.-W.; Sells, F.; Goddard, R. J.; Romão, M. J. *Organometallics*, **1985**, *4*, 948. (f) van Wijnkoop, M.; de Lange, P. P. M.; Frühauf, H.-W.; Vrieze, K.; Wang, Y.; Goubitz, K.; Stam, C. H. *Organometallics*, **1992**, *11*, 3607. (g) Feiken, N.; Schreuder, P.; Siebenlist, R.; Frühauf, H.-W.; Vrieze, K.; Kooijman, H.; Veldman, N.; Spek, A. L.; Fraanje, J.; Goubitz, K. *Organometallics*, **1996**, *15*, 2148.

19. Schmidt, M. W.; Baldrige, K. K.; Boatz, J. A.; Elbert, S. T.; Gordon, M. S.; Jensen, J. H.; Koseki, S.; Matsunaga, N.; Nguyen, K. A.; Su, S.; Windus, T. L.; Elbert, S. T. *J. Comp. Chem.* **1993**, *14*, 1347.

20. Zhao, Y.; Truhlar, D. G. *Theor. Chem. Acc.* **2007**, *118*, 215.

21. Moller, C.; Plesset, M. S.; *Phys. Rev.* **1934**, *46*, 618.

22. Fuentealba, P.; Preuss, H.; Stoll, H.; Szentpaly, L. V. *Chem. Phys. Lett.* **1989**, *89*, 418.

23. Martin, J. M. L.; Sundermann, A. *J. Chem. Phys.* **2001**, *114*, 3408.

24. Dunning, T. H. *J. Chem. Phys.* **1989**, *90*, 1007.

25. Bode, B. M.; Gordon, M. S. *J. Mol. Graph. Mod.* **1998**, *16*, 133.

26. Baldrige, K. K.; Greenberg, J. P. *J. Mol. Graphics* **1995**, *13*, 63.

27. For a proposed vinylcarbene-alkene Diels-Alder reaction: Trost, B. M.; Hashmi, A. S. K.; Ball, R. G. *Adv. Synth. Catal.* **2001**, *343*, 490.

28. An excellent precedent for the proposed Diels-Alder reactions of **11** is found in the [4 + 2]-cycloaddition reactions of an iridapyrylium complex: Bleeke, J. R. *Acc. Chem. Res.* **2007**, *40*, 1035.

29. The *reversible* Diels-Alder reaction of maleic anhydride with furan exhibits only a small kinetic preference for formation of the endo stereoisomer: Rulisek, L.; Sevek, P.; Havlas, Z.; Hrabal, R.; Capek, P.; Svatos, A. *J. Org. Chem.* **2005**, *70*, 6295.

30. Sauer, J.; Wiest, H.; Mielert, A. *Chem. Ber.* **1964**, *97*, 3183.

31. Ebersson, L.; Landström, L. *Acta Chem. Scand.* **1972**, *26*, 239.

32. (a) Hammett, L. P. *J. Am. Chem. Soc.* **1937**, *59*, 96. (b) McDaniel, D. H.; Brown, H. C. *J. Org. Chem.* **1958**, *23*, 420. (c) Hansch, C.; Leo, A.; Taft, R. W.; *Chem. Rev.* **1991**, *91*, 165.
33. Exner, O. *Collect. Czech. Chem. Commun.* **1966**, *31*, 65.
34. (a) Danishefsky, S.; Kitihara, T.; Schuda, P. F.; Etheredge, S. J. *J. Am. Chem. Soc.* **1976**, *98*, 3028. (b) Danishefsky, S. *Acc. Chem. Res.* **1981**, *14*, 400.
35. Jung, M. E.; Allen, D. A. *Org. Lett.* **2009**, *11*, 757.
36. Node, M.; Nishide, K.; Imazato, H.; Kurosaki, R.; Inoue, T.; Ikariya, T. *Chem. Commun.* **1996**, 2559.
37. Fleming, I. *Frontier Orbitals and Organic Chemical Reactions*; Wiley-Interscience, London, **1976**.
38. Furuya, T.; Benitez, D.; Tkatchouk, E.; Strom, A. E.; Tang, P.; Goddard III, W. A.; Ritter, T. *J. Am. Chem. Soc.* **2010**, *132*, 3793.
39. Holland, R. L.; O'Connor, J. M.; Bunker, K. D.; Qin, P.; Cope, S. K.; Baldrige, K. K.; Siegel, J. S. *Synlett*, **2015**, *26*, 2243.
40. (a) O'Connor, J. M.; Baldrige, K. K.; Vélez, C. L.; Rheingold, A. L.; Moore, C. E. *J. Am. Chem. Soc.* **2013**, *135*, 8826. (b) Vélez, C. L.; Ph.D. Dissertation, University of California, San Diego, CA, **2011**.
41. Mitsudo, T.-A. *Bull. Chem. Soc. Jpn.* **1998**, *71*, 1525.
42. (a) Dewar, M. *Bull. Soc. Chim. Fr.* **1951**, *18*, C71-C79. (b) Dewar, M. *Ann. Rep. Prog. Chem.* **1951**, *48*, 112. (c) Chatt, J.; Duncanson, L. A. *J. Chem. Soc.* **1953**, 2939. (d) Chatt, J.; Duncanson, L. A. *J. Chem. Soc.* **1955**, 4456.
43. Mitsudo, T.-A.; Nakanishi, H.; Inubushi, T.; Morishima, I.; Watanabe, Y.; Takegami, Y. *J. Chem. Soc. Chem. Commun.* **1976**, *11*, 416.
44. Nakatsu, K.; Mitsudo, T.-A.; Nakanishi, H.; Watanabe, Y.; Takegami, Y. *Chem. Lett.* **1977**, *6*, 1447.
45. Mitsudo, T.-A.; Watanabe, Y.; Nakanishi, H.; Morishima, I.; Inubushi, T.; Takegami, Y. *J. Chem. Soc., Dalton Trans.* **1978**, *10*, 1298.
46. Mitsudo, T.-A.; Sasaki, T.; Watanabe, Y.; Takegami, Y.; Nishigaki, S.; Nakatsu, K. *J. Chem. Soc., Chem. Commun.* **1978**, 252.

47. Mitsudo, T.-A.; Watanabe, H.; Komiya, Y.; Watanabe, Y.; Takaegami, Y. *J. Organomet. Chem.* **1980**, *190*, C39.
48. Mitsudo, T.-A.; Watanabe, H.; Watanabe, K.; Watanabe, Y.; Takegami, Y. *J. Organomet. Chem.* **1981**, *214*, 87.
49. Mitsudo, T.-A.; Watanabe, H.; Sasaki, T.; Takegami, Y.; Watanabe, Y.; Kafuku, K.; Nakatsu, K. *Organometallics*, **1989**, *8*, 368.
50. Mitsudo, T.-A.; Fujita, K.; Nagano, S.; Suzuki, T.; Watanabe, Y.; Masuda, H. *Organometallics*, **1995**, *14*, 4228.
51. Mitsudo, T.-A.; Watanabe, H.; Watanabe, K.; Watanabe, Y.; Kafuku, K.; Nakatsu, K. *Chem. Lett.* **1981**, *10*, 1687.
52. Mitsudo, T.-A.; Watanabe, H.; Sasaki, T.; Watanabe, Y.; Takegami, Y.; Kafuku, K.; Kinoshita, K.; Nakatsu, K. *J. Chem. Soc., Chem. Commun.* **1981**, 22.
53. Afarinkia, K.; Vinader, V.; Nelson, T. D.; Posner, G. H. *Tetrahedron*, **1992**, *48*, 9111.
54. (a) Goldstein, M. J.; Thayer, Jr., G. L. *J. Am. Chem. Soc.* **1965**, *87*, 1925. (b) Roth-Barton, J.; Goh, Y. W.; Karnezis, A.; White, J. M. *Aust. J. Chem.* **2009**, *62*, 407.
55. (a) Dötz, K. H. *Naturwissenschaften*, **1975**, *62*, 365. (b) Dötz, K. H. *Angew. Chem. Int. Ed. Engl.* **1975**, *14*, 644. (c) Dötz, K. H.; Dietz, R.; von Imhof, A.; Lorenz, H.; Huttner, G. *Chem. Ber.* **1976**, *109*, 2033. (d) Dötz, K. H.; Dietz, R. *Chem. Ber.* **1977**, *110*, 1555.
56. Titanium vinylcarbenes react with styrene at the Ti=C bond (**path a**, Scheme 2-18), but the vinylmetallacyclobutane intermediate undergoes either reductive elimination to vinylcyclopropanes or  $\beta$ -hydride elimination to 1,4-dienes: (a) Shono, T.; Kurashige, R.; Mukaiyama, R.; Tsubouchi, A.; Takeda, T. *Chem.-Eur. J.* **2007**, *13*, 4074.

Chapter 2 is adapted from **R. L. Holland**, K. D. Bunker, C. H. Chen, A. G.

DiPasquale, A. L. Rheingold, K. K. Baldrige, J. M. O'Connor, "Reactions of a Metallacyclobutene Complex with Alkenes" *J. Am. Chem. Soc.*, **2008**, *130*,

10093-10095. Copyright 2008 American Chemical Society. Permission to use

copyrighted images and data in the manuscript was also obtained from K. D.

Bunker, C. H. Chen, A. G. DiPasquale, A. L. Rheingold, K. K. Baldrige, and J. M.

O'Connor.

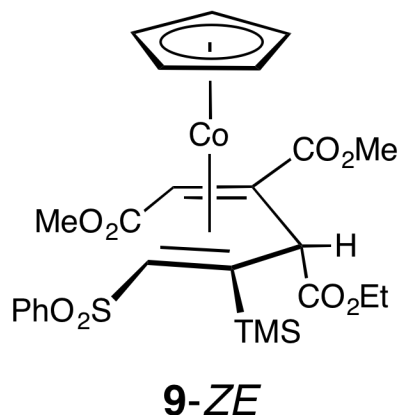
### **Experimental.**

**General Data.** All manipulations were performed under an atmosphere of nitrogen unless otherwise noted, or in a Vacuum Atmospheres inert atmosphere box equipped with a Dri-Train MO 40-1 purifier. NMR spectra were recorded on a Varian Mercury 300 ( $^1\text{H}$ , 300 MHz;  $^{31}\text{P}$ , 122 MHz;  $^{13}\text{C}$  75.5 MHz), a Varian Mercury 400 ( $^1\text{H}$ , 400 MHz;  $^{31}\text{P}$ , 163 MHz;  $^{13}\text{C}$  100.7 MHz), or a Varian UNITY 500 ( $^1\text{H}$ , 500MHz) spectrometer. Chemical shifts were referenced to residual protio-solvent or carbon-solvent signal. IR Spectra were recorded on a Nicolet Avatar 360 FT-IR. Benzene, toluene, hexanes and pentane were distilled over sodium/benzophenone ketyl under an atmosphere of nitrogen. Chloroform and methylene chloride were distilled over  $\text{CaH}_2$  under an atmosphere of nitrogen. Dimethyl maleate was obtained from Aldrich and purified by chromatography before use. All other reagents were obtained from commercial suppliers and used as received.

**Co( $\eta^5$ -C<sub>5</sub>H<sub>5</sub>)[ $\eta^4$ -CH(SO<sub>2</sub>Ph)=C(SiMe<sub>3</sub>)CH(CO<sub>2</sub>Et)C(CO<sub>2</sub>Me)=CH(CO<sub>2</sub>Me)]** (**9-ZE**). In the dry box, a 100-mL Schlenk flask equipped with a magnetic stir bar and a Teflon needle valve was charged with **2** (300 mg, 0.29 mmol), dimethyl fumarate (227.7 mg, 1.58 mmol) and toluene (25 mL). The vessel was sealed and the solution was stirred at 70 °C for 96 h. The reaction mixture was chromatographed on silica gel (12.5% EtOAc/hexanes) to afford **9-ZE** as a bright-orange air-stable solid in 87.4% crude yield. Analytically pure, crystalline **9-ZE** was obtained by slow diffusion of pentane into a concentrated CHCl<sub>3</sub> solution of **9-ZE**. For **9-ZE**: mp 172-174 °C. IR (KBr, thin film): 1726 (C=O), 1700 (C=O) cm<sup>-1</sup>. <sup>1</sup>H NMR (CDCl<sub>3</sub>):  $\delta$  0.35 (s, 9H, Si(CH<sub>3</sub>)<sub>3</sub>), 0.93 (t, 3H, *J* = 6.9 Hz, CO<sub>2</sub>CH<sub>2</sub>CH<sub>3</sub>), 2.87 (s, 1H, CH(SO<sub>2</sub>Ph)), 3.73 (s, 3H, CO<sub>2</sub>CH<sub>3</sub>), 3.74 (m, 1H, CO<sub>2</sub>CHH'CH<sub>3</sub>), 3.76 (s, 1H, CHCO<sub>2</sub>Me), 3.81 (s, 3H, CO<sub>2</sub>CH<sub>3</sub>), 3.93 (m, 1H, CO<sub>2</sub>CHH'CH<sub>3</sub>), 4.80 (s, 1H, CHCO<sub>2</sub>Et), 5.33 (s, 5H, C<sub>5</sub>H<sub>5</sub>), 7.54 (m, 3H, *m,p*-C<sub>6</sub>H<sub>5</sub>SO<sub>2</sub>), 7.92 (d, 2H, *J* = 7.4 Hz, *o*-C<sub>6</sub>H<sub>5</sub>SO<sub>2</sub>). <sup>13</sup>C{<sup>1</sup>H} NMR (CDCl<sub>3</sub>):  $\delta$  1.58 (Si(CH<sub>3</sub>)<sub>3</sub>), 14.05 (CO<sub>2</sub>CH<sub>2</sub>CH<sub>3</sub>), 28.30 (CCO<sub>2</sub>Me), 28.84 (CSiMe<sub>3</sub>), 39.06 (CHCO<sub>2</sub>CH<sub>3</sub>), 45.35 (CHCO<sub>2</sub>CH<sub>3</sub>), 52.50 (CHCO<sub>2</sub>CH<sub>3</sub> or CCO<sub>2</sub>CH<sub>3</sub>), 52.77 (CHCO<sub>2</sub>CH<sub>3</sub> or CCO<sub>2</sub>CH<sub>3</sub>), 60.28 (CHCO<sub>2</sub>CH<sub>2</sub>CH<sub>3</sub>), 81.42 (CHSO<sub>2</sub>Ph), 88.42 (C<sub>5</sub>H<sub>5</sub>), 127.17 (*o*-C<sub>6</sub>H<sub>5</sub>SO<sub>2</sub>), 128.84 (*m*-C<sub>6</sub>H<sub>5</sub>SO<sub>2</sub>), 132.60 (*p*-C<sub>6</sub>H<sub>5</sub>SO<sub>2</sub>), 143.44 (*ipso*-C<sub>6</sub>H<sub>5</sub>SO<sub>2</sub>), 169.10 (C=O), 173.57 (C=O), 175.42 (C=O). 2D-HSQC-NMR (CDCl<sub>3</sub>) provided the following <sup>1</sup>H-<sup>13</sup>C correlations (<sup>1</sup>H,  $\delta$ : <sup>13</sup>C,  $\delta$ ): (0.35: 1.58), (0.93: 14.05), (2.87: 81.42), (3.73: 52.50), (3.74: 60.28), (3.76: 39.06), (3.81: 52.77), (3.93: 60.28), (4.80: 45.35), (5.33: 88.42), (7.54: 127.17), (7.54: 128.84),

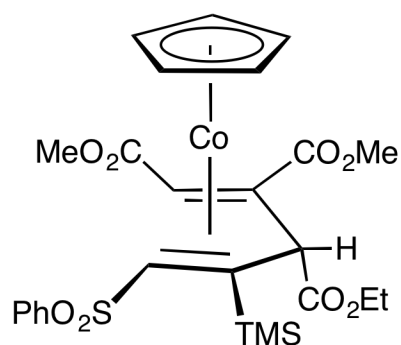


(7.92: 132.60). HRMS(EI),  $m/z$  calcd for  $C_{26}H_{33}O_8SiSCo$ : 592.0992, obsd: 592.0997. Anal Calcd for  $C_{26}H_{33}O_8SiSCo$ : C, 52.69%; H 5.61%. Found: C, 52.53%; H, 5.42%.



**$Co(\eta^5-C_5H_5)[\eta^4-CH(SO_2Ph)=C(SiMe_3)CH(CO_2Et)C(CO_2Me)=CH(CO_2Me)]$**  (9-ZZ). In the dry box, a 100-mL thick-walled reaction tube equipped with a threaded Teflon plug and O-ring, was charged with **2** (104.5 mg, 0.15 mmol), dimethyl fumarate (132.1 mg, 0.92 mmol, 45.8) and benzene (20 mL). The vessel was sealed and the solution was heated at 70 °C for 2.5 h. The reaction mixture was chromatographed on silica gel (25% EtOAc/hexanes) to afford **9-ZZ** as a bright orange/red air-stable solid in 58.2% crude yield. Analytically pure, crystalline **9-ZZ** was obtained by slow diffusion of pentane into a concentrated  $CHCl_3$  solution of **9-ZZ**. For **9-ZZ**: mp 160-161 °C. IR (KBr, thin film): 1731 (C=O), 1711 (C=O)  $cm^{-1}$ .  $^1H$  NMR ( $CDCl_3$ ):  $\delta$  0.35 (s, 9H,  $Si(CH_3)_3$ ), 0.88 (t, 3H,  $J = 6.9$  Hz,  $CO_2CH_2CH_3$ ), 2.32 (s, 1H,  $CHCO_2Me$ ), 2.58 (s, 1H,  $CHSO_2Ph$ ), 3.57 (m, 1H,  $CO_2CHH'CH_3$ ), 3.73 (s, 3H,  $CO_2CH_3$ ), 3.76 (s, 3H,  $CO_2CH_3$ ), 3.85 (m, 1H,

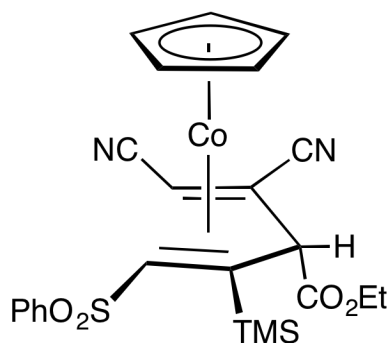
CO<sub>2</sub>CHH'CH<sub>3</sub>), 4.16 (s, 1H, CHCO<sub>2</sub>Et), 5.36 (s, 5H, C<sub>5</sub>H<sub>5</sub>), 7.48 (m, 2H, *m*-C<sub>6</sub>H<sub>5</sub>SO<sub>2</sub>), 7.52 (m, 1H, *p*-C<sub>6</sub>H<sub>5</sub>SO<sub>2</sub>), 7.87 (d, 2H, J = 7.9 Hz, *o*-C<sub>6</sub>H<sub>5</sub>SO<sub>2</sub>). <sup>13</sup>C{<sup>1</sup>H} NMR (CDCl<sub>3</sub>): δ 1.76 (Si(CH<sub>3</sub>)<sub>3</sub>), 13.87 (CH<sub>2</sub>CH<sub>3</sub>), 23.19 (CCO<sub>2</sub>Me), 38.31 (CSiMe<sub>3</sub>), 46.39 (CHCO<sub>2</sub>Me), 49.40 (CHCO<sub>2</sub>Et), 52.01 (CO<sub>2</sub>CH<sub>3</sub>), 52.90 (CO<sub>2</sub>CH<sub>3</sub>), 61.01 (CO<sub>2</sub>CH<sub>2</sub>CH<sub>3</sub>), 76.02 (CHSO<sub>2</sub>Ph), 89.72 (C<sub>5</sub>H<sub>5</sub>), 126.98 (*o*-C<sub>6</sub>H<sub>5</sub>SO<sub>2</sub>), 128.97 (*m*-C<sub>6</sub>H<sub>5</sub>SO<sub>2</sub>), 132.69 (*p*-C<sub>6</sub>H<sub>5</sub>SO<sub>2</sub>), 143.64 (*ipso*-C<sub>6</sub>H<sub>5</sub>SO<sub>2</sub>), 168.76 (C=O), 172.55 (C=O), 173.86 (C=O). HRMS(EI) *m/z* calcd for C<sub>26</sub>H<sub>33</sub>CoO<sub>8</sub>SSi: 592.0992, obsd: 592.1002. Anal Calcd for C<sub>26</sub>H<sub>33</sub>CoO<sub>8</sub>SSi: C, 52.69%; H, 5.61%. Found: C, 52.25%; H, 5.92%.



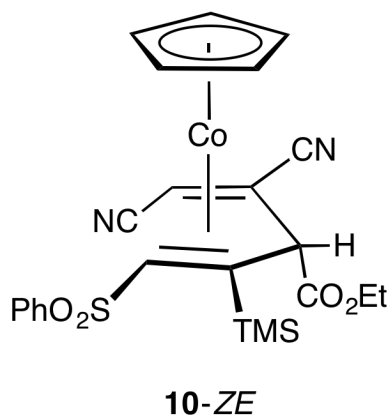
**9-ZZ**

**Co(η<sup>5</sup>-C<sub>5</sub>H<sub>5</sub>)[η<sup>4</sup>-CH(SO<sub>2</sub>Ph)=C(SiMe<sub>3</sub>)CH(CO<sub>2</sub>Et)C(CN)=CH(CN)] (10-ZZ).** In the dry box, a 100-mL thick-walled reaction tube equipped with a threaded Teflon plug and O-ring, was charged with **2** (190 mg, 0.27 mmol), fumaronitrile (237.3 mg, 3.03 mmol) and benzene (30 mL). The flask was sealed and the solution was stirred at 70 °C for 3 h. The reaction mixture was chromatographed on silica gel (12.5% EtOAc/hexanes) to afford **10-ZZ** as a bright orange/red air-stable solid in

78.2% crude yield. Analytically pure, crystalline **10-ZZ** was obtained by slow diffusion of pentane into a concentrated  $\text{CHCl}_3$  solution of **10-ZZ**. For **10-ZZ**: mp 196.8-199.7 °C. IR (KBr, thin film): 2216 (C≡N), 1731 (C=O)  $\text{cm}^{-1}$ .  $^1\text{H}$  NMR ( $\text{CDCl}_3$ ):  $\delta$  0.43 (s, 9H,  $\text{Si}(\text{CH}_3)_3$ ), 0.88 (t, 3H,  $J = 7.4$  Hz,  $\text{CO}_2\text{CH}_2\text{CH}_3$ ), 2.09 (s, 1H,  $\text{CHCN}$ ), 2.56 (s, 1H,  $\text{CHSO}_2\text{Ph}$ ), 3.63 (m, 1H,  $\text{CO}_2\text{CHH}'\text{CH}_3$ ), 3.84 (m, 1H,  $\text{CO}_2\text{CHH}'\text{CH}_3$ ), 4.08 (s, 1H,  $\text{CHCO}_2\text{Et}$ ), 5.56 (s, 5H,  $\text{C}_5\text{H}_5$ ), 7.52 (m, 2H,  $m\text{-C}_6\text{H}_5\text{SO}_2$ ), 7.59 (m, 1H,  $p\text{-C}_6\text{H}_5\text{SO}_2$ ), 7.80 (m, 2H,  $o\text{-C}_6\text{H}_5\text{SO}_2$ ).  $^{13}\text{C}\{^1\text{H}\}$  NMR ( $\text{CDCl}_3$ ):  $\delta$  1.61 ( $\text{Si}(\text{CH}_3)_3$ ), 10.81 ( $\text{CSi}(\text{CH}_3)_3$ ), 13.76 ( $\text{CO}_2\text{CH}_2\text{CH}_3$ ), 26.05 ( $\text{CHCN}$ ), 26.61 ( $\text{CCN}$ ), 48.29 ( $\text{CHCO}_2\text{Et}$ ), 61.89 ( $\text{CO}_2\text{CH}_2\text{CH}_3$ ), 77.48 ( $\text{CHSO}_2\text{Ph}$ ), 92.61 ( $\text{C}_5\text{H}_5$ ), 120.19 (CN), 121.11 (CN), 127.02 ( $o\text{-C}_6\text{H}_5\text{SO}_2$ ), 129.27 ( $m\text{-C}_6\text{H}_5\text{SO}_2$ ), 133.38 ( $p\text{-C}_6\text{H}_5\text{SO}_2$ ), 142.50 ( $ipso\text{-C}_6\text{H}_5\text{SO}_2$ ), 167.19 (C=O). HRMS(EI):  $m/z$  calcd for  $\text{C}_{24}\text{H}_{27}\text{CoN}_2\text{O}_4\text{SSi}$ : 526.0793, obsd: 526.0791. Anal Calcd for  $\text{C}_{24}\text{H}_{27}\text{CoN}_2\text{O}_4\text{SSi}$ : C, 54.74%, H, 5.17%; Found: C, 54.66%; H, 5.49%.

**10-ZZ**

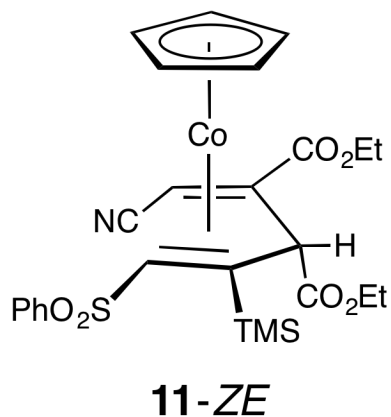
$\text{Co}(\eta^5\text{-C}_5\text{H}_5)[\eta^4\text{-CH}(\text{SO}_2\text{Ph})=\text{C}(\text{SiMe}_3)\text{CH}(\text{CO}_2\text{Et})\text{C}(\text{CN})=\text{CH}(\text{CN})]$  (**10-ZE**). A J-Young style NMR tube was charged with **2** (25 mg, 0.04 mmol) and maleonitrile (38 mg, 0.49 mmol), capped, and  $\text{CDCl}_3$  (~ 0.6 mL) was transferred in under reduced pressure. The NMR tube was heated at 70 °C, and the reaction was monitored by  $^1\text{H}$  NMR spectroscopy across several time points. The reaction was judged to be complete after 5.5 h by disappearance of starting material **2**. Analysis of the NMR spectrum was obfuscated by broadened peaks, but indicated the formation of a major product with resonances at  $\delta$  0.35 (s, 9H,  $\text{Si}(\text{CH}_3)_3$ ) and  $\delta$  5.47 (s, 5H,  $\text{C}_5\text{H}_5$ ). Thermal isomerization of maleonitrile to fumaronitrile was also observed. The reaction mixture was purified by preparative thin-layer chromatography (25% EtOAc/hexanes) to afford a small amount (< 2 mg) of **10-ZE**. A crystalline sample of **10-ZE** suitable for X-Ray diffraction analysis was obtained by slow diffusion of pentane into a concentrated  $\text{CHCl}_3$  solution of **10-ZE**.



**Co( $\eta^5$ -C<sub>5</sub>H<sub>5</sub>)( $\eta^4$ -CH(SO<sub>2</sub>Ph)=C(SiMe<sub>3</sub>)CH(CO<sub>2</sub>Et)C(CO<sub>2</sub>Et)=CH(CN))** (**11-ZE**). In the dry box, a 100-mL thick-walled reaction tube equipped with a threaded Teflon plug and O-ring, was charged with **2** (158.9 mg, 0.22 mmol), ethyl-cis- $\beta$ -cyanoacrylate (187.3 mg, 1.50 mmol) and dichloromethane (25 mL). The flask was sealed and the solution was stirred at 70 °C for 10 h 40 m. The reaction mixture was chromatographed on silica gel (25% EtOAc/hexanes) to afford **11-ZE** as bright orange/red air-stable crystals in 91.7% crude yield. Analytically pure, crystalline **11-ZE** was grown by slow diffusion of pentane into a concentrated CHCl<sub>3</sub> solution of **11-ZE**. For **11-ZE**: mp: 156.8-158.1 °C. IR (KBr, thin film): 2207 (C $\equiv$ N), 1731 (C=O), 1699 (C=O) cm<sup>-1</sup>. <sup>1</sup>H NMR (CDCl<sub>3</sub>):  $\delta$  0.41 (s, 9H, Si(CH<sub>3</sub>)<sub>3</sub>), 0.95 (t, 3H,  $J$  = 6.9 Hz, CO<sub>2</sub>CH<sub>2</sub>CH<sub>3</sub>), 1.37 (t, 3H,  $J$  = 6.6 Hz, CH<sub>3</sub>), 3.03 (s, 1H, CHSO<sub>2</sub>Ph), 3.27 (s, 1H, CHCN), 3.74 (m, 1H, CO<sub>2</sub>CHH'CH<sub>3</sub>), 3.92 (m, 1H, CO<sub>2</sub>CHH'CH<sub>3</sub>), 3.92 (m, 2H, CO<sub>2</sub>CH<sub>2</sub>CH<sub>3</sub>), 4.79 (s, 1H, CHCO<sub>2</sub>Et), 5.37 (s, 5H, C<sub>5</sub>H<sub>5</sub>), 7.55 (m, 3H,  $m,p$ -C<sub>6</sub>H<sub>5</sub>SO<sub>2</sub>), 7.97 (d, 2H,  $J$  = 7.4 Hz,  $\sigma$ -C<sub>6</sub>H<sub>5</sub>SO<sub>2</sub>). <sup>13</sup>C{<sup>1</sup>H} NMR (CDCl<sub>3</sub>):  $\delta$  1.82 (Si(CH<sub>3</sub>)<sub>3</sub>), 13.99 (CO<sub>2</sub>CH<sub>2</sub>CH<sub>3</sub>), 14.71 (CO<sub>2</sub>CH<sub>2</sub>CH<sub>3</sub>), 21.68 (CHCN), 27.85 (CCO<sub>2</sub>Et), 29.80 (CSiMe<sub>3</sub>), 46.86 (CHCO<sub>2</sub>Et), 61.40 (CHCO<sub>2</sub>CH<sub>2</sub>CH<sub>3</sub>), 62.54 (CCO<sub>2</sub>CH<sub>2</sub>CH<sub>3</sub>), 85.00 (CHSO<sub>2</sub>Ph), 88.96 (C<sub>5</sub>H<sub>5</sub>), 121.05 (CN), 127.43 ( $\sigma$ -C<sub>6</sub>H<sub>5</sub>SO<sub>2</sub>), 129.18 ( $m$ -C<sub>6</sub>H<sub>5</sub>SO<sub>2</sub>), 133.15 ( $p$ -C<sub>6</sub>H<sub>5</sub>SO<sub>2</sub>), 142.91 ( $ipso$ -C<sub>6</sub>H<sub>5</sub>SO<sub>2</sub>), 168.79 (C=O), 173.89 (C=O). 2D-HSQC-NMR (CDCl<sub>3</sub>) provided the following <sup>1</sup>H-<sup>13</sup>C correlations (<sup>1</sup>H,  $\delta$ : <sup>13</sup>C,  $\delta$ ): (0.41: 1.82), (0.95: 13.99), (1.38: 14.71), (3.03: 85.00), (3.27: 21.68), (3.74: 61.40), (3.93: 61.40), (4.28: 62.54), (4.79: 46.86), (5.37: 88.96), (7.53: 129.18), (7.55: 133.15), (7.98:

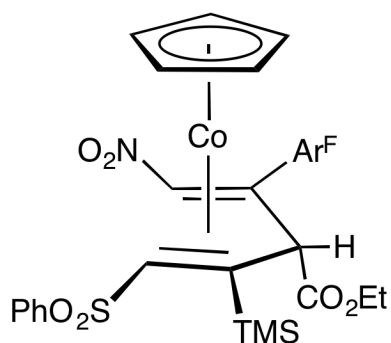
127.43). HRMS(EI):  $m/z$  calcd for  $C_{24}H_{27}CoN_2O_4SSi$ : 573.1046, obsd: 573.1038.

Anal Calcd for  $C_{24}H_{27}CoN_2O_4SSi$ : C, 54.44%; H, 5.62%. Found: C, 54.19%; H, 5.88%.



**Co( $\eta^5$ -C<sub>5</sub>H<sub>5</sub>)[ $\eta^4$ -CH(SO<sub>2</sub>Ph)=C(SiMe<sub>3</sub>)CH(CO<sub>2</sub>Et)C(*o*-C<sub>6</sub>H<sub>4</sub>F)=CH(NO<sub>2</sub>)]** (**12-ZZ-ortho**). In the dry box, a 100-mL thick-walled reaction tube equipped with a threaded Teflon plug and O-ring, was charged with **2** (202.6 mg, 0.29 mmol), 2-fluoro- $\beta$ -nitrostyrene (187.6 mg, 1.12 mmol) and toluene (40 mL). The vessel was sealed and the solution was heated at 70 °C for 26 h. The reaction mixture was chromatographed on silica gel (20% EtOAc/hexanes) to afford **12-ZZ-ortho** as a bright orange/red air-stable solid in 53.9% crude yield. Analytically pure, crystalline **12-ZZ-ortho** was obtained by slow diffusion of pentane into a concentrated CHCl<sub>3</sub> solution of **12-ZZ-ortho**. For **12-ZZ-ortho**: mp 135.9-137.6 °C. IR (KBr, thin film): 1724 (C=O). <sup>1</sup>H NMR (CDCl<sub>3</sub>):  $\delta$  0.33 (s, 9H, Si(CH<sub>3</sub>)<sub>3</sub>), 0.89 (t, 3H,  $J$  = 7.0 Hz, CO<sub>2</sub>CH<sub>2</sub>CH<sub>3</sub>), 3.20 (bs 1H, CH), 3.66 (m, 1H, CO<sub>2</sub>CHH'CH<sub>3</sub>), 3.83 (m, 1H, CO<sub>2</sub>CHH'CH<sub>3</sub>), 4.13 (bs, 1H, CH), 4.79 (bs, 1H,

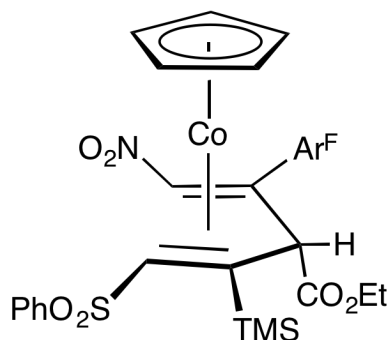
CH), 5.34 (s, 5H, C<sub>5</sub>H<sub>5</sub>), 6.94 (bs, 1H, C<sub>6</sub>H<sub>4</sub>F), 7.28 (m, 1H, *p*-C<sub>6</sub>H<sub>5</sub>SO<sub>2</sub>), 7.55 (m, 3H, *m*-C<sub>6</sub>H<sub>5</sub>SO<sub>2</sub> and C<sub>6</sub>H<sub>4</sub>F), 7.97 (d, 2H, *J* = 7.6 Hz, *o*-C<sub>6</sub>H<sub>5</sub>SO<sub>2</sub>), 8.18 (bs, 1H, C<sub>6</sub>H<sub>4</sub>F). <sup>13</sup>C{<sup>1</sup>H} NMR (CDCl<sub>3</sub>): δ 2.09 (Si(CH<sub>3</sub>)<sub>3</sub>), 13.77 (CH<sub>2</sub>CH<sub>3</sub>), 56.79, 61.26, 78.65, 85.46, 91.00 (C<sub>5</sub>H<sub>5</sub>), 115.56 (d, *J* = 18.8 Hz), 124.47 (d, *J* = 3.3 Hz), 127.02, 129.11, 129.37 (d, *J* = 8.3 Hz), 132.39 (d, *J* = 2.3 Hz), 133.00, 143.22, 158.25, 160.71, 167.95.



**12-ZZ-ortho**  
Ar<sup>F</sup> = *o*-F-C<sub>6</sub>H<sub>4</sub>

**Co(η<sup>5</sup>-C<sub>5</sub>H<sub>5</sub>)[η<sup>4</sup>-CH(SO<sub>2</sub>Ph)=C(SiMe<sub>3</sub>)CH(CO<sub>2</sub>Et)C(*p*-C<sub>6</sub>H<sub>4</sub>F)=CH(NO<sub>2</sub>)]** (**12-ZZ-para**). In the dry box, a 100-mL thick-walled reaction tube equipped with a threaded Teflon plug and O-ring, was charged with **2** (203.2 mg, 0.29 mmol), 4-fluoro-β-nitrostyrene (185.4 mg, 1.11 mmol) and toluene (40 mL). The vessel was sealed and the solution was heated at 70 °C for 26 h. The reaction mixture was chromatographed on silica gel (20% EtOAc/hexanes) to afford **12-ZZ-para** as a bright orange/red air-stable solid in 52.7% crude yield. Analytically pure, crystalline **12-ZZ-para** was obtained by slow diffusion of pentane into a

concentrated  $\text{CHCl}_3$  solution of **12-ZZ-para**. For **12-ZZ-para**: mp 159-163 °C. IR (KBr, thin film): 1721 (C=O).  $^1\text{H}$  NMR ( $\text{CDCl}_3$ ):  $\delta$  0.37 (s, 9H,  $\text{Si}(\text{CH}_3)_3$ ), 0.83 (t, 3H,  $J = 7.2$  Hz,  $\text{CO}_2\text{CH}_2\text{CH}_3$ ), 2.66 (s, 1H, CH), 2.58 (s, 1H, CH), 3.54 (m, 1H,  $\text{CO}_2\text{CHH}'\text{CH}_3$ ), 4.09 (s, 1H, CH), 4.53 (s, 1H, CH), 5.37 (s, 5H,  $\text{C}_5\text{H}_5$ ), 7.03 (t, 2H,  $J = 8.6$  Hz,  $\text{C}_6\text{H}_4\text{F}$ ), 7.54 (m, 5H, *m*- and *p*- $\text{C}_6\text{H}_5\text{SO}_2$  and  $\text{C}_6\text{H}_4\text{F}$ ), 7.94 (d, 2H,  $J = 7.6$  Hz, *o*- $\text{C}_6\text{H}_5\text{SO}_2$ ).  $^{13}\text{C}\{^1\text{H}\}$  NMR ( $\text{CDCl}_3$ ):  $\delta$  2.31 ( $\text{Si}(\text{CH}_3)_3$ ), 13.83 ( $\text{CH}_2\text{CH}_3$ ), 43.10, 57.58, 61.27, 79.40, 86.03, 90.71 ( $\text{C}_5\text{H}_5$ ), 115.60 (d,  $J = 21.4$  Hz), 127.16, 129.16, 131.07 (d,  $J = 8.1$  Hz), 133.11, 168.55. Anal Calcd for  $\text{C}_{28}\text{H}_{31}\text{CoFNO}_6\text{SSi}$ : C, 54.63%, H, 5.08%; Found: C, 54.14%; H, 5.33%.



**12-ZZ-para**  
 $\text{Ar}^{\text{F}} = p\text{-F-C}_6\text{H}_4$

**$\text{Co}(\eta^5\text{-C}_5\text{H}_5)[\kappa^2\text{-(C,C)-}\eta^1\text{-(O)-}$**

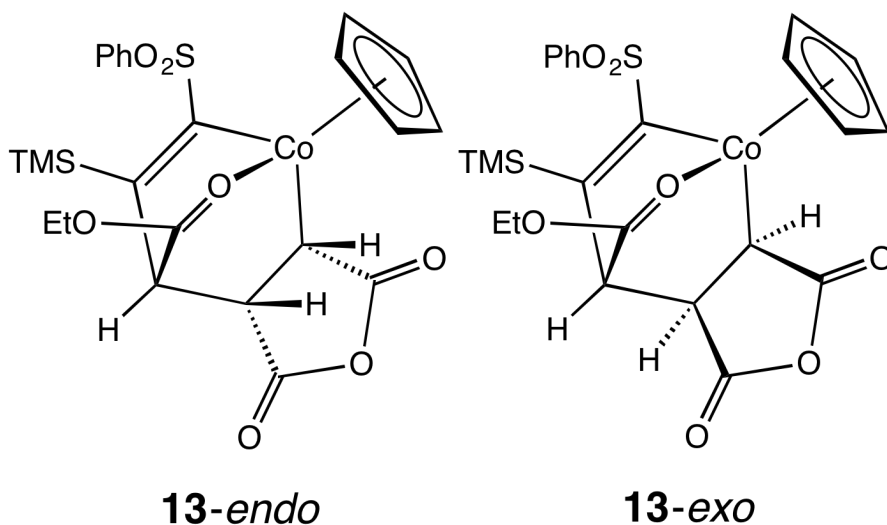
**$\text{CH}(\text{SO}_2\text{Ph})=\text{C}(\text{SiMe}_3)\text{CH}(\text{CO}_2\text{Et})\text{CH}(\text{C}=\text{O})\text{OC}(\text{O})\text{CH}]$**  (**13-endo**) and (**13-exo**).

In the dry box, a 100-mL thick-walled reaction tube equipped with a threaded Teflon plug and O-ring, was charged with **2** (456.6 mg, 0.64 mmol), maleic anhydride (301.8 mg, 3.08 mmol) and toluene (50 mL). The flask was sealed and



the solution was stirred at 70 °C for 3 h. The reaction mixture was chromatographed on silica gel. Eluting with 25% EtOAc/hexanes led to collection of a band from which **13-exo** was isolated in 50.0% yield (174.6 mg) as a dark-green solid. Analytically pure **13-exo** was obtained by slow diffusion of pentane into a concentrated CHCl<sub>3</sub> solution of **13-exo**. Subsequent elution with 40% EtOAc/hexanes led to collection of a second band containing **13-endo**, which was isolated in 41.5% yield (145.7 mg) as a dark red/brown solid. Analytically pure **13-endo** was obtained by slow diffusion of hexane into a concentrated CHCl<sub>3</sub> solution of **13-endo** at -25 °C. For **13-endo**: mp: 147.8-148.4 °C. IR (KBr, thin film): 1816 (C=O), 1753 (C=O), 1641 (C=O) cm<sup>-1</sup>. <sup>1</sup>H NMR (CDCl<sub>3</sub>): δ 0.34 (s, 9H, Si(CH<sub>3</sub>)<sub>3</sub>), 1.25 (t, 3H, *J* = 7.4 Hz, CH<sub>3</sub>), 2.60 (dd, 1H, *J* = 4.2, 9.0 Hz, CH(CO<sub>2</sub>Et)CH[C(=O)OC(=O)CH], 4.20 (m, 2H, CH<sub>2</sub>CH<sub>3</sub>), 4.45 (d, 1H, *J* = 4.2 Hz, CH(CO<sub>2</sub>Et)CH[C(=O)OC(=O)CH], 4.95 (s, 5H, C<sub>5</sub>H<sub>5</sub>), 5.57 (d, 1H, *J* = 9.0 Hz, CH(CO<sub>2</sub>Et)CH[C(=O)OC(=O)CH], 7.51 (m, 3H, *m,p*-C<sub>6</sub>H<sub>5</sub>SO<sub>2</sub>), 7.84 (dd, 2H, *J* = 1.6, 6.6 Hz, *o*-C<sub>6</sub>H<sub>5</sub>SO<sub>2</sub>). <sup>13</sup>C{<sup>1</sup>H} NMR (CDCl<sub>3</sub>): δ 3.27 (Si(CH<sub>3</sub>)<sub>3</sub>), 9.68 (CoCH[C(=O)OC(=O)CH], 13.95 (CO<sub>2</sub>CH<sub>2</sub>CH<sub>3</sub>), 42.15 (CH(CO<sub>2</sub>Et)CH[C(=O)OC(=O)CH], 49.65 (CHCO<sub>2</sub>Et), 65.80 (CO<sub>2</sub>CH<sub>2</sub>CH<sub>3</sub>), 76.74 (CSO<sub>2</sub>Ph), 88.14 (C<sub>5</sub>H<sub>5</sub>), 126.61 (*o*-C<sub>6</sub>H<sub>5</sub>SO<sub>2</sub>), 129.16 (*m*-C<sub>6</sub>H<sub>5</sub>SO<sub>2</sub>), 132.52 (*p*-C<sub>6</sub>H<sub>5</sub>SO<sub>2</sub>), 143.67 (*ipso*-C<sub>6</sub>H<sub>5</sub>SO<sub>2</sub>), 155.30 (CSiMe<sub>3</sub>), 172.51 (C=O), 180.32 (C=O), 180.63 (C=O). HRMS(EI): *m/z* calcd for C<sub>24</sub>H<sub>27</sub>CoO<sub>7</sub>SSi: 546.0573, obsd: 546.0575. Anal Calcd for C<sub>24</sub>H<sub>27</sub>CoO<sub>7</sub>SSi: C, 52.74%; H, 4.98%. Found: C, 52.75%; H, 5.18%.

For **13-exo**: mp: 168.7-169.2 °C. IR (KBr, thin film): 1813 (C=O), 1750 (C=O), 1638 (C=O)  $\text{cm}^{-1}$ .  $^1\text{H}$  NMR ( $\text{CDCl}_3$ ):  $\delta$  0.31 (s, 9H,  $\text{Si}(\text{CH}_3)_3$ ), 1.24 (t, 3H,  $J = 7.4$  Hz,  $\text{CH}_3$ ), 2.65 (dd, 1H,  $J = 5.3, 9.0$  Hz,  $\text{CH}(\text{CO}_2\text{Et})\text{CH}[\text{C}(=\text{O})\text{OC}(=\text{O})\text{CH}]$ ), 3.53 (d, 1H,  $J = 9.0$  Hz,  $\text{CH}(\text{CO}_2\text{Et})\text{CH}[\text{C}(=\text{O})\text{OC}(=\text{O})\text{CH}]$ ), 4.22 (m, 2H,  $\text{CH}_2\text{CH}_3$ ), 4.40 (d, 1H,  $J = 5.3$  Hz,  $\text{CH}(\text{CO}_2\text{Et})\text{CH}[\text{C}(=\text{O})\text{OC}(=\text{O})\text{CH}]$ ), 5.02 (s, 5H,  $\text{C}_5\text{H}_5$ ), 7.55 (m, 3H,  $m,p\text{-C}_6\text{H}_5\text{SO}_2$ ), 7.79 (d, 2H,  $J = 6.9$  Hz,  $o\text{-C}_6\text{H}_5\text{SO}_2$ )  $^{13}\text{C}\{^1\text{H}\}$  NMR ( $\text{CDCl}_3$ ):  $\delta$  3.75 ( $\text{Si}(\text{CH}_3)_3$ ), 12.56 ( $\text{CoCH}[\text{C}(=\text{O})\text{OC}(=\text{O})\text{CH}]$ ), 13.99 ( $\text{CO}_2\text{CH}_2\text{CH}_3$ ), 44.25 ( $\text{CHCO}_2\text{Et}$ ), 49.82 ( $\text{CoCH}[\text{C}(=\text{O})\text{OC}(=\text{O})\text{CH}]$ ), 65.97 ( $\text{CO}_2\text{CH}_2\text{CH}_3$ ), 76.86 ( $\text{CSO}_2\text{Ph}$ ), 87.87 ( $\text{C}_5\text{H}_5$ ), 125.69 ( $o\text{-C}_6\text{H}_5\text{SO}_2$ ), 129.40 ( $m\text{-C}_6\text{H}_5\text{SO}_2$ ), 132.45 ( $p\text{-C}_6\text{H}_5\text{SO}_2$ ), 144.08 ( $ipso\text{-C}_6\text{H}_5\text{SO}_2$ ), 158.65 ( $\text{CSiMe}_3$ ), 173.11 (C=O), 180.83 (C=O), 182.42 (C=O). HRMS(EI): calcd for  $\text{C}_{24}\text{H}_{27}\text{CoO}_7\text{SSi}$ : 546.0573, obsd: 546.0577. Anal Calcd for  $\text{C}_{24}\text{H}_{27}\text{CoO}_7\text{SSi}$ : C, 52.74%; H, 4.98%; Found: C, 52.48%; H, 4.62%.



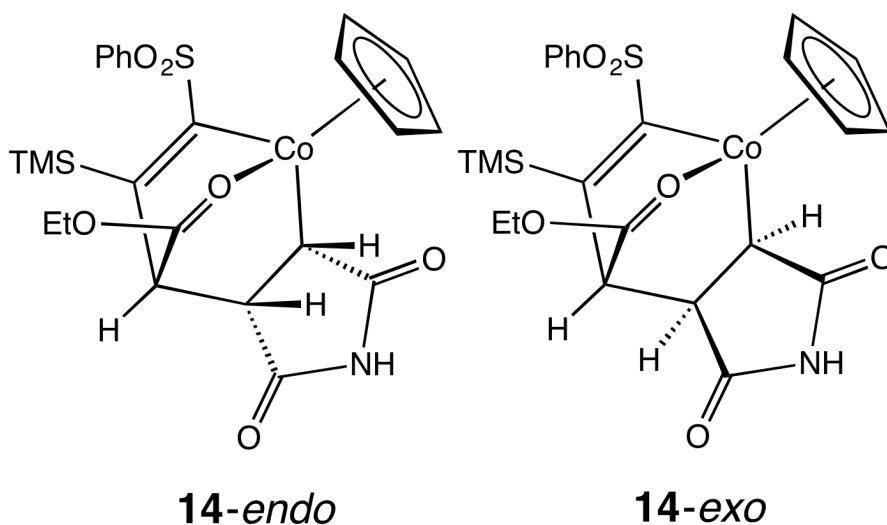
**Co( $\eta^5$ -C<sub>5</sub>H<sub>5</sub>)[ $\kappa^2$ -(C,C)- $\eta^1$ -(O)-**

**CH(SO<sub>2</sub>Ph)=C(SiMe<sub>3</sub>)CH(CO<sub>2</sub>Et)CH(C(=O)NHC(=O)CH)] (14-endo) and (14-**

*exo*). In the dry box, a 100-mL thick-walled reaction tube equipped with a threaded Teflon plug and O-ring, was charged with **2** (166.4 mg, 0.23 mmol), maleimide (172.3 mg, 1.78 mmol) and benzene (40 mL). The flask was sealed and the solution was stirred at 70 °C for 4 h. The reaction mixture was chromatographed on silica gel on silica gel. Eluting with 60% EtOAc/hexanes led to collection of a band from which **14-*exo*** was isolated in 42% yield (53.1 mg) as a dark-green solid. Analytically pure **14-*exo*** was obtained by slow diffusion of pentane into a concentrated CHCl<sub>3</sub> solution of **14-*exo***. Continued elution with 60% EtOAc/hexanes led to collection of a second band containing **14-*endo***, which was isolated in 60% yield (77.0 mg) as a dark red/brown solid. Analytically pure **14-*endo*** was obtained by layering hexane on a concentrated CHCl<sub>3</sub> solution of **14-*endo***. For **14-*endo***: mp: 153.9-155.2 °C. IR (KBr, thin film): 1740 (C=O), 1702 (C=O), 1638 (C=O) cm<sup>-1</sup>. <sup>1</sup>H NMR (CDCl<sub>3</sub>):  $\delta$  0.30 (s, 9H, Si(CH<sub>3</sub>)<sub>3</sub>), 1.25 (t, 3H,  $J$  = 7.2 Hz, CH<sub>3</sub>), 2.42 (dd, 1H,  $J$  = 4.0, 8.4 Hz, CH(CO<sub>2</sub>Et)CH[C(=O)NHC(=O)CH], 4.19 (m, 2H, CH<sub>2</sub>CH<sub>3</sub>), 4.44 (d, 1H,  $J$  = 4.0 Hz, CH(CO<sub>2</sub>Et)CH[C(=O)NHC(=O)CH], 4.97 (s, 5H, C<sub>5</sub>H<sub>5</sub>), 5.62 (d, 1H,  $J$  = 8.4 Hz, CH(CO<sub>2</sub>Et)CH[C(=O)NHC(=O)CH], 7.50 (m, 4H, *m,p*-C<sub>6</sub>H<sub>5</sub>SO<sub>2</sub> and NH), 7.82 (d, 2H,  $J$  = 7.2 Hz, *o*-C<sub>6</sub>H<sub>5</sub>SO<sub>2</sub>). <sup>13</sup>C{<sup>1</sup>H} NMR (CDCl<sub>3</sub>):  $\delta$  3.42 (Si(CH<sub>3</sub>)<sub>3</sub>), 13.45 (CoCH[C(=O)NHC(=O)CH], 14.09 (CO<sub>2</sub>CH<sub>2</sub>CH<sub>3</sub>), 42.73 (CH(CO<sub>2</sub>Et)CH[C(=O)NHC(=O)CH], 49.82 (CHCO<sub>2</sub>Et), 65.48 (CO<sub>2</sub>CH<sub>2</sub>CH<sub>3</sub>),

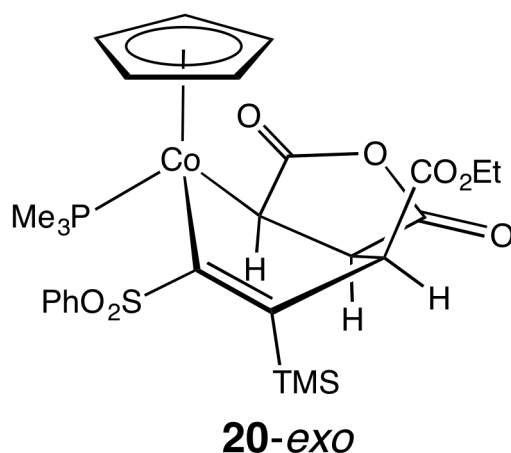
87.98 ( $C_5H_5$ ), 126.46 ( $o$ - $C_6H_5SO_2$ ), 128.93 ( $m$ - $C_6H_5SO_2$ ), 132.39 ( $p$ - $C_6H_5SO_2$ ), 144.54 ( $ipso$ - $C_6H_5SO_2$ ), 155.01 ( $CSiMe_3$ ), 176.95 (C=O), 181.13 (C=O), 186.87 (C=O). Anal Calcd for  $C_{24}H_{27}CoNO_6SSi$ : C, 52.84%; H, 5.17%. Found: C, 52.75%; H, 5.38%.

For **14-exo**: mp: 169.5-171.2°C. IR (KBr, thin film): 1745 (C=O), 1686 (C=O), 1639 (C=O)  $cm^{-1}$ .  $^1H$  NMR ( $CDCl_3$ ):  $\delta$  0.31 (s, 9H,  $Si(CH_3)_3$ ), 1.22 (t, 3H,  $J = 7.2$  Hz,  $CH_3$ ), 2.43 (dd, 1H,  $J = 4.4, 8.8$  Hz,  $CH(CO_2Et)CH[C(=O)NHC(=O)]CH$ ), 3.58 (d, 1H,  $J = 8.8$  Hz,  $CH(CO_2Et)CH[C(=O)NHC(=O)]CH$ ), 4.16 (m, 2H,  $CH_2CH_3$ ), 4.39 (d, 1H,  $J = 4.4$  Hz,  $CH(CO_2Et)CH[C(=O)NHC(=O)]CH$ ), 5.01 (s, 5H,  $C_5H_5$ ), 7.52 (m, 3H,  $m,p$ - $C_6H_5SO_2$ ), 7.64 (bs, NH), 7.78 (dd, 2H,  $J = 1.2$  Hz,  $o$ - $C_6H_5SO_2$ ).  $^{13}C\{^1H\}$  NMR ( $CDCl_3$ ):  $\delta$  3.88 ( $Si(CH_3)_3$ ), 14.12 ( $CoCH[C(=O)NHC(=O)]CH$ ), 16.16 ( $CO_2CH_2CH_3$ ), 45.09 ( $CHCO_2Et$ ), 50.00 ( $CoCH[C(=O)NHC(=O)]CH$ ), 65.54 ( $CO_2CH_2CH_3$ ), 87.58 ( $C_5H_5$ ), 125.76 ( $o$ - $C_6H_5SO_2$ ), 129.34 ( $m$ - $C_6H_5SO_2$ ), 132.30 ( $p$ - $C_6H_5SO_2$ ), 144.46 ( $ipso$ - $C_6H_5SO_2$ ), 159.01 ( $CSiMe_3$ ), 177.09 (C=O), 180.91 (C=O), 188.90 (C=O). Anal Calcd for  $C_{24}H_{28}CoNO_6SSi$ : C, 52.84%; H, 5.17%; Found: C, 52.45%; H, 4.98%.

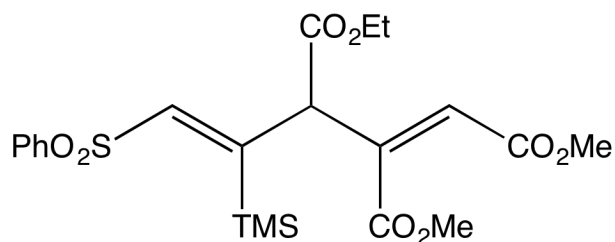


**CH(SO<sub>2</sub>Ph)=C(SiMe<sub>3</sub>)CH(CO<sub>2</sub>Et)CH(C(=O)OC(=O)CH)] (20-*exo*)**. In the dry box, a 100-mL thick-walled reaction tube equipped with a threaded Teflon plug and O-ring, was charged with **2** (644 mg, 0.91 mmol), maleic anhydride (354 mg, 3.61 mmol) and toluene (50 mL). The flask was sealed and the solution was stirred at 70 °C for 3.5 h. The reaction mixture was chromatographed on silica gel. Eluting with 35% EtOAc/hexanes led to collection of a band from which **10-*exo*** was isolated. Solvent was reduced *in vacuo*, and the r.b.f. containing **10-*exo*** was equipped with a Teflon-needle valve adapter, evacuated on a high-vacuum Schlenk line and subsequently transferred into the dry box. In the dry box, **10-*exo*** was dissolved in warm THF and 20 drops of PMe<sub>3</sub> (~400 mg, 5.26 mmol) were added dropwise while stirring. A color change from dark green to red-orange was

observed after the addition of the third drop of  $\text{PMe}_3$ . The solution was stirred for 5 m, and then recrystallized by layering with hexanes to yield a solid-state sample suitable for X-ray diffraction analysis. For **13-exo**:  $^1\text{H}$  NMR ( $\text{CDCl}_3$ ):  $\delta$  0.20 (s, 9H,  $\text{Si}(\text{CH}_3)_3$ ), 1.47 (t, 3H,  $J = 7.0$  Hz,  $\text{CH}_3$ ), 1.55 (d, 9H,  $J = 10$  Hz,  $\text{P}(\text{CH}_3)_3$ ), 1.97 (dd, 1H,  $J = 10.8, 12.0$  Hz,  $\text{CH}(\text{CO}_2\text{Et})\text{CH}[\text{C}(=\text{O})\text{OC}(=\text{O})\text{CH}]$ ), 2.72 (dd, 1H,  $J = 5.6, 10.8$  Hz,  $\text{CH}(\text{CO}_2\text{Et})\text{CH}[\text{C}(=\text{O})\text{OC}(=\text{O})\text{CH}]$ ), 4.14 (m, 1H,  $\text{CHH}'\text{CH}_3$ ), 4.43 (m, 1H,  $\text{CHH}'\text{CH}_3$ ), 4.51 (s, 5H,  $\text{C}_5\text{H}_5$ ), 5.06 (d, 1H,  $J = 5.6$  Hz,  $\text{CH}(\text{CO}_2\text{Et})\text{CH}[\text{C}(=\text{O})\text{OC}(=\text{O})\text{CH}]$ ), 7.51 (m, 3H,  $m,p\text{-C}_6\text{H}_5\text{SO}_2$ ), 8.00 (m, 2H,  $o\text{-C}_6\text{H}_5\text{SO}_2$ )  $^{13}\text{C}\{^1\text{H}\}$  NMR ( $\text{CDCl}_3$ ):  $\delta$  4.07 ( $\text{Si}(\text{CH}_3)_3$ ), 10.27 (d,  $J = 20.6$  Hz,  $\text{P}(\text{CH}_3)_3$ ), 14.37 ( $\text{CoCH}[\text{C}(=\text{O})\text{OC}(=\text{O})\text{CH}]$ ), 44.74 (d,  $J = 2.8$  Hz), 55.03 (d,  $J = 2.4$  Hz), 61.71, 76.86 ( $\text{CSO}_2\text{Ph}$ ), 87.36 (d,  $J = 2.1$  Hz,  $\text{C}_5\text{H}_5$ ), 126.07 ( $o\text{-C}_6\text{H}_5\text{SO}_2$ ), 128.84 ( $m\text{-C}_6\text{H}_5\text{SO}_2$ ), 132.04 ( $p\text{-C}_6\text{H}_5\text{SO}_2$ ), 145.75 ( $ipso\text{-C}_6\text{H}_5\text{SO}_2$ ), 172.42, 173.00 (d,  $J = 1.4$  Hz), 174.90, 185.13.

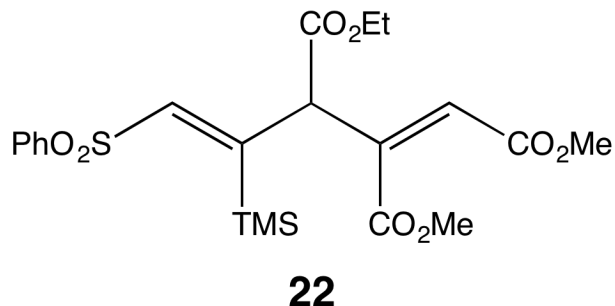


**CH(SO<sub>2</sub>Ph)=C(SiMe<sub>3</sub>)CH(CO<sub>2</sub>Et)C(CO<sub>2</sub>Me)=CH(CO<sub>2</sub>Me) (21)**. A J-Young style NMR tube was charged with **9-ZZ** (15.2 mg, 0.03 mmol) and iodine (25.0 mg, 0.10 mmol), fit with a Teflon cap, and evacuated on a high-vacuum Schlenk line. Several mL of rigorously dry C<sub>6</sub>D<sub>6</sub> was vacuum-transferred to the NMR tube under reduced pressure and sealed. Precipitate began to form immediately upon dissolution. The reaction was monitored by <sup>1</sup>H NMR and allowed to sit under fluorescent lab light overnight, at which time it was filtered and then quenched with an aqueous solution of Na<sub>2</sub>S<sub>2</sub>O<sub>3</sub>·5H<sub>2</sub>O. The organic layer was separated in a 5 mL scintillation vial and then added directly to a prepared silica gel column and purified by chromatography (50% EtOAc/hexanes) to afford **21** as a colorless oil. For **21**: <sup>1</sup>H NMR (C<sub>6</sub>D<sub>6</sub>): δ 0.78 (s, 9H, Si(CH<sub>3</sub>)<sub>3</sub>), 0.85 (t, 3H, *J* = 7.00 Hz, CO<sub>2</sub>CH<sub>2</sub>CH<sub>3</sub>), 3.06 (s, 3H, CO<sub>2</sub>Me), 3.10 (s, 3H, CO<sub>2</sub>Me), 3.88 (qd, 2H, *J*<sub>1</sub> = 7.00 Hz *J*<sub>2</sub> = 2.00 Hz, CO<sub>2</sub>CH<sub>2</sub>CH<sub>3</sub>) 5.92 (s, 1H, CHCO<sub>2</sub>Me), 6.68 (d, 1H, *J* = 0.50 Hz, CHCO<sub>2</sub>Et), 6.86 (t, 3H, *J* = 3.25 Hz, *m,p*-C<sub>6</sub>H<sub>5</sub>SO<sub>2</sub>), 6.89 (d, 1H, *J* = 0.50, CHSO<sub>2</sub>Ph), 7.97 (m, 2H, *o*-C<sub>6</sub>H<sub>5</sub>SO<sub>2</sub>).

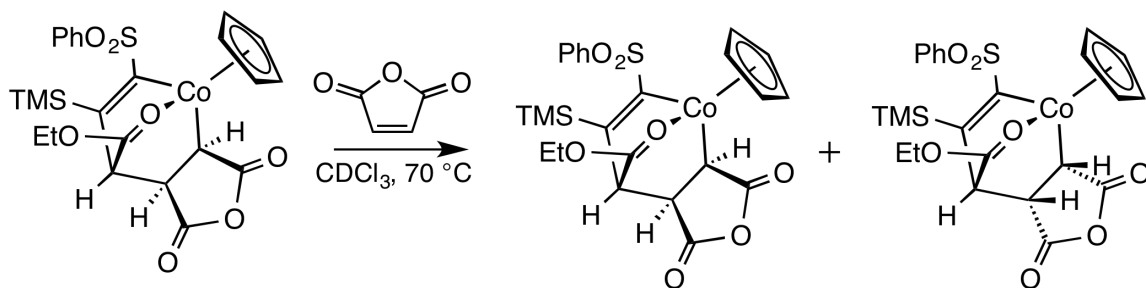
**21**

**CH(SO<sub>2</sub>Ph)=C(SiMe<sub>3</sub>)CH(CO<sub>2</sub>Et)C(CO<sub>2</sub>Me)=CH(CO<sub>2</sub>Me) (22)**. In the dry box, a 500-mL round bottom flask equipped with a magnetic stir bar was charged with **9-ZE** (132.8 mg, 0.224 mmol), iodine (232.6 mg, 0.930 mmol) and benzene (200 mL). The vessel was fit with a septum and the solution was stirred at r.t. for 17 h, at which time it sent out of the dry box, filtered, and then quenched with an aqueous solution of Na<sub>2</sub>S<sub>2</sub>O<sub>3</sub>·5H<sub>2</sub>O. The mixture was separated and the aqueous layer further extracted with diethyl ether. The combined fractions were dried with MgSO<sub>4</sub>, and solvent was removed *in vacuo*. The reaction mixture was chromatographed on silica gel (50% EtOAc/hexanes) to afford **22** as a colorless oil, which eventually solidified as a white crystalline solid in 98.7% crude yield. For **22**: <sup>1</sup>H NMR (C<sub>6</sub>D<sub>6</sub>): δ 0.76 (s, 9H, Si(CH<sub>3</sub>)<sub>3</sub>), 0.85 (t, 3H, *J* = 7.20 Hz, CO<sub>2</sub>CH<sub>2</sub>CH<sub>3</sub>), 3.08 (s, 3H, CO<sub>2</sub>Me), 3.11 (s, 3H, CO<sub>2</sub>Me), 3.88 (q, 2H, *J* = 7.20 Hz, CO<sub>2</sub>CH<sub>2</sub>CH<sub>3</sub>) 5.90 (s, 1H, CHCO<sub>2</sub>Me), 6.68 (d, 1H, *J* = 0.80 Hz, CHCO<sub>2</sub>Et), 6.88 (d, 1H, *J* = 0.80 Hz, CHSO<sub>2</sub>Ph), 6.88 (m, 3H, *m,p*-C<sub>6</sub>H<sub>5</sub>SO<sub>2</sub>), 7.96 (m, 2H, *o*-C<sub>6</sub>H<sub>5</sub>SO<sub>2</sub>) <sup>13</sup>C{<sup>1</sup>H} NMR (C<sub>6</sub>D<sub>6</sub>): δ 1.03 (Si(CH<sub>3</sub>)<sub>3</sub>), 14.01 (CO<sub>2</sub>CH<sub>2</sub>CH<sub>3</sub>), 50.75 (CHCO<sub>2</sub>Me or CHCO<sub>2</sub>Et), 51.63 (CHCO<sub>2</sub>Me or CHCO<sub>2</sub>Et), 52.32 (CHCO<sub>2</sub>Me or CHCO<sub>2</sub>Et), 61.53 (CO<sub>2</sub>CH<sub>2</sub>CH<sub>3</sub>), 127.45 (C<sub>6</sub>H<sub>5</sub>SO<sub>2</sub>), 128.81 (C<sub>6</sub>H<sub>5</sub>SO<sub>2</sub>), 129.11 (C<sub>6</sub>H<sub>5</sub>SO<sub>2</sub>), 132.73 (CHCO<sub>2</sub>Me), 139.97 (CHSiMe<sub>3</sub>), 142.28 (*ipso*-C<sub>6</sub>H<sub>5</sub>SO<sub>2</sub>), 144.83 (CCO<sub>2</sub>Me), 158.17 (CSO<sub>2</sub>Ph), 165.03 (C=O), 166.62 (C=O), 170.17 (C=O). HRMS(EI), *m/z* calcd for C<sub>21</sub>H<sub>28</sub>O<sub>8</sub>Si: 468.1269, obsd: 468.1279.

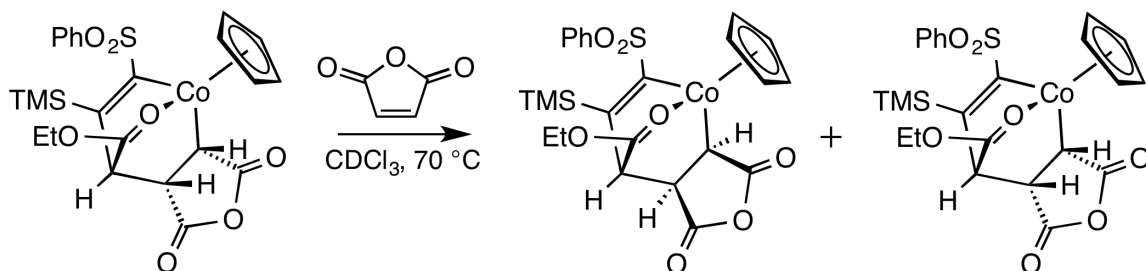




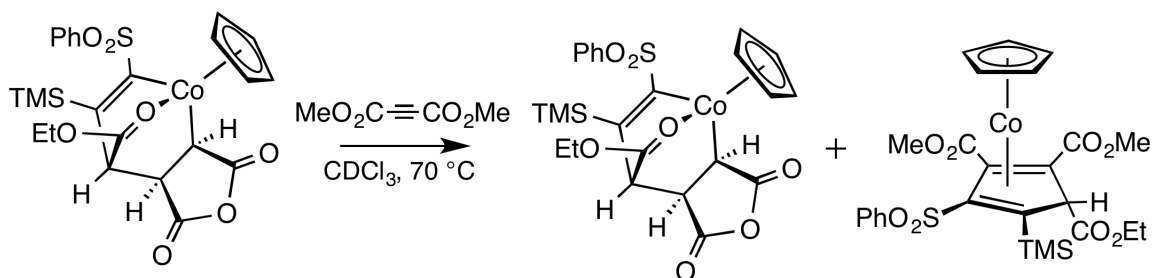
**Reaction of 13-*exo* with maleic anhydride.** A J-Young style NMR tube was charged with 4.3 mg of crystalline **13-*exo*** (13 mM), 6.5 mg of maleic anhydride (111 mM), and one crystal of 1,3,5-tri-*tert*-butyl-benzene (< 1 mg). The NMR tube was attached to a high-vacuum line and evacuated, rigorously-dried and degassed CDCl<sub>3</sub> was transferred in under reduced pressure (~ 0.6 mL), and the sample was sealed with a Teflon cap. An initial <sup>1</sup>H NMR spectrum was recorded, and the sample was heated at 70 °C for 3 h. The NMR tube sample was transferred into an inert-atmosphere dry-box, opened, and filtered into a second J-Young style NMR tube to remove precipitate. Analysis by <sup>1</sup>H NMR spectroscopy indicated the formation of a trace amount of the **13-*endo*** product, as well as decomposition of **13-*exo***. Further heating at 70 °C for 24 h followed by filtration and spectroscopic analysis revealed further decomposition, with no apparent increase in **13-*endo*** product.



**Reaction of **13-endo** with maleic anhydride.** A J-Young style NMR tube was charged with 3.4 mg of crystalline **13-endo** (10 mM), 6.5 mg of maleic anhydride (116 mM), and one crystal of 1,3,5-tri-*tert*-butyl-benzene (< 1 mg). The NMR tube was attached to a high-vacuum line and evacuated, rigorously-dried and degassed  $\text{CDCl}_3$  was transferred in under reduced pressure ( $\sim 0.6$  mL), and the sample was sealed with a Teflon cap. An initial  $^1\text{H}$  NMR spectrum was recorded, and the sample was heated at  $70^\circ\text{C}$  for 3 h. The NMR tube sample was transferred into an inert-atmosphere dry-box, opened, and filtered into a second J-Young style NMR tube to remove precipitate. Analysis by  $^1\text{H}$  NMR spectroscopy indicated only decomposition of **13-endo**, with no evidence for formation of **13-exo**. Further heating at  $70^\circ\text{C}$  for 12.5 h followed by filtration and spectroscopic analysis revealed further decomposition, with no appearance of **13-exo** product.

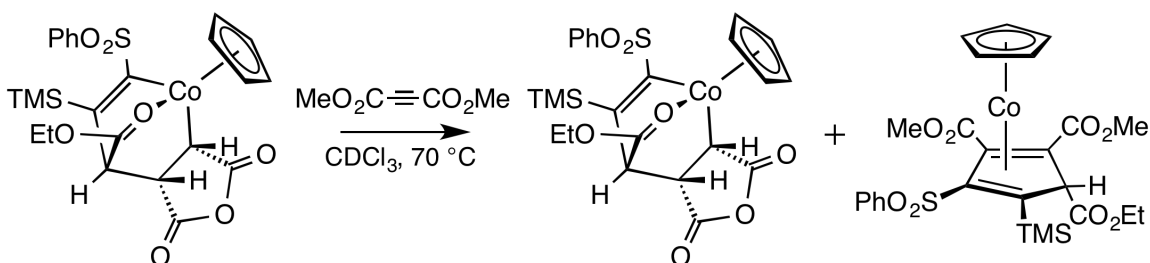


**Reaction of **13-*exo*** with dimethyl acetylenedicarboxylate.** A J-Young style NMR tube was charged with 4.5 mg of crystalline **13-*exo*** (14 mM), 20  $\mu$ L of dimethyl acetylenedicarboxylate (271 mM), and one crystal of 1,3,5-tri-*tert*-butylbenzene (< 1 mg). The NMR tube was attached to a high-vacuum line and evacuated, rigorously-dried and degassed  $\text{CDCl}_3$  was transferred in under reduced pressure ( $\sim 0.6$  mL), and the sample was sealed with a Teflon cap. An initial  $^1\text{H}$  NMR spectrum was recorded, and the sample was heated at  $70^\circ\text{C}$  for 4 h. Analysis by  $^1\text{H}$  NMR spectroscopy indicated the formation of a trace amount the  $\eta^4$ -cyclopentadiene DMAD product. Further heating at  $70^\circ\text{C}$  for 25 h revealed a similar spectrum, with only a trace amount of DMAD product.

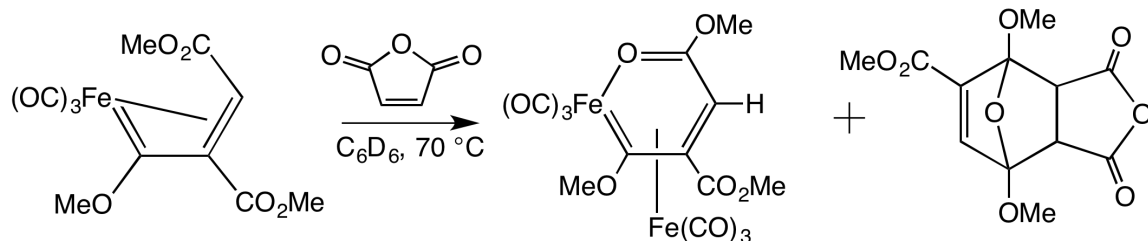


**Reaction of **13-*endo*** with dimethyl acetylenedicarboxylate.** A J-Young style NMR tube was charged with 4.5 mg of crystalline **13-*endo*** (13 mM), 20  $\mu$ L of dimethyl acetylenedicarboxylate (271 mM), and one crystal of 1,3,5-tri-*tert*-butylbenzene (< 1 mg). The NMR tube was attached to a high-vacuum line and evacuated, rigorously-dried and degassed  $\text{CDCl}_3$  was transferred in under reduced pressure ( $\sim 0.6$  mL), and the sample was sealed with a Teflon cap. An

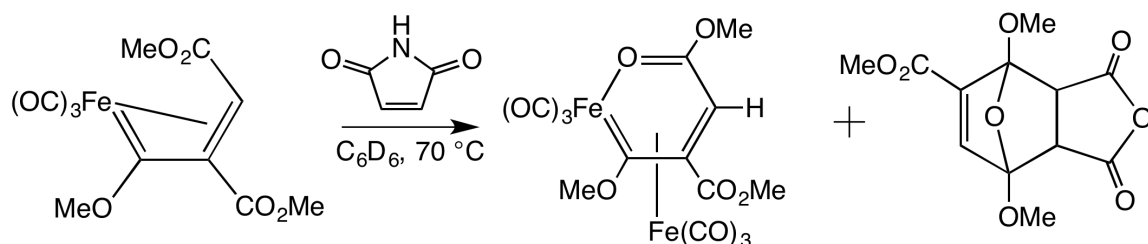
initial  $^1\text{H}$  NMR spectrum was recorded, and the sample was heated at  $70\text{ }^\circ\text{C}$  for 4 h. Analysis by  $^1\text{H}$  NMR spectroscopy indicated the formation of a trace amount the  $\eta^4$ -cyclopentadiene DMAD product. Further heating at  $70\text{ }^\circ\text{C}$  for 25 h revealed a similar spectrum, with only a trace amount of DMAD product.



**Reaction of 14 with maleic anhydride.** In the dry box, a 5 mL volumetric flask was charged with **25a** (13.1 mg,  $4.0\ \mu\text{mol}$ ), maleic anhydride (5.4 mg,  $5.6\ \mu\text{mol}$ ), and 5 mL  $\text{C}_6\text{D}_6$ . The sample was dissolved and a  $500\ \mu\text{L}$  aliquot was removed via syringe, transferred to a J-Young style NMR tube, and sealed with a Teflon cap. The reaction mixture was analyzed by  $^1\text{H}$  NMR ( $\text{C}_6\text{D}_6$ , 400.1 MHz) to obtain initial conditions, and then heated at  $70\text{ }^\circ\text{C}$ . Subsequent analysis of the proton spectrum after 6 h of heating indicated the formation of a dinuclear iron species **30** and formation of a new product identified as **31**. Analysis after 20 h of heating at  $70\text{ }^\circ\text{C}$  indicated that the reaction had reached completion, with formation of a 1:1 mixture of **30** and **31**. For **31**:  $^1\text{H}$  NMR ( $\text{C}_6\text{D}_6$ ):  $\delta$  2.79 (s, 3H,  $\text{CH}_3$ ), 3.28 (s, 3H,  $\text{CH}_3$ ), 3.32 (d, 1H,  $J = 8.0\text{ Hz}$ , CH), 3.46 (s, 3H,  $\text{CH}_3$ ), 3.85 (d, 1H,  $J = 8.0\text{ Hz}$ , CH), 4.64 (s, 1H, CH).



**Reaction of 25a with maleimide (32).** In the dry box, a 5 mL volumetric flask was charged with **25a** (9.6 mg, 3.1  $\mu\text{mol}$ ), maleimide (6.5 mg, 5.6  $\mu\text{mol}$ ), and 5 mL  $\text{C}_6\text{D}_6$ . The sample was dissolved and a 500  $\mu\text{L}$  aliquot was removed via syringe, transferred to a J-Young style NMR tube, and sealed with a Teflon cap. The reaction mixture was analyzed by  $^1\text{H}$  NMR ( $\text{C}_6\text{D}_6$ , 400.1 MHz) to obtain initial conditions, and then heated at 70  $^\circ\text{C}$ . Subsequent analysis of the proton spectrum after 16 h of heating indicated that the reaction had reached completion, with formation of a 1:1 mixture of **30** and **32**. For **32**:  $^1\text{H}$  NMR ( $\text{C}_6\text{D}_6$ ):  $\delta$  2.93 (s, 3H,  $\text{CH}_3$ ), 3.28 (d, 1H,  $J = 7.6$  Hz, CH), 3.32 (s, 3H,  $\text{CH}_3$ ), 3.57 (s, 3H,  $\text{CH}_3$ ), 3.92 (d, 1H,  $J = 7.6$  Hz, CH), 4.72 (s, 1H, CH), 6.58 (bs, 1H, NH).



## Calculations and Equations for the Geometric Analysis of $\eta^4$ -1,4-Pentadiene Complexes.

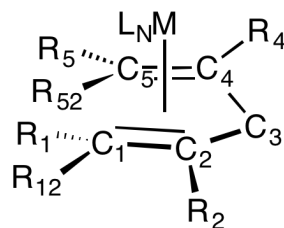


**Figure 2-10.** Generic numbering and geometric analysis schema for  $\eta^4$ -1,4-pentadienes.

Definitions and Equations:

Equation of a plane  $\vec{n}$ :  $ax + by + cz = d$

Angle between two planes  $\angle \vec{n}_1 - \vec{n}_2 = \alpha(\vec{n}_1, \vec{n}_2)$

$\vec{n}_1$ :  $a_1x + a_2y + a_3z + a_4 = 0$

$\vec{n}_2$ :  $b_1x + b_2y + b_3z + b_4 = 0$

$$\mathbf{a} = \begin{bmatrix} a_1 \\ a_2 \\ a_3 \end{bmatrix} \quad \mathbf{b} = \begin{bmatrix} b_1 \\ b_2 \\ b_3 \end{bmatrix} \quad |\mathbf{a}| = \sqrt{a_1^2 + a_2^2 + a_3^2} \quad |\mathbf{b}| = \sqrt{b_1^2 + b_2^2 + b_3^2}$$

$$\angle \vec{n}_1 - \vec{n}_2 = \alpha(\vec{n}_1, \vec{n}_2) \text{ bend-back parameter: } \cos \alpha = \frac{|a_1b_1 + a_2b_2 + a_3b_3|}{|\mathbf{a}||\mathbf{b}|}$$

$$\alpha(\vec{n}_1, \vec{n}_2) = \cos^{-1} \frac{|a_1b_1 + a_2b_2 + a_3b_3|}{|\mathbf{a}||\mathbf{b}|}$$

$$\angle \vec{n}_{C1-C2-C4-C5} - \vec{n}_{C2-C3-C4} \text{ fold angle}$$

Generic Analysis Scheme:

CSD Refcode

C1-C2 = [ $\text{\AA}$ ]

$\vec{n}_{R1-C1-R12}$ :  $ax + by + cz - d = 0$

$\vec{n}_{R2-C2-C3}$ :  $ax + by + cz - d = 0$

$\alpha_1 = [^\circ]$

C4-C5 = [ $\text{\AA}$ ]

$\vec{n}_{R5-C5-R52}$ :  $ax + by + cz - d = 0$

$\vec{n}_{C3-C4-R4}$ :  $ax + by + cz - d = 0$

$\alpha_2 = [^\circ]$

$\angle \vec{n}_{C1-C2-C4-C5} - \vec{n}_{C2-C3-C4} \text{ fold angle} = [^\circ]$

(all atom numbering is from the respective crystallographic information file)

BUCNIT10 ((tBuNC)<sub>2</sub>Ni(C(CN)<sub>2</sub>=C(CN)<sub>2</sub>) – test structure)<sup>16a</sup>

$\vec{n}_{H7-C5-H8}$ :  $0.795x - 0.176y - 0.581z - 4.295 = 0$

$\vec{n}_{H10-C6-H9}$ :  $0.069x + 0.184y + 0.980z + 5.371 = 0$

$$\alpha_1 = 56.84^\circ; \text{ reported } 56.8(5)^\circ$$

KCLETP03 (Zeise's Salt – test structure)<sup>16b</sup>

$$\vec{n}_{\text{H7-C5-H8}}: 0.979x + 0.041y + 0.200z + 4.940 = 0$$

$$\vec{n}_{\text{H10-C6-H9}}: 0.930x + 0.093y - 0.356z + 4.537 = 0$$

$$\alpha_1 = 32.55^\circ; \text{ reported } 32.5^\circ$$

BZAMCR10

$$\text{C15-C8} = 1.4055(13) \text{ \AA}$$

$$\vec{n}_{\text{C9-C15-H27}}: 0.711x - 0.480y - 0.514z - 2.598 = 0$$

$$\vec{n}_{\text{C1-C8-H21}}: 0.916x - 0.066y - 0.396z - 2.951 = 0$$

$$\alpha_1 = 27.22447^\circ$$

$$\text{C22-C23} = 1.4159(13) \text{ \AA}$$

$$\vec{n}_{\text{C1-C22-H28}}: 0.979x - 0.105y + 0.175z - 5.391 = 0$$

$$\vec{n}_{\text{C16-C23-H29}}: 0.783x - 0.524y + 0.334z - 6.103 = 0$$

$$\alpha_2 = 28.3178133^\circ$$

$$\angle \vec{n}_{\text{C15-C8-C22-C23}}-\vec{n}_{\text{C8-C1-C22}} \text{ fold angle} = 27.47(3)^\circ$$

MVHFUI10<sup>a</sup>

$$\text{C5-C2} = 1.4027(6) \text{ \AA}$$

$$\text{C6-C4} = 1.3697(6) \text{ \AA}$$

$$\angle \vec{n}_{\text{C5-C2-C4-C6}}-\vec{n}_{\text{C2-C3-C4}} \text{ fold angle} = 52.41(3)^\circ$$

(a) – no H-atom coordinates available from crystallographic information file

PONFED

$$\text{C15-C14} = 1.397(12) \text{ \AA}$$

$$\vec{n}_{\text{H21-C15-H22}}: -0.644x + 0.762y + 0.063z - 8.049 = 0$$

$$\vec{n}_{\text{H20-C14-C13}}: 0.239x + 0.948y + 0.208z + 6.343 = 0$$

$$\alpha_1 = 54.4073569^\circ$$

$$\text{C11-C12} = 1.332(10) \text{ \AA}$$

$$\vec{n}_{\text{H17-C11-H16}}: -0.174x + 0.563y + 0.808z + 1.637 = 0$$

$$\vec{n}_{\text{C13-C12-H18}}: -0.702x - 0.129y + 0.700z - 9.944 = 0$$

$$\alpha_1 = 52.0293134^\circ$$

$$\angle \vec{n}_{\text{C15-C14-C12}}-\vec{n}_{\text{C14-C13-C12}} \text{ fold angle}^b = 39.8(4)^\circ$$

(b) – fold angle measured from the plane of three alkene carbons instead of four

**9-ZE**

$$\text{C10-C11} = 1.433(4) \text{ \AA}$$

$$\vec{n}_{\text{H11-C11-Si1}}: 0.549x + 0.750y + 0.369z + 2.322 = 0$$

$$\vec{n}_{\text{C9-C10-Si1}}: -0.062x + 0.998y - 0.019z + 2.970 = 0$$

$$\alpha_1 = 44.9798711^\circ$$

$$\text{C7-C8} = 1.423(5) \text{ \AA}$$

$$\vec{n}_{\text{H7-C7-C6}}: 0.821x + 0.276y - 0.499z + 1.666 = 0$$

$$\vec{n}_{\text{C13-C8-C9}}: -0.219x - 0.433y + 0.874z - 2.279 = 0$$

$$\alpha_1 = 42.6108592^\circ$$

$$\angle \vec{n}_{\text{C7-C8-C10-C11}} - \vec{n}_{\text{C8-C9-C10}} \text{ fold angle} = 58.1(3)^\circ$$

### 9-ZZ

$$\text{C5-C4} = 1.4298(16) \text{ \AA}$$

$$\vec{n}_{\text{H5-C5-S1}}: 0.334x + 0.849y + 0.409z + 5.265 = 0$$

$$\vec{n}_{\text{C3-C4-Si1}}: -0.315x + 0.948y + 0.043z + 1.016 = 0$$

$$\alpha_1 = 44.1565993^\circ$$

$$\text{C1-C2} = 1.4208(16) \text{ \AA}$$

$$\vec{n}_{\text{H1-C1-C6}}: -0.057x + 0.120y + 0.991z + 3.298 = 0$$

$$\vec{n}_{\text{C3-C2-C7}}: 0.837x - 0.148y - 0.527z + 2.140 = 0$$

$$\alpha_1 = 54.0027799^\circ$$

$$\angle \vec{n}_{\text{C1-C2-C4-C5}} - \vec{n}_{\text{C2-C3-C4}} \text{ fold angle} = 61.26(10)^\circ$$

### 10-ZE

$$\text{C1-C2} = 1.417(6) \text{ \AA}$$

$$\vec{n}_{\text{H1-C1-S1}}: -0.624x - 0.067y + 0.778z - 0.415 = 0$$

$$\vec{n}_{\text{C3-C2-Si1}}: 0.216x + 0.745y - 0.631z + 0.136 = 0$$

$$\alpha_1 = 47.4714066^\circ$$

$$\text{C4-C5} = 1.436(6) \text{ \AA}$$

$$\vec{n}_{\text{H5-C5-C(CN)}}: 0.994x + 0.060y + 0.094z + 5.211 = 0$$

$$\vec{n}_{\text{C3-C4-C(CN)}}: 0.629x + 0.645y + 0.433z + 5.409 = 0$$

$$\alpha_1 = 45.189875^\circ$$

$$\angle \vec{n}_{\text{C1-C2-C4-C5}} - \vec{n}_{\text{C2-C3-C4}} \text{ fold angle} = 61.7(4)^\circ$$

### 10-ZZ

$$\text{C10-C9} = 1.428(3) \text{ \AA}$$

$$\vec{n}_{\text{H10-C10-S1}}: 0.920x - 0.298y - 0.255z - 4.430 = 0$$

$$\vec{n}_{\text{C8-C9-Si1}}: 0.828x - 0.099y + 0.552z - 0.856 = 0$$

$$\alpha_1 = 49.4283395^\circ$$

$$\text{C6-C7} = 1.437(3) \text{ \AA}$$

$$\vec{n}_{\text{H6-C6-C11}}: 0.581x + 0.639y - 0.505z - 0.088 = 0$$

$$\vec{n}_{\text{C12-C7-C8}}: 0.463x + 0.855y + 0.235z + 3.234 = 0$$

$$\alpha_1 = 45.881722^\circ$$

$$\angle \vec{n}_{\text{C10-C9-C6-C7}} - \vec{n}_{\text{C9-C8-C7}} \text{ fold angle} = 60.18(13)^\circ$$

### 11-ZE

$$\text{C1-C2} = 1.430(2) \text{ \AA}$$

$$\vec{n}_{\text{H1-C1-S1}}: 0.536x + 0.794y + 0.287z + 11.822 = 0$$

$$\vec{n}_{\text{C3-C2-Si1}}: 0.275x + 0.836y - 0.475z + 1.155 = 0$$

$$\alpha_1 = 47.5632682^\circ$$



$$C4-C5 = 1.428(2) \text{ \AA}$$

$$\vec{n}_{H5-C5-C24}: -0.391x + 0.720y + 0.573z - 7.017 = 0$$

$$\vec{n}_{C23-C4-C3}: -0.731x + 0.678y - 0.072z - 3.181 = 0$$

$$\alpha_1 = 42.848825^\circ$$

$$\angle \vec{n}_{C1-C2-C4-C5} - \vec{n}_{C2-C3-C4} \text{ fold angle} = 59.96(14)^\circ$$

### 12-ZZ-ortho

$$C1-C2 = 1.449(9) \text{ \AA}$$

$$\vec{n}_{H1-C1-S1}: -0.700x - 0.472y + 0.536z - 1.557 = 0$$

$$\vec{n}_{C3-C2-Si1}: 0.080x - 0.443y + 0.893z + 9.445 = 0$$

$$\alpha_1 = 50.8252461^\circ$$

$$C4-C5 = 1.414(10) \text{ \AA}$$

$$\vec{n}_{H5-C5-N1}: 0.232x + 0.919y + 0.320z + 7.321 = 0$$

$$\vec{n}_{C23-C4-C3}: -0.552x + 0.828y - 0.097z - 4.539 = 0$$

$$\alpha_1 = 53.009465^\circ$$

$$\angle \vec{n}_{C1-C2-C4-C5} - \vec{n}_{C2-C3-C4} \text{ fold angle} = 61.4(5)^\circ$$

### 12-ZZ-para

$$C1-C2 = 1.431(3) \text{ \AA}$$

$$\vec{n}_{H1-C1-S1}: -0.203x + 0.639y + 0.741z + 2.539 = 0$$

$$\vec{n}_{C3-C2-Si1}: 0.797x - 0.593y - 0.118z + 6.871 = 0$$

$$\alpha_1 = 51.0717224^\circ$$

$$C4-C5 = 1.425(3) \text{ \AA}$$

$$\vec{n}_{H5-C5-N1}: 0.512x + 0.852y - 0.105z + 6.872 = 0$$

$$\vec{n}_{C23-C4-C3}: -0.184x + 0.773y - 0.607z - 3.244 = 0$$

$$\alpha_1 = 51.0629257^\circ$$

$$\angle \vec{n}_{C1-C2-C4-C5} - \vec{n}_{C2-C3-C4} \text{ fold angle} = 60.97(18)^\circ$$

**Computational Methods.** The conformational analyses described in this study, including structural and orbital arrangements as well as property calculations, were carried out using the GAMESS<sup>19</sup> software package. Structural computations on **12** were performed using the new M06-2X<sup>20</sup> DFT method of Truhlar, *et al.*, as well as the MP2<sup>21</sup> second order perturbation method. The relativistic effective core potential, Stuttgart/Dresden-double- $\zeta$  (6d, 10f) (SDD)<sup>22</sup> was used for the transition metal, with the state-averaged optimum f exponents 1.019 and 4.076 from Martin and Sundermann,<sup>23</sup> while all other atoms were treated with the Dunning correlation consistent basis set, cc-pVDZ, a [3s2p1d] contraction of a (9s4p1d) primitive set.<sup>24</sup> Full geometry optimizations were performed and uniquely characterized via second derivatives (Hessian) analysis to determine the number of imaginary frequencies (0 = minima; 1 = transition state), and zero point contributions. Molecular orbital and electrostatic contour plots, used as an aid in the analysis of results, were generated and depicted using the programs MacMolPlt,<sup>25</sup> and QMView.<sup>26</sup>

**General Experimental for X-Ray Structure Determinations.** A single crystal with general dimensions of  $a \times b \times c$  was immersed in Paratone and placed on a Cryoloop. Data were collected on a Bruker SMART (APEX) CCD diffractometer, using a graphite monochromator with Mo  $K\alpha$  radiation ( $\lambda = 0.71073 \text{ \AA}$ ) at the defined temperature. The data were integrated using the Bruker SAINT software program and scaled using the SADABS software program. Solution by direct methods (SIR-2004) produced a complete heavy-atom phasing model consistent with the proposed structure. All non-hydrogen atoms were refined anisotropically by full-matrix least-squares (SHELXL-97). All hydrogen atoms were placed using a riding model. Their positions were constrained relative to their parent atom using the appropriate HFIX command in SHELXL-97.

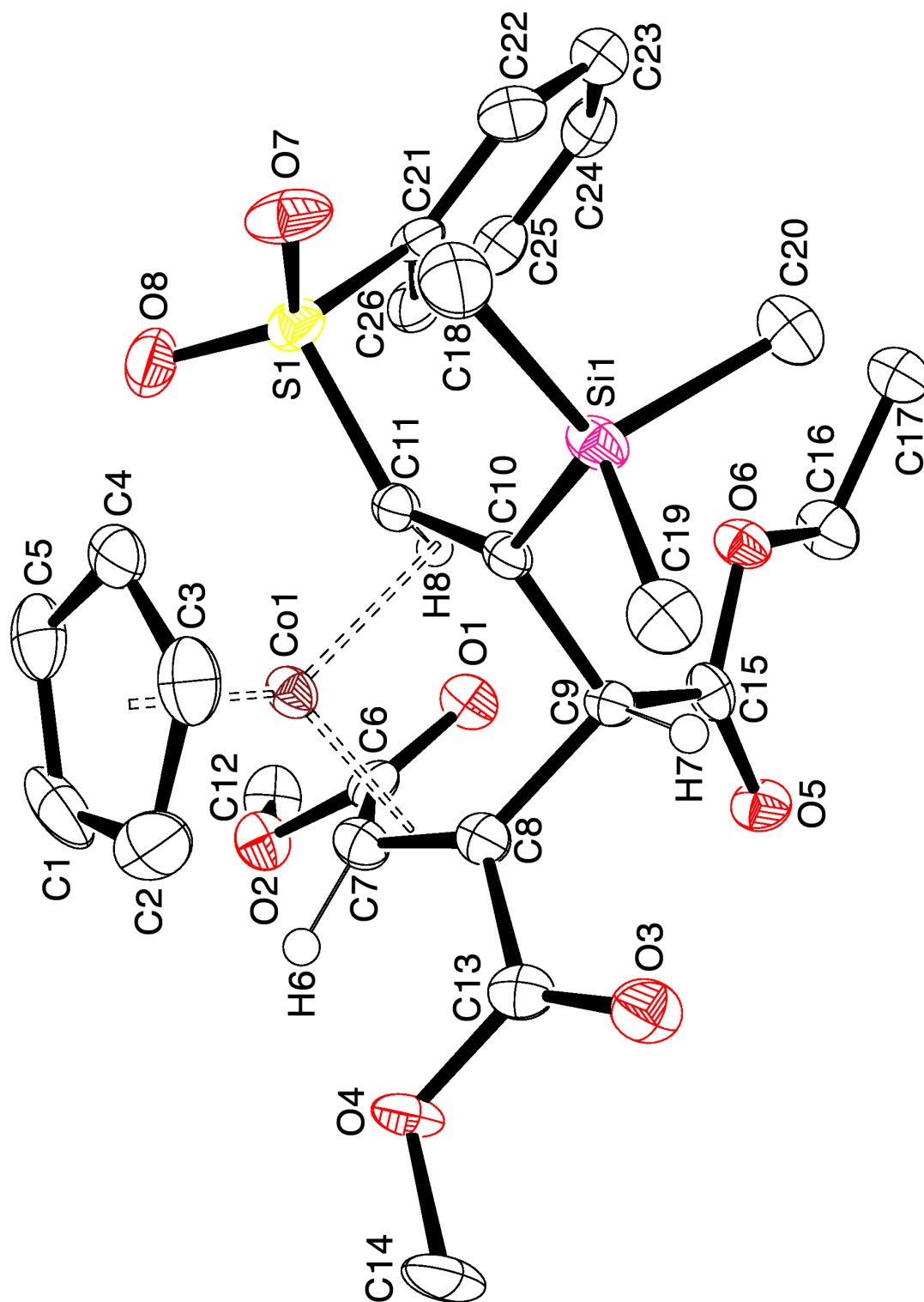


**Figure 2-11.** ORTEP of orthorhombic cobalt complex **9-ZE**. Ellipsoids shown at 50% probability. Most hydrogens are omitted for clarity.

**Table 2-3.** Crystal data and structure refinement for **9-ZE**.

CCDC Refcode	JOGWIM	
CCDC Deposition No.	703132	
Sample/notebook ID	rlh2044	
Empirical formula	C <sub>26</sub> H <sub>33</sub> Co O <sub>8</sub> S Si	
Formula weight	592.60	
Temperature	100(2) K	
Wavelength	0.71073 Å	
Crystal system	Orthorhombic	
Space group	<i>Pca</i> 2 <sub>1</sub>	
Unit cell dimensions	a = 15.359(3) Å	$\alpha = 90^\circ$
	b = 12.065(2) Å	$\beta = 90^\circ$
	c = 14.452(3) Å	$\gamma = 90^\circ$
Volume	2678.1(8) Å <sup>3</sup>	
Z	4	
Density (calculated)	1.470 Mg/m <sup>3</sup>	
Absorption coefficient	0.811 mm <sup>-1</sup>	
F(000)	1240	
Crystal size	0.14 x 0.12 x 0.08 mm <sup>3</sup>	
Crystal color/habit	red prism	
Theta range for data collection	1.69 to 28.26°	
Index ranges	-20 ≤ h ≤ 20, -15 ≤ k ≤ 15, -18 ≤ l ≤ 14	
Reflections collected	21491	
Independent reflections	5064 [R(int) = 0.0690]	
Completeness to theta = 25.00°	100.0 %	
Max. and min. transmission	0.9379 and 0.8949	
Refinement method	Full-matrix least-squares on F <sup>2</sup>	
Data / restraints / parameters	5064 / 1 / 341	
Goodness-of-fit on F <sup>2</sup>	1.019	
Final R indices [I > 2σ(I)]	R1 = 0.0458, wR2 = 0.0916	
R indices (all data)	R1 = 0.0577, wR2 = 0.0982	
Absolute structure parameter	0.22(2)	
Largest diff. peak and hole	0.819 and -0.295 e.Å <sup>-3</sup>	

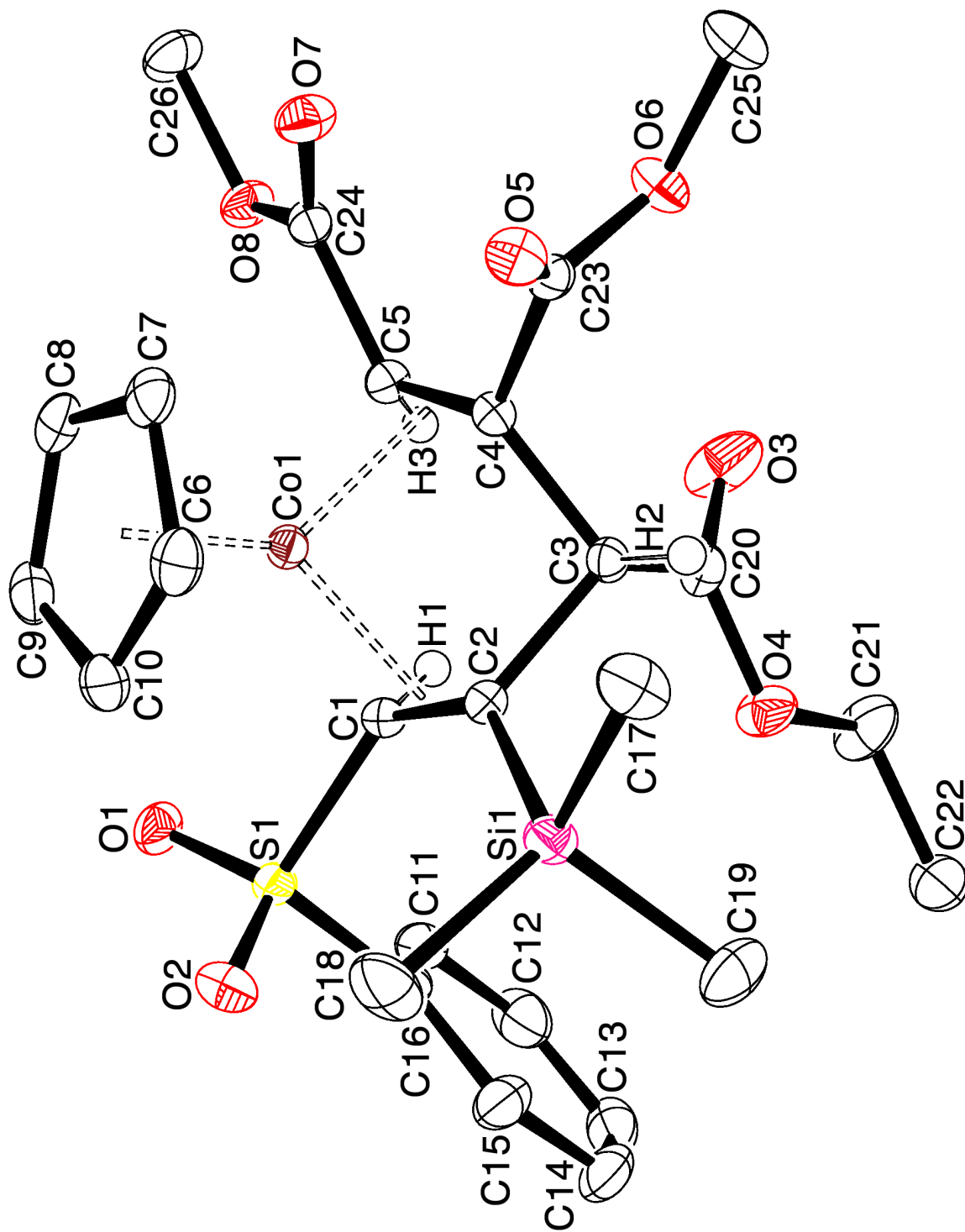


**Figure 2-12.** ORTEP of monoclinic cobalt complex **9-ZZ**. Ellipsoids shown at 50% probability. Most hydrogens are omitted for clarity.

**Table 2-4.** Crystal data and structure refinement for **9-ZZ**.

CSD Refcode	JOKXAJ	
CCDC Deposition No.	703133	
Sample/notebook ID	rlh2208	
Empirical formula	C <sub>26</sub> H <sub>33</sub> Co O <sub>8</sub> S Si	
Formula weight	592.60	
Temperature	100(2) K	
Wavelength	0.71073 Å	
Crystal system	Monoclinic	
Space group	<i>P</i> 2 <sub>1</sub> / <i>n</i>	
Unit cell dimensions	<i>a</i> = 8.5050(7) Å	$\alpha = 90^\circ$
	<i>b</i> = 22.6260(18) Å	$\beta = 94.9220(10)^\circ$
	<i>c</i> = 14.2390(11) Å	$\gamma = 90^\circ$
Volume	2730.0(4) Å <sup>3</sup>	
Z	4	
Density (calculated)	1.442 Mg/m <sup>3</sup>	
Absorption coefficient	0.796 mm <sup>-1</sup>	
F(000)	1240	
Crystal size	0.26 x 0.24 x 0.22 mm <sup>3</sup>	
Crystal color/habit	orange plate	
Theta range for data collection	1.69 to 28.25°	
Index ranges	-11 ≤ <i>h</i> ≤ 11, -28 ≤ <i>k</i> ≤ 29, -18 ≤ <i>l</i> ≤ 18	
Reflections collected	44594	
Independent reflections	6370 [R(int) = 0.0187]	
Completeness to theta = 25.00°	100.0 %	
Absorption correction	Semi-empirical from equivalents	
Max. and min. transmission	0.8444 and 0.8198	
Refinement method	Full-matrix least-squares on F <sup>2</sup>	
Data / restraints / parameters	6370 / 0 / 340	
Goodness-of-fit on F <sup>2</sup>	1.037	
Final R indices [ <i>I</i> > 2σ( <i>I</i> )]	R1 = 0.0261, wR2 = 0.0695	
R indices (all data)	R1 = 0.0273, wR2 = 0.0703	
Largest diff. peak and hole	0.693 and -0.297 e.Å <sup>-3</sup>	

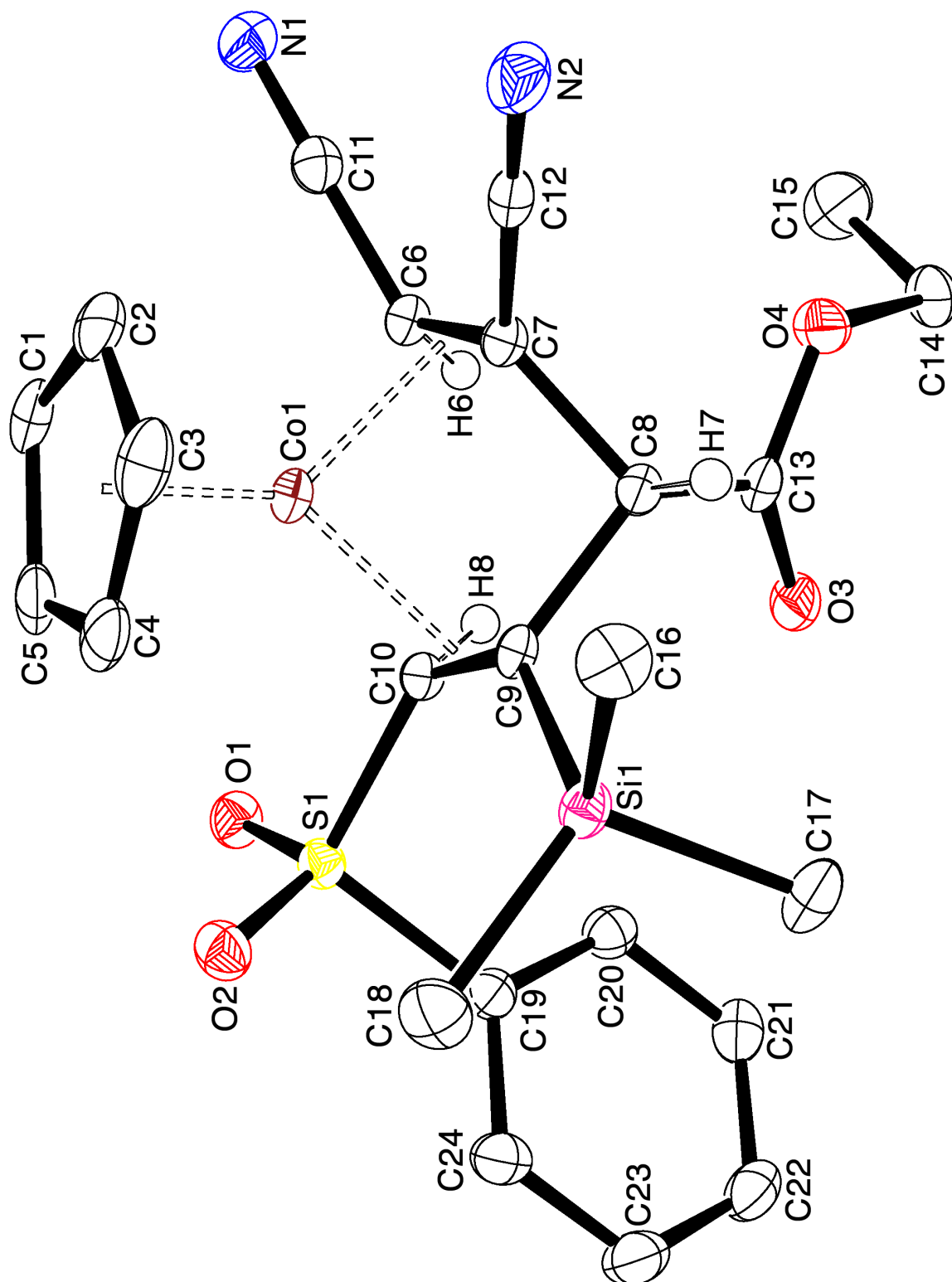


**Figure 2-13.** ORTEP of monoclinic cobalt complex 10-ZZ. Ellipsoids shown at 50% probability. Most hydrogens are omitted for clarity.



**Table 2-5.** Crystal data and structure refinement for **10-ZZ**.

CCDC X-ray ID	JOGWOS	
CCDC Deposition No.	703134	
Sample/notebook ID	rlh2140	
Empirical formula	C <sub>24</sub> H <sub>27</sub> Co N <sub>2</sub> O <sub>4</sub> S Si	
Formula weight	526.56	
Temperature	100(2) K	
Wavelength	0.71073 Å	
Crystal system	Triclinic	
Space group	<i>P</i> -1	
Unit cell dimensions	a = 9.2160(4) Å	$\alpha = 101.3900(10)^\circ$
	b = 11.2160(5) Å	$\beta = 101.1400(10)^\circ$
	c = 13.5220(9) Å	$\gamma = 112.0290(10)^\circ$
Volume	1213.98(11) Å <sup>3</sup>	
Z	2	
Density (calculated)	1.440 Mg/m <sup>3</sup>	
Absorption coefficient	0.875 mm <sup>-1</sup>	
F(000)	548	
Crystal size	0.27 x 0.24 x 0.04 mm <sup>3</sup>	
Crystal color/habit	orange plate	
Theta range for data collection	1.61 to 28.12°	
Index ranges	-12 ≤ h ≤ 12, -14 ≤ k ≤ 14, -17 ≤ l ≤ 17	
Reflections collected	25219	
Independent reflections	5483 [R(int) = 0.0289]	
Completeness to theta = 25.00°	99.5 %	
Absorption correction	Semi-empirical from equivalents	
Max. and min. transmission	0.9658 and 0.7980	
Refinement method	Full-matrix least-squares on F <sup>2</sup>	
Data / restraints / parameters	5483 / 0 / 302	
Goodness-of-fit on F <sup>2</sup>	1.028	
Final R indices [I > 2σ(I)]	R1 = 0.0299, wR2 = 0.0673	
R indices (all data)	R1 = 0.0393, wR2 = 0.0720	
Largest diff. peak and hole	0.442 and -0.336 e.Å <sup>-3</sup>	

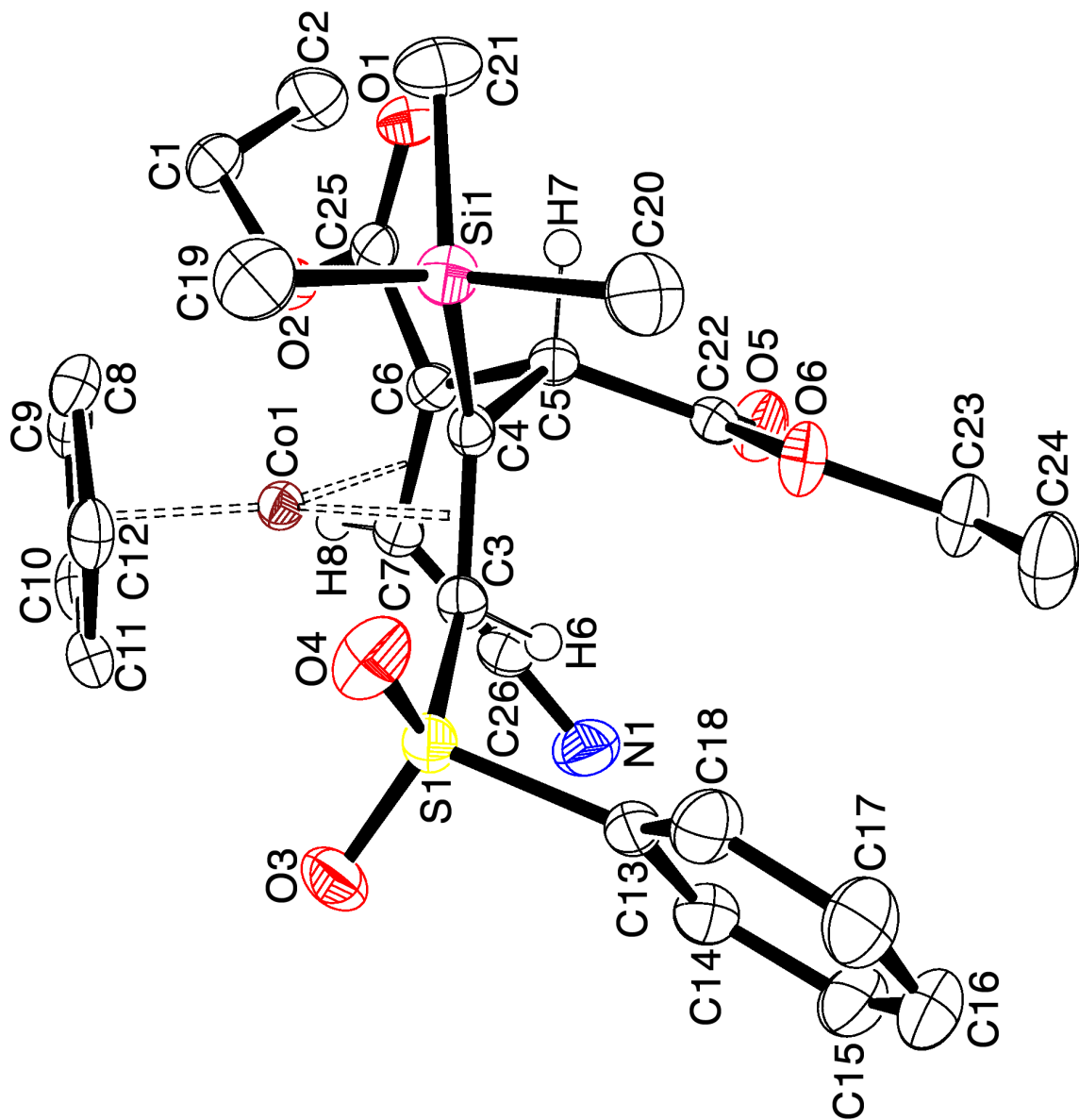


**Figure 2-14.** ORTEP of monoclinic cobalt complex 11-ZE. Ellipsoids shown at 50% probability. Most hydrogens are omitted for clarity.

**Table 2-6.** Crystal data and structure refinement for **11-ZE**.

CSD Refcode	JOGWUY	
CCDC Deposition No.	703135	
Sample/notebook ID	rlh2230	
Empirical formula	C <sub>26</sub> H <sub>32</sub> Co N O <sub>6</sub> S Si	
Formula weight	573.61	
Temperature	208(2) K	
Wavelength	0.71073 Å	
Crystal system	Triclinic	
Space group	<i>P</i> 2 <sub>1</sub> / <i>c</i>	
Unit cell dimensions	<i>a</i> = 14.884(2) Å	$\alpha = 90^\circ$
	<i>b</i> = 11.4118(18) Å	$\beta = 98.671(2)^\circ$
	<i>c</i> = 15.750(2) Å	$\gamma = 90^\circ$
Volume	2644.6(7) Å <sup>3</sup>	
Z	4	
Density (calculated)	1.441 Mg/m <sup>3</sup>	
Absorption coefficient	0.815 mm <sup>-1</sup>	
F(000)	1200	
Crystal size	0.65 x 0.28 x 0.06 mm <sup>3</sup>	
Crystal color/habit	orange plate	
Theta range for data collection	1.38 to 28.33°	
Index ranges	-19 ≤ <i>h</i> ≤ 19, -15 ≤ <i>k</i> ≤ 15, -19 ≤ <i>l</i> ≤ 20	
Reflections collected	28543	
Independent reflections	6151 [R(int) = 0.0420]	
Completeness to theta = 25.00°	99.7 %	
Absorption correction	Semi-empirical from equivalents	
Max. and min. transmission	0.9528 and 0.6195	
Refinement method	Full-matrix least-squares on F <sup>2</sup>	
Data / restraints / parameters	6151 / 0 / 331	
Goodness-of-fit on F <sup>2</sup>	0.984	
Final R indices [ <i>I</i> > 2σ( <i>I</i> )]	R1 = 0.0330, wR2 = 0.0757	
R indices (all data)	R1 = 0.0479, wR2 = 0.0817	
Largest diff. peak and hole	0.366 and -0.334 e.Å <sup>-3</sup>	

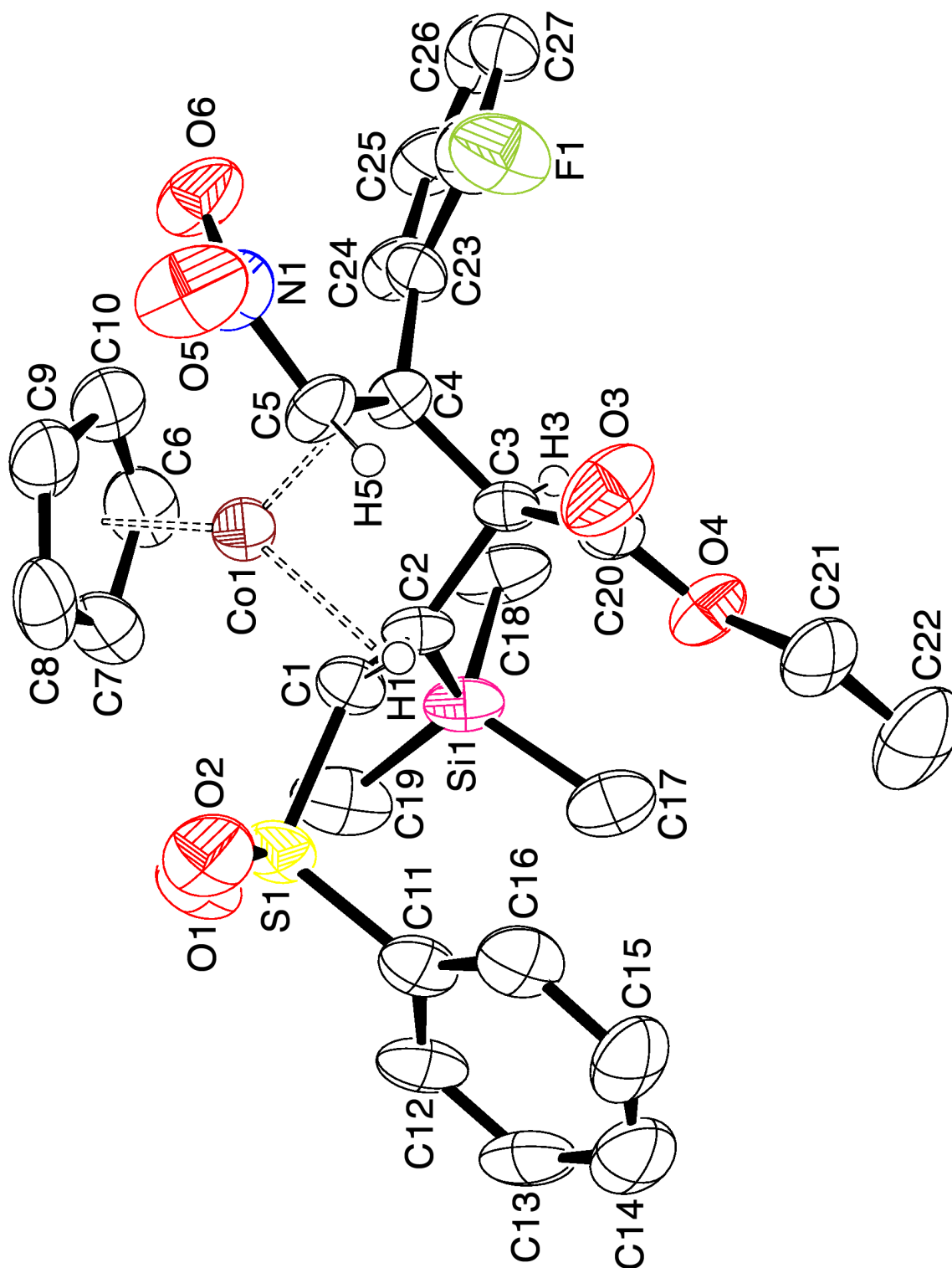


**Figure 2-15.** ORTEP of monoclinic cobalt complex **12-ZZ-ortho**. Ellipsoids shown at 50% probability. Most hydrogens are omitted for clarity.

**Table 2-7.** Crystal data and structure refinement for **12-ZZ-ortho**.

Sample/notebook ID	rlh3106	
Empirical formula	C <sub>28</sub> H <sub>31</sub> Co F N O <sub>6</sub> S Si	
Formula weight	615.63	
Temperature	293(2) K	
Wavelength	0.71073 Å	
Crystal system	Triclinic	
Space group	<i>P</i> 2 <sub>1</sub> / <i>n</i>	
Unit cell dimensions	a = 12.75(3) Å	$\alpha = 90^\circ$
	b = 17.79(4) Å	$\beta = 98.72(3)^\circ$
	c = 12.99(3) Å	$\gamma = 90^\circ$
Volume	2911(11) Å <sup>3</sup>	
Z	4	
Density (calculated)	1.405 Mg/m <sup>3</sup>	
Absorption coefficient	0.750 mm <sup>-1</sup>	
F(000)	1280	
Crystal size	0.24 x 0.22 x 0.18 mm <sup>3</sup>	
Crystal color/habit	red plate	
Theta range for data collection	1.96 to 25.67°	
Index ranges	-15 ≤ h ≤ 15, -21 ≤ k ≤ 21, -15 ≤ l ≤ 15	
Reflections collected	17428	
Independent reflections	4582 [R(int) = 0.0814]	
Completeness to theta = 25.00°	82.9 %	
Absorption correction	None	
Max. and min. transmission	0.8768 and 0.8405	
Refinement method	Full-matrix least-squares on F <sup>2</sup>	
Data / restraints / parameters	4582 / 0 / 356	
Goodness-of-fit on F <sup>2</sup>	1.176	
Final R indices [I > 2σ(I)]	R1 = 0.0906, wR2 = 0.2670	
R indices (all data)	R1 = 0.1248, wR2 = 0.3052	
Largest diff. peak and hole	1.249 and -1.075 e.Å <sup>-3</sup>	

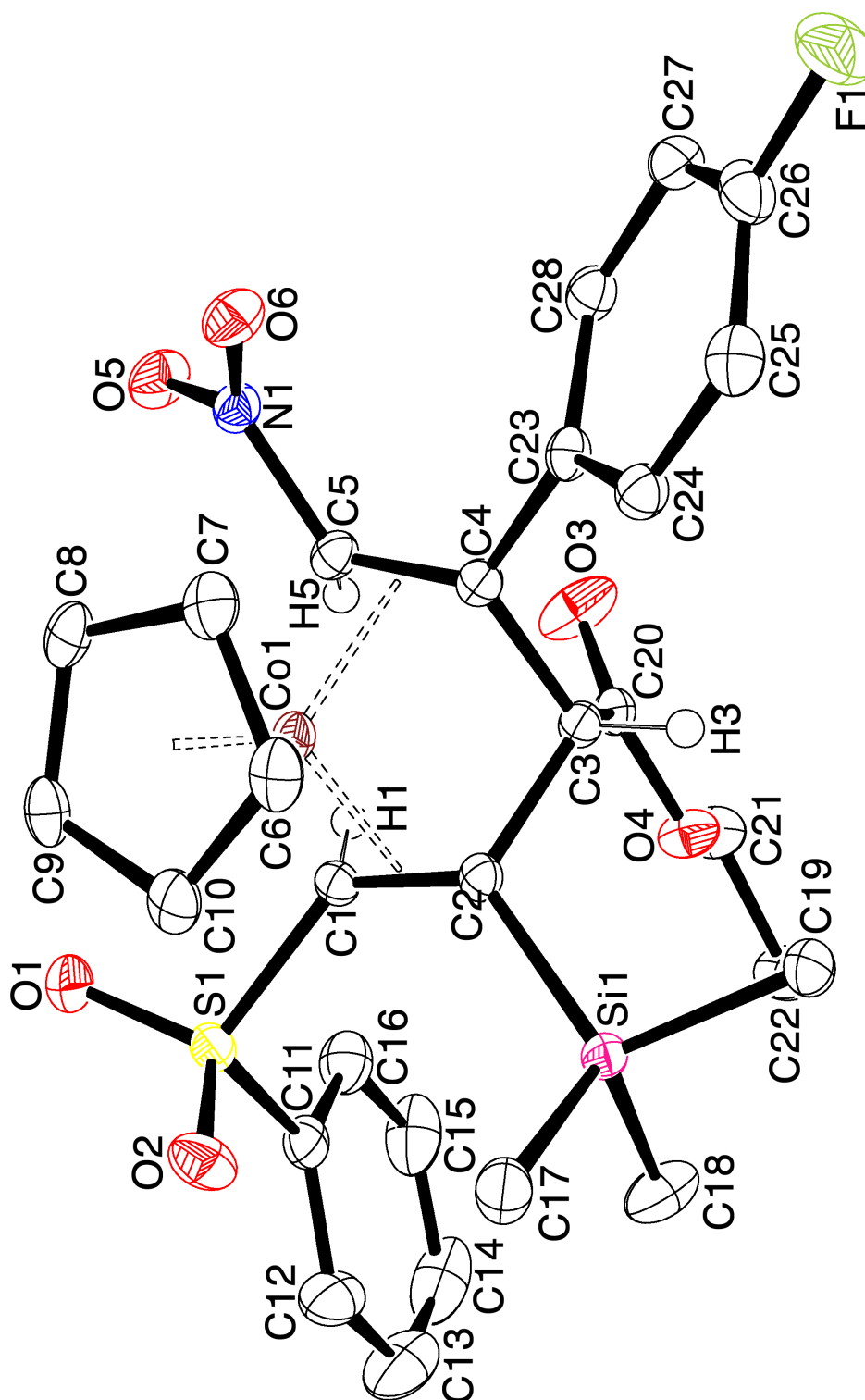


**Figure 2-16.** ORTEP of monoclinic cobalt complex **12-ZZ-para**. Ellipsoids shown at 50% probability. Most hydrogens are omitted for clarity.

**Table 2-8.** Crystal data and structure refinement for **12-ZZ-para**.

Sample/notebook ID	rlh4001	
Empirical formula	C <sub>28</sub> H <sub>31</sub> Co F N O <sub>6</sub> S Si	
Formula weight	615.63	
Temperature	100(2) K	
Wavelength	0.71073 Å	
Crystal system	Triclinic	
Space group	<i>P</i> -1	
Unit cell dimensions	a = 13.754(3) Å	$\alpha = 90^\circ$
	b = 13.838(3) Å	$\beta = 114.507(2)^\circ$
	c = 15.648(3) Å	$\gamma = 90^\circ$
Volume	2709.9(9) Å <sup>3</sup>	
Z	4	
Density (calculated)	1.487 Mg/m <sup>3</sup>	
Absorption coefficient	0.805 mm <sup>-1</sup>	
F(000)	1244	
Crystal size	0.24 x 0.16 x 0.08 mm <sup>3</sup>	
Crystal color/habit	red plate	
Theta range for data collection	1.66 to 25.74°	
Index ranges	-16 ≤ h ≤ 16, -16 ≤ k ≤ 16, -19 ≤ l ≤ 19	
Reflections collected	58773	
Independent reflections	5104 [R(int) = 0.0440]	
Completeness to theta = 25.00°	99.0 %	
Absorption correction	Semi-empirical from equivalents	
Max. and min. transmission	0.9384 and 0.8303	
Refinement method	Full-matrix least-squares on F <sup>2</sup>	
Data / restraints / parameters	5104 / 0 / 353	
Goodness-of-fit on F <sup>2</sup>	1.057	
Final R indices [I > 2σ(I)]	R1 = 0.0338, wR2 = 0.0973	
R indices (all data)	R1 = 0.0372, wR2 = 0.1008	
Largest diff. peak and hole	0.865 and -0.387 e.Å <sup>-3</sup>	

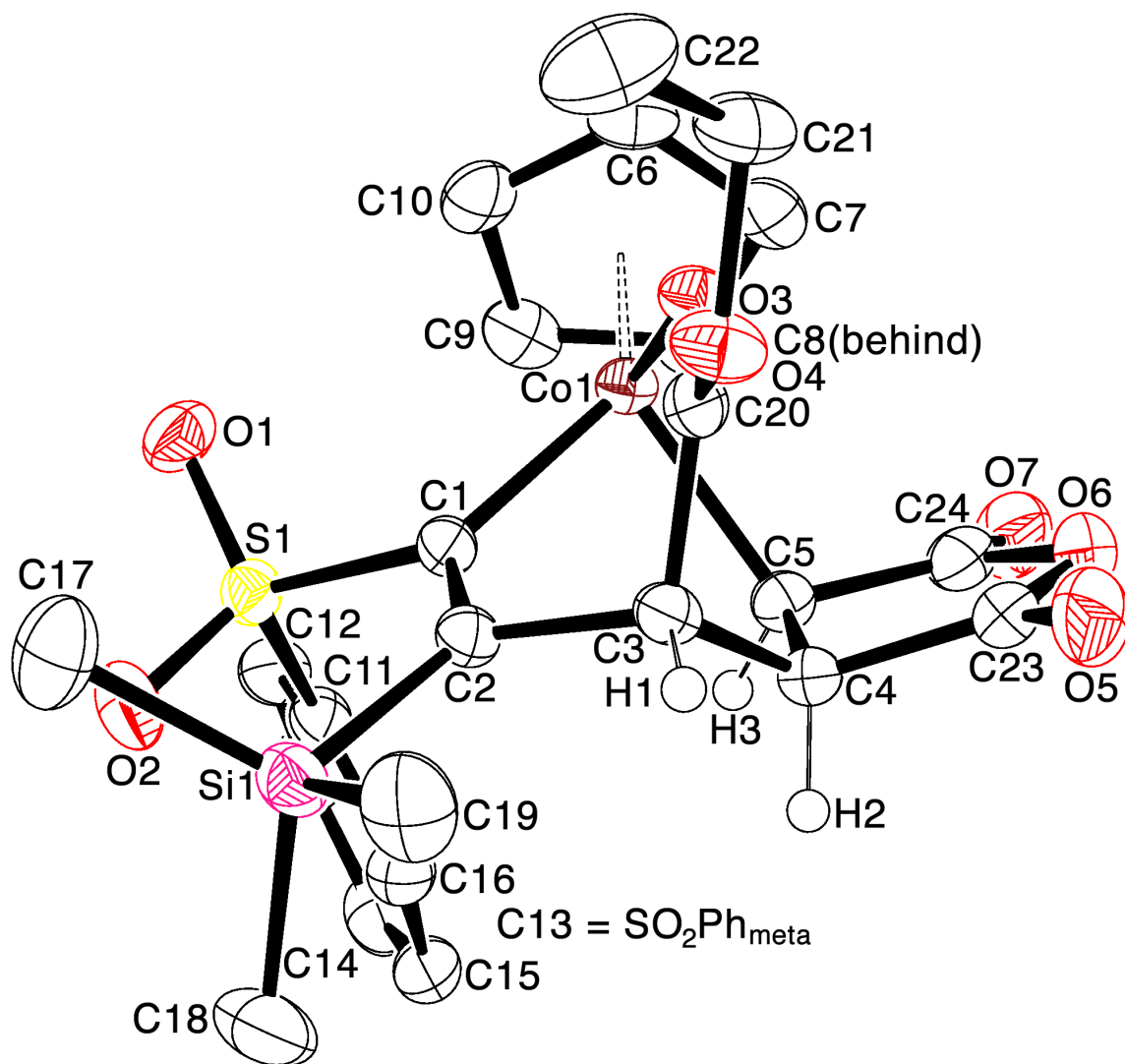


**Figure 2-17.** ORTEP of monoclinic cobalt complex **13-exo**. Ellipsoids shown at 20% probability. Most hydrogens are omitted for clarity.



**Table 2-9.** Crystal data and structure refinement for **13-exo**.

CSD Refcode	JOKXEN	
CCDC Deposition No.	703137	
Sample/notebook ID	rlh2203	
Empirical formula	C <sub>24</sub> H <sub>27</sub> Co O <sub>7</sub> S Si	
Formula weight	546.54	
Temperature	203(2) K	
Wavelength	0.71073 Å	
Crystal system	Monoclinic	
Space group	<i>P</i> 2 <sub>1</sub> / <i>n</i>	
Unit cell dimensions	<i>a</i> = 11.309(2) Å	$\alpha$ = 90.000(4)°
	<i>b</i> = 11.898(4) Å	$\beta$ = 91.096(4)°
	<i>c</i> = 17.955(5) Å	$\gamma$ = 90.000(4)°
Volume	2415.5(12) Å <sup>3</sup>	
Z	4	
Density (calculated)	1.503 Mg/m <sup>3</sup>	
Absorption coefficient	0.890 mm <sup>-1</sup>	
F(000)	1136	
Crystal size	0.18 x 0.17 x 0.08 mm <sup>3</sup>	
Crystal color/habit	black	
Theta range for data collection	2.05 to 28.26°	
Index ranges	-14 ≤ <i>h</i> ≤ 13, -14 ≤ <i>k</i> ≤ 15, -23 ≤ <i>l</i> ≤ 23	
Reflections collected	30654	
Independent reflections	5547 [R(int) = 0.0371]	
Completeness to theta = 25.00°	100.0 %	
Max. and min. transmission	0.9322 and 0.8421	
Refinement method	Full-matrix least-squares on F <sup>2</sup>	
Data / restraints / parameters	5547 / 0 / 311	
Goodness-of-fit on F <sup>2</sup>	1.029	
Final R indices [ <i>I</i> > 2σ( <i>I</i> )]	R1 = 0.0277, wR2 = 0.0736	
R indices (all data)	R1 = 0.0305, wR2 = 0.0758	
Largest diff. peak and hole	0.343 and -0.472 e.Å <sup>-3</sup>	

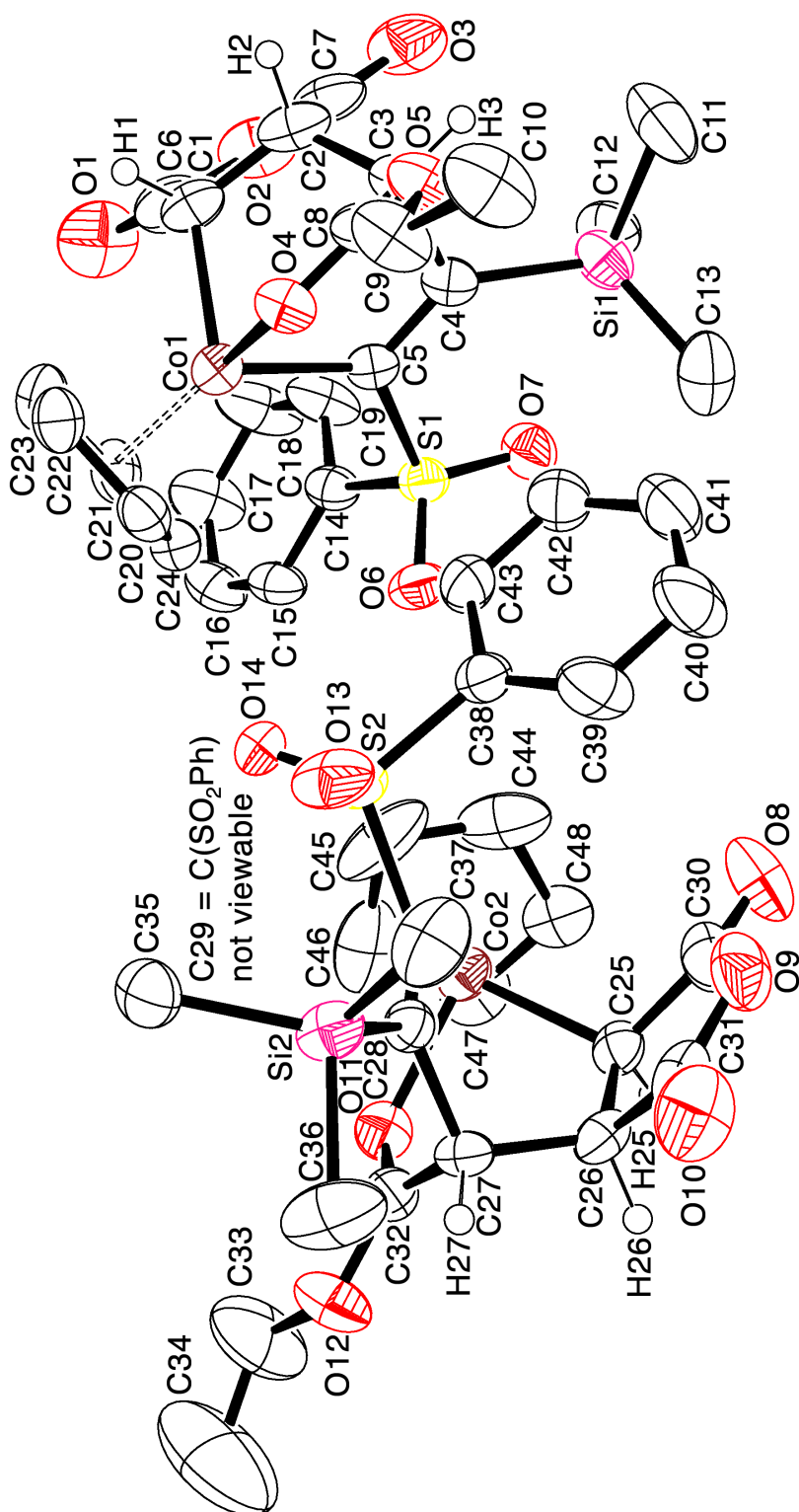


**Figure 2-18.** ORTEP of monoclinic cobalt complex **13-endo**. Ellipsoids shown at 30% probability. Most hydrogens are omitted for clarity.

**Table 2-10.** Crystal data and structure refinement for **13-endo**.

CSD Refcode	JOGXAF	
CCDC Deposition No.	724841	
Sample/notebook ID	rlh2205	
Empirical formula	C <sub>48</sub> H <sub>54</sub> Co <sub>2</sub> O <sub>14</sub> S <sub>2</sub> Si <sub>2</sub>	
Formula weight	1093.07	
Temperature	203(2) K	
Wavelength	0.71073 Å	
Crystal system	Triclinic	
Space group	<i>P</i> -1	
Unit cell dimensions	a = 8.293(2) Å	$\alpha = 73.484(4)^\circ$
	b = 16.275(4) Å	$\beta = 81.053(4)^\circ$
	c = 19.621(5) Å	$\gamma = 87.930(4)^\circ$
Volume	2508.0(12) Å <sup>3</sup>	
Z	2	
Density (calculated)	1.447 Mg/m <sup>3</sup>	
Absorption coefficient	0.857 mm <sup>-1</sup>	
F(000)	1136	
Crystal size	0.20 x 0.16 x 0.08 mm <sup>3</sup>	
Crystal color/habit	black block	
Theta range for data collection	2.19 to 25.03°	
Index ranges	-9 ≤ h ≤ 9, -19 ≤ k ≤ 19, -23 ≤ l ≤ 23	
Reflections collected	29855	
Independent reflections	8720 [R(int) = 0.0441]	
Completeness to theta = 25.00°	98.5 %	
Absorption correction	Semi-empirical from equivalents	
Max. and min. transmission	0.9346 and 0.8473	
Refinement method	Full-matrix least-squares on F <sup>2</sup>	
Data / restraints / parameters	8720 / 0 / 621	
Goodness-of-fit on F <sup>2</sup>	1.028	
Final R indices [I > 2σ(I)]	R1 = 0.0458, wR2 = 0.1049	
R indices (all data)	R1 = 0.0665, wR2 = 0.1149	
Largest diff. peak and hole	0.362 and -0.366 e.Å <sup>-3</sup>	

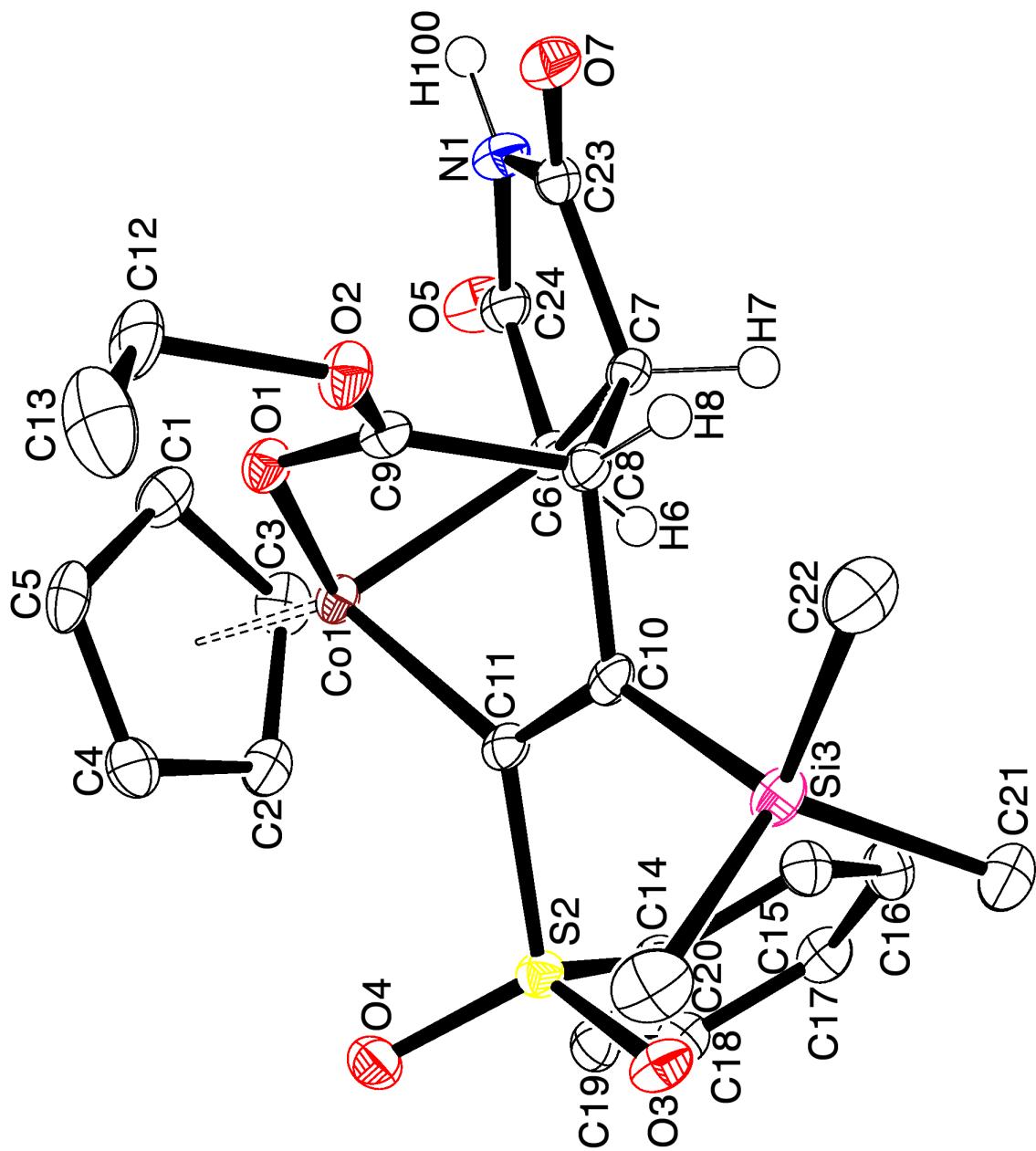


**Figure 2-19.** ORTEP of monoclinic cobalt complex **14-exo**. Ellipsoids shown at 20% probability. Most hydrogens are omitted for clarity.

**Table 2-11.** Crystal data and structure refinement for **14-exo**.

Sample/notebook ID	rlh2254	
Empirical formula	C <sub>24</sub> H <sub>27</sub> Co N <sub>2</sub> O <sub>4</sub> S Si	
Formula weight	526.56	
Temperature	293(2) K	
Wavelength	0.71073 Å	
Crystal system	Monoclinic	
Space group	<i>P</i> 2 <sub>1</sub> / <i>n</i>	
Unit cell dimensions	a = 11.263(3) Å	$\alpha = 90^\circ$
	b = 14.395(3) Å	$\beta = 99.981(3)^\circ$
	c = 15.537(4) Å	$\gamma = 90^\circ$
Volume	2480.9(10) Å <sup>3</sup>	
Z	4	
Density (calculated)	1.410 Mg/m <sup>3</sup>	
Absorption coefficient	0.857 mm <sup>-1</sup>	
F(000)	1096	
Crystal size	0.18 x 0.17 x 0.08 mm <sup>3</sup>	
Crystal color/habit	black	
Theta range for data collection	1.94 to 28.28°	
Index ranges	-14 ≤ h ≤ 8, -18 ≤ k ≤ 19, -20 ≤ l ≤ 20	
Reflections collected	20169	
Independent reflections	5650 [R(int) = 0.0446]	
Completeness to theta = 25.00°	99.6 %	
Max. and min. transmission	0.9322 and 0.8421	
Refinement method	Full-matrix least-squares on F <sup>2</sup>	
Data / restraints / parameters	5650 / 0 / 315	
Goodness-of-fit on F <sup>2</sup>	1.038	
Final R indices [I > 2σ(I)]	R1 = 0.0348, wR2 = 0.0905	
R indices (all data)	R1 = 0.0414, wR2 = 0.0956	
Largest diff. peak and hole	0.898 and -0.520 e.Å <sup>-3</sup>	

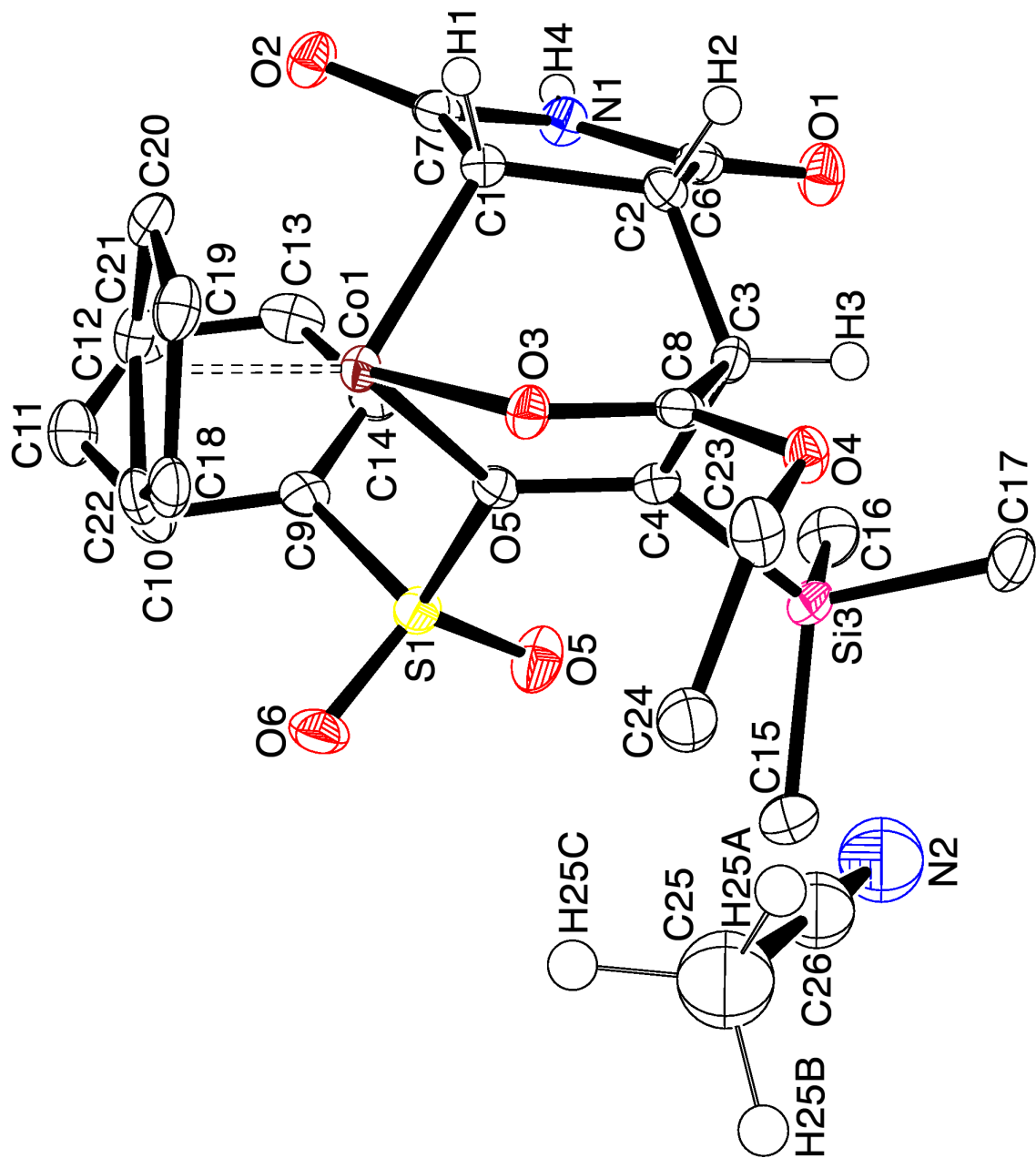


**Figure 2-20.** ORTEP of monoclinic cobalt complex **14-endo**. Ellipsoids shown at 20% probability. Most hydrogens are omitted for clarity.

**Table 2-12.** Crystal data and structure refinement for **14-endo**.

Sample/notebook ID	rlh2255	
Empirical formula	C <sub>24</sub> H <sub>28</sub> Co N O <sub>6</sub> S Si, C <sub>2</sub> H <sub>3</sub> N	
Formula weight	545.07, 41.03	
Temperature	293(2) K	
Wavelength	0.71073 Å	
Crystal system	Triclinic	
Space group	<i>P</i> -1	
Unit cell dimensions	a = 8.2830(10) Å	$\alpha = 83.969(2)^\circ$
	b = 11.0299(14) Å	$\beta = 75.301(2)^\circ$
	c = 15.5542(19) Å	$\gamma = 85.333(2)^\circ$
Volume	1364.7(3) Å <sup>3</sup>	
Z	2	
Density (calculated)	1.245 Mg/m <sup>3</sup>	
Absorption coefficient	0.776 mm <sup>-1</sup>	
F(000)	532	
Crystal size	0.10 x 0.04 x 0.03 mm <sup>3</sup>	
Crystal color/habit	black	
Theta range for data collection	2.72 to 28.14°	
Index ranges	-10 ≤ h ≤ 10, -14 ≤ k ≤ 14, -20 ≤ l ≤ 20	
Reflections collected	23467	
Independent reflections	6159 [R(int) = 0.0600]	
Completeness to theta = 25.00°	100.0 %	
Max. and min. transmission	0.746 and 0.680	
Refinement method	Full-matrix least-squares on F <sup>2</sup>	
Data / restraints / parameters	6159 / 0 / 328	
Goodness-of-fit on F <sup>2</sup>	1.033	
Final R indices [I > 2σ(I)]	R1 = 0.0418, wR2 = 0.0852	
R indices (all data)	R1 = 0.0633, wR2 = 0.0951	
Largest diff. peak and hole	0.64 and -0.46 e.Å <sup>-3</sup>	

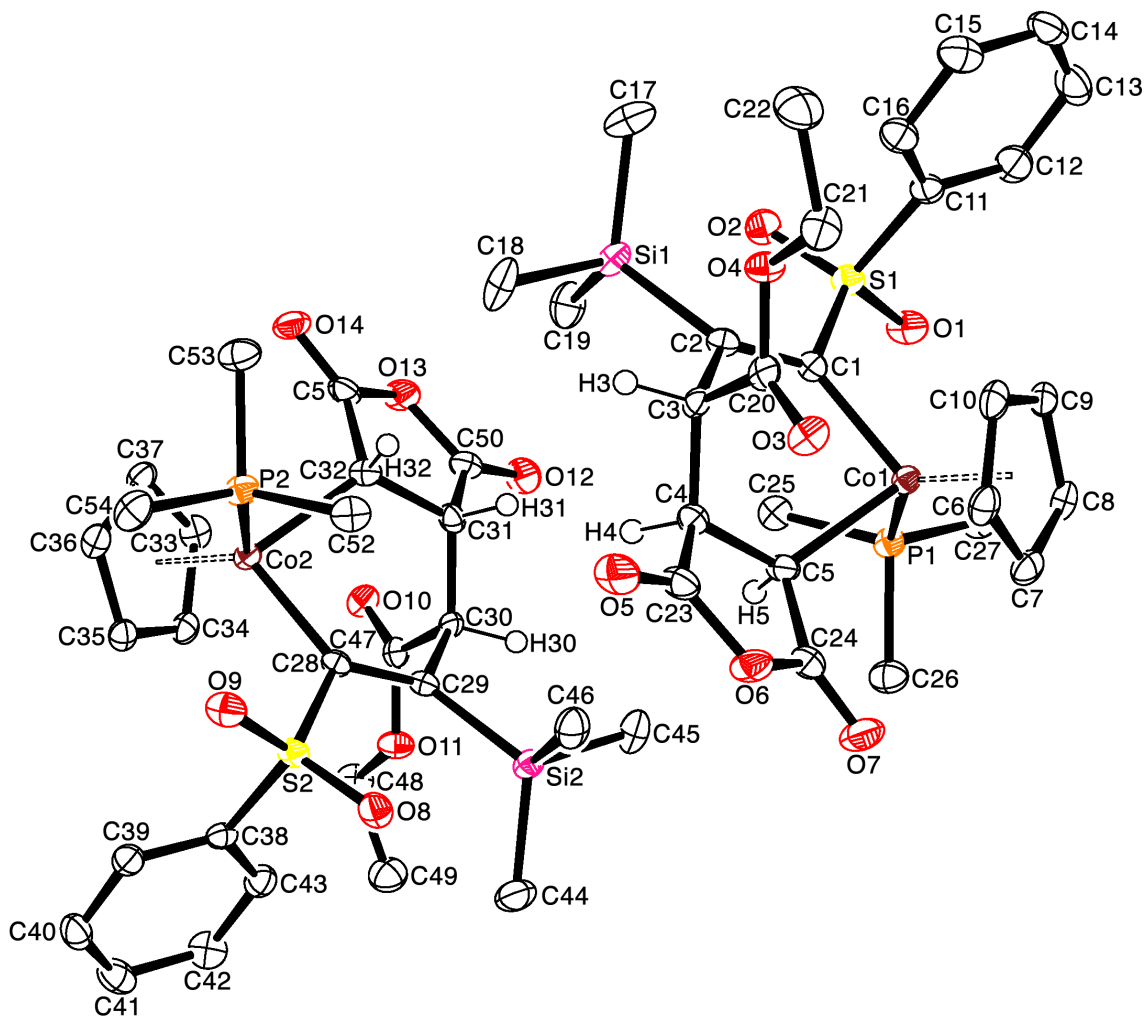


**Figure 2-21.** ORTEP of monoclinic cobalt complex **20-exo**. Ellipsoids shown at 20% probability. Most hydrogens are omitted for clarity.



**Table 2-13.** Crystal data and structure refinement for **20-exo**.

Sample/notebook ID	rlh3126	
Empirical formula	C <sub>27</sub> H <sub>36</sub> Co O <sub>7</sub> P S Si	
Formula weight	622.61	
Temperature	100(2) K	
Wavelength	0.71073 Å	
Crystal system	Monoclinic	
Space group	<i>P</i> 2 <sub>1</sub> / <i>n</i>	
Unit cell dimensions	<i>a</i> = 9.7659(12) Å	$\alpha = 90^\circ$
	<i>b</i> = 19.310(2) Å	$\beta = 97.630(2)^\circ$
	<i>c</i> = 30.643(4) Å	$\gamma = 90^\circ$
Volume	5727.6(12) Å <sup>3</sup>	
Z	8	
Density (calculated)	1.444 Mg/m <sup>3</sup>	
Absorption coefficient	0.813 mm <sup>-1</sup>	
F(000)	2608	
Crystal size	0.30 x 0.28 x 0.04 mm <sup>3</sup>	
Crystal color/habit	black plates	
Theta range for data collection	1.25 to 24.76°	
Index ranges	-11 ≤ <i>h</i> ≤ 11, -22 ≤ <i>k</i> ≤ 22, -35 ≤ <i>l</i> ≤ 36	
Reflections collected	77630	
Independent reflections	9770 [R(int) = 0.0597]	
Completeness to theta = 25.00°	99.4 %	
Absorption correction	Semi-empirical from equivalents	
Max. and min. transmission	0.9682 and 0.7925	
Refinement method	Full-matrix least-squares on F <sup>2</sup>	
Data / restraints / parameters	9770 / 0 / 699	
Goodness-of-fit on F <sup>2</sup>	1.121	
Final R indices [ <i>I</i> > 2σ( <i>I</i> )]	R1 = 0.0425, wR2 = 0.0800	
R indices (all data)	R1 = 0.0552, wR2 = 0.0857	
Largest diff. peak and hole	0.339 and -0.361 e.Å <sup>-3</sup>	

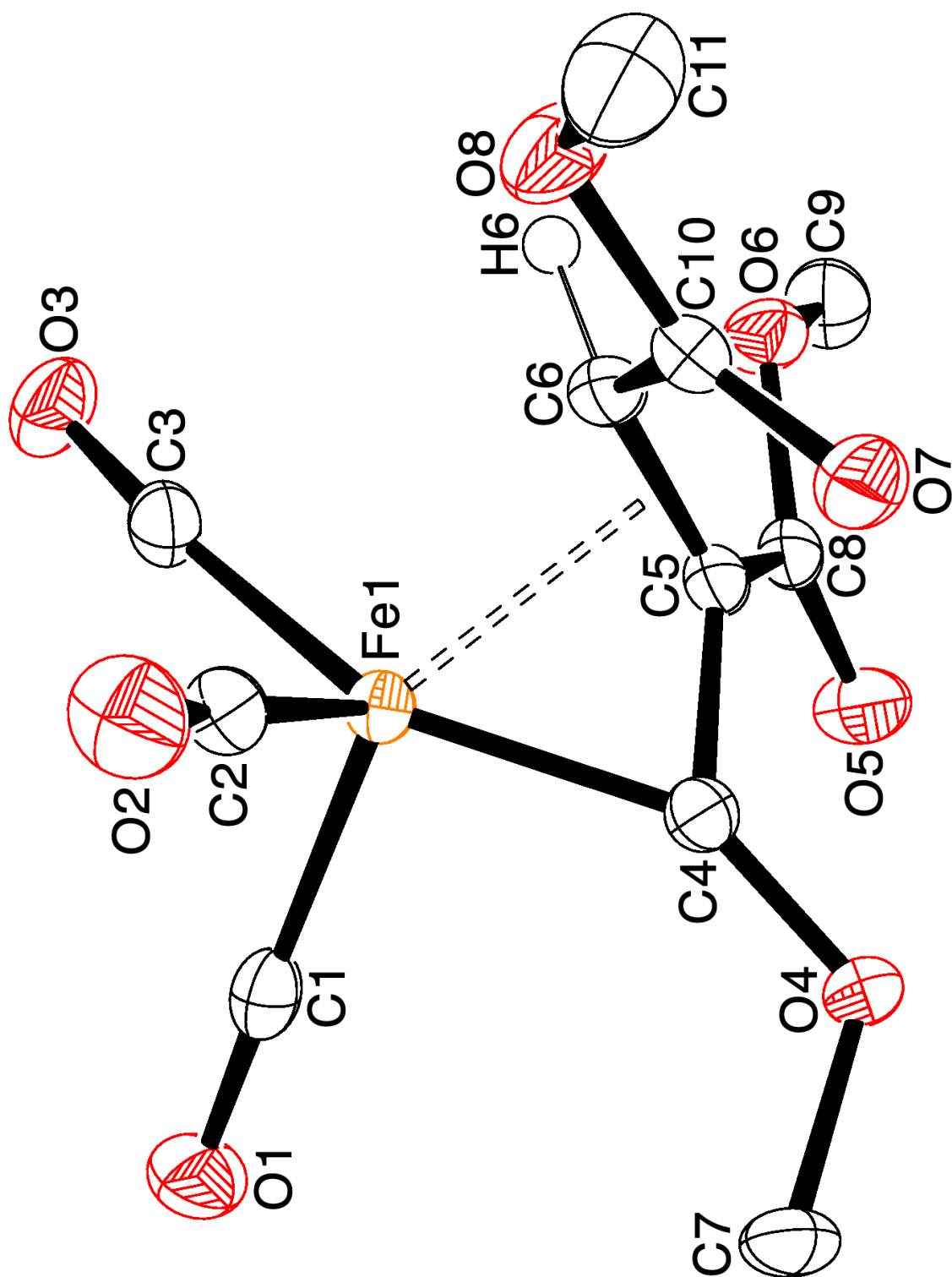


**Figure 2-22.** ORTEP of monoclinic cobalt complex **25a**. Ellipsoids shown at 20% probability. Most hydrogens are omitted for clarity.

**Table 2-14.** Crystal data and structure refinement for **25a**.

Sample/notebook ID	rlh3005	
Empirical formula	C <sub>11</sub> H <sub>10</sub> Fe O <sub>8</sub>	
Formula weight	326.04	
Temperature	100(2) K	
Wavelength	0.71073 Å	
Crystal system	Monoclinic	
Space group	<i>C</i> <sub>2</sub> / <i>c</i>	
Unit cell dimensions	a = 17.765(3) Å	$\alpha = 90^\circ$
	b = 9.6825(17) Å	$\beta = 97.500(2)^\circ$
	c = 15.769(3) Å	$\gamma = 90^\circ$
Volume	2689.2(8) Å <sup>3</sup>	
Z	4	
Density (calculated)	1.611 Mg/m <sup>3</sup>	
Absorption coefficient	1.155 mm <sup>-1</sup>	
F(000)	1328	
Crystal size	0.16 x 0.13 x 0.11 mm <sup>3</sup>	
Crystal color/habit	orange plate	
Theta range for data collection	2.31 to 25.59°	
Index ranges	-21 ≤ h ≤ 21, -11 ≤ k ≤ 11, -19 ≤ l ≤ 19	
Reflections collected	8949	
Independent reflections	2516 [R(int) = 0.0369]	
Completeness to theta = 25.00°	99.9 %	
Max. and min. transmission	0.8835 and 0.8368	
Refinement method	Full-matrix least-squares on F <sup>2</sup>	
Data / restraints / parameters	2516 / 0 / 184	
Goodness-of-fit on F <sup>2</sup>	1.047	
Final R indices [I > 2σ(I)]	R1 = 0.0255, wR2 = 0.0640	
R indices (all data)	R1 = 0.0301, wR2 = 0.0667	
Largest diff. peak and hole	0.267 and -0.233 e.Å <sup>-3</sup>	

**Table 2-15.** Selected bond distances [Å] for complexes **9-ZZ**, **9-ZE**, **10-ZZ**, **10-ZE**, **11-ZE**, **12-ZZ-ortho**, and **12-ZZ-para**.

<b>Cmpd No.:</b>	<b>9-ZE</b>	<b>9-ZZ</b>	<b>10-ZE</b>	<b>10-ZZ</b>	<b>11-ZE</b>	<b>12-ZZ-ortho</b>	<b>12-ZZ-para</b>
Co-C(1)	2.009(4)	2.016(1)	2.028(4)	2.023(2)	2.019(2)	2.027(8)	2.016(3)
Co-C(2)	2.059(4)	2.053(1)	2.067(4)	2.074(2)	2.063(2)	2.060(7)	2.054(2)
Co-C(4)	2.030(4)	2.013(1)	2.004(4)	1.991(2)	2.032(2)	2.034(8)	2.042(2)
Co-C(5)	2.058(4)	2.050(1)	2.030(4)	2.031(2)	2.034(2)	2.001(8)	2.031(2)
C(1)-C(2)	1.433(4)	1.430(2)	1.417(6)	1.428(3)	1.430(2)	1.449(9)	1.431(3)
C(2)-C(3)	1.545(6)	1.550(2)	1.542(5)	1.537(3)	1.541(3)	1.574(9)	1.552(3)
C(3)-C(4)	1.520(5)	1.519(2)	1.518(5)	1.522(3)	1.514(3)	1.537(9)	1.535(4)
C(4)-C(5)	1.423(5)	1.421(2)	1.436(6)	1.437(3)	1.428(2)	1.414(9)	1.425(3)
C(1)-C(5)	2.875(5)	2.831(2)	2.941(5)	2.798(3)	2.903(3)	2.78(1)	2.758(4)
H(1)- O(7)/N(1)	2.032		2.713		2.712		
( $\eta^5$ -C <sub>5</sub> H <sub>5</sub> ) <sub>plane</sub> - C(1)	3.034	3.099	3.070	3.108	3.045	3.104	3.120
( $\eta^5$ -C <sub>5</sub> H <sub>5</sub> ) <sub>plane</sub> - C(2)	3.160	3.151	3.264	3.200	3.189	3.239	3.201
( $\eta^5$ -C <sub>5</sub> H <sub>5</sub> ) <sub>plane</sub> - C(3)	4.059	4.034	4.159	4.021	4.093	4.114	4.016
( $\eta^5$ -C <sub>5</sub> H <sub>5</sub> ) <sub>plane</sub> - C(4)	3.189	3.133	3.159	3.083	3.194	3.156	3.096
( $\eta^5$ -C <sub>5</sub> H <sub>5</sub> ) <sub>plane</sub> - C(5)	2.930	2.984	2.824	2.954	2.898	2.917	2.976

**Table 2-16.** Selected bond distances [ $\text{\AA}$ ] for complexes **13-*exo***, **13-*endo***, **14-*exo***, and **14-*endo***.

<b>Cmpd No.:</b>	<b>13-<i>exo</i></b>	<b>13-<i>endo</i></b>	<b>14-<i>exo</i></b>	<b>14-<i>endo</i></b>
Co(1)-C(1)	1.965(1)	1.982(4) 1.955(3)	1.968(2)	1.966(3)
C(1)-C(2)	1.356(2)	1.358(5) 1.360(4)	1.359(3)	1.359(3)
C(2)-C(3)	1.541(2)	1.550(5) 1.535(5)	1.545(2)	1.546(3)
C(3)-C(4)	1.495(2)	1.493(4) 1.485(5)	1.490(2)	1.485(4)
C(4)-O(1)	1.230(2)	1.234(5) 1.228(4)	1.237(2)	1.236(3)
O(1)-Co(1)	1.959(1)	1.955(3) 1.961(3)	1.978(1)	1.965(2)
C(4)-C(5)	1.546(2)	1.549(5) 1.545(6)	1.541(3)	1.547(3)
C(5)-C(6)	1.522(2)	1.505(6) 1.521(4)	1.530(3)	1.523(3)
C(6)-Co(1)	2.030(2)	2.026(3) 2.008(4)	2.031(2)	2.024(2)

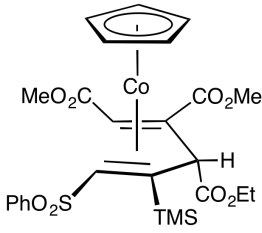
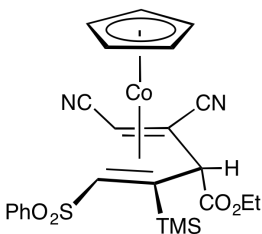
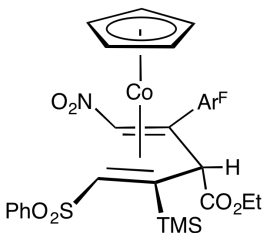
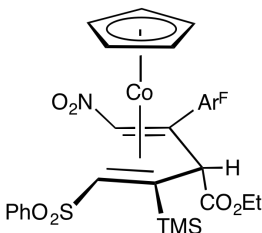
(a) Two independent molecules in the asymmetric unit cell.

**Table 2-17.** Selected angles [°] for complexes **13-*exo***, **13-*endo***, **14-*exo***, and **14-*endo***.

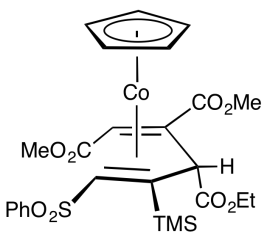
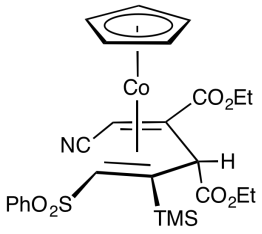
<b>Cmpd No.:</b>	<b>13-<i>exo</i></b>	<b>13-<i>endo</i><sup>a</sup></b>	<b>14-<i>exo</i></b>	<b>14-<i>endo</i></b>
Co(1)-C(1)-C(2)	121.8(1)	122.5(3) 122.0(3)	122.1(1)	122.0(2)
C(1)-C(2)-C(3)	113.2(1)	112.5(3) 113.6(3)	112.8(1)	113.6(2)
C(2)-C(3)-C(4)	106.9(1)	108.5(3) 107.9(3)	106.1(1)	106.9(2)
C(3)-C(4)-O(1)	120.8(1)	122.0(3) 122.4(3)	121.0(2)	122.3(2)
C(4)-O(1)-Co(1)	120.23(9)	119.7(2) 119.7(2)	118.9(1)	119.8(2)
O(1)-Co(1)-C(1)	89.94(5)	88.8(1) 89.4(1)	89.54(6)	89.43(8)
C(4)-C(3)-C(5)	109.0(1)	109.0(3) 108.5(3)	109.3(1)	110.1(2)
C(2)-C(3)-C(5)	110.8(1)	110.5(3) 110.3(3)	111.4(1)	109.8(2)
C(3)-C(5)-C(6)	117.1(1)	115.7(3) 115.6(3)	117.2(3)	115.8(2)
C(5)-C(6)-Co(1)	110.3(1)	113.7(2) 113.7(2)	108.8(1)	113.5(2)
C(6)-Co(1)-C(1)	83.88(6)	89.3(1) 88.3(1)	83.58(7)	88.4(1)
C(6)-Co(1)-O(1)	94.35(5)	89.4(1) 89.9(1)	95.57(6)	89.39(8)
Co(1)-C(6)-C(8)	111.7(1)	112.9(3) 113.2(3)	111.5(1)	113.5(2)
C(3)-C(5)-C(7)	110.3(1)	110.5(3) 110.3(3)	83.30 -6.70 <sup>a</sup>	108.8(2)

(a) Two independent molecules in the asymmetric unit cell.

**Table 2-18.** Selected spectroscopic data for  $\eta^4$ -1,4-pentadiene complexes ( $\text{CDCl}_3$ ).

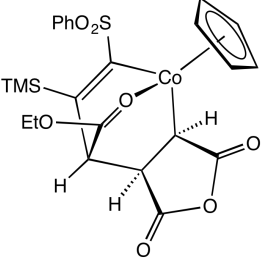
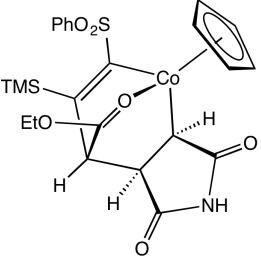
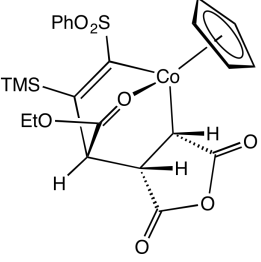
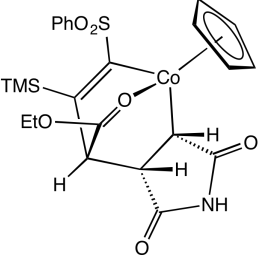
Complex	$^1\text{H}$ NMR, [ $\delta$ ]	$^{13}\text{C}\{^1\text{H}\}$ NMR, [ $\delta$ ]
 <p><b>9-ZZ</b></p>	<p><b>9-ZZ</b></p> <p>0.35 (s, 9H, TMS)</p> <p>0.88 (t, 3H, <math>J = 6.9</math> Hz, <math>\text{CH}_3</math>)</p> <p>2.32 (s, 1H, <math>\text{CH}(\text{CO}_2\text{Me})</math>)</p> <p>2.58 (s, 1H, <math>\text{CH}(\text{SO}_2\text{Ph})</math>)</p> <p>4.16 (s, 1H, <math>\text{CH}(\text{CO}_2\text{Et})</math>)</p> <p>5.36 (s, 5H, Cp)</p>	<p>1.76 (TMS)</p> <p>89.72 (Cp)</p>
 <p><b>10-ZZ</b></p>	<p><b>10-ZZ</b></p> <p>0.43 (s, 9H, TMS)</p> <p>0.88 (t, 3H, <math>J = 7.4</math> Hz, <math>\text{CH}_3</math>)</p> <p>2.09 (s, 1H, <math>\text{CH}(\text{CN})</math>)</p> <p>2.56 (s, 1H, <math>\text{CH}(\text{SO}_2\text{Ph})</math>)</p> <p>4.08 (s, 1H, <math>\text{CH}(\text{CO}_2\text{Et})</math>)</p> <p>5.56 (s, 5H, Cp)</p>	<p>1.61 (TMS)</p> <p>92.16 (Cp)</p>
 <p><b>12-ZZ-ortho</b>  <math>\text{Ar}^{\text{F}} = o\text{-F-C}_6\text{H}_4</math></p>	<p><b>12-ZZ-ortho</b></p> <p>0.33 (s, 9H, TMS)</p> <p>0.89 (t, 3H, <math>J = 7.0</math> Hz, <math>\text{CH}_3</math>)</p> <p>3.20 (bs, 1H, CH)</p> <p>4.13 (bs, 1H, CH)</p> <p>4.79 (bs, 1H, CH)</p> <p>5.34 (s, 5H, Cp)</p>	<p>2.09 (TMS)</p> <p>91.00 (Cp)</p>
 <p><b>12-ZZ-para</b>  <math>\text{Ar}^{\text{F}} = p\text{-F-C}_6\text{H}_4</math></p>	<p><b>12-ZZ-para</b></p> <p>0.37 (s, 9H, TMS)</p> <p>0.83 (t, 3H, <math>J = 7.0</math> Hz, <math>\text{CH}_3</math>)</p> <p>2.68 (s, 1H, CH)</p> <p>4.09 (s, 1H, CH)</p> <p>4.53 (s, 1H, CH)</p> <p>5.37 (s, 5H, Cp)</p>	<p>2.31 (TMS)</p> <p>90.71 (Cp)</p>

**Table 2-18.** Selected spectroscopic data for  $\eta^4$ -1,4-pentadiene complexes ( $\text{CDCl}_3$ ) (continued).

Complex	$^1\text{H}$ NMR, [ $\delta$ ]	$^{13}\text{C}\{^1\text{H}\}$ NMR, [ $\delta$ ]
 <p><b>9-ZE</b></p>	<p><b>9-ZE</b></p> <p>0.35 (s, 9H, TMS)</p> <p>0.93 (t, 3H, <math>J = 6.9</math> Hz, <math>\text{CH}_3</math>)</p> <p>2.87 (s, 1H, <math>\text{CH}(\text{SO}_2\text{Ph})</math>)</p> <p>3.76 (s, 1H, <math>\text{CH}(\text{CO}_2\text{Me})</math>)</p> <p>4.80 (s, 1H, <math>\text{CH}(\text{CO}_2\text{Et})</math>)</p> <p>5.33 (s, 5H, Cp)</p>	<p>1.58 (TMS)</p> <p>88.42 (Cp)</p>
 <p><b>11-ZE</b></p>	<p><b>11-ZE</b></p> <p>0.41 (s, 9H, TMS)</p> <p>0.95 (t, 3H, <math>J = 6.9</math> Hz, <math>\text{CH}_3</math>)</p> <p>3.03 (s, 1H, <math>\text{CH}(\text{SO}_2\text{Ph})</math>)</p> <p>3.27 (s, 1H, <math>\text{CH}(\text{CN})</math>)</p> <p>4.79 (s, 1H, <math>\text{CH}(\text{CO}_2\text{Et})</math>)</p> <p>5.37 (s, 5H, Cp)</p>	<p>1.82 (TMS)</p> <p>88.96 (Cp)</p>



**Table 2-19.** Selected spectroscopic data for 2-oxa-1-metalla-(7,8)-dihydrobarrelene complexes (CDCl<sub>3</sub>).

Complex	<sup>1</sup> H NMR, [δ]	<sup>13</sup> C{ <sup>1</sup> H} NMR, [δ]
 <p><b>13-<i>exo</i></b></p>	<p><b>13-<i>exo</i></b></p> <p>0.31 (s, 9H, TMS)</p> <p>1.24 (t, 3H, <i>J</i> = 7.4 Hz, CH<sub>3</sub>)</p> <p>2.65 (dd, 1H, <i>J</i> = 5.3, 9.0 Hz C(5)<i>H</i>)</p> <p>3.53 (d, 1H, <i>J</i> = 9.0 Hz C(6)<i>H</i>)</p> <p>4.40 (d, 1H, <i>J</i> = 5.3 Hz C(3)<i>H</i>)</p> <p>5.02 (s, 5H, Cp)</p>	<p>3.75 (TMS)</p> <p>87.87 (Cp)</p>
 <p><b>14-<i>exo</i></b></p>	<p><b>14-<i>exo</i></b></p> <p>0.31 (s, 9H, TMS)</p> <p>1.22 (t, 3H, <i>J</i> = 7.2 Hz, CH<sub>3</sub>)</p> <p>2.43 (dd, 1H, <i>J</i> = 4.4, 8.8 Hz C(5)<i>H</i>)</p> <p>3.58 (d, 1H, <i>J</i> = 8.8 Hz C(6)<i>H</i>)</p> <p>4.39 (d, 1H, <i>J</i> = 4.4 Hz C(3)<i>H</i>)</p> <p>5.01 (s, 5H, Cp)</p>	<p>3.88 (TMS)</p> <p>87.58 (Cp)</p>
 <p><b>13-<i>endo</i></b></p>	<p><b>13-<i>endo</i></b></p> <p>0.34 (s, 9H, TMS)</p> <p>1.25 (t, 3H, <i>J</i> = 7.4 Hz, CH<sub>3</sub>)</p> <p>2.60 (dd, 1H, <i>J</i> = 4.2, 9.0 Hz C(5)<i>H</i>)</p> <p>4.45 (d, 1H, <i>J</i> = 4.2 Hz C(3)<i>H</i>)</p> <p>4.95 (s, 5H, Cp)</p> <p>5.57 (d, 1H, <i>J</i> = 9.0 Hz C(6)<i>H</i>)</p>	<p>3.27 (TMS)</p> <p>88.14 (Cp)</p>
 <p><b>14-<i>endo</i></b></p>	<p><b>14-<i>endo</i></b></p> <p>0.30 (s, 9H, TMS)</p> <p>1.25 (t, 3H, <i>J</i> = 7.2 Hz, CH<sub>3</sub>)</p> <p>2.42 (dd, 1H, <i>J</i> = 4.0, 8.4 Hz C(5)<i>H</i>)</p> <p>4.44 (d, 1H, <i>J</i> = 4.0 Hz C(3)<i>H</i>)</p> <p>4.97 (s, 5H, Cp)</p> <p>5.62 (d, 1H, <i>J</i> = 8.4 Hz C(6)<i>H</i>)</p>	<p>3.42 (TMS)</p> <p>87.98 (Cp)</p>

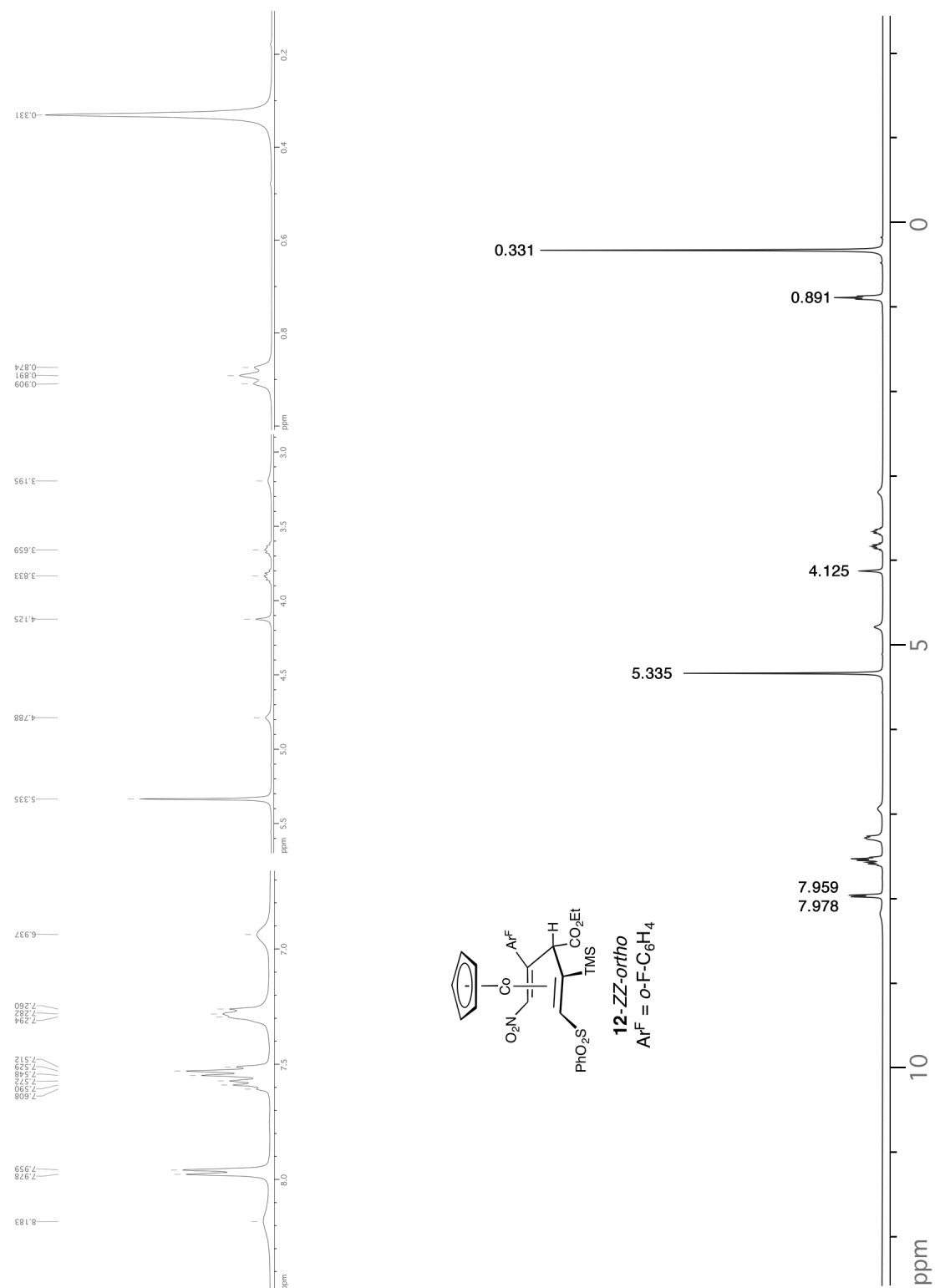
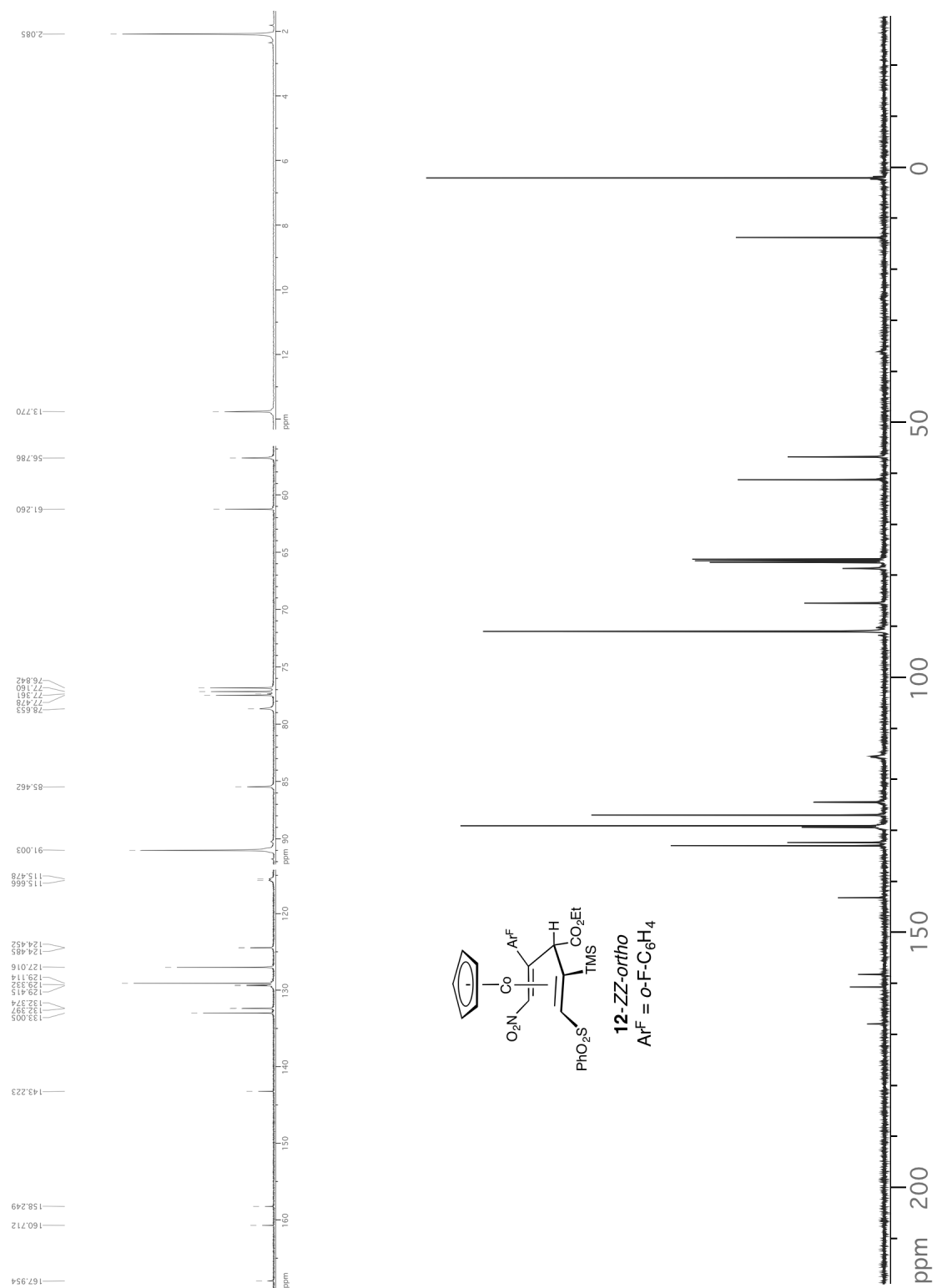


Figure 2-23. 12-ZZ-ortho <sup>1</sup>H (400.053 MHz, CDCl<sub>3</sub>).



**Figure 2-24.** 12-ZZ-ortho <sup>13</sup>C (100.567 MHz, CDCl<sub>3</sub>).

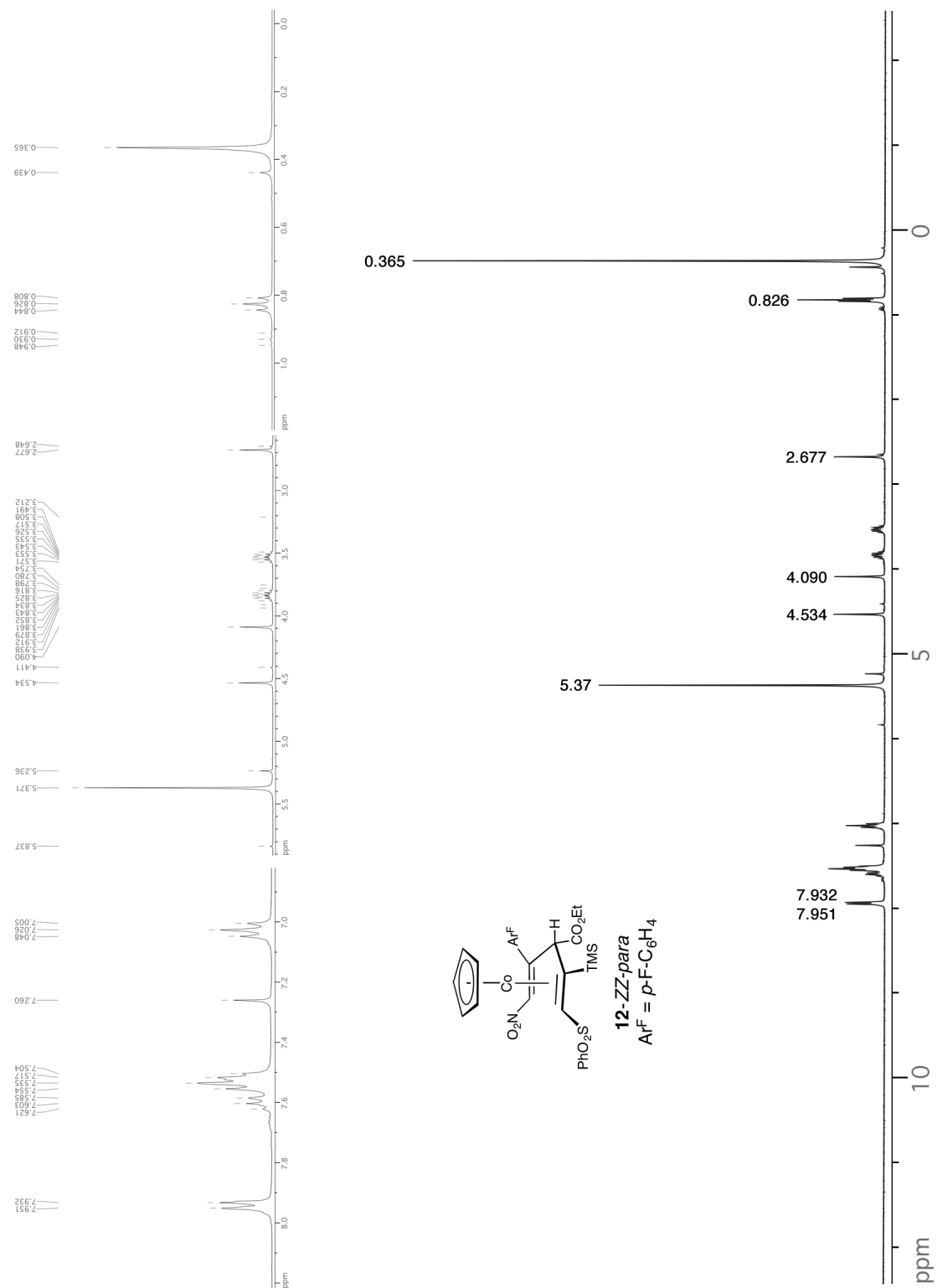
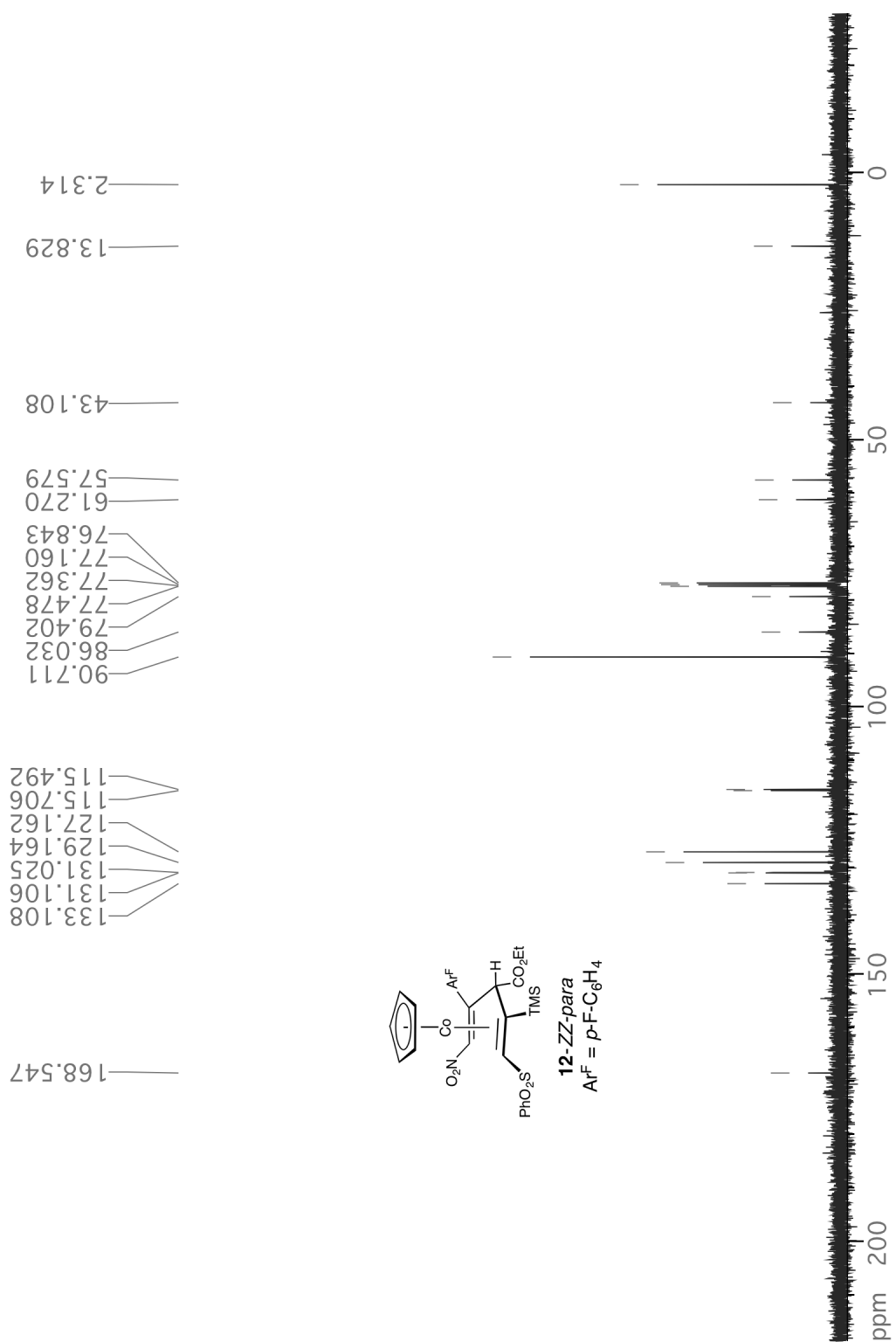


Figure 2-25. **12-ZZ-para**  $^1\text{H}$  (400.053 MHz,  $\text{CDCl}_3$ ).



**Figure 2-26.** 12-ZZ-*para* <sup>13</sup>C (100.567 MHz, CDCl<sub>3</sub>).

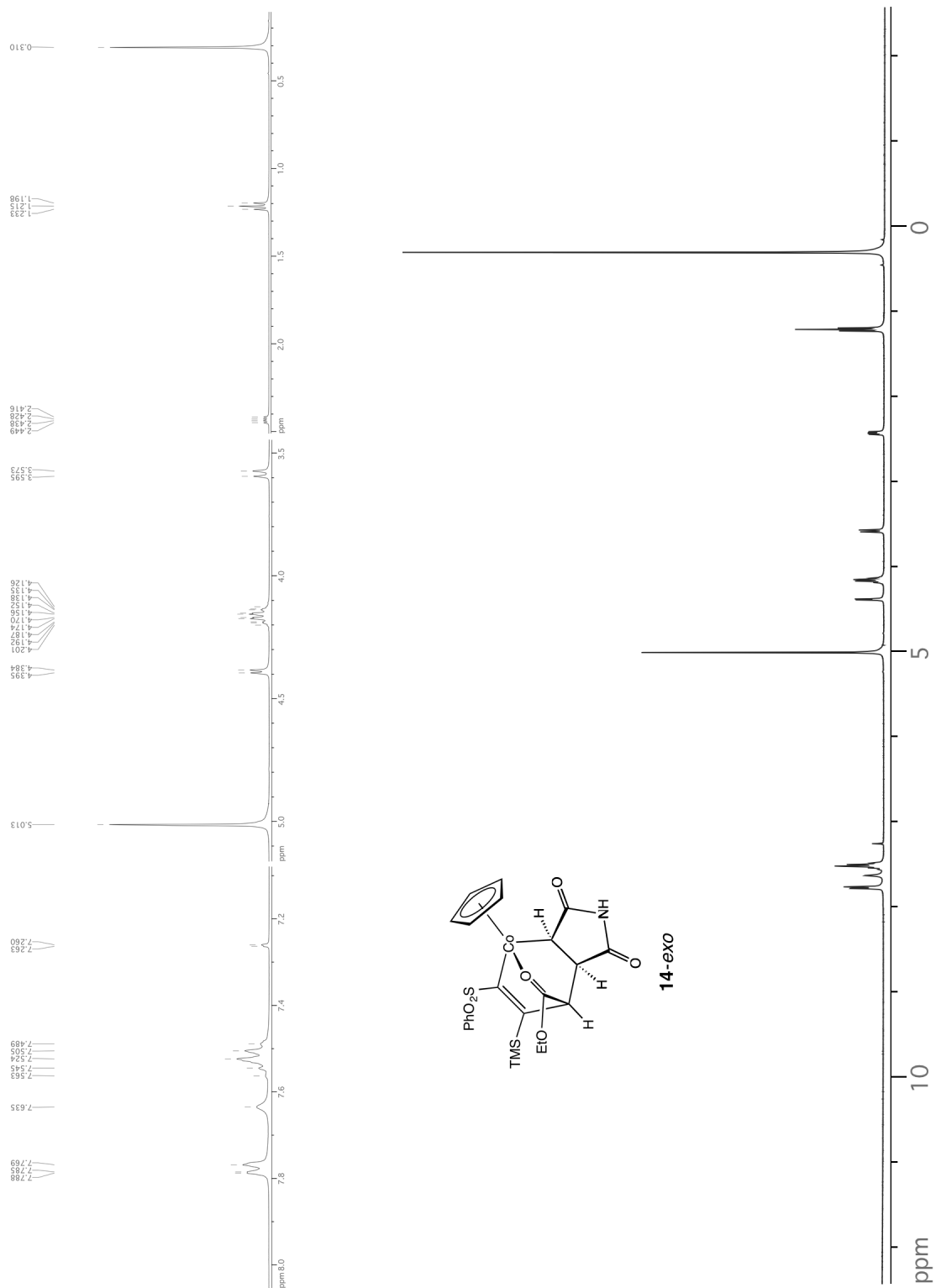
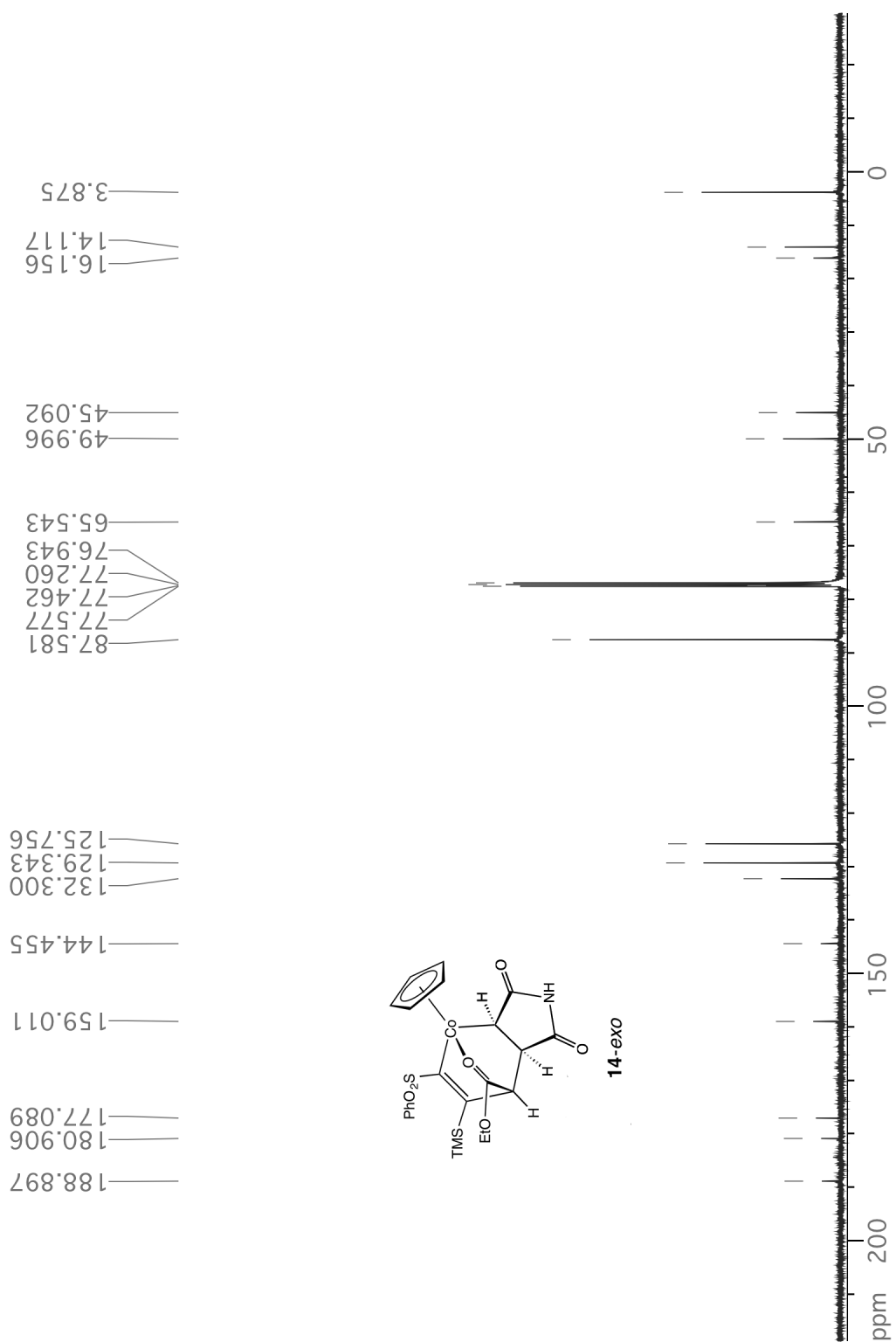


Figure 2-27. 14-exo  $^1\text{H}$  (400.053 MHz,  $\text{CDCl}_3$ ).



**Figure 2-28.** **14-exo**  $^{13}\text{C}$  (100.567 MHz,  $\text{CDCl}_3$ ).

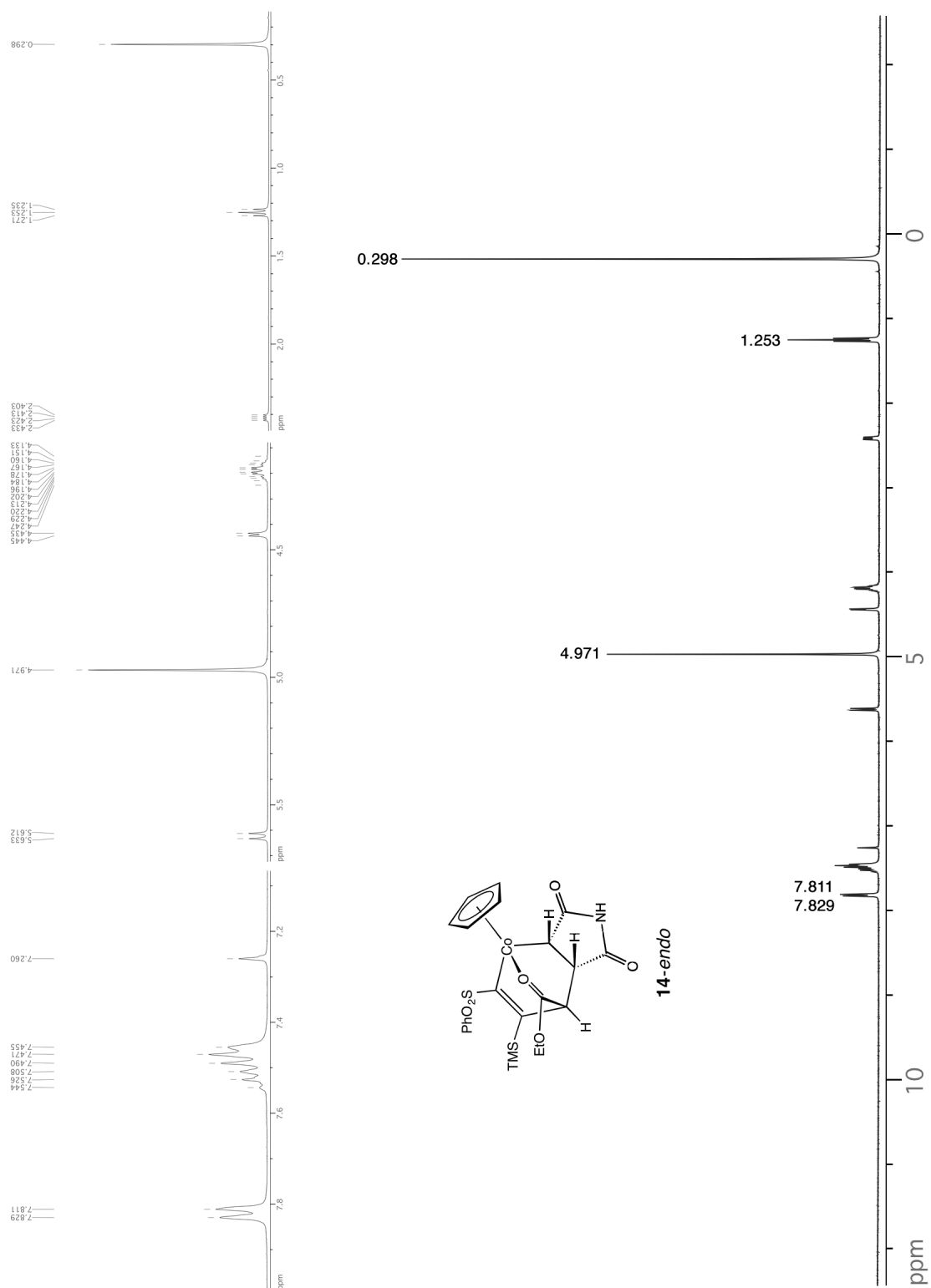
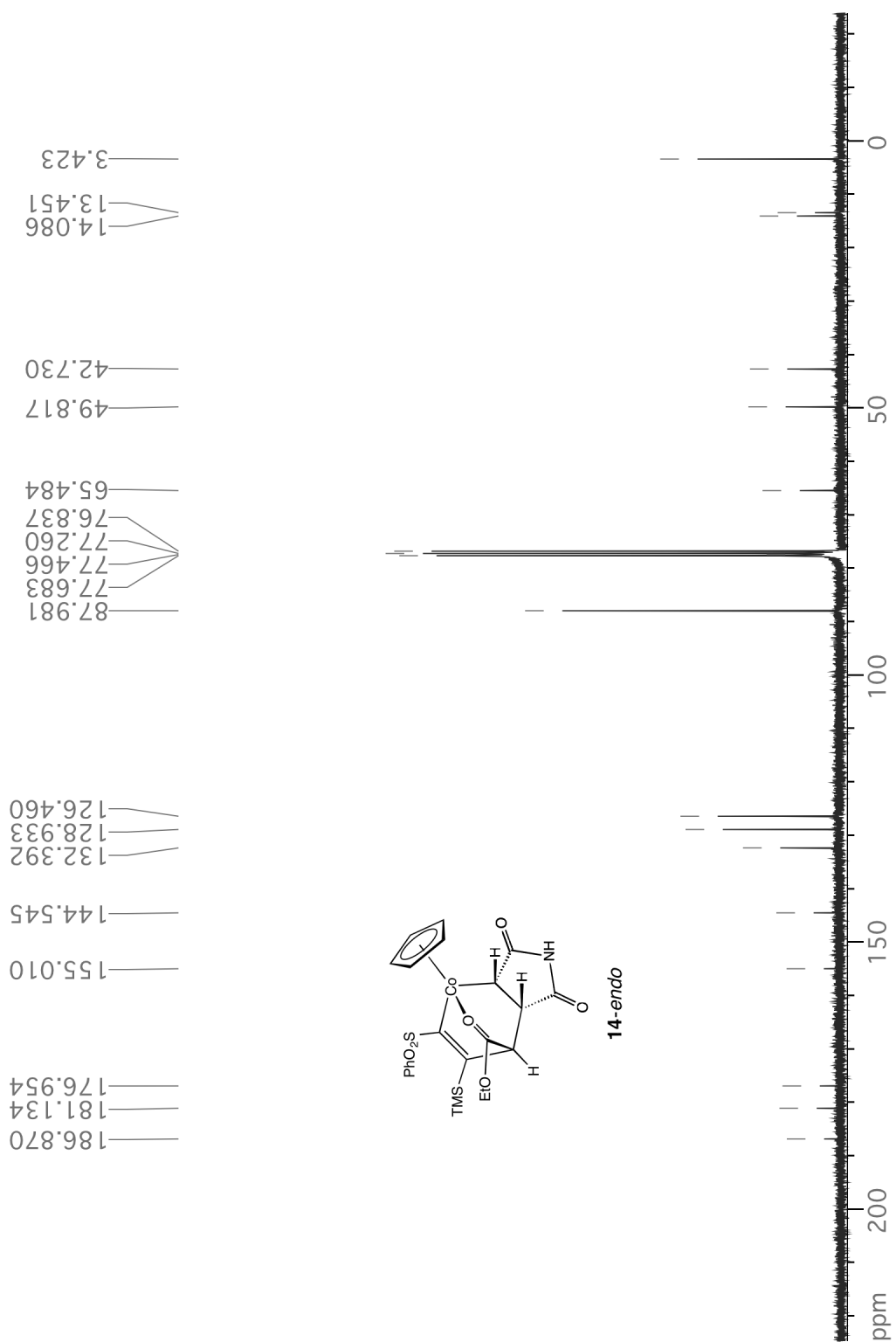


Figure 2-29. **14-endo**  $^1\text{H}$  (400.053 MHz,  $\text{CDCl}_3$ ).





**Figure 2-30.** **14-endo**  $^{13}\text{C}$  (100.567 MHz,  $\text{CDCl}_3$ ).

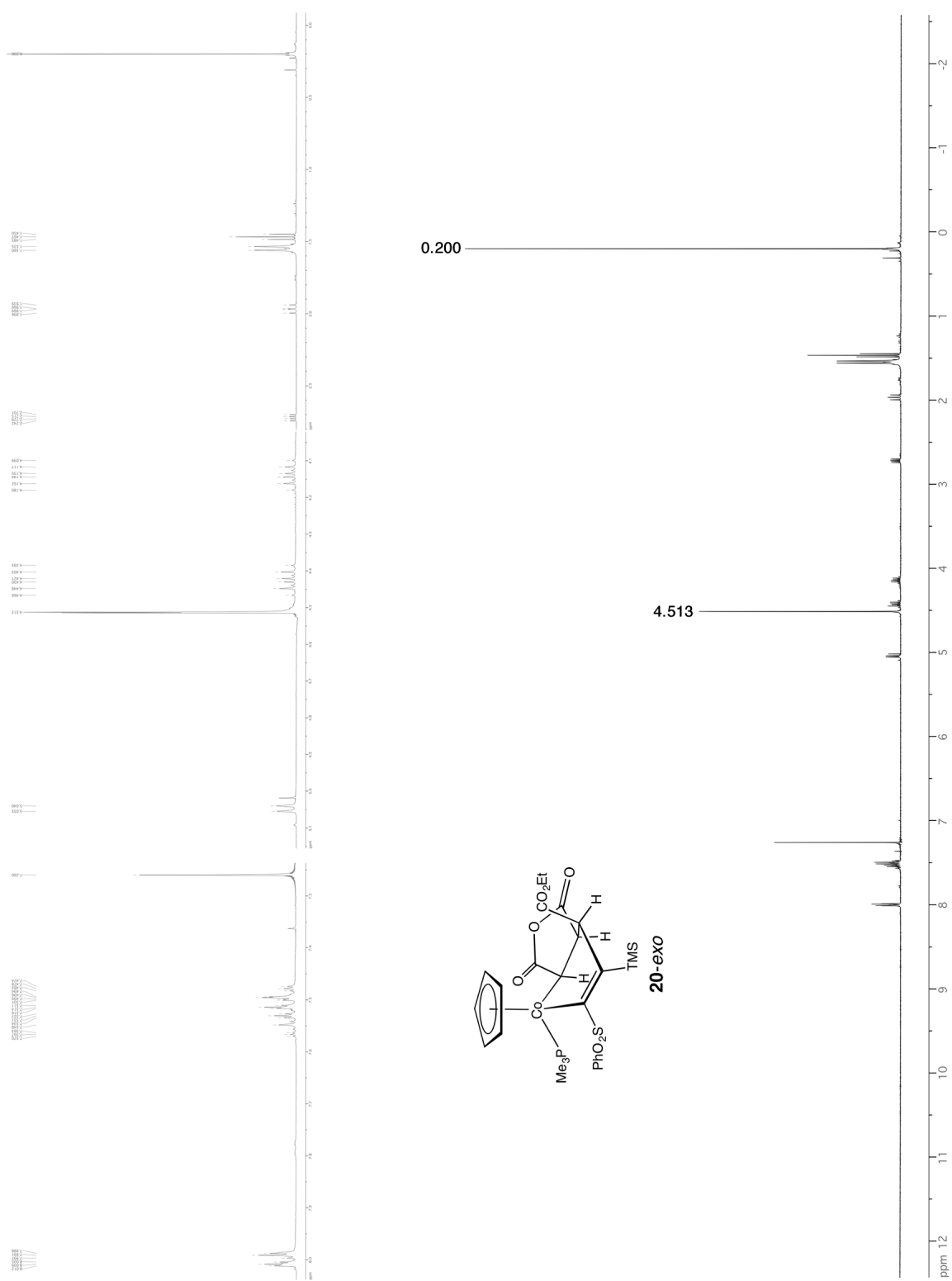


Figure 2-31. **20-exo**  $^1\text{H}$  (400.053 MHz,  $\text{CDCl}_3$ ).

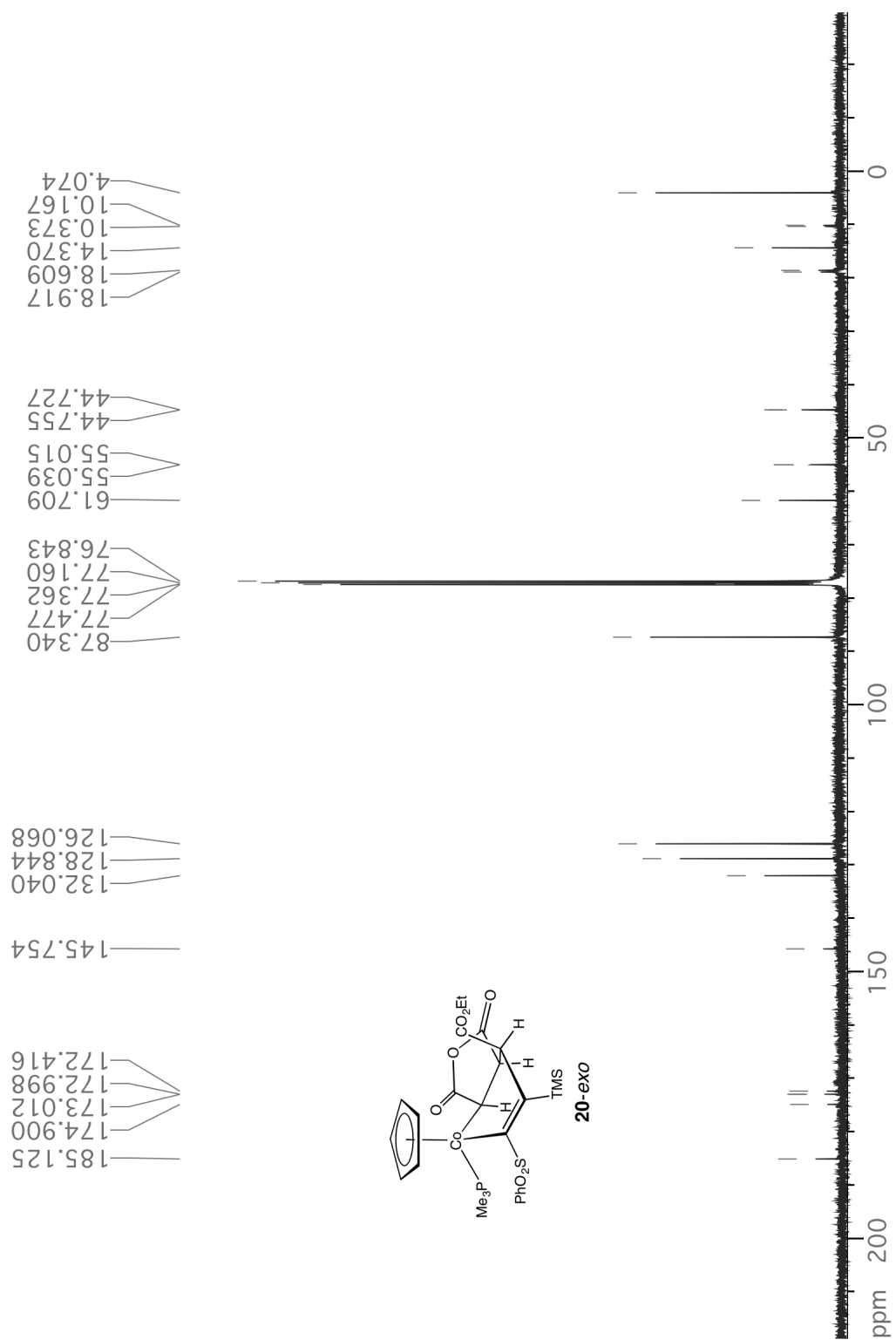


Figure 2-32. **20-exo**  $^{13}\text{C}$  (100.567 MHz,  $\text{CDCl}_3$ ).



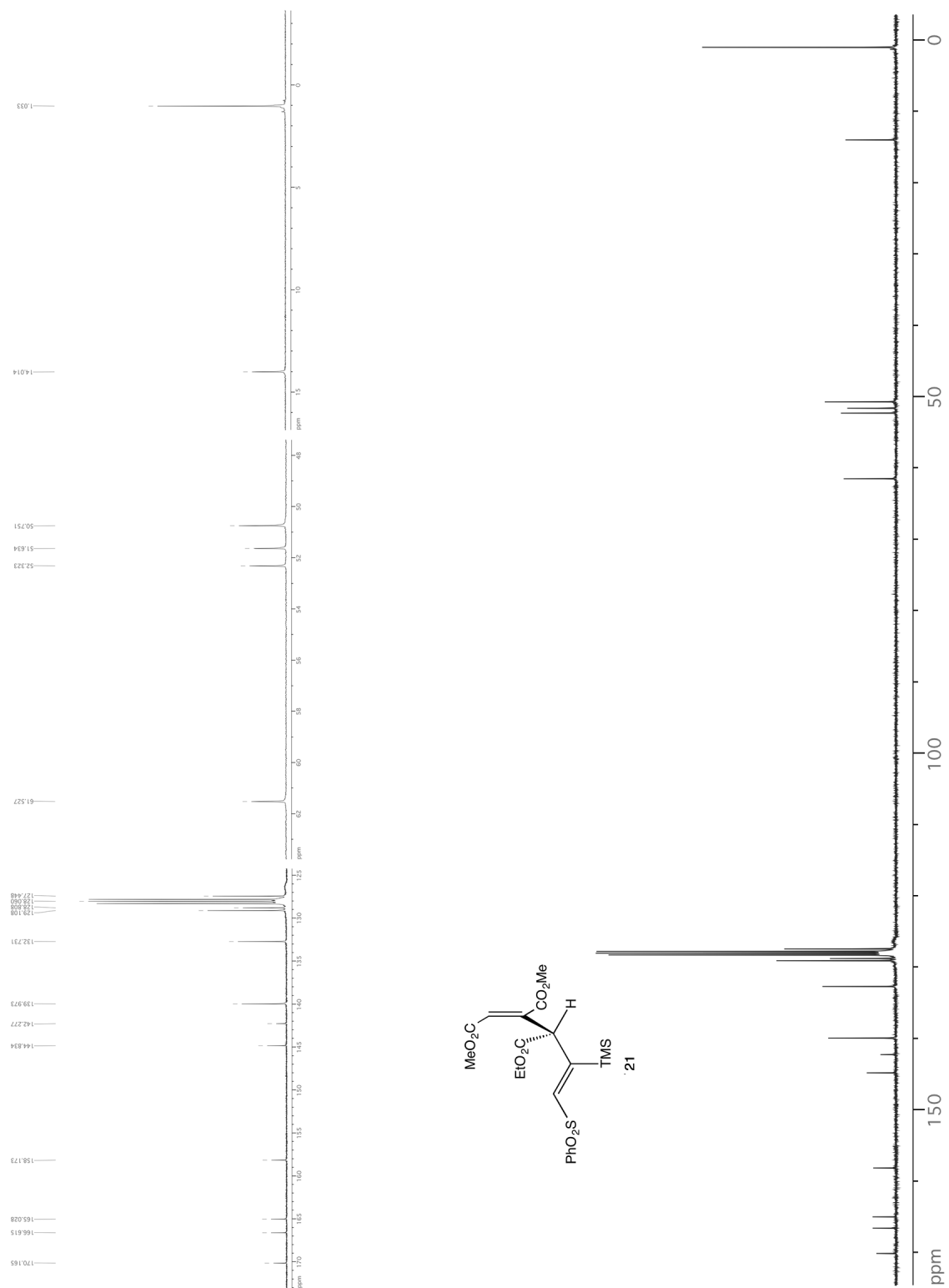


Figure 2-34. **21**  $^{13}\text{C}$  (100.567 MHz,  $\text{CDCl}_3$ ).

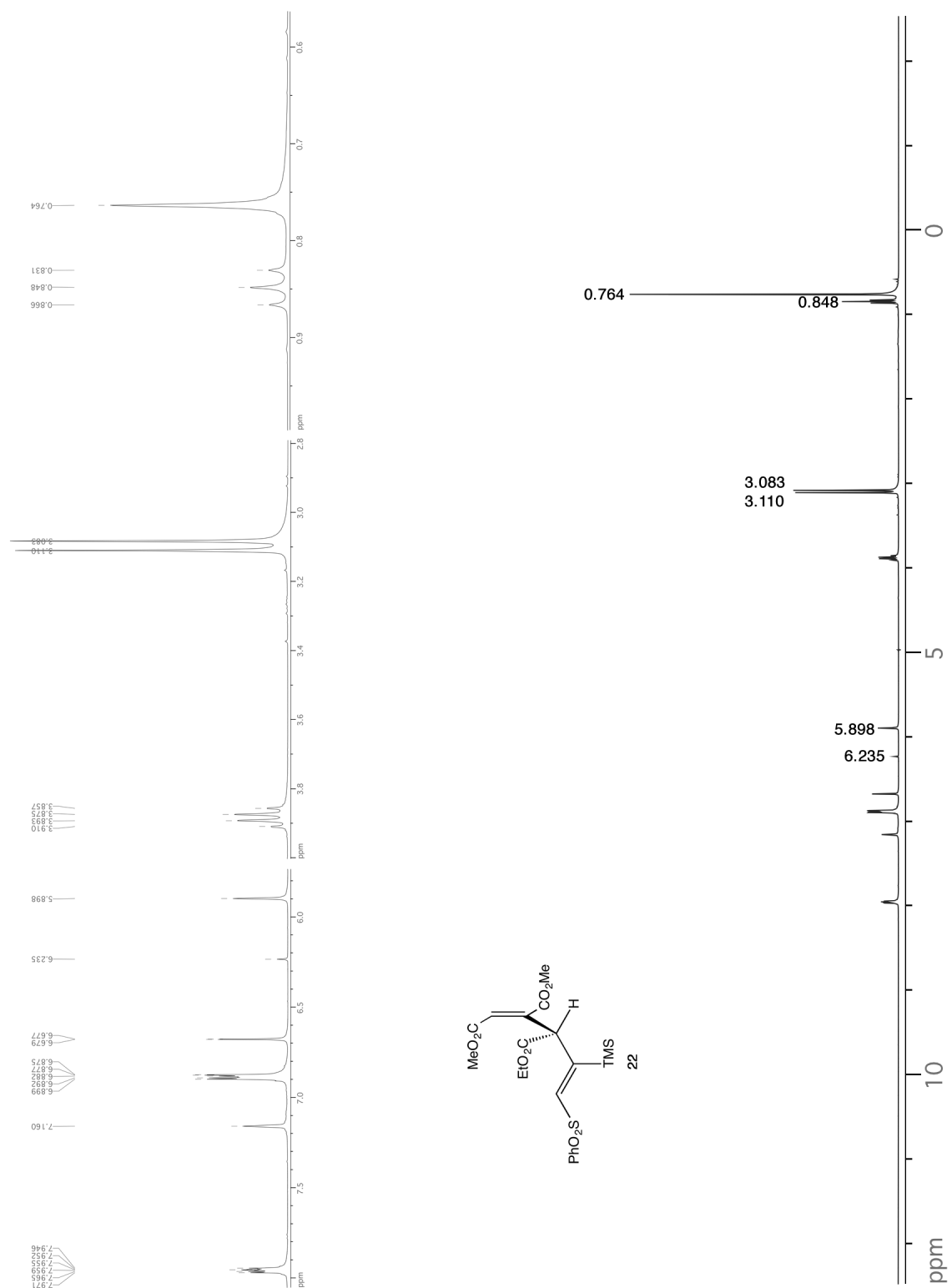
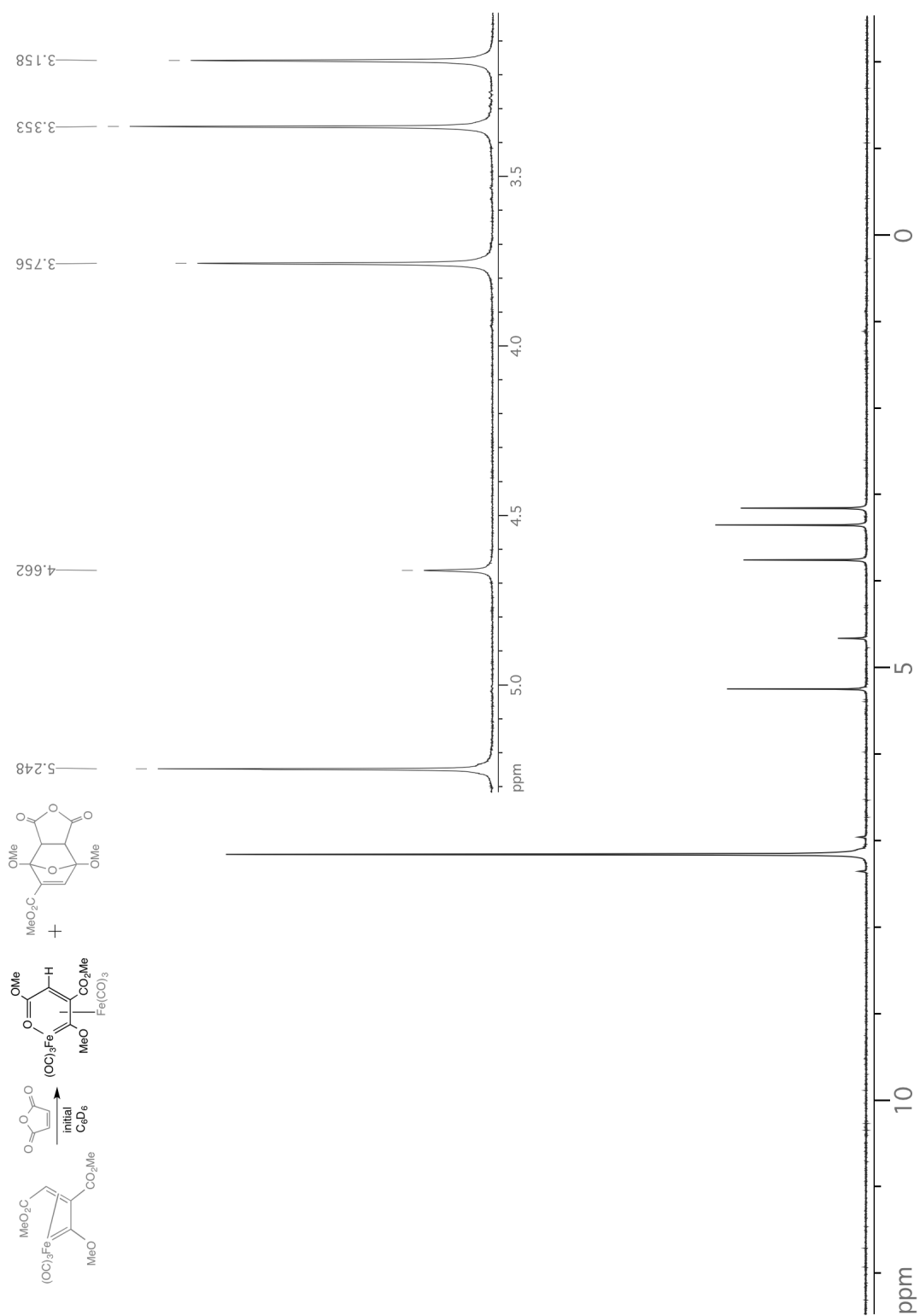
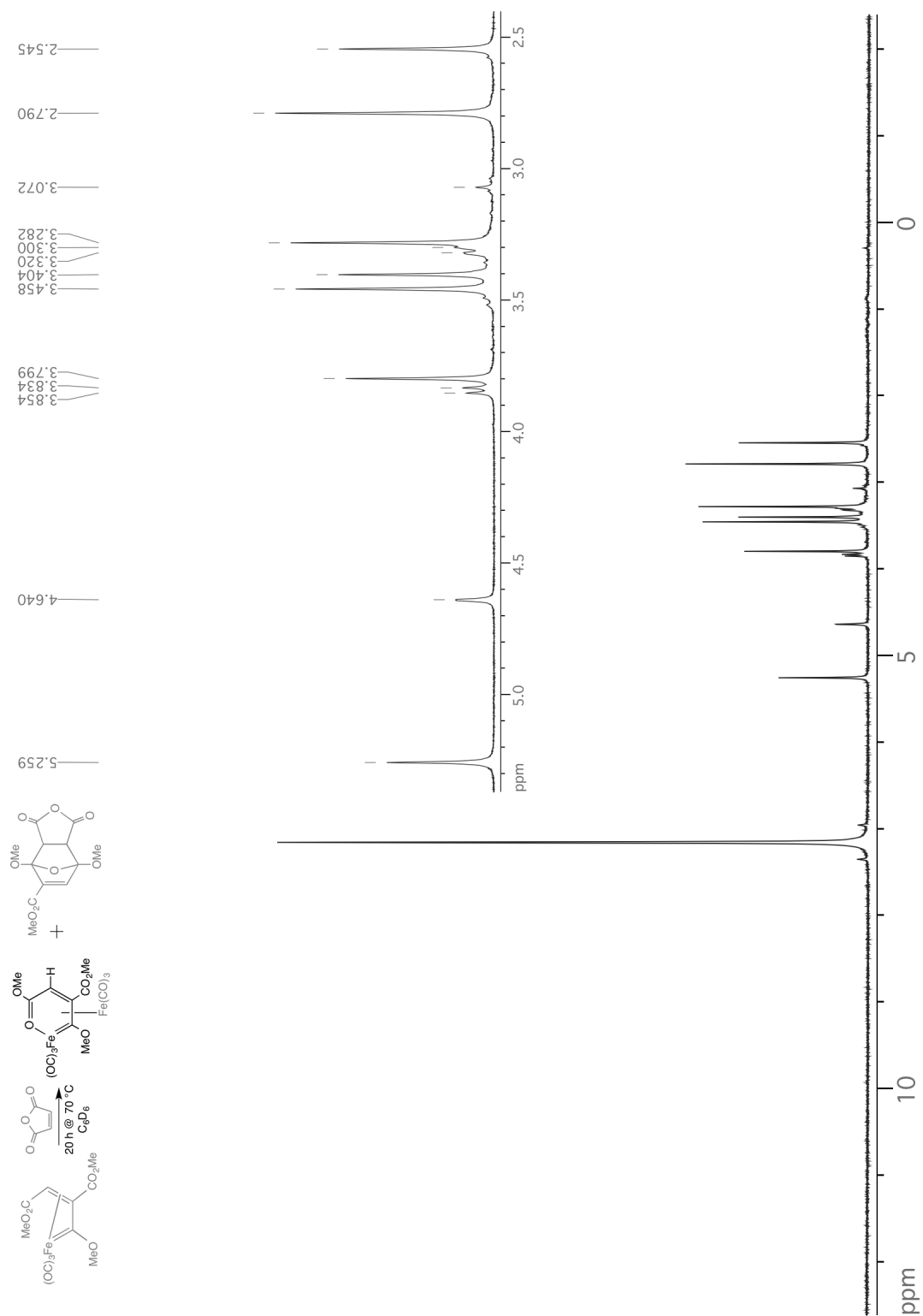


Figure 2-35. 22  $^1\text{H}$  (400.053 MHz,  $\text{CDCl}_3$ ).



**Figure 2-36.** Reaction of **25a** with maleic anhydride (initial)  $^1\text{H}$  (400.053 MHz,  $\text{CDCl}_3$ ).



**Figure 2-37.** Reaction of **25a** with maleic anhydride (final)  $^1H$  (400.053 MHz,  $CDCl_3$ ).



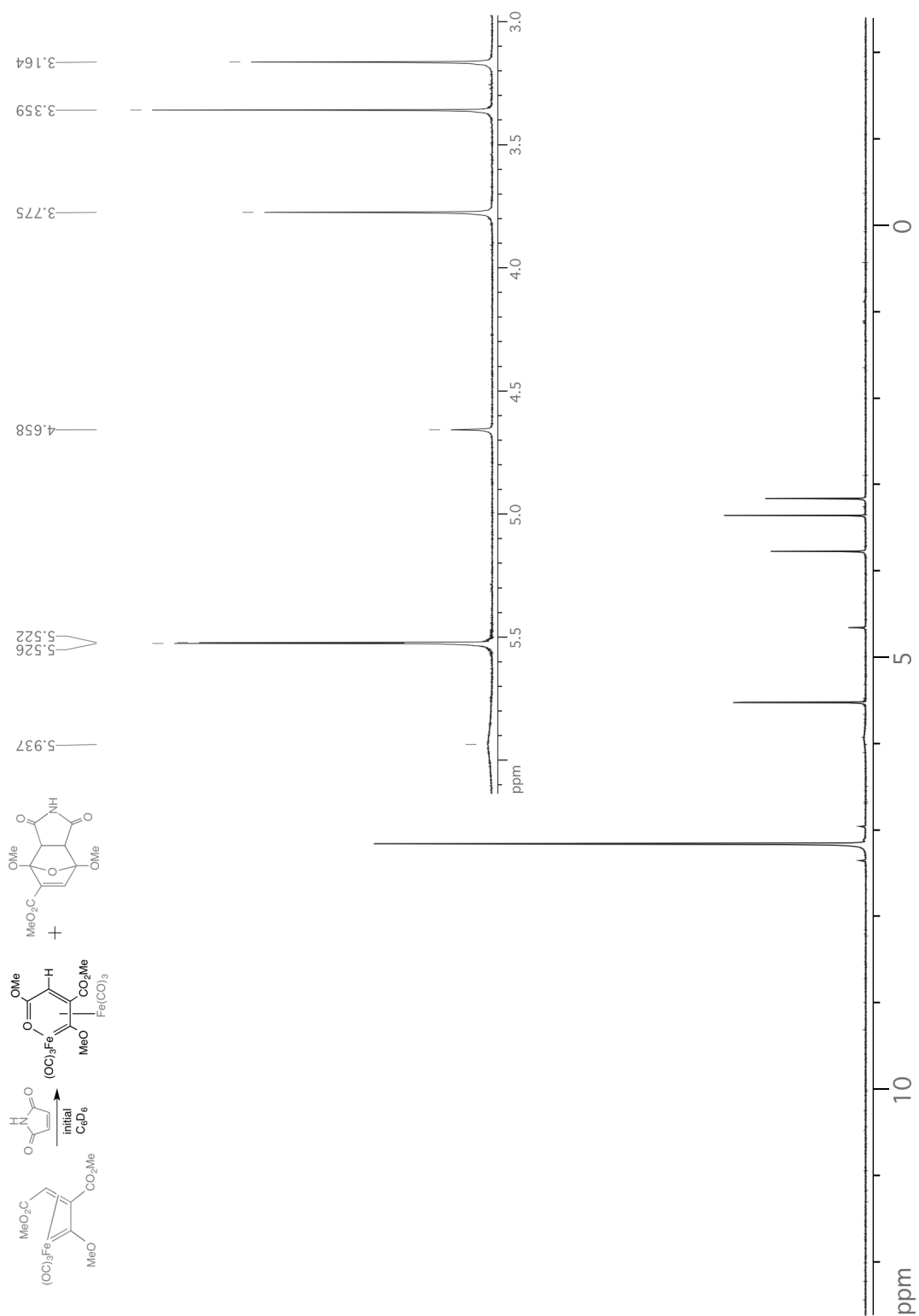


**Figure 2-38.** Reaction of **25a** with maleimide (initial)  $^1\text{H}$  (400.053 MHz,  $\text{CDCl}_3$ ).

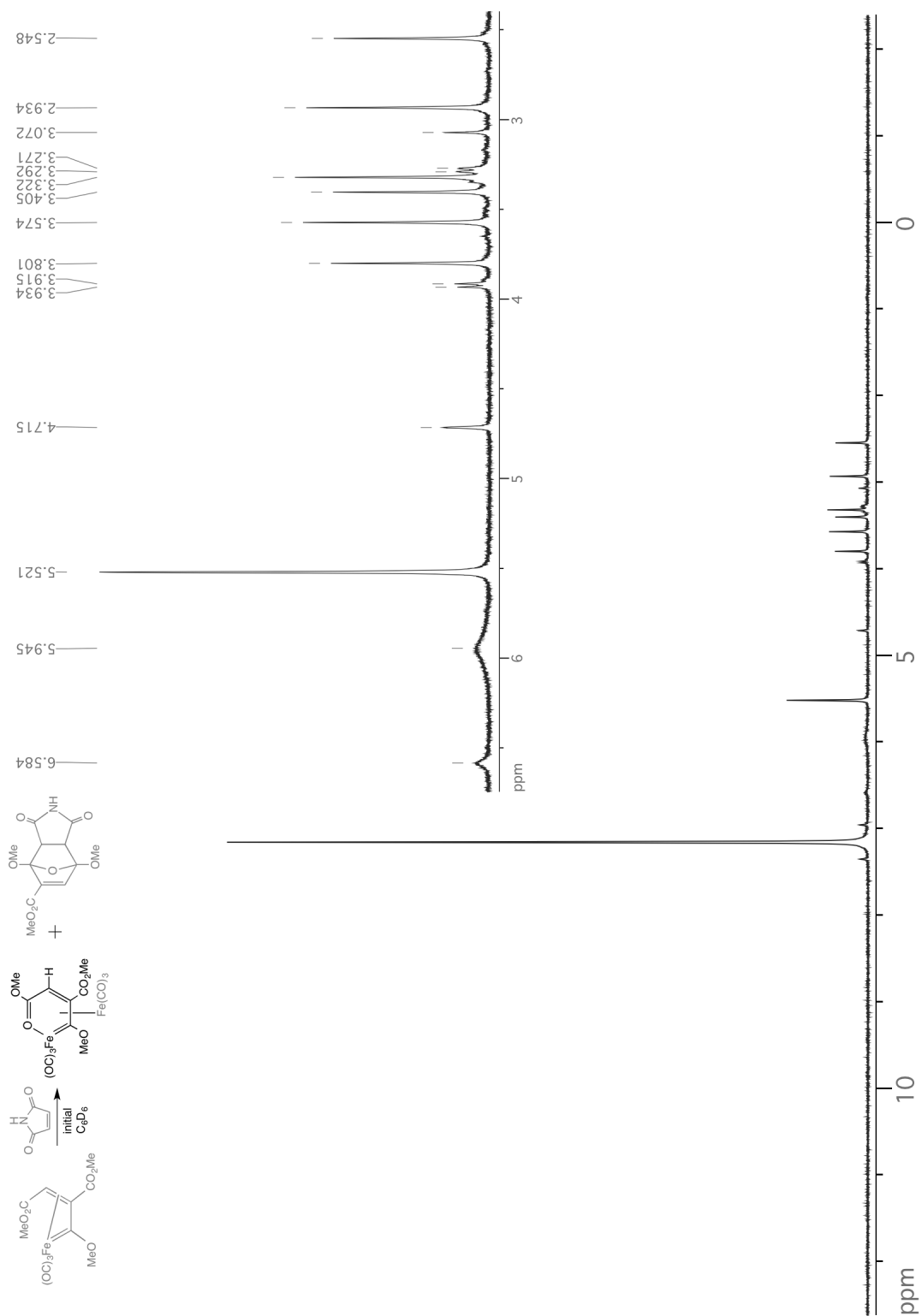


**Figure 2-39.** Reaction of **25a** with maleimide (final)  $^1H$  (400.053 MHz,  $CDCl_3$ ).

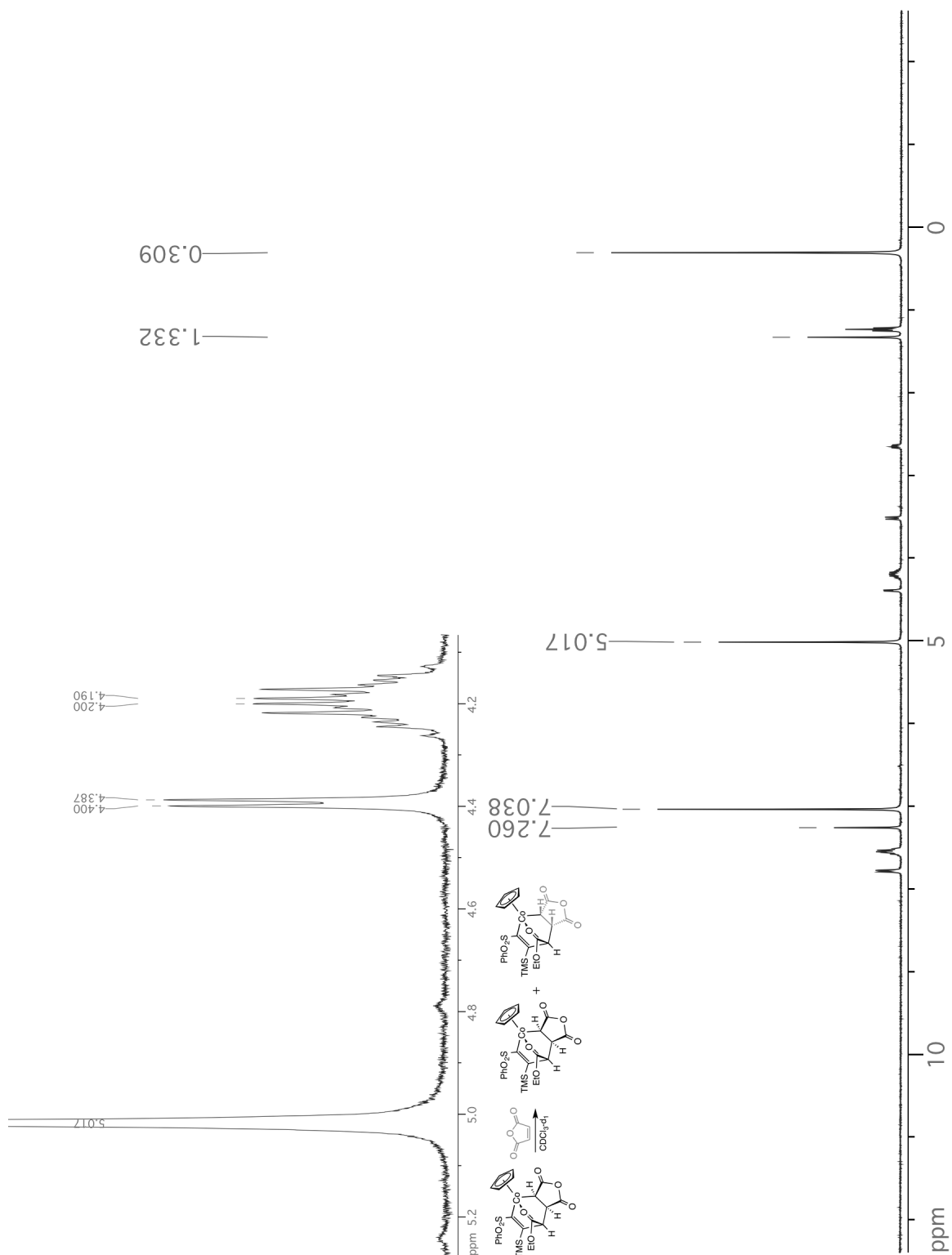


**Figure 2-40.** Reaction of **13-exo** with maleic anhydride (initial)  $^1\text{H}$  (400.053 MHz,  $\text{CDCl}_3$ ).

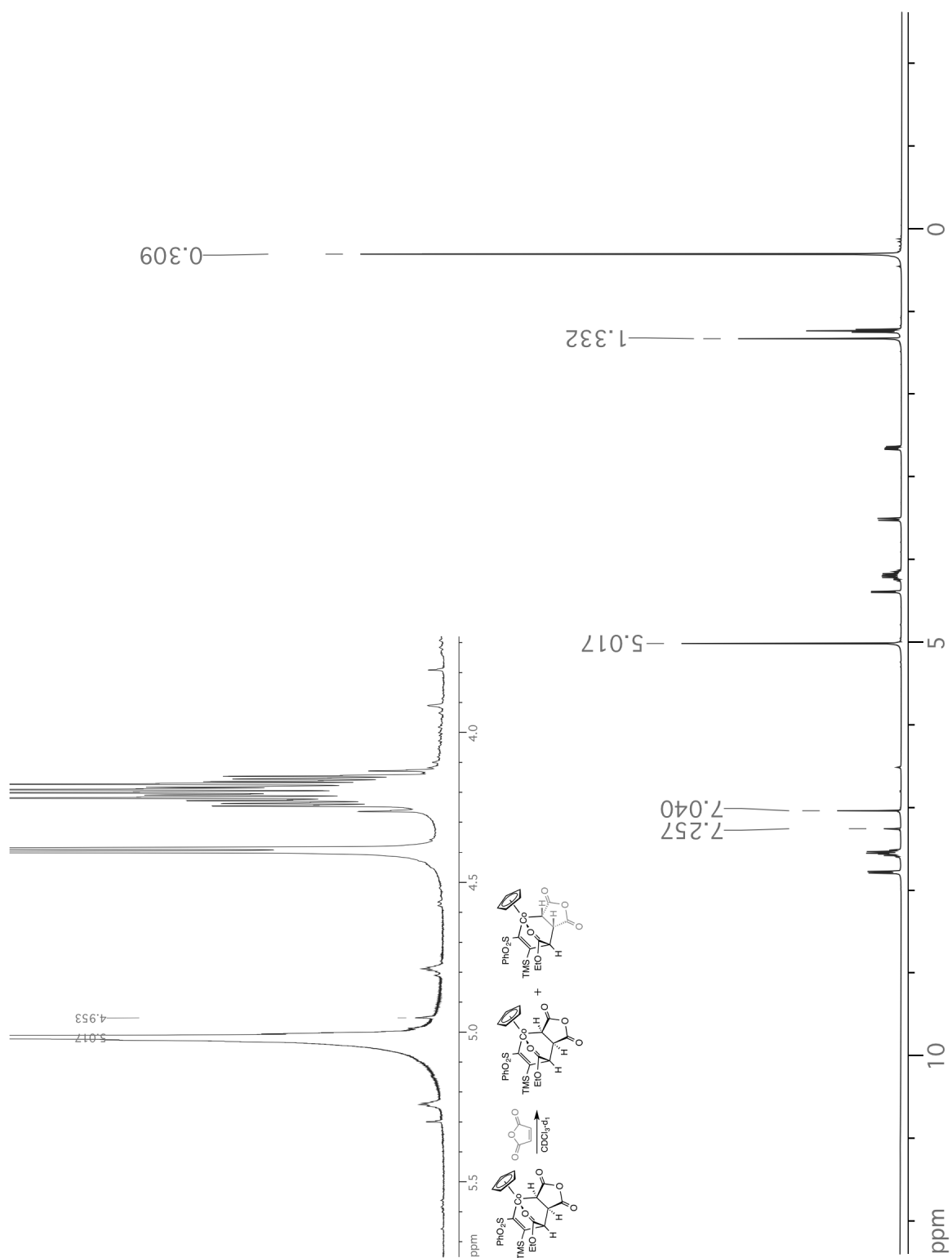


**Figure 2-41.** Reaction of **13-*exo*** with maleic anhydride (final)  $^1\text{H}$  (400.053 MHz,  $\text{CDCl}_3$ ).

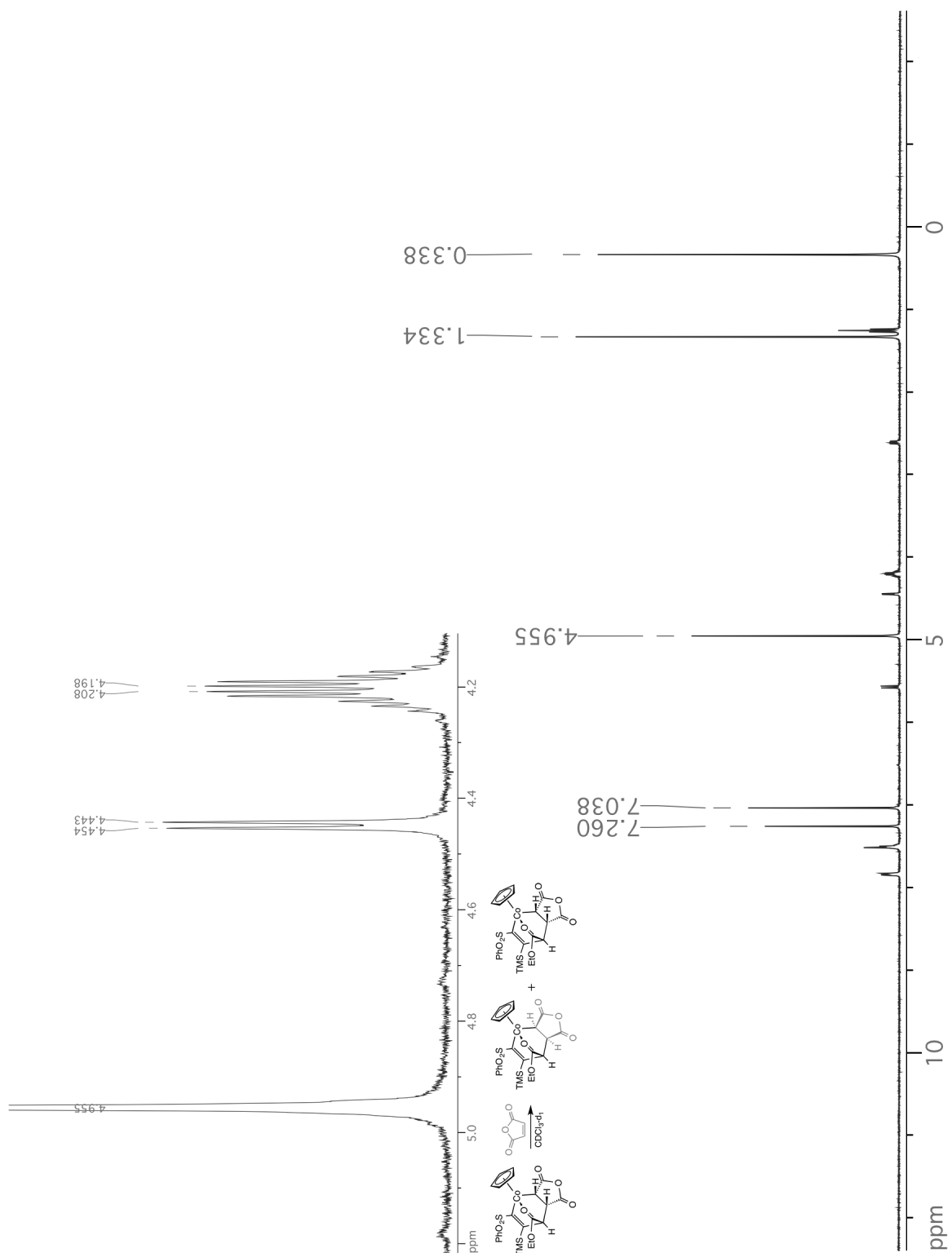


**Figure 2-42.** Reaction of **13-endo** with maleic anhydride (initial)  $^1\text{H}$  (400.053 MHz,  $\text{CDCl}_3$ ).

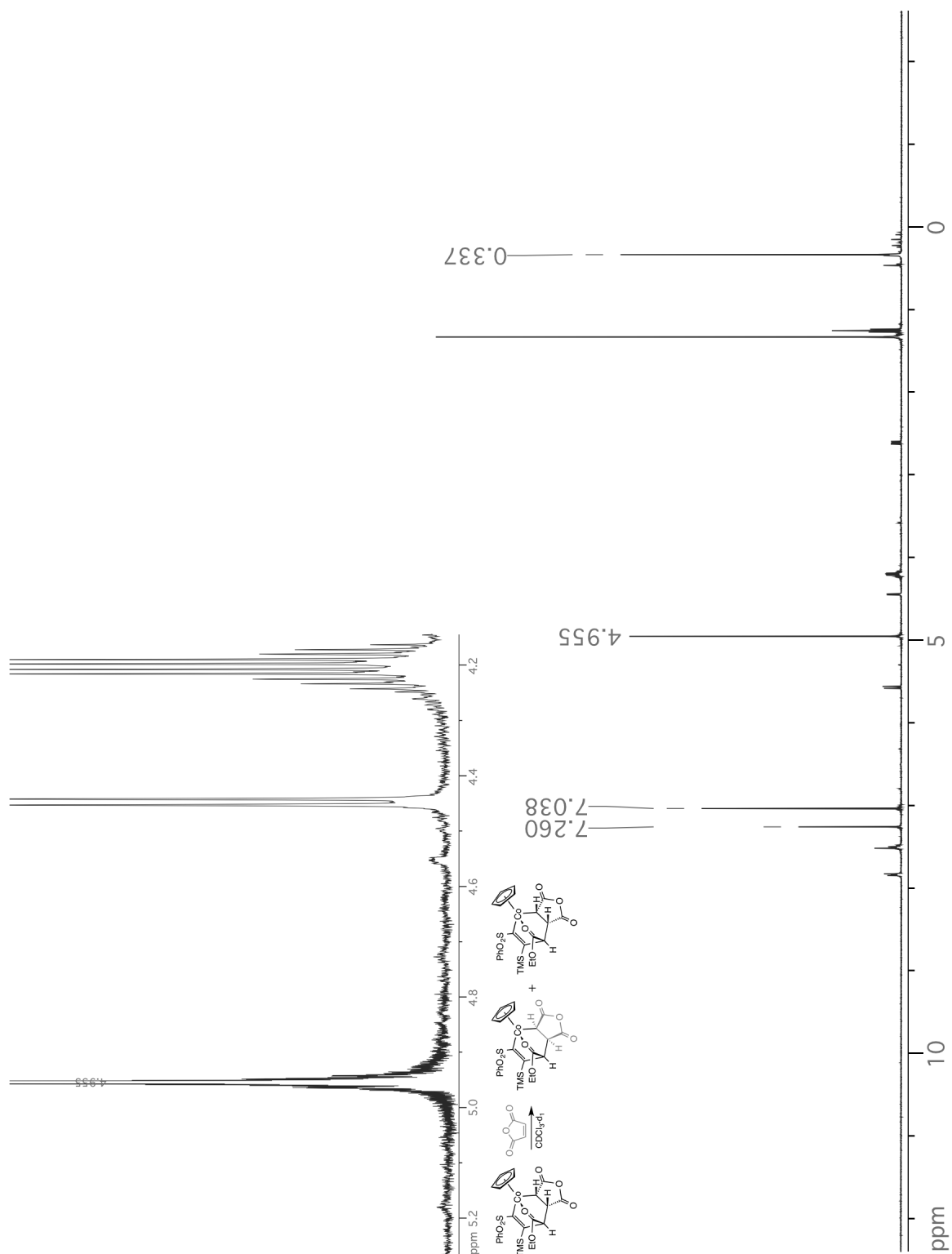


**Figure 2-43.** Reaction of **13-endo** with maleic anhydride (final)  $^1\text{H}$  (400.053 MHz,  $\text{CDCl}_3$ ).

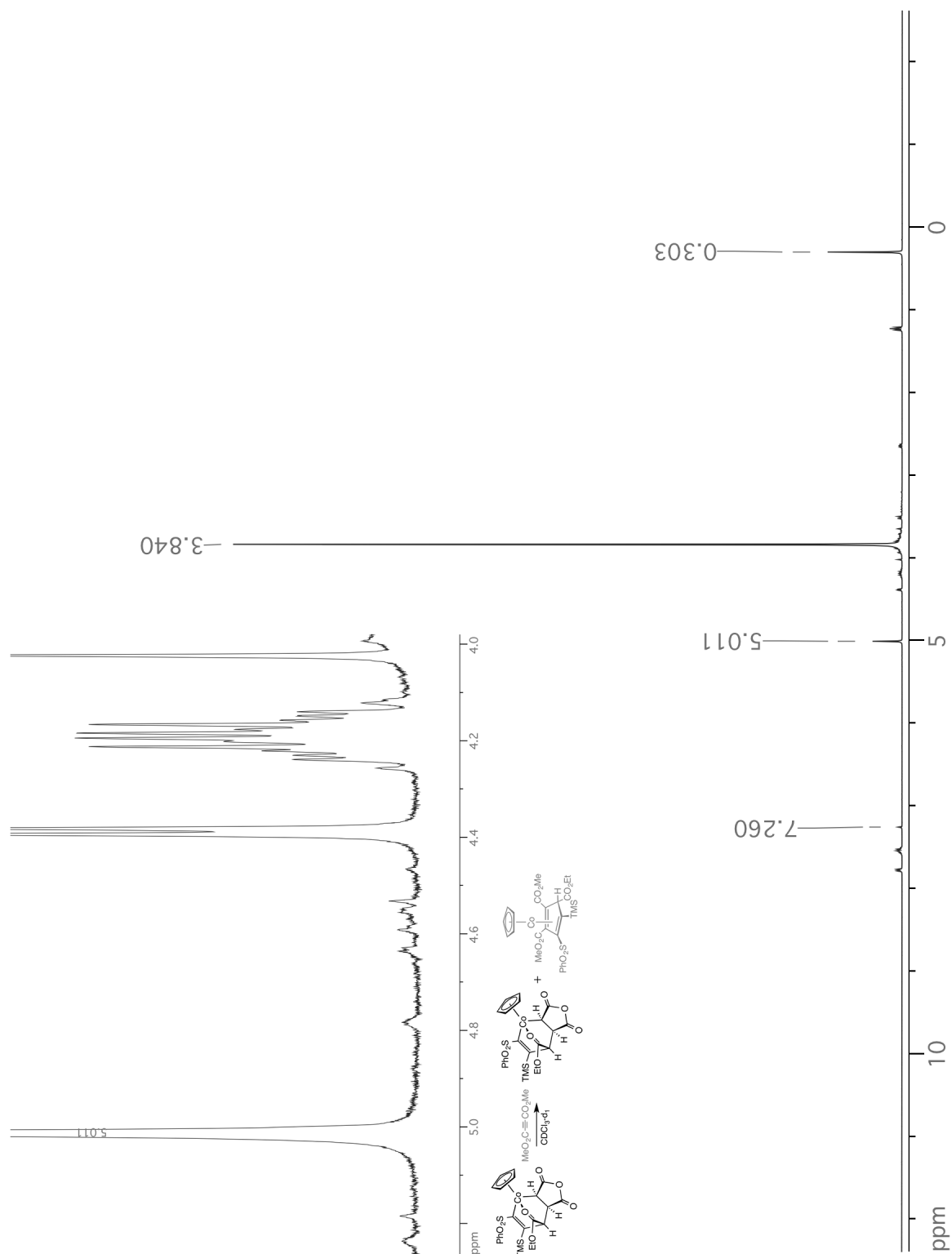


**Figure 2-44.** Reaction of **13-*exo*** with dimethyl acetylenedicarboxylate (initial)  $^1\text{H}$  (400.053 MHz,  $\text{CDCl}_3$ ).

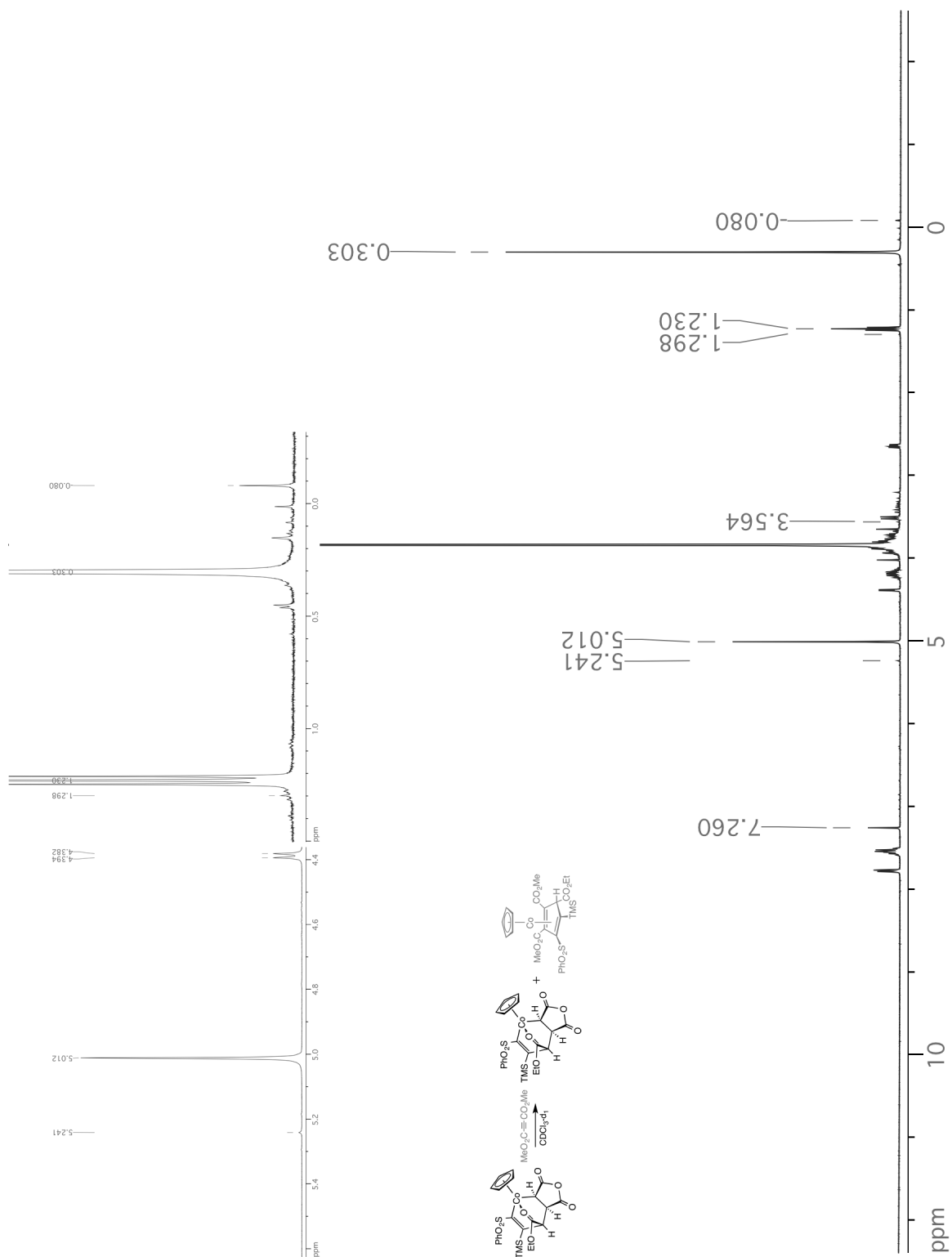


**Figure 2-45.** Reaction of **13-exo** with dimethyl acetylenedicarboxylate (final)  $^1\text{H}$  (400.053 MHz,  $\text{CDCl}_3$ ).



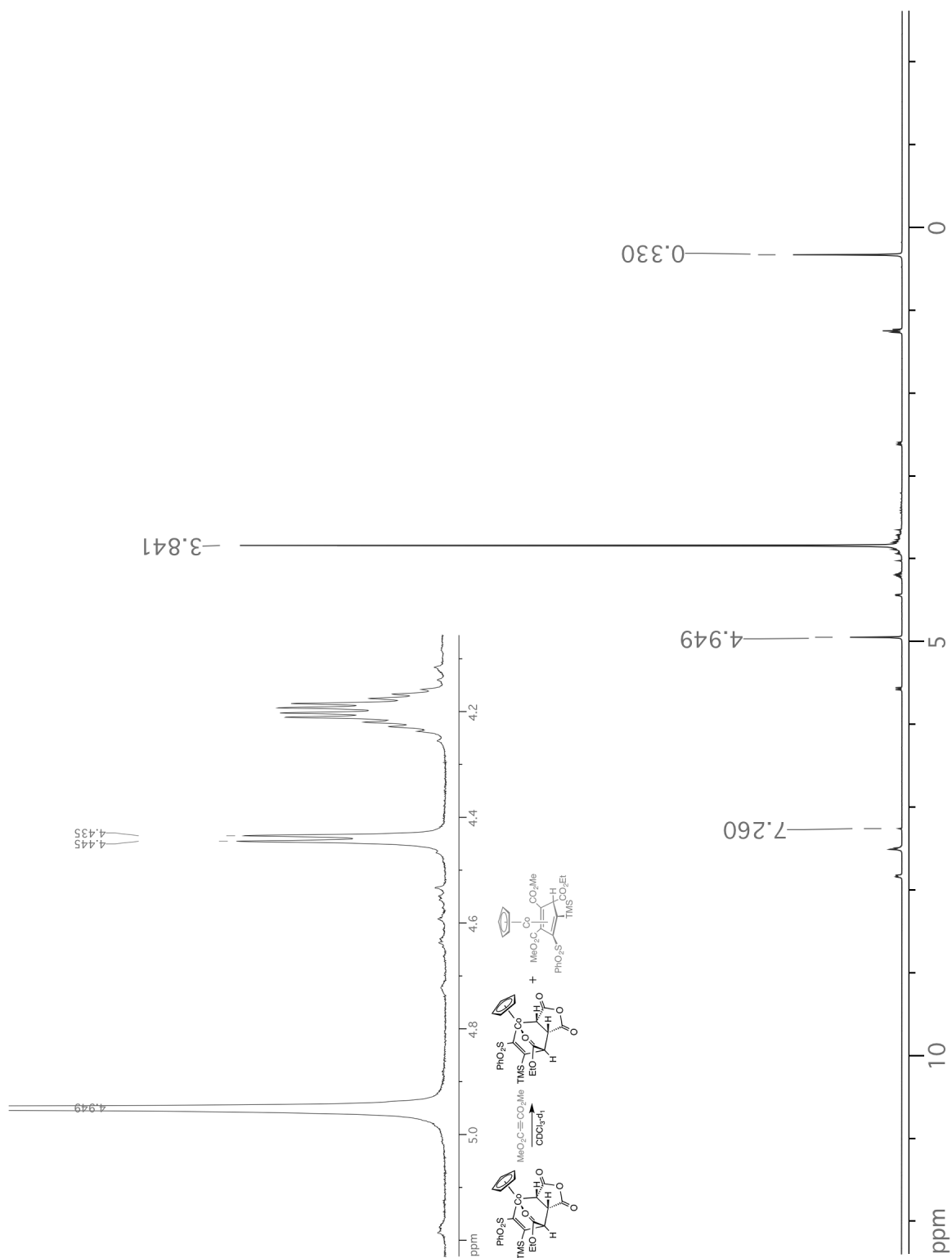


**Figure 2-46.** Reaction of **13-endo** with dimethyl acetylenedicarboxylate (initial)  $^1\text{H}$  (400.053 MHz,  $\text{CDCl}_3$ ).

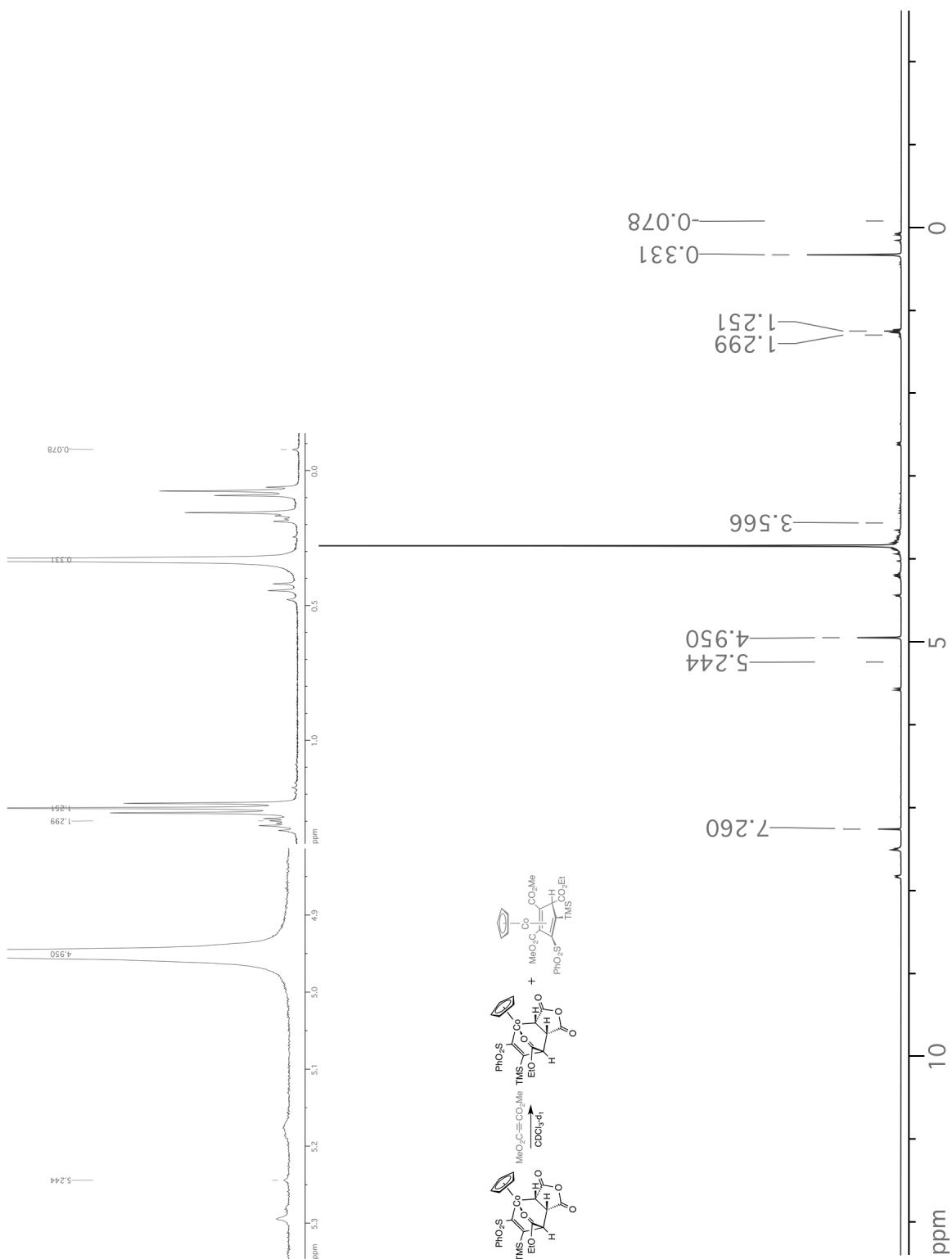


**Figure 2-47.** Reaction of **13-endo** with dimethyl acetylenedicarboxylate (final)  $^1\text{H}$  (400.053 MHz,  $\text{CDCl}_3$ ).

## **Chapter 3**

### Reactivity of Stable Metallacyclobutenes with *C*-Nitroso Reagents

*N,N*-Dialkylhydroxylamido complexes, **I** and **II**, are intriguing intermediates that may prove useful for the formation of highly functionalized organic compounds (Figure 3-1).<sup>1</sup> Both bidentate (**I**) and monodentate (**II**) dialkylhydroxylamine coordination to transition metals has been observed, with early metals more often adopting  $\eta^2$  (**I**)<sup>2,3</sup> bonding and late metals typically adopting  $\kappa^1$  bonding (**II**) (Figure 3-2).<sup>4-8</sup> Of particular interest for potential synthetic applications are the less oxophilic late-metal hydroxylamido complexes. The most common synthetic routes toward late-metal hydroxylamido complexes employ preformed nitroxyl<sup>5</sup> or hydroxylamine<sup>6</sup> reagents. The development of late-metal hydroxylamido chemistry would be facilitated by new methods for the preparation of  $\eta^2$ -(*N,O*)-*N,N*-dialkylhydroxylamido complexes which contain two different alkyl groups bound to nitrogen. Here we describe the first syntheses of late-metal  $\eta^2$ -(*N,O*)-*N,N*-dialkylhydroxylamido complexes via a formal insertion of nitroso compounds into a metal-carbon bond.<sup>9-11</sup>

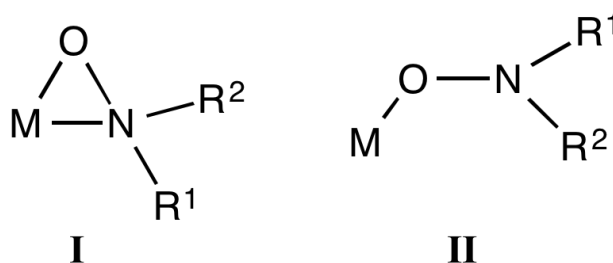


**Figure 3-1.**  $\eta^2$ -(*N,O*)- and  $\kappa^1$ -(*O*)-hydroxylamido coordination.

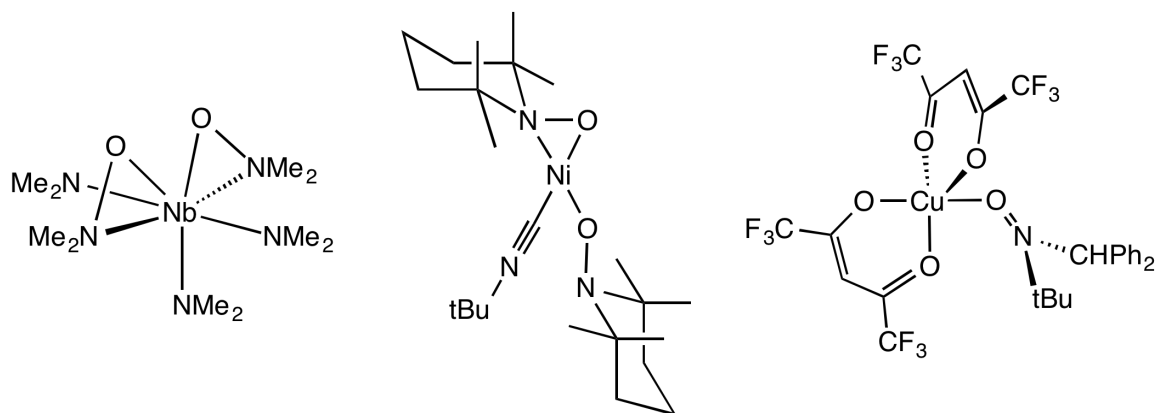
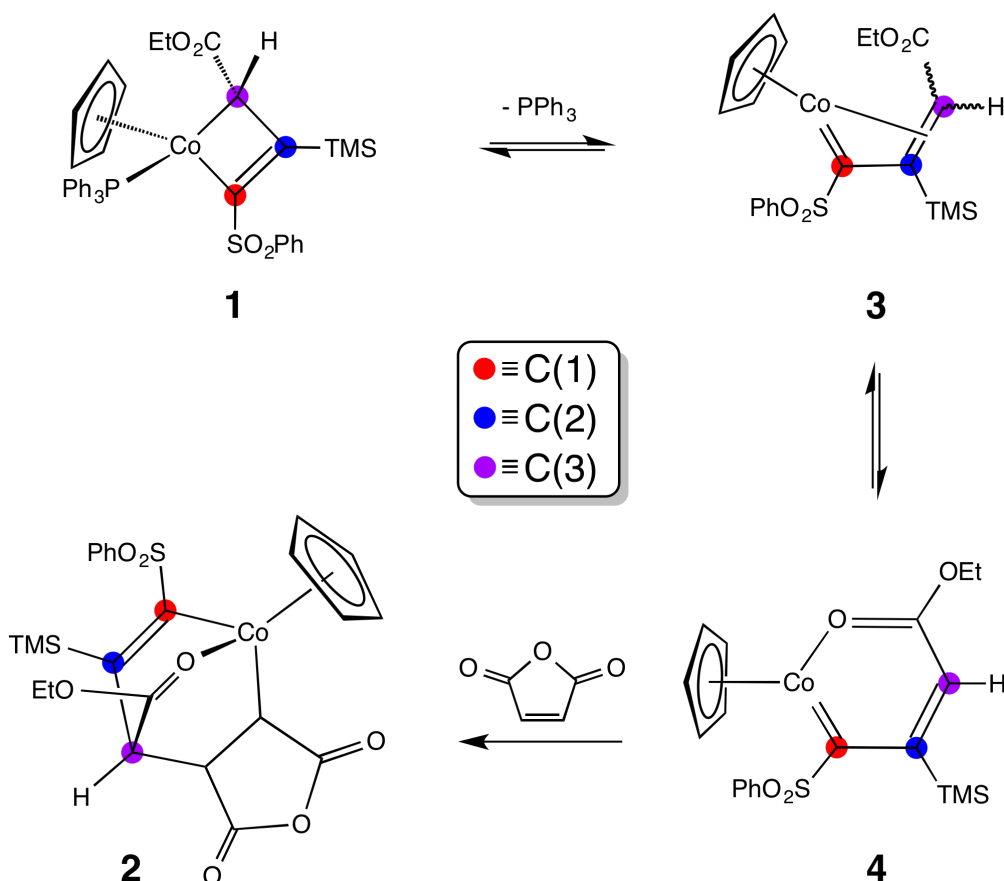


**Figure 3-2.** Crystallographically characterized examples of dihapto  $[\text{Nb}(\text{NMe}_2)_3(\eta^2\text{-N}(\text{O})\text{Me}_2)_2]$  (GAJHEG),<sup>8a</sup> ambidentate  $[(\text{tBuNC})\text{Ni}(\eta^2\text{-2,2,6,6-Me}_4\text{-N}(\text{O})\text{C}_5\text{H}_3)(\kappa^1\text{-2,2,6,6-Me}_4\text{-N}(\text{O})\text{C}_5\text{H}_3)]$  (IWUPUM),<sup>8b</sup> and monohapto  $[\eta^2\text{-(1,3-(CF}_3)_2\text{-acac)}_2\text{Cu}(\eta^1\text{-N}(\text{O})(\text{CHPh}_2)(\text{tBu}))]$  (YUBDII),<sup>8c</sup> binding modes.

We recently reported the reaction of the cobaltacyclobutene complex ( $\eta^5\text{-C}_5\text{H}_5$ )(PPh<sub>3</sub>)Co[ $\kappa^2\text{-C}(\text{SO}_2\text{Ph})=\text{C}(\text{TMS})\text{CH}(\text{CO}_2\text{Et})$ ] (**1**) with maleic anhydride to give metallacyclohexene products (**2**, Scheme 3-1).<sup>12</sup> The observed selectivity for reaction at C(3) in preference to C(1) of the metallacycle contrasts with the reactions of **1** with carbon monoxide, ethyl diazoacetate, and isocyanides, all of which undergo coupling at the Co-C(1) bond to form vinylketene, vinylketenimine, and 1,3-diene products.<sup>13</sup> In principle, all four reactions of **1** could proceed via the vinylcarbene intermediate **3** (Scheme 3-1).<sup>14</sup> Reaction of **3** with CO, isocyanides, and carbenes would involve substrate coordination to cobalt followed by coupling to the carbene ligand. In the case of maleic anhydride, a [4 + 2] cycloaddition reaction involving **3** or oxametallacycle **4** would lead directly to metallacyclohexene **2** (see Chapter 2). In this respect, **3** and **4** may be viewed as “metalladiene” participants in a Diels-Alder reaction with activated alkenes. This

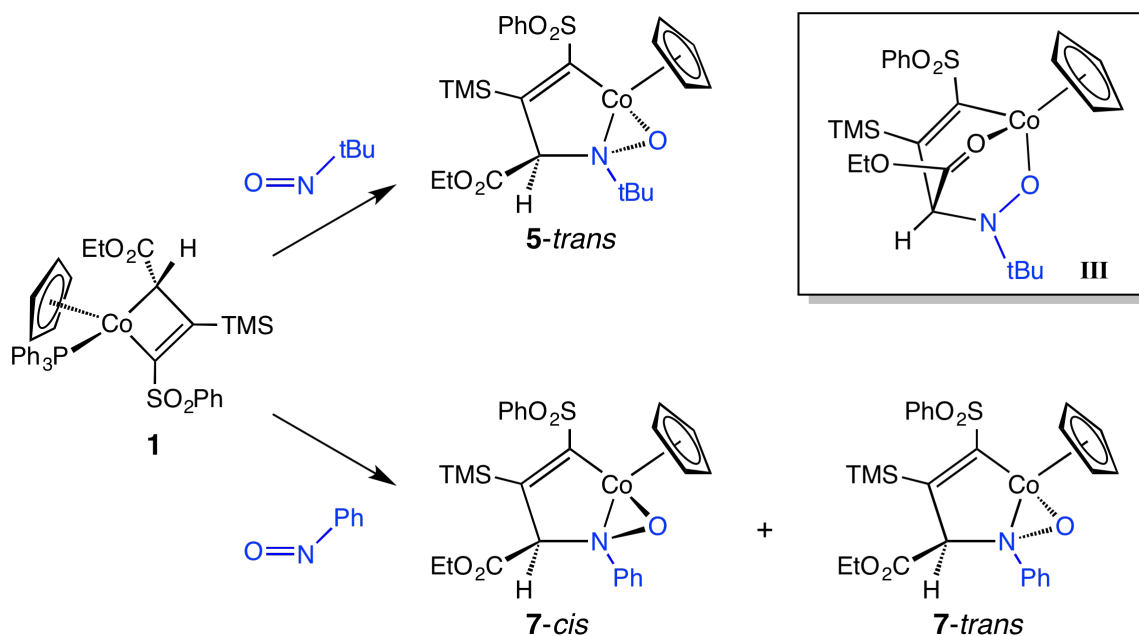
speculation led us to examine the reactions of **1** with the classic heterodienophiles, nitrosobenzene and 2-methyl-2-nitrosopropane. As described below, nitroso compounds undergo regioselective coupling to C(3) of the metallacycle and formation of ring-expanded metallacycles which contain an  $\eta^2$ -(*N,O*)-*N,N*-dialkylhydroxylamido ligand.



**Scheme 3-1.** Mechanistic speculation for the conversion of **1** and maleic anhydride to **2**.<sup>12</sup>

A toluene solution (25 mL) of metallacycle **1** (245 mg, 0.35 mmol) and excess 2-methyl-2-nitrosopropane dimer (0.66 mmol) was heated under a nitrogen atmosphere at 70 °C for 4 h, followed by chromatography on silica gel

(35% ethyl acetate/hexanes), to provide **5-trans** as a dark burgundy powder in 83% yield (Scheme 3-2). Analytically pure **5-trans** was obtained by recrystallization from chloroform/hexanes. In the  $^1\text{H}$  NMR spectrum ( $\text{CDCl}_3$ ) of **5-trans**, singlets were observed at  $\delta$  4.93 ( $\text{C}_5\text{H}_5$ ) and 4.08 ( $\text{CHCO}_2\text{Et}$ ). Both resonances were significantly downfield of the corresponding signals for **1** ( $\delta$  4.20 ( $\text{C}_5\text{H}_5$ ), 1.43 (d,  $J_{\text{PH}} = 7.0$  Hz,  $\text{CHCO}_2\text{Et}$ )) and appeared at chemical shift values very similar to those observed for metallacyclohexene **2** ( $\delta$  5.02 ( $\text{C}_5\text{H}_5$ ), 4.05 (d,  $J_{\text{HH}} = 4.2$  Hz,  $\text{CHCO}_2\text{Et}$ )). In the  $^{13}\text{C}\{^1\text{H}\}$  NMR spectrum ( $\text{CDCl}_3$ ) of **5-trans**, the carbon bearing the ester substituent was observed at  $\delta$  80.6 ( $\text{CHCO}_2\text{Et}$ ), which is substantially downfield of the  $\delta$  49.6 ( $\text{CHCO}_2\text{Et}$ ) resonance observed for the corresponding carbon in **2**. In the IR spectrum (thin film) of **5-trans**, a strong ester  $\nu(\text{C}=\text{O})$  stretch was observed at  $1748\text{ cm}^{-1}$ , which is at much higher frequency than that observed for **2** ( $1638\text{ cm}^{-1}$ ), suggesting that the ester carbonyl oxygen of **5-trans** is not coordinated to cobalt. Thus, the spectroscopic data for **5-trans** suggested that nitroso coupling to C(3) had occurred, but the data were inconsistent with the anticipated structure **III** (Scheme 3-2).

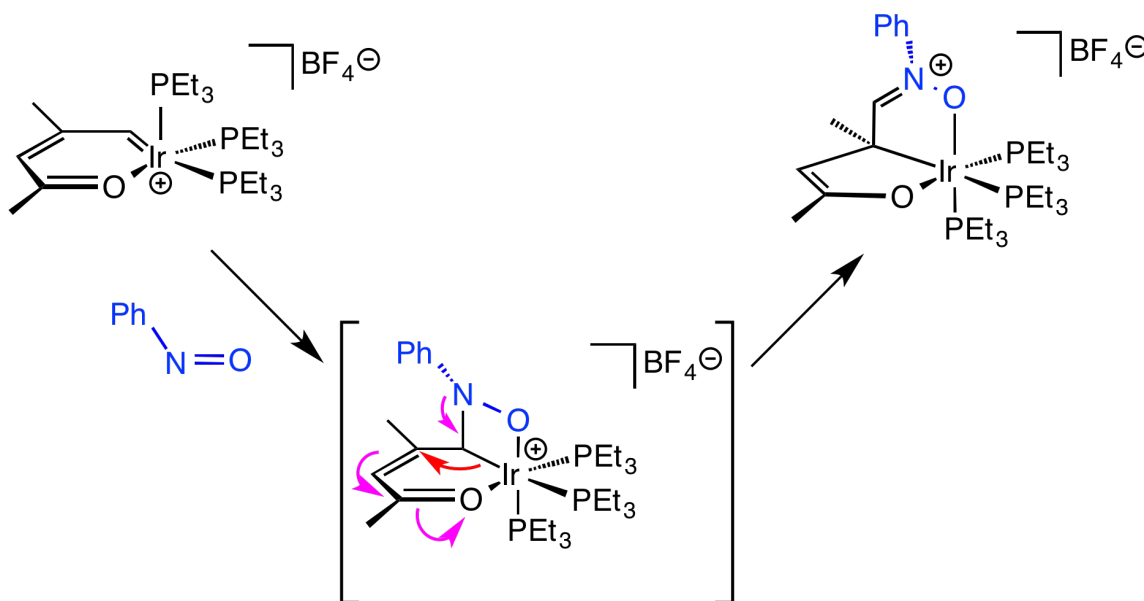


**Scheme 3-2.** Formation of  $\eta^2$ -(*N,O*)-*N,N*-dialkylhydroxylamido complexes from **1** and nitroso reagents.

A second possibility for **5-trans** would be a [2 + 2] cycloaddition reaction between 2-methyl-2-nitrosopropane and either a vinylcarbene species such as **3** or an oxametallacyclobenzene such as **4** (Scheme 3-1). Work by Bleeker<sup>10a</sup> and co-workers have established the viability of [4 + 2]-cycloaddition reactions of metallabenzene,<sup>10b</sup> and related metallapyrylium<sup>10d</sup> and metallathiabenzene<sup>10f</sup> species. Iridabenzene<sup>10c</sup> and iridathiabenzene<sup>10f</sup> react with nitrosobenzene to form dihydro-(*N,O*)-metallabarrelenes and dihydro-(*N,O*)-metallathiabarrelenes, respectively – both of which adopt a type **III** structure. In the case of iridapyrylium however,<sup>10e</sup> nitrosobenzene undergoes a formal [2 + 2] reaction to give a bicyclic [4.2.0] intermediate before a skeletal rearrangement to generate the observed [3.3.0] product (Scheme 3-3). Such a species would be consistent with the spectral data for **5-trans** and would be interesting in context of the



cobaltacyclobutene chemistry since  $C_2$ -cycloaddends couple either exclusively at the C(3)  $\gamma$ -sp<sup>3</sup> carbon (alkenes), or in ambiguous fashion at both C(1) and C(3) carbons to give cyclopentadienes (alkynes).<sup>12,13c</sup>



**Scheme 3-3.** Reaction of an iridapyrylium with nitrosobenzene to give a bicyclic [3.3.0] metallacycle.<sup>10e</sup>

A single-crystal X-ray diffraction study on **5-trans** confirmed that the ester oxygen was not chelating and revealed a much different type of bicyclic structure, with  $\kappa^1$ -(C)- $\eta^2$ -(N,O) coordination to cobalt (Figure 3-3, Table 3-1 and 3-2).<sup>15</sup> The relative stereochemistry at the cobalt, nitrogen, and carbon stereocenters is  $S^{Co}S^N R^C, R^{Co}R^N S^C$ , with O(1) and the ester located on opposite faces of the five-membered azametallacycle ring defined by (Co, C(1), C(2), C(3), N). The trans relationship for the ester substituent and O(1) is reflected in a C(13)-C(3)-N(1)-O(1) dihedral angle of 172.95(0.12)°. The fold angle between the Co-N(1)-O(1) and C(1)-Co-N(1) planes is 87.37(5)°, and the largest deviations of ring atoms

from the C(1)-Co-N(1) plane are 0.150(2) Å for C(2), 0.410(2) Å for C(3), and -1.289(1) Å for O(1). The quaternary carbon of the *tert*-butyl substituent, C(16), is displaced only 0.207(2) Å from the C(1)-Co-N(1) plane. To our knowledge, **5-trans** is the first cobalt(III)- $\eta^2$ -(*N,O*)-hydroxylamido complex and the only example of an  $\eta^2$ -(*N,O*)-hydroxylamido group which is incorporated into a [3.1.0] fused-ring framework. The constraints of this bicyclic structure cause significant perturbations on the geometry at N(1). The Co-N(1)-O angle is constrained to 68.4(1)° by the three-membered ring, the Co-N(1)-C(3) angle is constrained to 111.51(10)° by the five-membered ring, and the Co-N(1)-C(16) angle is opened up to 127.6(1)°. The corresponding Co-N-C angles in the cobalt(I) complex (triphos)Co[ $\eta^2$ -(*N,O*)-Me<sub>2</sub>NO] (**6**)<sup>6a</sup> are 121.5(5) and 122.7(4)°. The Co-N and N-O bond distances in **6** are similar to the 1.917(1) and 1.388(2) Å distances in **5-trans**; however, the 1.908(1) Å Co-O(1) bond distance in **5-trans** is significantly longer than the 1.854(4) Å distance observed in **6**. For comparison the Co-N and N-O bond distances in the  $\kappa^1$ -(*N*)-nitroso complex ( $\eta^5$ -C<sub>5</sub>H<sub>5</sub>)(PPh<sub>3</sub>)Co[ $\kappa^1$ -(*N*)-N(=O)CH<sub>3</sub>] are 1.7822(16) and 1.2846(19) Å, respectively.<sup>16</sup>



combined yield. The structure of the minor isomer, **7-trans**, was tentatively assigned on the basis of the  $^1\text{H}$  NMR spectral data, by comparison to those for **5-trans**. Specifically, in the  $^1\text{H}$  NMR spectrum ( $\text{CDCl}_3$ ) of the minor isomer, singlets are observed at  $\delta$  4.78 ( $\text{C}_5\text{H}_5$ ) and 3.90 ( $\text{CHCO}_2\text{Et}$ ), which are chemical shift values similar to those observed for **5-trans** ( $\delta$  4.93 ( $\text{C}_5\text{H}_5$ ) and 4.08 ( $\text{CHCO}_2\text{Et}$ )). In contrast, the major isomer, **7-cis**, exhibits resonances in the  $^1\text{H}$  NMR spectrum ( $\text{CDCl}_3$ ) at  $\delta$  4.48 ( $\text{C}_5\text{H}_5$ ) and 5.23 ( $\text{CHCO}_2\text{Et}$ ). Attempts to separate the two isomers by silica gel chromatography failed, and extended heating at  $70\text{ }^\circ\text{C}$  led to the formation of several unidentified new products.

An analytically pure sample of the mixture was obtained by recrystallization from chloroform/hexanes, and an X-ray diffraction study was carried out on a crystal of **7-cis** (Figure 3-4, Table 3-1, and Table 3-2). The structural data for **7-cis** revealed a bicyclic structure with  $\kappa^1\text{-}(C)\text{-}\eta^2\text{-}(N,O)$  coordination to cobalt, as was observed for **5-trans**, but with the ester substituent and O(1) on the same face of the five-membered azametallacycle ring. The cis relationship of the ester substituent and O(1) leads to a C(13)-C(3)-N(1)-O(1) dihedral angle of  $-62.80(0.23)^\circ$ . The ipso carbon of the phenyl substituent, C(16), is displaced only  $-0.354(2)\text{ \AA}$  from the C(1)-Co-N(1) plane. The relative stereochemistry at the cobalt, nitrogen, and carbon stereocenters is  $S^{\text{Co}}S^{\text{N}}S^{\text{C}}, R^{\text{Co}}R^{\text{N}}R^{\text{C}}$ . With the exception of a  $6.8^\circ$  smaller Co-N(1)-C(16) angle in **7-cis** and the difference in stereochemistry at C(3), the bond distance and angle data for **7-cis** are very similar to those observed for **5-trans** (Table 3-1).



**Table 3-1.** Selected bond distances [ $\text{\AA}$ ] for complexes **5-trans**, **7-cis**, **8-cis**, and **9-cis**. (a) Two independent molecules in the unit cell.

<b>Cmpd No.:</b>	<b>5-trans</b>	<b>7-cis</b>	<b>8-cis<sup>a</sup></b>	<b>9-cis</b>
Co-O(1)	1.908(1)	1.909(2)	1.891(3) 1.897(3)	1.892(8)
Co-N(1)	1.917(1)	1.895(2)	1.911(4) 1.912(4)	1.915(1)
Co-C(1)	1.935(2)	1.928(3)	1.952(4) 1.944(4)	1.938(2)
C(1)-C(2)	1.345(2)	1.353(2)	1.337(7) 1.348(7)	1.351(2)
C(2)-C(3)	1.523(2)	1.527(3)	1.517(6) 1.529(6)	1.519(2)
C(3)-N(1)	1.503(2)	1.504(3)	1.500(5) 1.497(6)	1.505(2)
N(1)-O(1)	1.388(2)	1.387(2)	1.391(4) 1.386(4)	1.391(2)

**Table 3-2.** Selected angles [°] for complexes **5-trans**, **7-cis**, **8-cis**, and **9-cis**. (a)  
Two independent molecules in the unit cell.

<b>Cmpd No.:</b>	<b>5-trans</b>	<b>7-cis</b>	<b>8-cis<sup>a</sup></b>	<b>9-cis</b>
Co(1)-C(1)-C(2)	117.71(12)	117.70(18)	118.8(3) 119.0(3)	118.3(1)
C(1)-C(2)-C(3)	112.10(14)	112.4(2)	113.2(4) 112.8(4)	113.0(1)
C(2)-C(3)-N(1)	109.96(13)	109.4(2)	109.3(3) 108.9(3)	109.6(1)
Co(1)-O(1)-N(1)	69.09(7)	68.06(11)	69.3(2) 69.2(2)	69.43(7)
C(3)-N(1)-C(16)	115.7(1)	117.4(2)	119.4(3) 119.1(3)	116.1(1)
Co(1)-N(1)-O(1)	68.4(1)	69.2(1)	67.8(2) 68.1(2)	67.71(6)
Co(1)-N(1)-C(3)	115.7(1)	113.43(14)	115.8(2) 116.3(3)	114.57(9)
Co(1)-N(1)-C(16)	127.6(1)	120.8(1)	117.8(3) 117.4(3)	121.64(9)
O(1)-N(1)-C(3)	110.5(1)	112.9(2)	108.8(3) 108.8(3)	112.8(1)
N(1)-Co(1)-C(1)	84.15(6)	83.90(10)	82.6(2) 82.6(2)	83.20(5)
N(1)-Co(1)-O(1)	42.6(1)	42.8(1)	42.9(1) 42.7(1)	42.86(5)
C(13)-C(3)-N(1)-C(16)	-57.69(0.17)	72.51(0.25)	85.2(4) 84.6(9)	-79.7(1)
C(13)-C(3)-N(1)-O(1)	172.95(0.12)	-62.80(0.23)	-86.5(4) 49.5(4)	55.3(1)

Surprisingly, dissolution of a crystalline sample of **7-cis** in  $\text{CDCl}_3$  gave a mixture of both the **7-cis** and **7-trans** isomers. It is not known whether **7-trans** reformed from a pure solid-state sample of **7-cis** through rapid re-equilibration, or whether both compounds co-crystallized. Co-crystallization would imply that a careful screening might yield a crystallographic analysis of the **7-trans** stereoisomer, which would be quite useful in elucidating the cause of diastereomerism and selectivity in the course of these reactions. It might also be possible to separate crystals of the two isomers by the “method of Pasteur,” however visual inspection of the crystalline sample did not reveal two different crystalline habits or morphologies.<sup>17</sup>

In an effort to further elucidate the role of sterics on the diastereoselectivity of *C*-nitroso compounds, the reactivity of cobaltacyclobutene **1** with *o*-nitrosotoluene was investigated. The exclusive formation of **5-trans** from 2-methyl-2-nitrosopropane, coupled with the formation of both *cis* and *trans* stereoisomers in the reaction of the relatively smaller nitrosobenzene suggests that increased bulk favors formation of the *trans* product. When metallacyclobutene **1** (0.17 mmol) was heated in the presence of *o*-nitrosotoluene (0.93 mmol) at 100 °C in toluene (50 mL), followed by chromatographic workup, product **8-cis** was formed in 95% crude yield. Product analysis by <sup>1</sup>H NMR spectroscopy indicated formation of a major product – identified as **8-cis** by comparison to **7-cis** (Table 3-7). In addition to the major product, two partial sets of proton resonances were identified that may indicate



formation of an **8-trans** isomer (by comparison to established trends), as well as a second unidentified complex. The **8-trans** isomer existed in solution in a 36:1 ratio relative to **8-cis**, while the second unidentified product was present in a 30:1 ratio.

Hexane diffusion into a concentrated solution of **8-cis** in chloroform provided a crystalline sample that permitted an X-ray diffraction analysis, which confirmed the structural assignment and the *syn* relationship of the ethyl ester and the oxametallaziridine ring. As shown in Tables 3-1 and 3-2, the structural parameters of **8-cis** are very similar to those found for **5-trans** and **7-cis**. In addition, dissolution of crystals of **8-cis** contained trace impurities of the two minor complexes formed in the course of the reaction – in like fashion to the solid-state sample of **7-cis** subjected to crystallographic analysis. Again, these impurities may have co-crystallized, or they may be in equilibrium with the parent complex.

As part of an effort to expand the scope of the reaction between metallacyclobutenes and *C*-nitroso compounds, and also in consideration of the potential elaboration of organic molecules for use in drug discovery and synthesis,<sup>18</sup> the reaction of 1,3-difluoro-2-nitroso-benzene with cobaltacyclobutene **1** was studied. A solution of **1** (125 mg, 0.18 mmol), one equivalent of 1,3-difluoro-2-nitroso-benzene (26 mg, 0.18 mmol), and toluene (50 mL) were sealed in a reaction flask and then heated at 70 °C for 3 h, followed by chromatographic workup in air to afford **9-cis** and **9-trans** as a dark blue air-stable

solid in 33.2% yield. Analysis by NMR spectroscopy ( $\text{CDCl}_3$ ) was more ambiguous in comparison to the previous *C*-nitroso products, as compounds **9** did not show characteristic peaks near  $\delta$  4.5 ( $\text{CHCO}_2\text{Et}$ ) and 5.0 ( $\text{C}_5\text{H}_5$ ) for the *cis* complex, or peaks near  $\delta$  4.0 ( $\text{C}_5\text{H}_5$ ) and 5.0 ( $\text{CHCO}_2\text{Et}$ ) for the *trans* product (Table 3-7). What was observed was a set of peaks at  $\delta$  4.66 ( $\text{C}_5\text{H}_5$ ) and 4.73 ( $\text{CHCO}_2\text{Et}$ ) in a 6:1 ratio with a second set of peaks at  $\delta$  4.86 ( $\text{C}_5\text{H}_5$ ) and 4.01 ( $\text{CHCO}_2\text{Et}$ ). As before, analytically pure, crystalline **9-cis** was obtained by slow diffusion of hexane into a concentrated  $\text{CHCl}_3$  solution of **9-cis** and **9-trans**. When crystalline **9-cis** was re-dissolved for spectroscopic characterization, the same ratio of 6:1 *cis* to *trans* product was observed. This ratio is the smallest of the three reactions of aryl *C*-nitroso compounds observed, and likely indicates that 1,3-difluoro-2-nitroso-benzene is very similar in steric bulk to the unsubstituted nitrosobenzene derivative.<sup>19</sup>

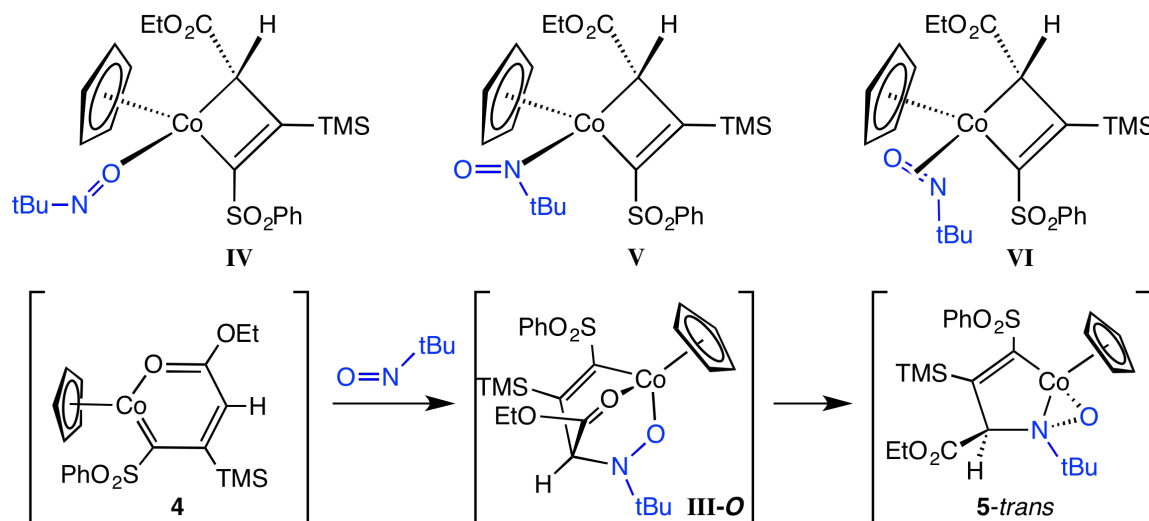
The chemical shift perturbations mentioned previously are attributable to the pronounced through-space effect of fluorine atoms on the chemical shifts of hydrogen.<sup>20</sup> Although it is safe to assume that the N(1)-C(16) bond rotates freely in solution, there are close chemical contacts between the proton on C(3) and one of the *o*-fluorine atoms on the nitrogen phenyl substituent (2.668 Å) in the crystal structure of **9-cis**, as well as between this same fluorine and two ring hydrogens on the cyclopentadienyl ring (2.635 and 3.383 Å). Steric effects are unlikely to be the cause of this chemical shift perturbation as fluorine atoms are

comparable in size to hydrogen atoms (the hydrogen atom van der Waals radius is 1.10 Å and the fluorine atom van der Waals radius is 1.46 Å).<sup>21</sup>

In addition to the reactions of *C*-nitroso compounds with metallacyclobutene **1**, the reactions of *N*-nitroso compounds were also briefly probed. In an exploratory set of NMR-scale reactions, the cobaltacyclobutene compound **1** was heated in a sealed NMR tube with *N*-nitrosopyrrolidine, and separately, with the diazomethane generator *N*-nitroso-*N*-methyl-*p*-toluenesulfonamide (Diazald®). Under the conditions employed (CDCl<sub>3</sub>, 70 °C), **1** failed to evince any reactivity toward these two compounds, which is consistent with literature results that show a lack of [4 + 2] cycloadditions with *N*-nitroso compounds.<sup>22</sup> As was described previously (Chapter 3), the vinylcarbene and oxametallabenzene intermediates **3** and **4** may require a sufficient degree of electronic activation in their dienophile and heterodienophile reaction partners in order to undergo reaction. In consideration of the reactants' frontier molecular orbitals, these heterodienophiles might be insufficiently matched in terms of their LUMO energy level with the participating HOMO of an intermediate such as **3** or **4** to participate in a 'normal' electron demand Diels-Alder reaction. *N*-nitroso compounds – which have an electron-donating substituent immediately attached to the reactive moiety – might be unreactive toward an electron-rich diene such as **3** or **4**.

In the reactions of cobaltacyclobutene **1** with nitroso compounds, the available data do not allow us to distinguish between a traditional metallacycle

insertion mechanism, involving intermediates such as **IV-VI**, from a [4 + 2] cycloaddition reaction involving the nitroso compound and intermediate **4** (Scheme 3-4).<sup>23</sup>



**Scheme 3-4.** Mechanistic speculation for the formation of **5-trans** from **1** and *C*-nitroso reagents.

Speculatively, loss of phosphine and coordination by the *C*-nitroso reagent could be accomplished via nitrogen, oxygen, or both nitrogen and oxygen, as depicted (*vide supra*), followed by regioselective insertion into the Co-C(3) sp<sup>3</sup>-hybridized bond. Alternatively, the nitroso compound could approach an intermediate such as **4** in a regio- and stereoselective fashion to give a Diels-Alder-like transition state, with the cyclopentadienyl ring providing steric shielding and preventing the formation of a structure such as **TS-N-endo** or **TS-N-exo** (Figure 3-5). *A priori*, the steric bulk of the 2-methyl-2-nitrosopropane would also appear to disfavor a transition state in which the *tert*-butyl group of the nitroso

adduct is *syn* with the trimethylsilyl substituent of the metallacycle, such as in transition TS-*O-endo* (Figure 3-5).

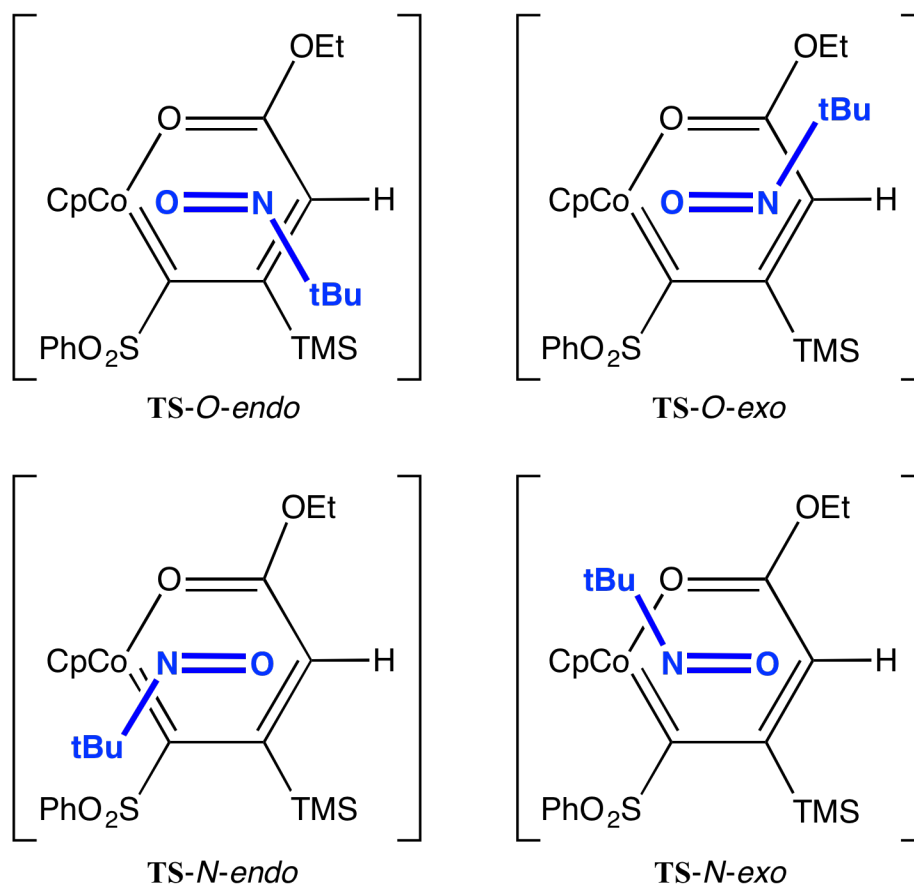


**Figure 3-5.** Possible transition state structures arising from intermediate **4**.

In an effort to explain the diastereoselectivity of these reactions, it was thought that perhaps a careful scrutiny of the crystal structures might yield some insight. As such, a number of potentially useful observations were brought to mind: (1) across the plane of the five-membered ring formed by Co-C(1)-C(2)-C(3)-N(1), seven different functional groups are extant (Cp, O, NR, H, CO<sub>2</sub>Et, TMS, SO<sub>2</sub>Ph), each of which might contribute some level of steric pressure; (2) that among these groups, the cyclopentadienyl group, trimethylsilyl, and the alkyl

or aryl substituents on nitrogen present bilaterally, whereas the phenyl sulfone, ethyl ester, and oxametallaziridine all fall on one side or the other of the five-membered ring; (3) finally, some combinations of these groups would likely render the product sterically inaccessible and thermodynamically unstable.

The reaction of **1** with 2-methyl-2-nitrosopropane was completely selective to give the **5-trans** product, and examination of the crystal structure indicates a sterically congested system. The ethyl ester substituent is sandwiched between the bulky trimethylsilyl and *tert*-butyl groups on the C(2) and N(1) ring atoms, respectively, and is located trans to the oxametallaziridine ring oxygen. Inspection of the space-filling model for this complex suggests that a cis arrangement of ethyl ester and the oxametallaziridine ring oxygen might be sterically inaccessible (Figure 3-6).

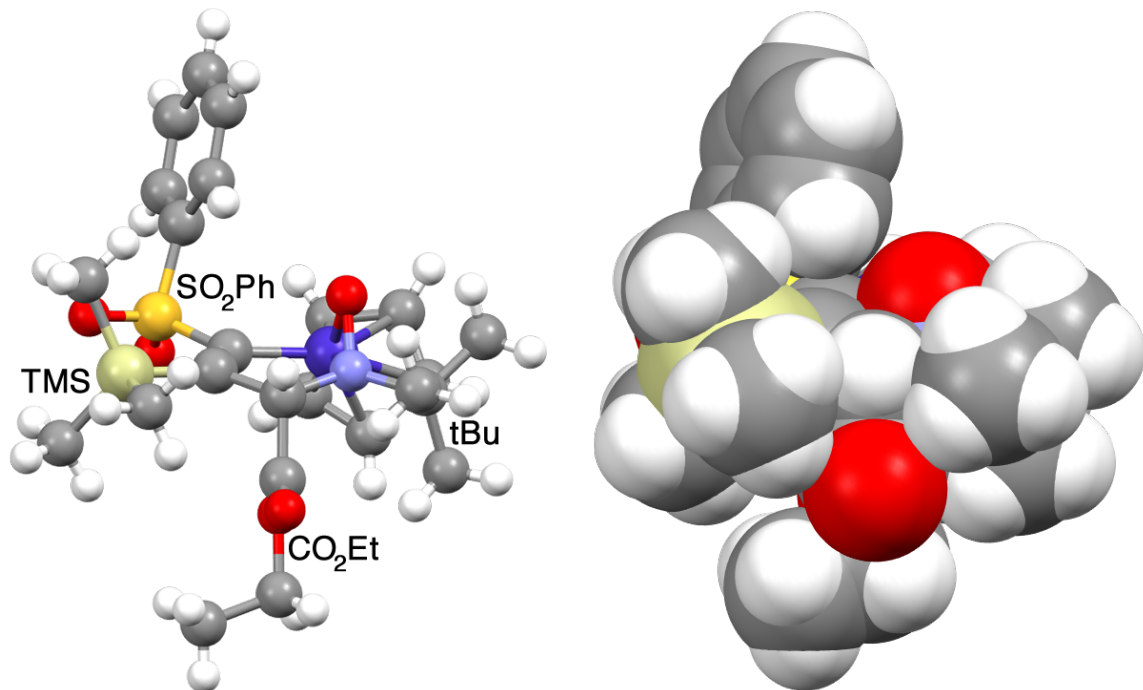
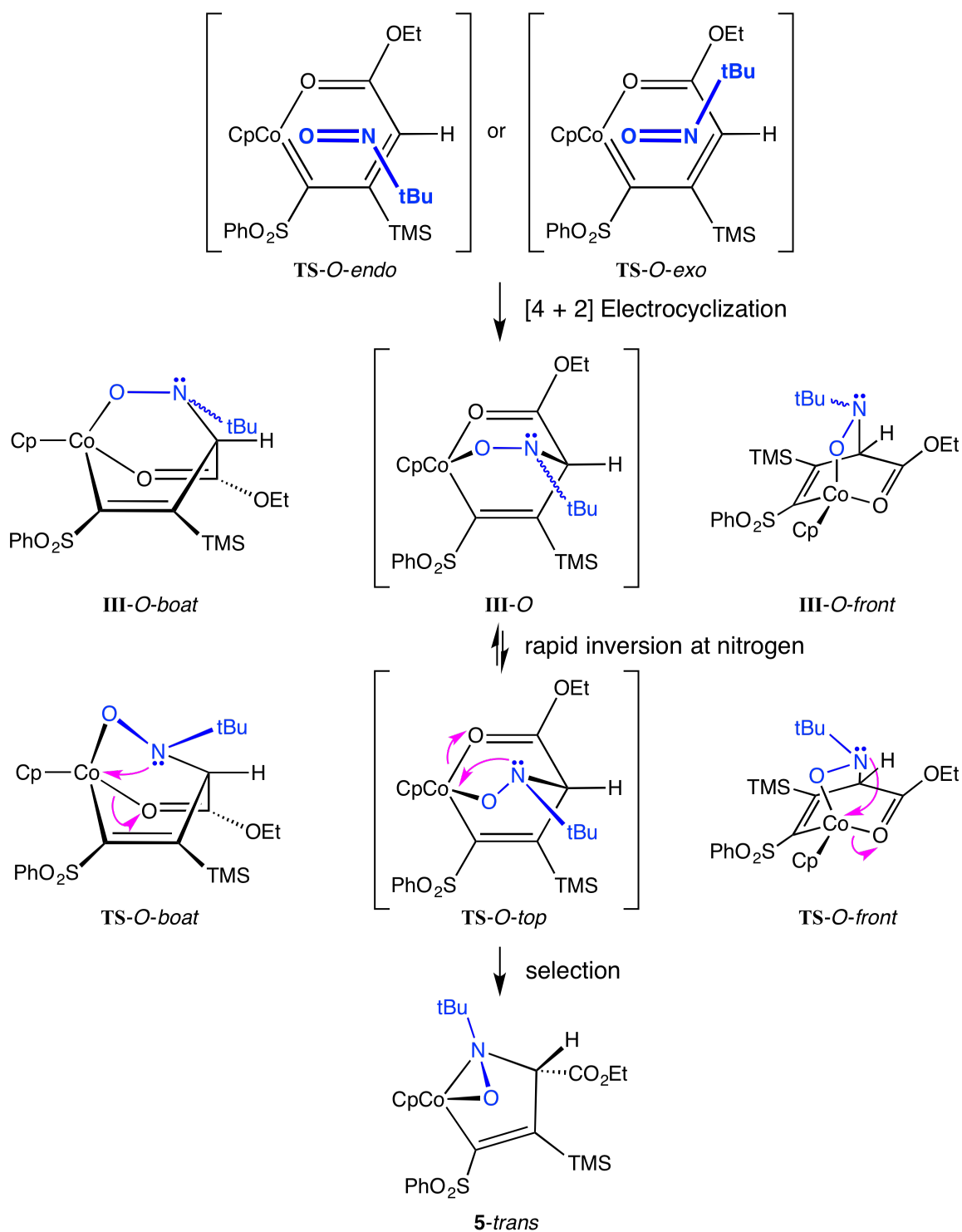


**Figure 3-6.** Ball-and-Stick and Spacefill representations of **5-trans**. An orientation with both the ethyl ester (in red; bottom) and the oxametallaziridine ring oxygen (in red, top) on the same face of the five-membered ring is likely inaccessible.

Based on these observations it was postulated that the diastereoselectivity observed in these nitroso reactions might be thermodynamic rather than kinetic in nature. Thermodynamic control of reactivity would imply that product formation is reversible under the reaction conditions. To our knowledge, such reversibility would be the only example of a retro-metalla-hetero-Diels-Alder. In addition, the presence of two products in the reactions of aryl *C*-nitroso reagents with **1** both before and after recrystallization is consistent with rapid equilibration upon dissolution of the crystallized product – although not definitively conclusive (for  $^1\text{H}$  NMR spectra, see Figure 3-11, Figure 3-13, and Figure 3-14).

Mechanistically, metallacyclobutene **1** may react with unsaturated substrates through an electrocyclization reaction in which it first dissociates  $\text{PPh}_3$  to give an  $\eta^1$ - or  $\eta^3$ -vinylcarbene **3**, which could rearrange to give oxametallabenzene **4** (Scheme 3-1). The oxametallabenzene might also form directly upon loss of phosphine. From either **3** or **4**, a Diels-Alder cycloaddition reaction would generate an intermediate type **III-O**,<sup>24</sup> which is formally  $\kappa^2$ -(C,O)- $\eta^1$ -(O) (Scheme 3-3). From such an intermediate, nitrogen could coordinate to the cobalt metal center in an associative (cyclopentadienyl ring-slippage) or  $\text{S}_{\text{N}}2$ -type process, displacing the coordinated ester oxygen to form the observed product (Scheme 3-5). Alternatively, the ester oxygen could dissociate from cobalt to form a 16-electron intermediate, followed by nitrogen coordination. Importantly, the configuration at nitrogen during the ring-closure step determines product stereochemistry.





**Scheme 3-5.** Possible mechanism for product selection and formation. III-*O* and TS-*O-top* are shown from two additional perspectives for clarity.

For instance, with 2-methyl-2-nitrosopropane, product formation could occur via either *TS-O-endo* or *TS-O-exo* (Scheme 3-5). From a metallacyclohexene intermediate **III-O**, as the nitrogen lone pair moves toward coordination with the metal to form the oxametallaziridine ring, the  $\kappa^1$ -oxygen from the nitroso moiety is displaced either toward the side of the ethyl ester or the hydrogen atom on C(3). For the *tert*-butyl nitrosoalkane, coordination from nitrogen gives the **5-trans** product when the substituent on nitrogen and the ethyl ester are *anti* – despite having an *endo* configuration in which the *tert*-butyl group and the trimethylsilyl group are *syn* (*TS-O-endo*; Figure 3-5). When the *tert*-butyl substituent on nitrogen is *syn* to the ethyl ester, product **5-cis** either fails to form due to steric constraints, or is formed as a thermodynamically unstable species. Nitrogen either fails to coordinate to the metal, or de-coordinates and the molecular species returns to a type **III-O** intermediate. From a (*N,O*)-metallacyclohexene type intermediate such as **III-O**, nitrogen inversion should be energetically accessible, which will epimerize the substituent on nitrogen as well as the lone pair, and allow access to a form that can lead to stable product.<sup>25</sup> Product selection would thus occur via nitrogen epimerization as an equilibrating process through a type **III-O** intermediate, giving a mixture of two products when the relative difference in energies for the *cis* and *trans* isomers is small. For the particular case of **1** with 2-methyl-2-nitrosopropane, this equilibrium lies on the side of the *trans* product exclusively, but for cases such as nitrosobenzene

derivatives, this mechanism could account for the formation of both cis and trans products.

Although the mechanism proposed above is merely hypothetical, it does account for the empirical observations for this nitroso adduct system, *a posteriori*. *In silico* analysis might provide supporting evidence for the above proposal in the form of relative energies for the cis and trans products, as well as in the availability of energetically accessible intermediates and transition states. In addition, the pathways suggested above led to the supposition that the nitroso adducts formed from the reaction of C-nitroso reagents with **1** could potentially be used to access an intermediate – free from trapping phosphine – that would lead to products with unsaturated substrates typically only available from thermally forced conditions ( $\geq 60$  °C). Regardless of the mechanism, it is becoming clear that, for the late-metal metallacyclobutene **1**, one-atom addends (CO, carbenes, and isocyanides)<sup>13</sup> exhibit selective coupling at the Co-C(1)  $sp^2$  bond, whereas two-atom cycloaddends (alkenes,<sup>12</sup> nitroso compounds, and possibly alkynes<sup>13c</sup>) exhibit selective coupling at the Co-C(3)  $sp^3$  bond. It is anticipated that follow up studies may successfully extend this novel nitroso reaction chemistry to acyclic late-metal alkyl and vinyl complexes.

## References.

1. Complexes with the connectivity shown for **I** and **II** are also referred to in the literature as “hydroxylaminato”, “hydroxylamino”, “nitroxide”, and “nitroxyl” complexes. The last two terms typically are used for paramagnetic complexes. Nitroxyl also refers to  $\text{HN}=\text{O}$ .
2. For leading references to early-metal  $\kappa^1$ -hydroxylamido complexes: (a) Kraft, B. M.; Huang, K.-W.; Cole, A. P.; Waymouth, R. M. *Helv. Chim. Acta* **2006**, *89*, 1589. (b) Rehder, D.; Jaitner, P. *J. Organomet. Chem.* **1987**, *329*, 337. (c) Jochmann, P.; Stephan, D. W. *Chem. Commun.* **2014**, *50*, 8395. (d) Davies, H. O.; Peek, B.; Rochford, J.; O'Brien, P.; Afzaal, M.; Murin, C.; Dawson, C. P. *Inorg. Chem. Commun.* **2014**, *44*, 180. (e) Reis, S. G.; del Águila-Sánchez, M. A.; Guedes, G. P.; Ferreira, G. B.; Novak, M. A.; Speziali, N. L.; López-Ortiz, F.; Vaz, M. G. F. *Dalton Trans.* **2014**, *43*, 14889.
3. For leading references to early-metal  $\eta^2$ -hydroxylamido complexes: (a) Smee, J. J.; Epps, J. A.; Teissedre, G.; Maes, M.; Harding, N.; Yang, L.; Baruah, B.; Miller, S. M.; Anderson, O. P.; Willsky, G. R.; Crans, D. C. *Inorg. Chem.* **2007**, *46*, 9827. (b) Dove, A. P.; Xie, X.; Waymouth, R. M. *Chem. Commun.* **2005**, 2152. (c) Wieghardt, K.; Quilitzsch, U.; Nuber, B.; Weiss, J. *Angew. Chem., Int. Ed.* **1978**, *17*, 351. (d) Smee, J. J.; Epps, J. A.; Ooms, K.; Bolte, S. E.; Polenova, T.; Baruah, B.; Yang, L.; Ding, W.; Li, M.; Willsky, G. R.; la Cour, A.; Anderson, O. P.; Crans, D. C. *J. Inorg. Biochem.* **2009**, *103*, 575. (e) Pedersen, S. F.; Dewan, J. C.; Eckman, R. R.; Sharpless, K. B. *J. Am. Chem. Soc.* **1987**, *109*, 1279. (f) Willner, A.; Niemeyer, J.; Mitzel, N. W. *Dalton Trans.* **2009**, 4473.
4. Late-metal  $\kappa^1$ -nitroxyl complexes often display interesting magnetic properties: (a) Sessoli, R. *Angew. Chem., Int. Ed.* **2008**, *47*, 5508, and references therein. (b) Ishii, N.; Okamura, Y.; Chiba, S.; Nogami, T.; Ishida, T. *J. Am. Chem. Soc.* **2008**, *130*, 24. (c) Demir, S.; Jeon, I.-R.; Long, J. R.; Harris, T. D. *Coord. Chem. Rev.* **2015**, *289-290*, 149.
5. For leading references to late-metal  $\eta^2$ -hydroxylamido complexes prepared from nitroxyl radicals: (a) Mindiola, D. J.; Waterman, R.; Jenkins, D. M.; Hillhouse, G. L. *Inorg. Chim. Acta* **2003**, *345*, 299. (b) Laugier, J.; Latour, J. M.; Caneschi, A.; Rey, P. *Inorg. Chem.* **1991**, *30*, 4474. (c) Fullmer, B. C.; Fan, H.; Pink, M.; Caulton, K. G. *Inorg. Chim. Acta* **2011**, *369*, 49. (d) Isrow, D.; Captain, B. *Inorg. Chem.* **2011**, *50*, 5864. (e) Zhu, Z.; Fetting, J. C.; Olmstead, M. M.; Power, P. P. *Organometallics* **2009**, *28*, 2091. (f) Ito, M.; Matsumoto, T.; Tatsumi, K. *Inorg. Chem.* **2009**, *48*, 2215. (g) Wright, A. M.; Zaman, H. T.; Wu, G.; Hayton, T. W. *Inorg. Chem.* **2013**, *52*, 3207.

6. For leading references to late-metal  $\eta^2$ -hydroxylamidos prepared from hydroxylamines: (a) Vogel, S.; Huttner, G.; Zsolnai, L.; Emmerich, C. *Z. Naturforsch.* **1993**, *48b*, 353. (b) Middleton, A. R.; Thornback, J. R.; Wilkinson, G. *J. Chem. Soc., Dalton Trans.* **1980**, 174. Belock, C. W.; Çetin, A.; Barone, N. V.; Ziegler, C. J. *Inorg. Chem.* **2008**, *47*, 7714.
7. For a late-metal  $\eta^2$ -hydroxylamido complex prepared from a metal nitrosyl complex: Kura, S.; Kuwata, S.; Ikariya, T. *Angew. Chem., Int. Ed.* **2005**, *44*, 6406.
8. For representative examples of crystallographically-characterized hydroxylamido complexes: (a) Chen, S.-J.; Zhang, J.; Yu, X.; Bu, X.; Chen, X.-T.; Xue, Z.-L. *Inorg. Chem.* **2010**, *49*, 4017. (b) Isrow, D.; Captain, B. *Inorg. Chem.* **2011**, *50*, 5864. (c) Ovcharenko, V. I.; Lanfranc de Panthou, F.; Pervukhina, N. V.; Reznikov, V. A.; Rey, P.; Sagdeev, R. Z. *Inorg. Chem.* **1995**, *34*, 2263.
9. Nitroso insertions into early-transition-metal-carbon bonds have been observed: (a) Erker, G.; Humphrey, M. G. *J. Organomet. Chem.* **1989**, *378*, 163. (b) Doxsee, K. M.; Juliette, J. J. J.; Weakley, T. J. R.; Zientara, K. *Inorg. Chim. Acta* **1994**, *222*, 305. (c) Nakamoto, M.; Tilley, T. D. *Organometallics* **2001**, *20*, 5515. (d) Cummings, S. A.; Radford, R.; Erker, G.; Kehr, G.; Fröhlich, R. *Organometallics* **2006**, *25*, 839.
10. The reactions of nitroso compounds with aromatic iridacycles give addition products without ring expansion: (a) Bleeke, J. R. *Acc. Chem. Res.* **2007**, *40*, 1035. (b) Bleeke, J. R. *Acc. Chem. Res.* **1991**, *24*, 271. (c) Bleeke, J. R.; Behm, R.; Xie, Y.-F.; Chiang, M. Y.; Robinson, K. D.; Beatty, A. M. *Organometallics* **1997**, *16*, 606. (d) Bleeke, J. R.; Blanchard, J. M. B. *J. Am. Chem. Soc.* **1997**, *119*, 5443. (e) Bleeke, J. R.; Blanchard, J. M. B.; Donnay, E. *Organometallics* **2001**, *20*, 324. (f) Bleeke, J. R.; Hinkle, P. V.; Rath, N. P. *Organometallics* **2001**, *20*, 1939.
11. Portions of this chapter were previously communicated: Holland, R. L.; O'Connor, J. M. *Organometallics*, **2009**, *28*, 394.
12. Complex **2** was formed as both endo and exo products: Holland, R. L.; Bunker, K. D.; Chen, C. H.; DiPasquale, A. G.; Rheingold, A. L.; Baldrige, K. K.; O'Connor, J. M. *J. Am. Chem. Soc.* **2008**, *130*, 10093.
13. (a) O'Connor, J. M.; Ji, H.; Iranpour, M.; Rheingold, A. L. *J. Am. Chem. Soc.* **1993**, *115*, 1586. (b) O'Connor, J. M.; Ji, H.-L.; Rheingold, A. L. *J. Am. Chem. Soc.* **1993**, *115*, 9846. (c) O'Connor, J. M.; Fong, B. S.; Ji, H.-L.; Hiibner, K.; Rheingold, A. L. *J. Am. Chem. Soc.* **1995**, *117*, 8029. (d) O'Connor, J. M.; Chen, M.-C.; Frohn, M.; Rheingold, A. L.; Guzei, I. A. *Organometallics* **1997**, *16*, 5589.

(e) O'Connor, J. M.; Chen, M.-C.; Rheingold, A. L. *Tetrahedron Lett.* **1997**, *38*, 5241.

14. A model structure for intermediate **4**, ( $\eta^5\text{-C}_5\text{H}_5$ )Co[ $\kappa^2\text{-(C,O)-C(SO}_2\text{Me)C(SiH}_3\text{)CH(CO}_2\text{Me)}$ ], has been studied using quantum-mechanical methods, and the electrostatic potential map indicates relatively high charge density at the CH ring carbon.<sup>12</sup>

15. The reactions of nitroso compounds with early-transition-metal metallacyclobutenes also leads to insertion into the metal-carbon ( $\text{sp}^3$ ) bond, but the ring-expanded product does not engage in metal-nitrogen bonding.<sup>8b</sup>

16. O'Connor, J. M.; Bunker, K. D. *Organometallics* **2003**, *22*, 5268.

17. (a) Fox, A. R.; Clough, C. R.; Piro, N. A.; Cummins, C. C. *Angew. Chem. Int. Ed.* **2007**, *46*, 973. (b) Geison, G. L. *The Private Life of Louis Pasteur*, Princeton University Press, Princeton **1995**.

18. (a) Montgomery, J. A.; Hewson, K. *J. Am. Chem. Soc.* **1957**, *79*, 4559. (b) Sun, S.; Adejare, A. *Curr. Top. Med. Chem.* **2006**, *6*, 1457.

19. O'Hagan, D.; Rzepa, H. S. *Chem. Commun.* **1997**, 645.

20. Abraham, R. J.; Warne, M. A.; Griffiths, L. *J. Chem. Soc., Perkin Trans. 2* **1997**, 2151.

21. Rowland, R. S.; Taylor, R. *J. Phys. Chem.* **1996**, *100*, 7384.

22. Hamer, J. *1,4-Cycloaddition Reactions, the Diels-Alder Reaction in Heterocyclic Syntheses*; Hamer, J., Ed. *Organic Chemistry: A Series of Monographs Vol. 8*, Academic Press, New York **1967**.

23. We are also unable to rule out associative mechanisms. Attempts at kinetic studies were unsuccessful due to the reaction of the Nitroso compounds with triphenylphosphine.

24. (a) Kresze, G.; Firl, J. *Fort. Chem. Forsch.* **1969**, *11*, 245. (b) Kresze, G.; Saitner, H.; Firl, J.; Kosbahn, W. *Tetrahedron* **1971**, *27*, 1941.

25. Katritzky, A. R.; Patel, R. C.; Riddell, F. G. *Angew. Chem. Int. Ed. Engl.* **1981**, *20*, 521.

Chapter 3 is adapted from **R. L. Holland**, J. M. O'Connor, "Nitroso Compounds Serve as Precursors to Late-Metal  $\eta^2$ -(N,O)-Hydroxylamido Complexes" *Organometallics*, **2009**, *28*, 394-396. Copyright 2009 American Chemical Society. Permission to use copyrighted images and data in the manuscript was also obtained from J. M. O'Connor. The dissertation author is the first author of this paper.

### **Experimental.**

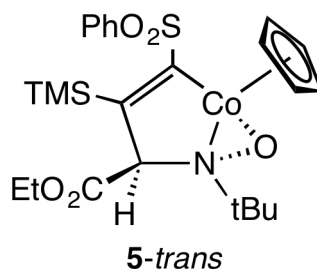
**General Data.** All manipulations were performed under an atmosphere of nitrogen or in a Vacuum Atmospheres inert atmosphere box equipped with a Dri-Train MO 40-1 purifier, unless otherwise noted. NMR spectra were recorded on a Varian Mercury 400 ( $^1\text{H}$ , 400 MHz;  $^{31}\text{P}$ , 163MHz;  $^{13}\text{C}$  100.7 MHz), or a Varian UNITY 500 ( $^1\text{H}$ , 500MHz) spectrometer. Chemical shifts were referenced to residual protio-solvent or carbon-solvent signal. IR Spectra were recorded on a Nicolet Avatar 360 FT-IR. Toluene was distilled over sodium/benzophenone ketyl under an atmosphere of nitrogen. Deuterated chloroform was distilled over  $\text{CaH}_2$  under an atmosphere of nitrogen. Nitrosobenzene, 2-methyl-2-nitrosopropane, 2-methyl-nitrosotoluene, and 1,3-difluoro-2-nitroso-benzene were purchased from Aldrich and used as received.

$(\eta^5\text{-C}_5\text{H}_5)\text{Co}[\kappa^2\text{-(C,O)-}\eta^1\text{-(M)-CH(SO}_2\text{Ph)=C(TMS)CH(CO}_2\text{Et)N}^i\text{(Bu)O}]$  (*5-trans*).

In the dry box, a 50-mL thick-walled reaction tube equipped with a threaded Teflon plug and O-ring, was charged with **1** (245.2 mg, 0.35 mmol), 2-methyl-2-nitrosopropane dimer (115.8 mg, 1.33 mmol) and toluene (25 mL). The flask was sealed and the solution was heated at 70 °C for 4 h. The reaction mixture was chromatographed on silica gel. Eluting with 35% EtOAc/hexanes led to collection of a burgundy/brown band from which *5-trans* was obtained in 83.2% yield. Analytically pure *5-trans* was obtained by slow diffusion of hexanes into a concentrated  $\text{CHCl}_3$  solution of *5-trans*. For *5-trans*: mp: 152.9-153.6 °C. IR (KBr, thin film): 1746 (C=O)  $\text{cm}^{-1}$ .  $^1\text{H}$  NMR ( $\text{CDCl}_3$ ):  $\delta$  0.15 (s, 9H,  $\text{Si}(\text{CH}_3)_3$ ), 1.35 (t, 3H,  $J = 7.03$  Hz,  $\text{CH}_3$ ), 1.50 (s, 9H,  $\text{C}(\text{CH}_3)_3$ ), 4.08 (s, 1H,  $\text{CHCO}_2\text{Et}$ ), 4.22 (m, 2H,  $\text{CH}_2\text{CH}_3$ ), 4.93 (s, 5H,  $\text{C}_5\text{H}_5$ ), 7.53 (m, 3H,  $m,p\text{-C}_6\text{H}_5\text{SO}_2$ ), 7.87 (m, 2H,  $o\text{-C}_6\text{H}_5\text{SO}_2$ ).  $^{13}\text{C}\{^1\text{H}\}$  NMR ( $\text{CDCl}_3$ ):  $\delta$  2.89 ( $\text{Si}(\text{CH}_3)_3$ ), 14.14 ( $\text{CO}_2\text{CH}_3$ ), 28.56 ( $\text{C}(\text{CH}_3)_3$ ), 61.77 ( $\text{CO}_2\text{CH}_2\text{CH}_3$ ), 68.03 ( $\text{C}[(\text{CH}_3)_3]$ ), 80.57 ( $\text{CHCO}_2\text{Et}$ ), 83.48 ( $\text{C}_5\text{H}_5$ ), 125.70 ( $o\text{-SO}_2\text{Ph}$ ), 128.87 ( $m\text{-SO}_2\text{Ph}$ ), 131.69 ( $p\text{-SO}_2\text{Ph}$ ), 144.68 (*ipso*- $\text{SO}_2\text{Ph}$ ), 157.83 ( $\text{C}[\text{Si}(\text{CH}_3)_3]$ ), 168.03 ( $\text{C}[\text{SO}_2\text{Ph}]$ ), 180.50 ( $\text{CO}_2\text{Et}$ ). 2D-HSQC-NMR ( $\text{CDCl}_3$ ) provided the following  $^1\text{H}$ - $^{13}\text{C}$  correlations ( $^1\text{H}$ ,  $\delta$ :  $^{13}\text{C}$ ,  $\delta$ ): (0.15: 2.89), (1.35: 14.14), (1.50: 28.56), (4.08: 80.57), (4.22: 61.77), (4.93: 83.48), (7.53: 128.87), (7.53: 131.69), (7.87: 125.70). 2D-HMBC-NMR ( $\text{CDCl}_3$ ) provided the following  $^1\text{H}$ - $^{13}\text{C}$  multiple bond correlations ( $^1\text{H}$ ,  $\delta$ :  $^{13}\text{C}$ ,  $\delta$ ): (0.15: 157.83), (1.35: 61.77), (1.50: 68.03), (4.08: 157.83, 168.03, 180.50), (7.53: 125.70, 128.87, 144.68), (7.87: 128.87, 131.69). HRMS(EI):  $m/z$  calcd for

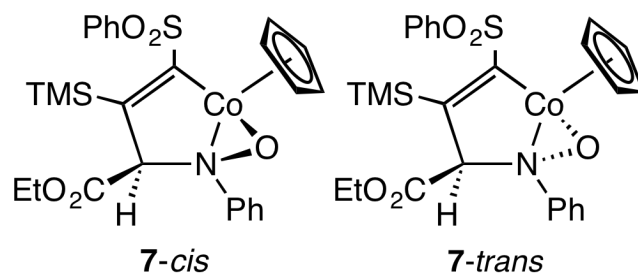


$C_{26}H_{30}CoNO_5SSi$ : 535.1262, obsd: 535.1253. Anal Calcd for  $C_{26}H_{30}CoNO_5SSi$ : C, 53.82%; H, 6.40%. Found: C, 53.71%; H, 6.57%.



$(\eta^5-C_5H_5)Co[\kappa^2-(C,O)-\eta^1-(N)-CH(SO_2Ph)=C(TMS)CH(CO_2Et)N(Ph)O]$  (**7-cis** and **7-trans**). In the dry box, a 50-mL thick-walled reaction tube equipped with a threaded Teflon plug and O-ring, was charged with **1** (263.1 mg, 0.37 mmol), nitrosobenzene (136.2 mg, 1.27 mmol) and toluene (25 mL). The flask was sealed and the solution was heated at 70 °C for 4 h. The reaction mixture was chromatographed on silica gel. Eluting with 35% EtOAc/hexanes led to collection of a dark blue band from which **7** was obtained in 70.9% yield as an 8:1 mixture of **7-cis**:**7-trans**. Analytically pure material was as obtained by slow diffusion of hexanes into a concentrated  $CHCl_3$  solution of **7-cis** and **7-trans**. For **7-cis** and **7-trans**: mp: 157.1-158.5 °C. IR (KBr, thin film): 1741 (C=O)  $cm^{-1}$ .  $^1H$  NMR ( $CDCl_3$ ):  $\delta$  0.11 (s, 9H,  $Si(CH_3)_3$ -*trans*), 0.21 (s, 9H,  $Si(CH_3)_3$ -*cis*), 1.05 (t, 3H,  $J = 7.15$  Hz,  $CH_3$ -*cis*), 1.11 (t, 3H,  $J = 7.18$  Hz,  $CH_3$ -*trans*), 3.90 (s, 1H,  $CHCO_2Et$ -*trans*), 4.00 (m, 2H,  $CH_2CH_3$ -*cis*), 4.07 (m, 2H,  $CH_2CH_3$ -*trans*), 4.48 (s, 5H,  $C_5H_5$ -*cis*), 4.78 (s, 5H,  $C_5H_5$ -*trans*), 5.23 (s, 1H,  $CHCO_2Et$ -*cis*), 7.34 (t, 3H  $J = 7.45$  Hz), 7.40 (m), 7.46 (m, broad), 7.55 (m, 2H), 7.92 (m, 2H).  $^{13}C\{^1H\}$  NMR ( $CDCl_3$ ):  $\delta$  2.30

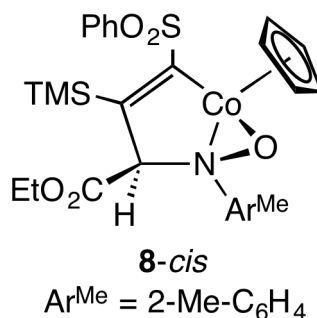
(Si(CH<sub>3</sub>)<sub>3</sub>-*cis*), 2.60 (Si(CH<sub>3</sub>)<sub>3</sub>-*trans*), 13.88 (CO<sub>2</sub>CH<sub>3</sub>-*trans*), 13.95 (CO<sub>2</sub>CH<sub>3</sub>-*cis*), 61.73 (CO<sub>2</sub>CH<sub>2</sub>CH<sub>3</sub>-*cis*), 61.95 (CO<sub>2</sub>CH<sub>2</sub>CH<sub>3</sub>-*trans*), 84.48 (C<sub>5</sub>H<sub>5</sub>-*trans*), 84.63 (C<sub>5</sub>H<sub>5</sub>-*cis*), 86.05 (CHCO<sub>2</sub>Et-*cis*), 88.71 (CHCO<sub>2</sub>Et-*trans*), 124.91, 125.68, 126.08, 127.22, 128.76, 128.90, 129.00, 129.40, 131.70, 145.12 (*ipso*-SO<sub>2</sub>Ph-*cis*), 153.17 (C[Si(CH<sub>3</sub>)<sub>3</sub>]-*cis*), 164.06, 165.50, 170.84 (CO<sub>2</sub>Et-*cis*). HRMS(EI): *m/z* calcd for C<sub>26</sub>H<sub>30</sub>CoNO<sub>5</sub>SSi: 555.0940, obsd: 555.0942. Anal Calcd for C<sub>26</sub>H<sub>30</sub>CoNO<sub>5</sub>SSi: C, 56.21%; H, 5.44%. Found: C, 55.82%; H, 5.80%.



**( $\eta^5$ -C<sub>5</sub>H<sub>5</sub>)Co[ $\kappa^2$ -(C,O)- $\eta^1$ -(M)-CH(SO<sub>2</sub>Ph)=C(TMS)CH(CO<sub>2</sub>Et)N(2-Me-C<sub>6</sub>H<sub>4</sub>)O]**

**(8-cis)**. In the dry box, a 100-mL thick-walled reaction tube equipped with a threaded Teflon plug and O-ring, was charged with **1** (118 mg, 0.17 mmol), *o*-nitrosotoluene (113 mg, 0.93 mmol) and toluene (50 mL). The flask was sealed and the solution was stirred at 100 °C for 70 m. The reaction mixture was chromatographed on silica gel. Eluting with 20% EtOAc/hexanes afforded **8-cis** as a dark blue air-stable solid in 95.2% crude yield. Analytically pure, crystalline **8-cis** was obtained by slow diffusion of hexane into a concentrated CHCl<sub>3</sub> solution of **8-cis**. For **8-cis**: mp: 182.3-183.4 °C. IR (KBr, thin film): 1743 (C=O) cm<sup>-1</sup>. <sup>1</sup>H NMR (CDCl<sub>3</sub>):  $\delta$  0.19 (s, 9H, Si(CH<sub>3</sub>)<sub>3</sub>), 1.15 (t, 3H, *J* = 7.20 Hz,

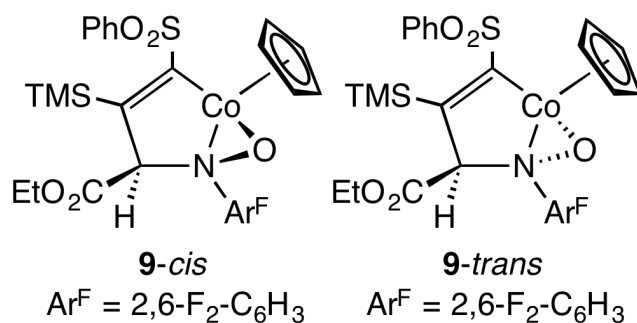
CO<sub>2</sub>CH<sub>2</sub>CH<sub>3</sub>), 2.85 (s, 3H, PhCH<sub>3</sub>), 4.06 (m, 2H, CH<sub>2</sub>CH<sub>3</sub>), 4.49 (s, 5H, C<sub>5</sub>H<sub>5</sub>), 4.92 (s, 1H, CHCO<sub>2</sub>Et), 7.20 (td, 1H,  $J_1 = 8$  Hz,  $J_2 = 1.2$  Hz, *p*-2-Me-C<sub>6</sub>H<sub>4</sub>NO), 7.32 (qt, 2H,  $J_1 = 8$  Hz,  $J_2 = 1.2$  Hz, *m*-2-Me-C<sub>6</sub>H<sub>4</sub>NO), 7.47 (dd, 1H,  $J_1 = 8$  Hz,  $J_2 = 1.2$  Hz, *o*-2-Me-C<sub>6</sub>H<sub>4</sub>NO), 7.57 (m, 3H, *o,p*-SO<sub>2</sub>Ph), 7.97 (m, 2H, *o*-SO<sub>2</sub>Ph). <sup>13</sup>C{<sup>1</sup>H} NMR (CDCl<sub>3</sub>): δ 2.22 (Si(CH<sub>3</sub>)<sub>3</sub>), 14.06 (CO<sub>2</sub>CH<sub>2</sub>CH<sub>3</sub>), 19.45 (PhCH<sub>3</sub>), 61.85 (CO<sub>2</sub>CH<sub>2</sub>CH<sub>3</sub>), 83.86 (CHCO<sub>2</sub>Et), 84.69 (C<sub>5</sub>H<sub>5</sub>), 121.24, 126.16, 126.80, 127.80, 128.95, 129.41, 131.74, 132.01, 145.07 (*ipso*-SO<sub>2</sub>Ph), 151.44 (C[Si(CH<sub>3</sub>)<sub>3</sub>]), 165.05, 165.72, 168.73 (CO<sub>2</sub>Et). HRMS(EI): *m/z* calcd for C<sub>27</sub>H<sub>32</sub>CoNO<sub>5</sub>SSi: 592.0995, obsd: 592.0997. Anal Calcd for C<sub>27</sub>H<sub>32</sub>CoNO<sub>5</sub>SSi: C, 56.93%; H, 5.66%. Found: C, 57.19%; H, 6.00%.



**( $\eta^5$ -C<sub>5</sub>H<sub>5</sub>)Co[ $\kappa^2$ -(C,O)- $\eta^1$ -(M)-CH(SO<sub>2</sub>Ph)=C(TMS)CH(CO<sub>2</sub>Et)N(2,6-F<sub>2</sub>-C<sub>6</sub>H<sub>3</sub>)O]**

**(9-cis and 9-trans)**. In the dry box, a 100-mL thick-walled reaction tube equipped with a threaded Teflon plug and O-ring, was charged with **1** (125 mg, 0.18 mmol), 1,3-difluoro-2-nitroso-benzene (26 mg, 0.18 mmol) and toluene (50 mL). The flask was sealed and the solution was stirred at 70 °C for 3 h. The reaction mixture was chromatographed on silica gel (20% EtOAc/hexanes) to afford **9-cis**

and **9-trans** as a dark blue air-stable solid in 33.2% crude yield. Analytically pure, crystalline **9-cis** and **9-trans** was obtained by slow diffusion of hexane into a concentrated  $\text{CHCl}_3$  solution of **9-cis** and **9-trans**. For **9-cis** and **9-trans**: mp 175.4-176.1 °C. IR (KBr, thin film): 1747 (C=O)  $\text{cm}^{-1}$ .  $^1\text{H}$  NMR ( $\text{CDCl}_3$ ):  $\delta$  0.12 (s, 9H,  $\text{Si}(\text{CH}_3)_3$ -*trans*), 0.19 (s, 9H,  $\text{Si}(\text{CH}_3)_3$ -*cis*), 1.18 (t, 3H,  $J = 7.18$  Hz,  $\text{CO}_2\text{CH}_2\text{CH}_3$ -*trans*), 1.21 (t, 3H,  $J = 7.18$  Hz,  $\text{CO}_2\text{CH}_2\text{CH}_3$ -*cis*), 4.01 (s, 1H,  $\text{CHCO}_2\text{Et}$ -*trans*), 4.14 (m, 2H,  $\text{CH}_2\text{CH}_3$ ), 4.66 (s, 5H,  $\text{C}_5\text{H}_5$ -*cis*), 4.73 (s, 1H,  $\text{CHCO}_2\text{Et}$ -*cis*), 4.86 (s, 5H,  $\text{C}_5\text{H}_5$ -*trans*), 6.96 (m, 2,6- $\text{F}_2$ - $\text{C}_6\text{H}_3$ -*cis*), 7.04 (m, 2,6- $\text{F}_2$ - $\text{C}_6\text{H}_3$ -*trans*), 7.15 (m, 2,6- $\text{F}_2$ - $\text{C}_6\text{H}_3$ ), 7.40 (m, 2,6- $\text{F}_2$ - $\text{C}_6\text{H}_3$ ), 7.55 (m, 2H, *o*- $\text{SO}_2\text{Ph}$ ), 7.94 (m, 3H, *m,p*- $\text{SO}_2\text{Ph}$ ).  $^{13}\text{C}\{^1\text{H}\}$  NMR ( $\text{CDCl}_3$ ):  $\delta$  2.23 ( $\text{Si}(\text{CH}_3)_3$ -*cis*), 2.55 ( $\text{Si}(\text{CH}_3)_3$ -*trans*), 13.88 ( $\text{CO}_2\text{CH}_2\text{CH}_3$ -*cis*), 13.89 ( $\text{CO}_2\text{CH}_2\text{CH}_3$ -*trans*), 62.46 ( $\text{CO}_2\text{CH}_2\text{CH}_3$ -*cis*), 84.25, 84.38 ( $\text{C}_5\text{H}_5$ -*cis*), 85.40 ( $\text{C}_5\text{H}_5$ -*trans*), 85.42 ( $\text{CHCO}_2\text{Et}$ ), 112.13, 112.33, 113.21, 113.42, 125.73, 126.15 (*o*- $\text{SO}_2\text{Ph}$ -*cis*), 128.97 (*m*- $\text{SO}_2\text{Ph}$ -*cis*), 129.48, 131.73 (*p*- $\text{SO}_2\text{Ph}$ -*cis*), 131.77, 145.05 (*ipso*- $\text{SO}_2\text{Ph}$ -*cis*), 152.99, 154.71, 155.62, 157.23, 162.98, 165.80, 170.40 ( $\text{CO}_2\text{Et}$ -*cis*). HRMS(EI):  $m/z$  calcd for  $\text{C}_{26}\text{H}_{28}\text{CoF}_2\text{NO}_5\text{SSi}$ : 614.0650, obsd: 614.0646. Anal Calcd for  $\text{C}_{26}\text{H}_{28}\text{CoF}_2\text{NO}_5\text{SSi}$ : C, 52.79%; H, 4.77%. Found: C, 52.62%; H, 5.27%.



**Reaction with *N*-nitrosopyrrolidine.** A J-Young style NMR tube was charged with **1** (3.2 mg, 45.0  $\mu\text{mol}$ ) and *N*-nitrosopyrrolidine (2  $\mu\text{L}$ , 21.7  $\mu\text{mol}$ ). The NMR tube was attached to a vacuum gas manifold and evacuated, and  $\text{CDCl}_3$  was transferred *in vacuo*. The reaction mixture was analyzed by  $^1\text{H}$  NMR spectroscopy ( $\text{CDCl}_3$ , 399.9 MHz) to obtain initial conditions, and then heated at 70  $^\circ\text{C}$  for 100 m. Subsequent analysis of the  $^1\text{H}$  NMR spectrum indicated formation of dinuclear cobalt complexes and no reactivity between **1** and *N*-nitrosopyrrolidine.

**Reaction with *N*-nitroso-*N*-methyl-*p*-toluenesulfonamide.** A J-Young style NMR tube was charged with **1** (8.7 mg, 12.2  $\mu\text{mol}$ ) and *N*-nitroso-*N*-methyl-*p*-toluenesulfonamide (3 mg, 14.0  $\mu\text{mol}$ ). The NMR tube was attached to a vacuum gas manifold and evacuated, and  $\text{CDCl}_3$  was transferred *in vacuo*. The reaction mixture was analyzed by  $^1\text{H}$  NMR spectroscopy ( $\text{CDCl}_3$ , 400.1 MHz) to obtain initial conditions, and then heated at 70  $^\circ\text{C}$  for 2 h. Subsequent analysis of the  $^1\text{H}$  NMR spectrum indicated formation of dinuclear cobalt complexes and no reactivity between **1** and *N*-nitroso-*N*-methyl-*p*-toluenesulfonamide.

**General Experimental for X-Ray Structure Determinations.** A single crystal with general dimensions of  $a \times b \times c$  was immersed in Paratone and placed on a Cryoloop. Data were collected on a Bruker SMART (APEX) CCD diffractometer, using a graphite monochromator with Mo  $K\alpha$  radiation ( $\lambda = 0.71073 \text{ \AA}$ ) at the defined temperature. The data were integrated using the Bruker SAINT software program and scaled using the SADABS software program. Solution by direct methods (SIR-2004) produced a complete heavy-atom phasing model consistent with the proposed structure. All non-hydrogen atoms were refined anisotropically by full-matrix least-squares (SHELXL-97). All hydrogen atoms were placed using a riding model. Their positions were constrained relative to their parent atom using the appropriate HFIX command in SHELXL-97.

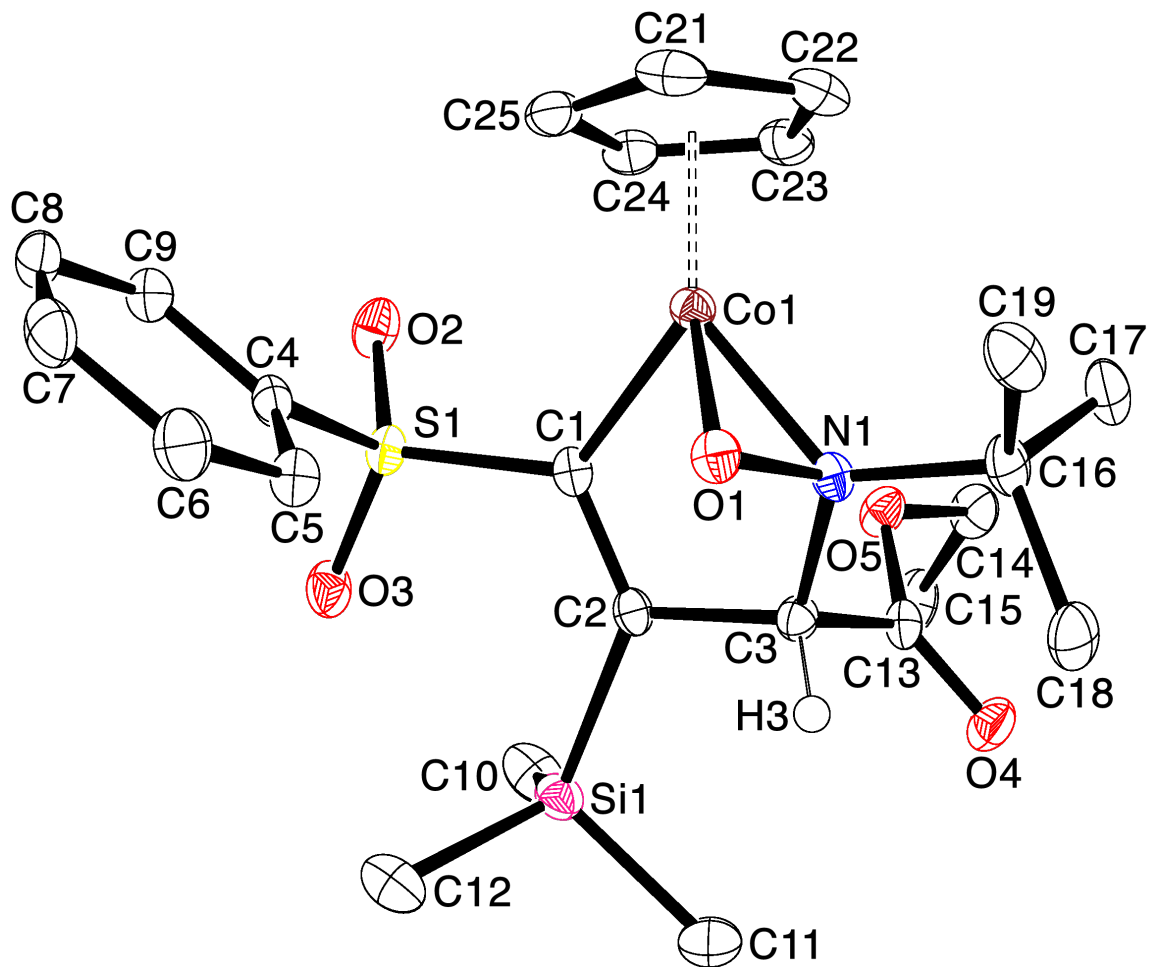
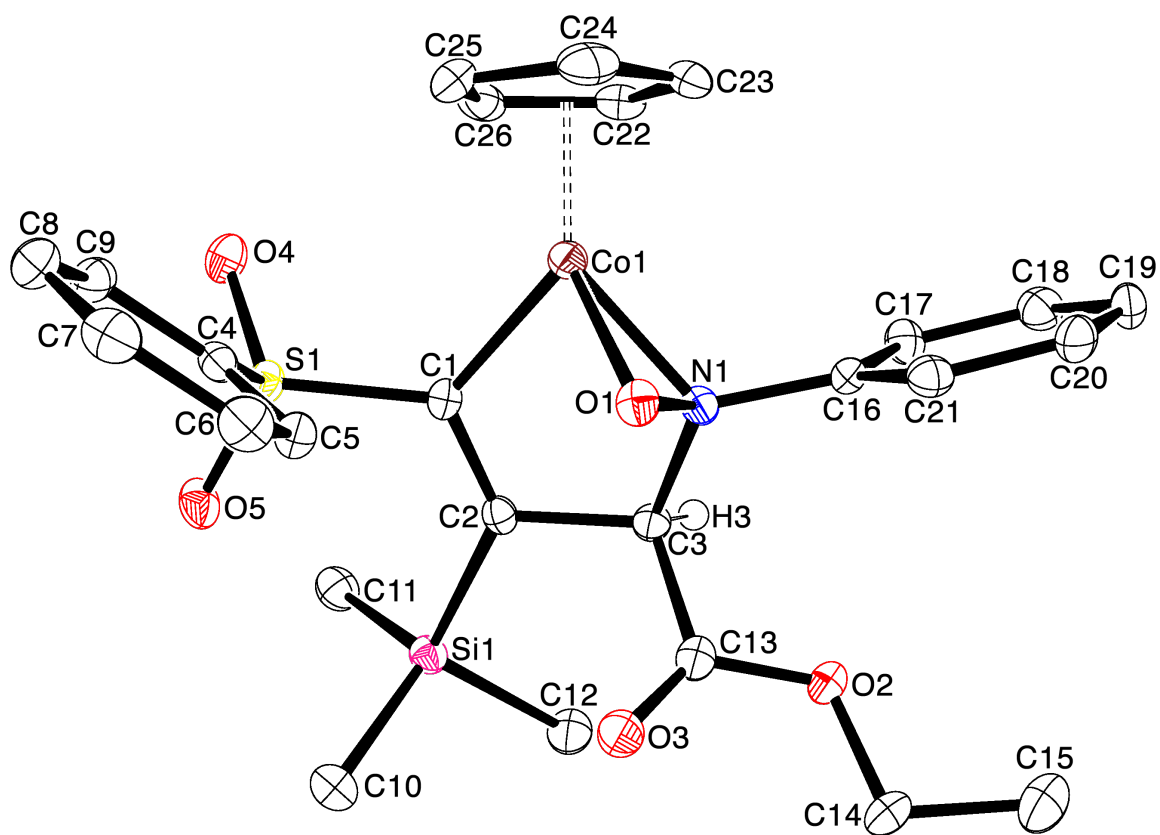


**Figure 3-7.** ORTEP of monoclinic cobalt complex *5-trans*. Ellipsoids shown at 50% probability. Most hydrogens removed for clarity.

**Table 3-3.** Crystal data and structure refinement for **5-trans**.

CSD Refcode	DOWDID	
CCDC Deposition No.	724840	
Sample/notebook ID	rlh3076	
Empirical formula	C <sub>24</sub> H <sub>34</sub> Co N O <sub>5</sub> S Si	
Formula weight	535.60	
Temperature	100(2) K	
Wavelength	0.71073 Å	
Crystal system	Monoclinic	
Space group	<i>P</i> 2 <sub>1</sub> / <i>n</i>	
Unit cell dimensions	a = 12.4106(9) Å	$\alpha = 90^\circ$
	b = 12.1402(9) Å	$\beta = 92.6420(10)^\circ$
	c = 16.7732(13) Å	$\gamma = 90^\circ$
Volume	2524.5(3) Å <sup>3</sup>	
Z	4	
Density (calculated)	1.409 Mg/m <sup>3</sup>	
Absorption coefficient	0.845 mm <sup>-1</sup>	
F(000)	1128	
Crystal size	0.18 x 0.12 x 0.06 mm <sup>3</sup>	
Crystal color/habit	red plate	
Theta range for data collection	2.00 to 28.13°	
Index ranges	-15 ≤ h ≤ 16, -16 ≤ k ≤ 16, -20 ≤ l ≤ 22	
Reflections collected	23879	
Independent reflections	5832 [R(int) = 0.0316]	
Completeness to theta = 25.00°	100.0 %	
Absorption correction	Semi-empirical from equivalents	
Max. and min. transmission	0.9511 and 0.8628	
Refinement method	Full-matrix least-squares on F <sup>2</sup>	
Data / restraints / parameters	5832 / 0 / 305	
Goodness-of-fit on F <sup>2</sup>	1.031	
Final R indices [I > 2σ(I)]	R1 = 0.0313, wR2 = 0.0690	
R indices (all data)	R1 = 0.0408, wR2 = 0.0737	
Largest diff. peak and hole	0.356 and -0.299 e.Å <sup>-3</sup>	

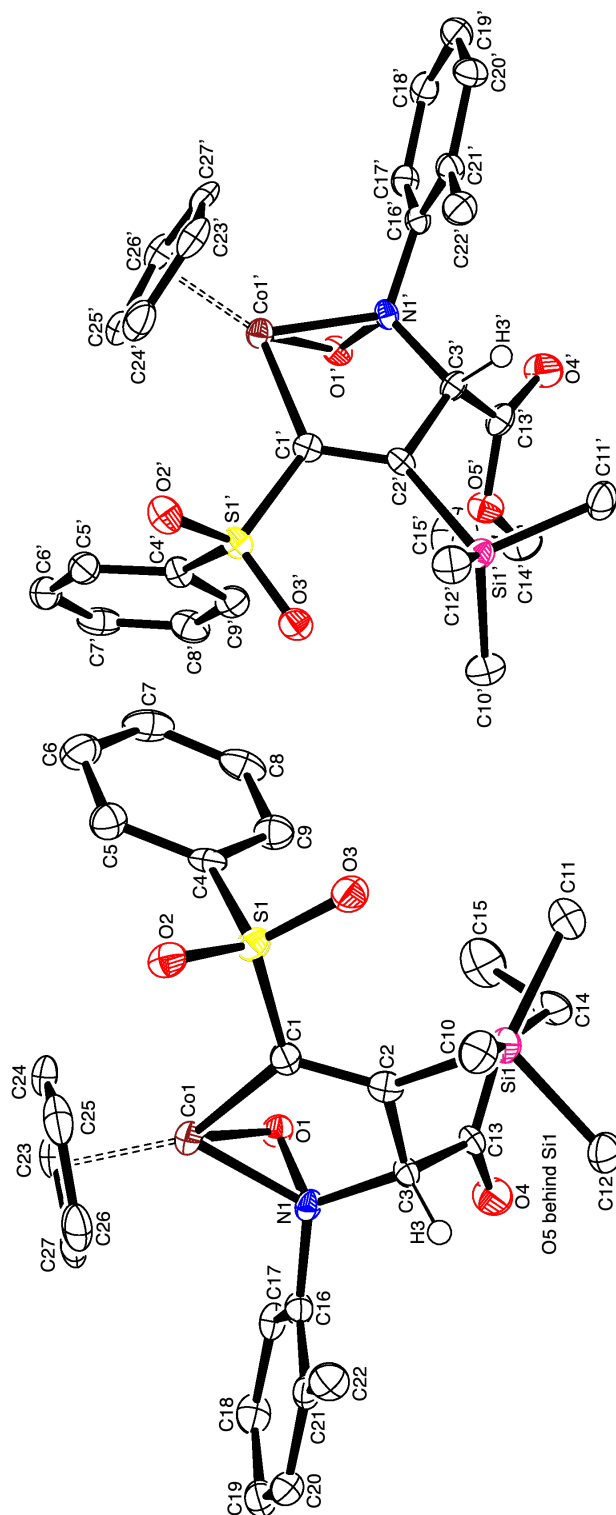




**Figure 3-8.** ORTEP of monoclinic cobalt complex *7-cis*. Ellipsoids shown at 50% probability. Most hydrogens removed for clarity.

**Table 3-4.** Crystal data and structure refinement for **7-cis**.

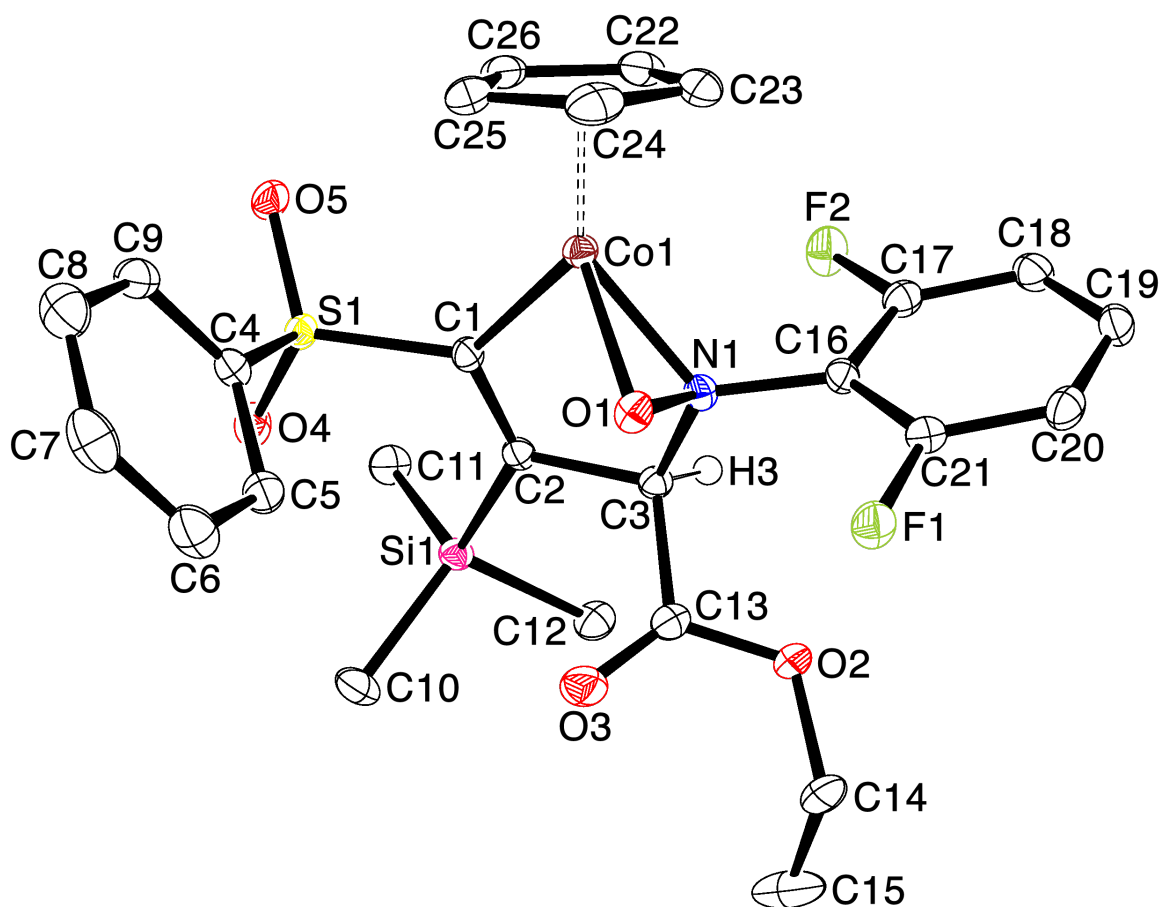
CSD Refcode	DOWDOJ	
CCDC Deposition No.	724841	
Sample/notebook ID	rlh22165	
Empirical formula	C <sub>26</sub> H <sub>30</sub> Co N O <sub>5</sub> S Si	
Formula weight	555.59	
Temperature	100(2) K	
Wavelength	0.71073 Å	
Crystal system	Monoclinic	
Space group	<i>P</i> 2 <sub>1</sub> / <i>n</i>	
Unit cell dimensions	a = 9.6140(7) Å	$\alpha = 90^\circ$
	b = 12.2740(9) Å	$\beta = 96.2460(10)^\circ$
	c = 21.9780(16) Å	$\gamma = 90^\circ$
Volume	2578.1(3) Å <sup>3</sup>	
Z	4	
Density (calculated)	1.431 Mg/m <sup>3</sup>	
Absorption coefficient	0.830 mm <sup>-1</sup>	
F(000)	1160	
Crystal size	0.60 x 0.20 x 0.04 mm <sup>3</sup>	
Crystal color/habit	purple plate	
Theta range for data collection	1.86 to 28.23°	
Index ranges	-12 ≤ h ≤ 12, -15 ≤ k ≤ 16, -29 ≤ l ≤ 29	
Reflections collected	24366	
Independent reflections	5928 [R(int) = 0.0662]	
Completeness to theta = 25.00°	100.0 %	
Absorption correction	Semi-empirical from equivalents	
Max. and min. transmission	0.9675 and 0.6357	
Refinement method	Full-matrix least-squares on F <sup>2</sup>	
Data / restraints / parameters	5928 / 0 / 320	
Goodness-of-fit on F <sup>2</sup>	1.024	
Final R indices [I > 2σ(I)]	R1 = 0.0421, wR2 = 0.0806	
R indices (all data)	R1 = 0.0770, wR2 = 0.0927	
Largest diff. peak and hole	0.477 and -0.516 e.Å <sup>-3</sup>	



**Figure 3-9.** ORTEP of triclinic cobalt complex **8-cis**. Ellipsoids shown at 50% probability. Most hydrogens removed for clarity.

**Table 3-5.** Crystal data and structure refinement for **8-cis**.

Sample/notebook ID	RLH3137	
Empirical formula	C <sub>27</sub> H <sub>32</sub> Co N O <sub>5</sub> S Si	
Formula weight	569.61	
Temperature	100 K	
Wavelength	0.71073 Å	
Crystal system	Triclinic	
Space group	<i>P</i> -1	
Unit cell dimensions	a = 10.3250(6) Å	$\alpha = 88.493(3)^\circ$
	b = 10.5582(7) Å	$\beta = 86.125(3)^\circ$
	c = 25.3414(17) Å	$\gamma = 74.412(3)^\circ$
Volume	2654.8(3) Å <sup>3</sup>	
Z	4	
Density (calculated)	1.425 Mg/m <sup>3</sup>	
Absorption coefficient	0.808 mm <sup>-1</sup>	
F(000)	1192	
Crystal size	0.253 x 0.217 x 0.155 mm <sup>3</sup>	
Theta range for data collection	0.805 to 25.422°	
Index ranges	-12 ≤ h ≤ 12, -12 ≤ k ≤ 12, -30 ≤ l ≤ 30	
Reflections collected	14758	
Independent reflections	14758 [R(int) = ?]	
Completeness to theta = 68.47°	98.9 %	
Absorption correction	Semi-empirical from equivalents	
Max. and min. transmission	0.091638 and 0.060790	
Refinement method	Full-matrix least-squares on F <sup>2</sup>	
Data / restraints / parameters	14758 / 0 / 660	
Goodness-of-fit on F <sup>2</sup>	1.014	
Final R indices [I > 2σ(I)]	R1 = 0.0452, wR2 = 0.1130	
R indices (all data)	R1 = 0.0505, wR2 = 0.1161	
Extinction coefficient	n/a	
Largest diff. peak and hole	0.558 and -0.798 e.Å <sup>-3</sup>	

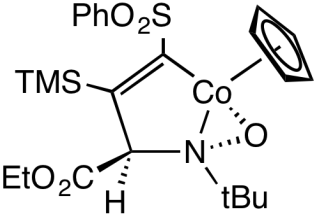
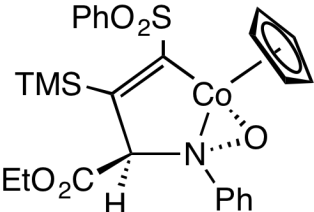
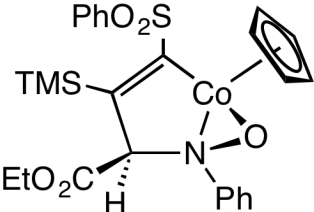
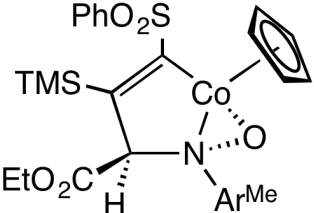


**Figure 3-10.** ORTEP of triclinic cobalt complex **9-cis**. Ellipsoids shown at 50% probability. Most hydrogens removed for clarity.

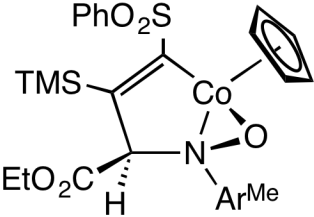
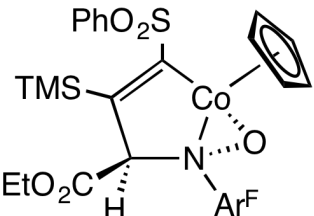
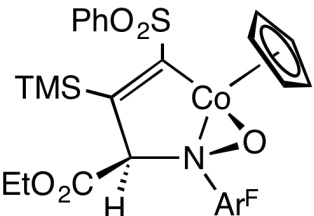
**Table 3-6.** Crystal data and structure refinement for **9-cis**.

Sample/notebook ID	rlh3093_0m	
Empirical formula	C <sub>26</sub> H <sub>28</sub> Co F <sub>2</sub> N O <sub>5</sub> S Si	
Formula weight	591.57	
Temperature	100(2) K	
Wavelength	0.71073 Å	
Crystal system	Triclinic	
Space group	<i>P</i> -1	
Unit cell dimensions	a = 10.1864(30) Å	$\alpha = 87.7195(45)^\circ$
	b = 10.5493(31) Å	$\beta = 73.9070(41)^\circ$
	c = 14.2180(41) Å	$\gamma = 61.4816(39)^\circ$
Volume	1282.0(6) Å <sup>3</sup>	
Z	2	
Density (calculated)	1.532 Mg/m <sup>3</sup>	
Absorption coefficient	0.851 mm <sup>-1</sup>	
F(000)	612	
Crystal size	0.15 x 0.14 x 0.13 mm <sup>3</sup>	
Theta range for data collection	1.50 to 28.17°	
Index ranges	-13 ≤ h ≤ 13, -13 ≤ k ≤ 14, -18 ≤ l ≤ 18	
Reflections collected	35393	
Independent reflections	5813 [R(int) = 0.0181]	
Completeness to theta = 25.00°	99.1 %	
Absorption correction	Semi-empirical from equivalents	
Max. and min. transmission	0.8974 and 0.8830	
Refinement method	Full-matrix least-squares on F <sup>3</sup>	
Data / restraints / parameters	5813 / 0 / 338	
Goodness-of-fit on F <sup>2</sup>	1.035	
Final R indices [I > 2σ(I)]	R1 = 0.0239, wR2 = 0.0624	
R indices (all data)	R1 = 0.0255, wR2 = 0.0637	
Largest diff. peak and hole	0.406 and -0.271 e.Å <sup>-3</sup>	

**Table 3-7.** Selected spectroscopic data for *N,N*-Dialkylhydroxylamido complexes (CDCl<sub>3</sub>).

Complex	<sup>1</sup> H NMR, [δ]	<sup>13</sup> C{ <sup>1</sup> H} NMR, [δ]
 <p><b>5-trans</b></p>	0.15 (s, 9H, TMS) 1.35 (t, 3H, <i>J</i> = 7.03 Hz, CH <sub>3</sub> ) 4.08 (s, 1H, CHCO <sub>2</sub> Et) 4.93 (s, 5H, Cp)	2.89 (TMS) 14.14 (CH <sub>2</sub> CH <sub>3</sub> ) 80.57 (CHCO <sub>2</sub> Et) 83.48 (Cp)
 <p><b>7-trans</b></p>	0.11 (s, 9H, TMS) 1.11 (t, 3H, <i>J</i> = 7.18 Hz, CH <sub>3</sub> ) 3.90 (s, 1H, CHCO <sub>2</sub> Et) 4.78 (s, 5H, Cp)	2.60 (TMS) 13.88 (CH <sub>2</sub> CH <sub>3</sub> ) 84.48 (Cp) 88.71 (CHCO <sub>2</sub> Et)
 <p><b>7-cis</b></p>	0.21 (s, 9H, TMS) 1.05 (t, 3H, <i>J</i> = 7.15 Hz, CH <sub>3</sub> ) 5.23 (s, 1H, CHCO <sub>2</sub> Et) 4.48 (s, 5H, Cp)	2.30 (TMS) 13.95 (CH <sub>2</sub> CH <sub>3</sub> ) 84.63 (Cp) 86.05 (CHCO <sub>2</sub> Et)
 <p><b>8-trans</b> Ar<sup>Me</sup> = 2-Me-C<sub>6</sub>H<sub>4</sub></p>	0.11 (s, 9H, TMS) 1.13 (t, 3H, <i>J</i> = 7.20 Hz, CH <sub>3</sub> ) 4.85 (s, 5H, Cp)	

**Table 3-7.** Selected spectroscopic data for *N,N*-Dialkylhydroxylamido complexes (CDCl<sub>3</sub>) (continued).

Complex	<sup>1</sup> H NMR, [δ]	<sup>13</sup> C{ <sup>1</sup> H} NMR, [δ]
 <p><b>8-cis</b> Ar<sup>Me</sup> = 2-Me-C<sub>6</sub>H<sub>4</sub></p>	0.19 (s, 9H, TMS) 1.15 (t, 3H, <i>J</i> = 7.20 Hz, CH <sub>3</sub> ) 4.49 (s, 5H, Cp) 4.92 (s, 1H, CHCO <sub>2</sub> Et)	2.22 (TMS) 14.06 (CH <sub>2</sub> CH <sub>3</sub> ) 83.86 (CHCO <sub>2</sub> Et) 84.68 (Cp)
 <p><b>9-trans</b> Ar<sup>F</sup> = 2,6-F<sub>2</sub>-C<sub>6</sub>H<sub>3</sub></p>	0.19 (s, 9H, TMS) 1.21 (t, 3H, <i>J</i> = 7.18 Hz, CH <sub>3</sub> ) 4.86 (s, 5H, Cp) 4.01 (s, 1H, CHCO <sub>2</sub> Et)	2.24 (TMS) 13.88 (CH <sub>2</sub> CH <sub>3</sub> ) 84.39 (Cp) 85.42 (CHCO <sub>2</sub> Et)
 <p><b>9-cis</b> Ar<sup>F</sup> = 2,6-F<sub>2</sub>-C<sub>6</sub>H<sub>3</sub></p>	0.12 (s, 9H, TMS) 1.18 (t, 3H, <i>J</i> = 7.18 Hz, CH <sub>3</sub> ) 4.66 (s, 5H, Cp) 4.73 (s, 1H, CHCO <sub>2</sub> Et)	2.55 (TMS) 13.89 (CH <sub>2</sub> CH <sub>3</sub> ) 85.41 (Cp) 85.42 (CHCO <sub>2</sub> Et)



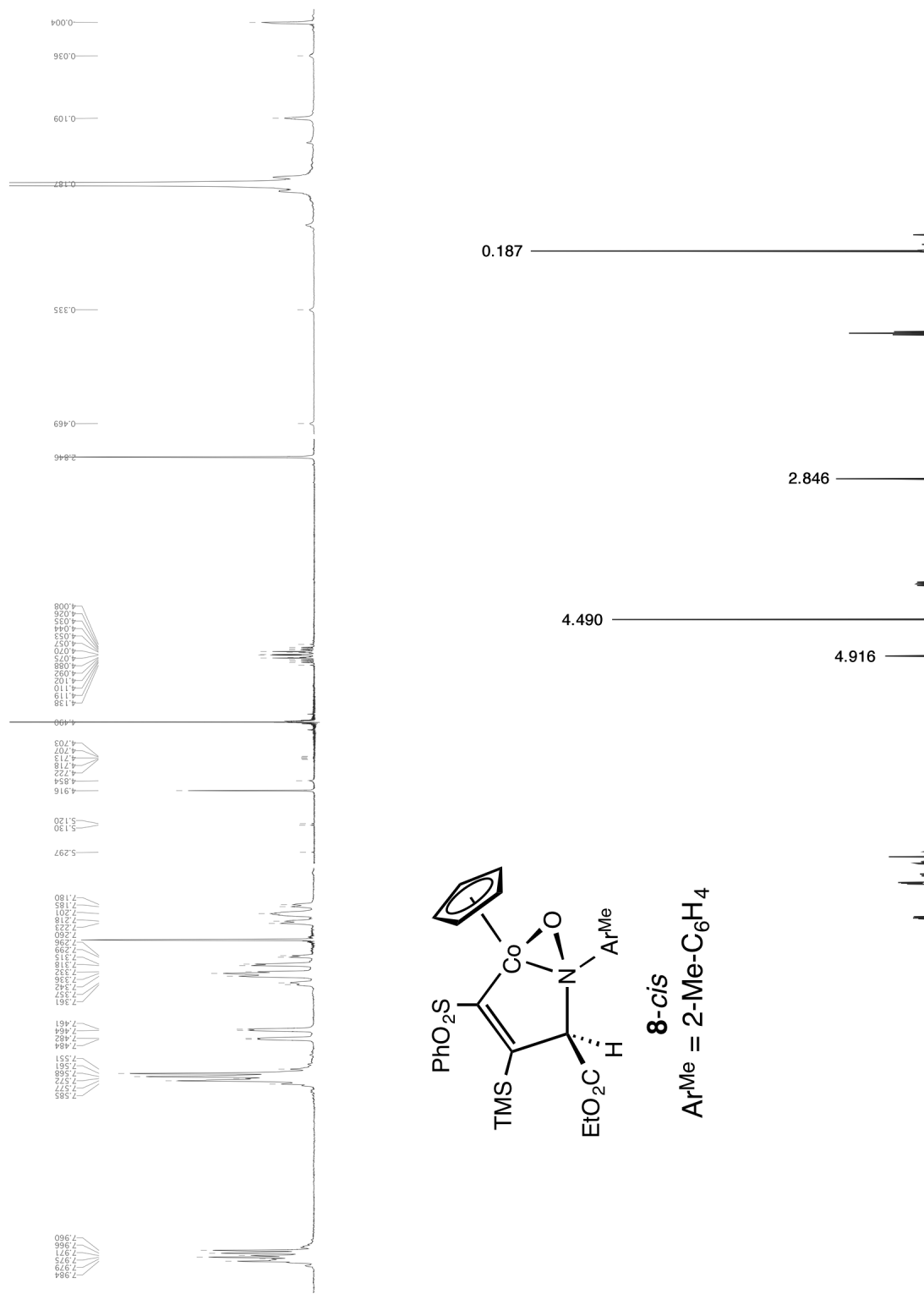


**Figure 3-11.** Compound **8-cis**  $^1H$  NMR spectrum (400.053 MHz,  $CDCl_3$ ).

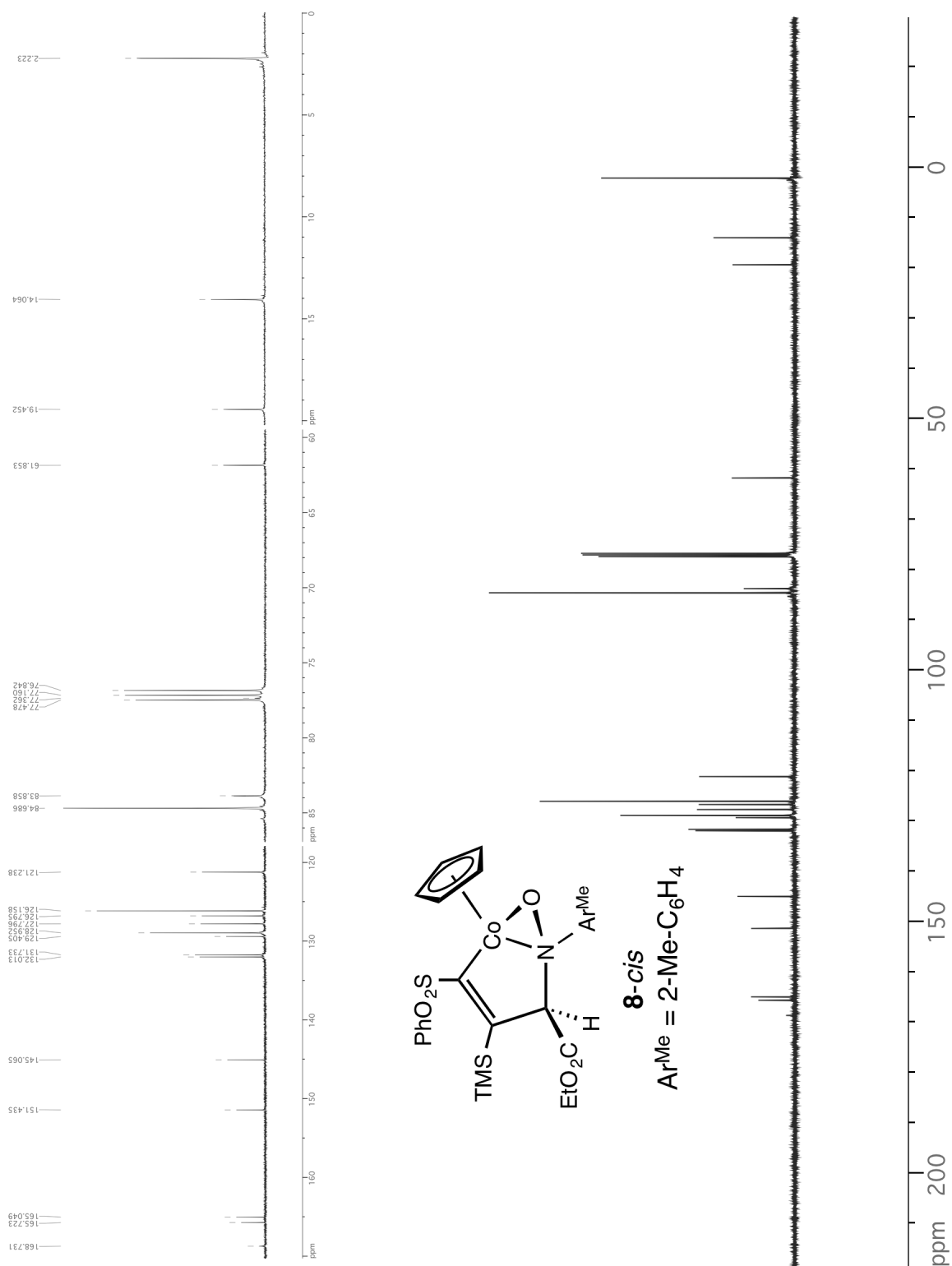


**Figure 3-12.** **8-cis**  $^{13}\text{C}$  NMR spectrum (100.567 MHz,  $\text{CDCl}_3$ ).

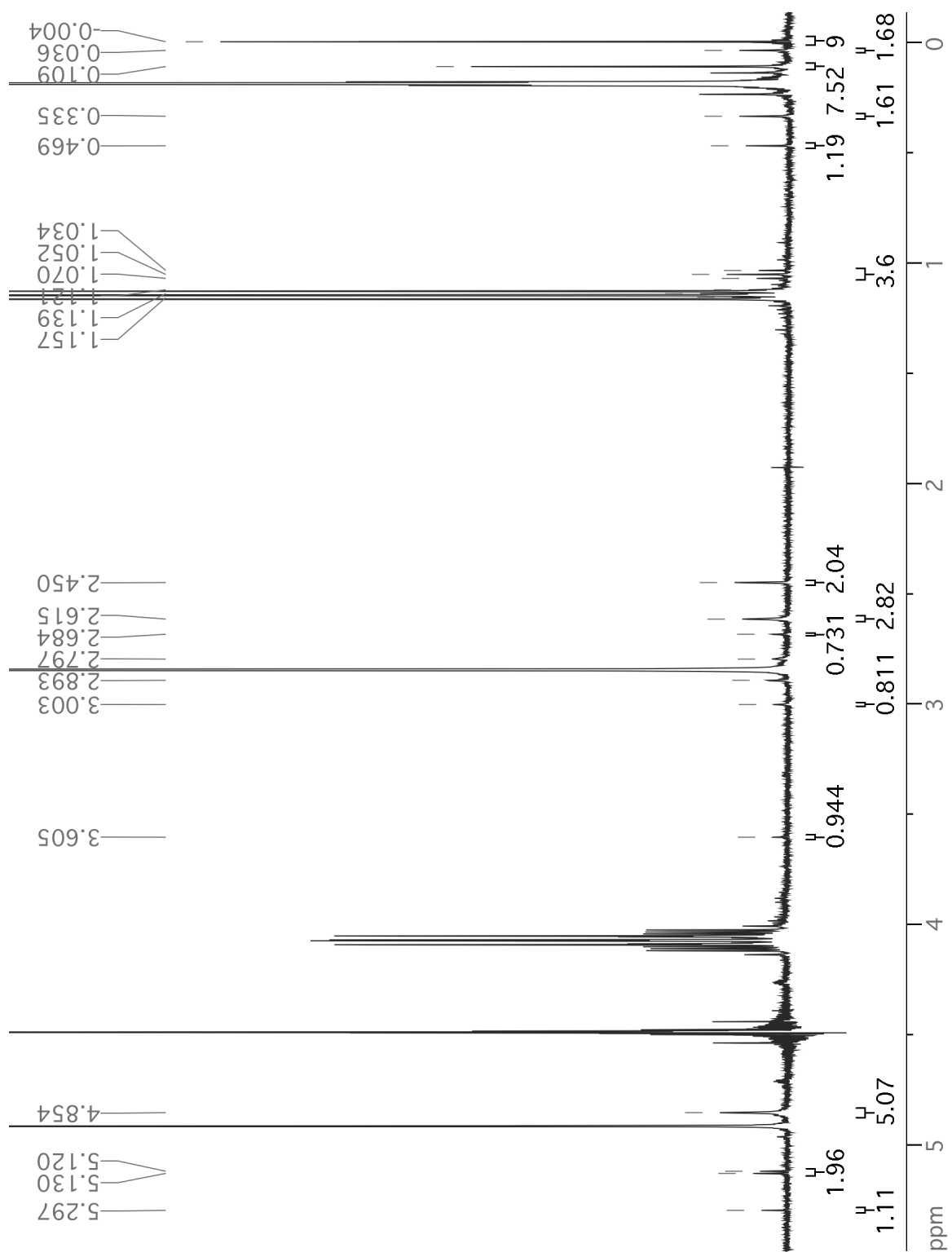


**Figure 3-13.** Minor peaks in 8-*cis*  $^1\text{H}$  NMR spectrum (400.053 MHz,  $\text{CDCl}_3$ ).

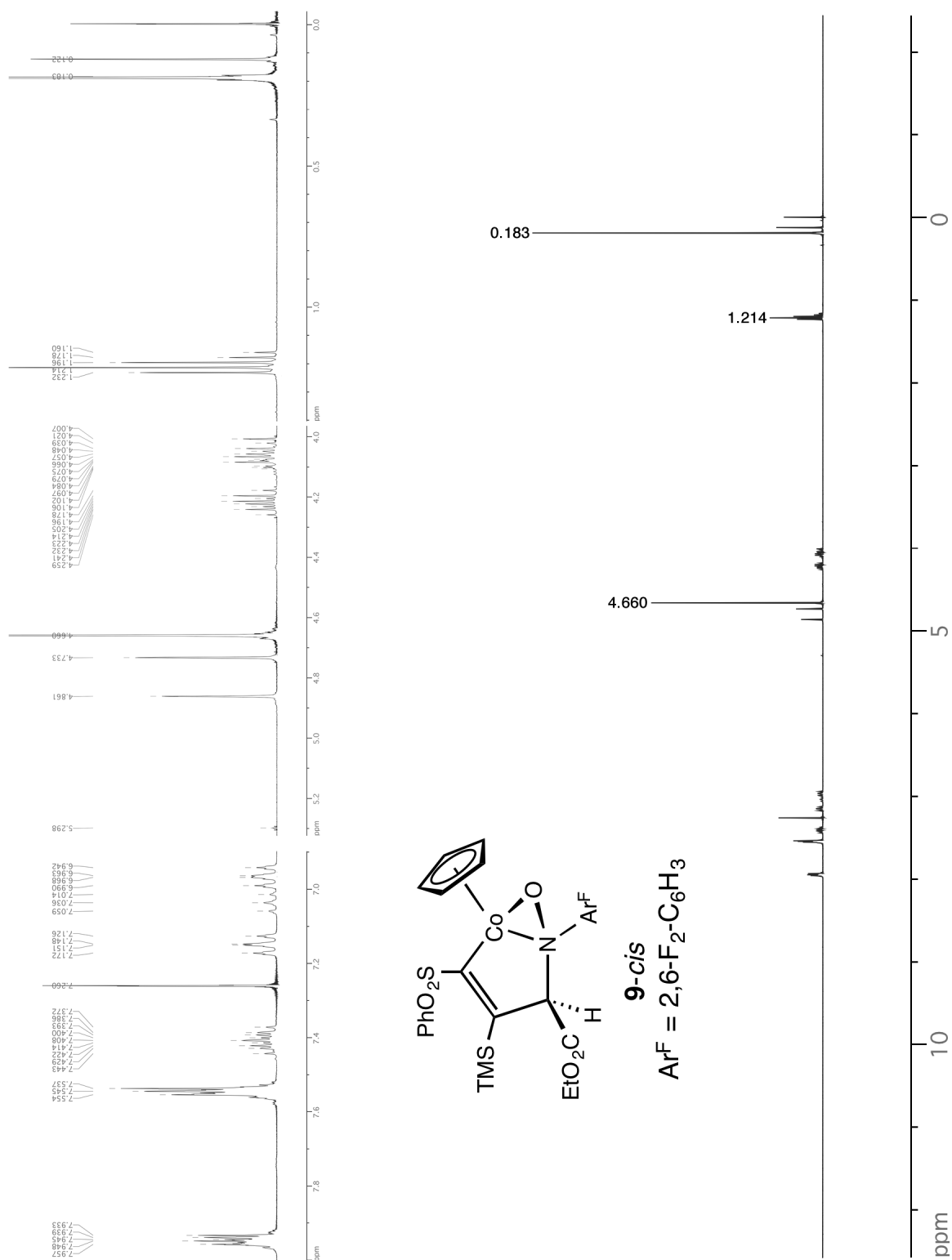
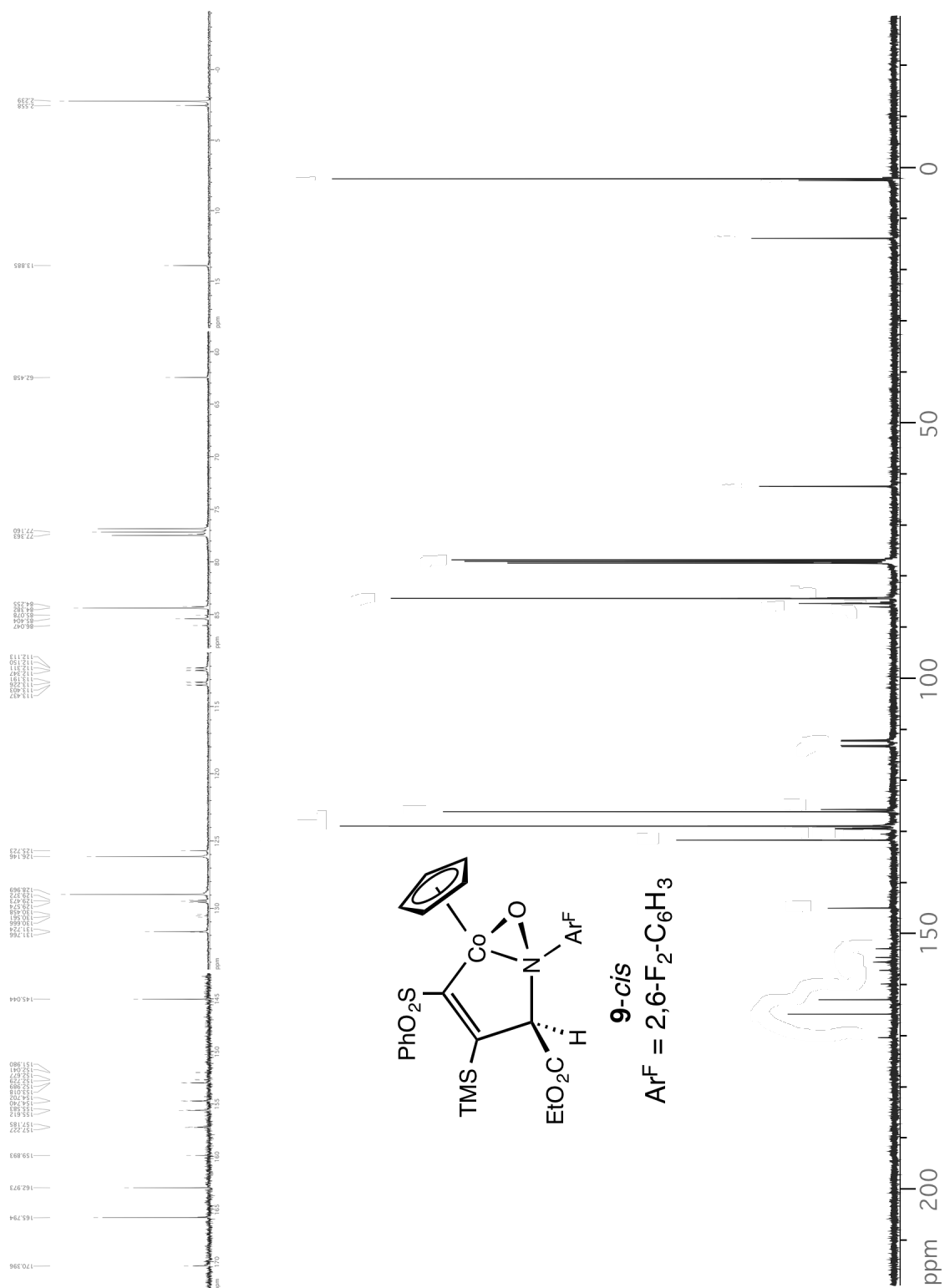


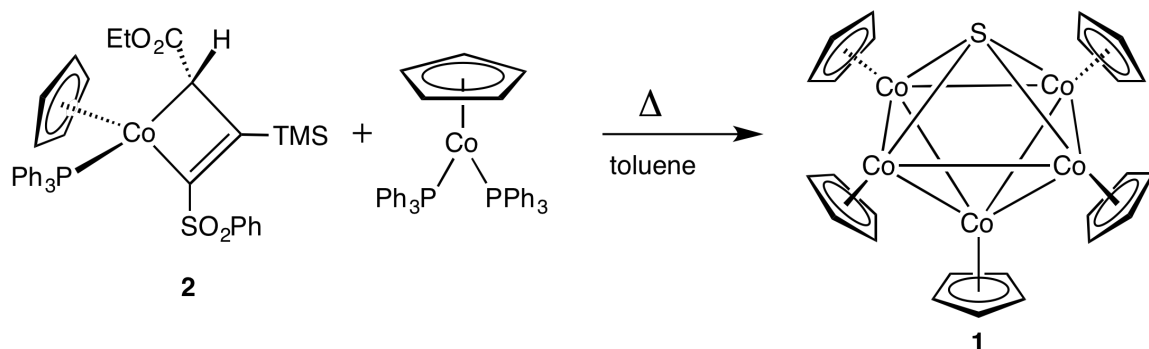
Figure 3-14. 9-cis  $^1\text{H}$  NMR spectrum (400.053 MHz,  $\text{CDCl}_3$ ).



## Chapter 4

The Isolation of a Large Cyclopentadienylcobaltsulfide Cluster – Synthesis and  
Crystal Structure of Octahedral *closo*-[( $\eta^5$ -C<sub>5</sub>H<sub>5</sub>)Co]<sub>5</sub>S

Transition-metal clusters containing main group elements in their framework are, among other things, of interest as models for metal-sulfur clusters in biologically important systems, as precursors to conducting and thermoelectric phases, and as catalysts.<sup>1,2</sup> Progress in this field has been characterized by the creative selection of cluster-forming precursors, while letting nature dictate the outcome. Few large clusters have been designed and prepared in the more systematic and rational manner characterizing organic synthesis. Our studies into the reactivity of late-metal metallacyclobutene complexes led to the serendipitous isolation of an unusual pentanuclear cobalt chalcogenido cluster, the compound *closo*- $[(\eta^5\text{-C}_5\text{H}_5)\text{Co}]_5\text{S}$  (**1**) from cobaltacycle **2** (Scheme 4-1).<sup>3</sup>



**Scheme 4-1.** Synthesis of title cluster compound **1**.<sup>3</sup>

Presumably, complex **1** forms from the oligomerization of  $(\eta^5\text{-C}_5\text{H}_5)\text{Co}$  moieties and a sulfide ion in solution. It appears that the sulfur present in **1** is derived from the phenyl sulfone in complex **2**, although the small quantities of **1** do not allow us to rule out that traces of sulfur-containing impurities may have been present in the starting material.<sup>4,5</sup> Mechanistically, the six-electron reduction of the sulfone to a terminal sulfido presents difficulty, though this transformation

may be facilitated by a metal-mediated oxidation of free triphenylphosphine to triphenylphosphine oxide and subsequent metal-mediated C–S bond cleavages.<sup>6–10</sup>

The core atoms of *closo*-[( $\eta^5$ -C<sub>5</sub>H<sub>5</sub>)Co]<sub>5</sub>S, **1**, form an octahedral structure (Figure 4-1).<sup>1,2,11</sup> Selected bond distances and angles are presented in Table 4-1. The core structure electron count is 74, but if the sulfur atom is considered as the isolobal equivalent of a 16-electron transition-metal fragment,<sup>2</sup> then the valence electron count is the same as required for a *closo* structure of all transition-metal atoms obeying the 18-electron rule. With five ( $\eta^5$ -C<sub>5</sub>H<sub>5</sub>)Co fragments, it is the largest ( $\eta^5$ -C<sub>5</sub>H<sub>5</sub>)Co-based cluster known. There are several clusters containing [( $\eta^5$ -C<sub>5</sub>H<sub>5</sub>)Co]<sub>4</sub>, one being the related disulfide complex, *trans*-[( $\eta^5$ -C<sub>5</sub>H<sub>5</sub>)Co]<sub>4</sub>S<sub>2</sub> (**3**) (Figure 4-2).<sup>12</sup> As a *closo*-octahedral cluster, **1** is isolobally related to the group-9, 86-electron octahedral clusters, M<sub>6</sub>(CO)<sub>16</sub>, M = Co,<sup>13</sup> Rh,<sup>14</sup> and Ir<sup>15</sup> and both isolobal and isostructural analogues of the group-8 clusters, M<sub>5</sub>(CO)<sub>15</sub>S, M = Ru<sup>16</sup> and Os.<sup>17</sup>



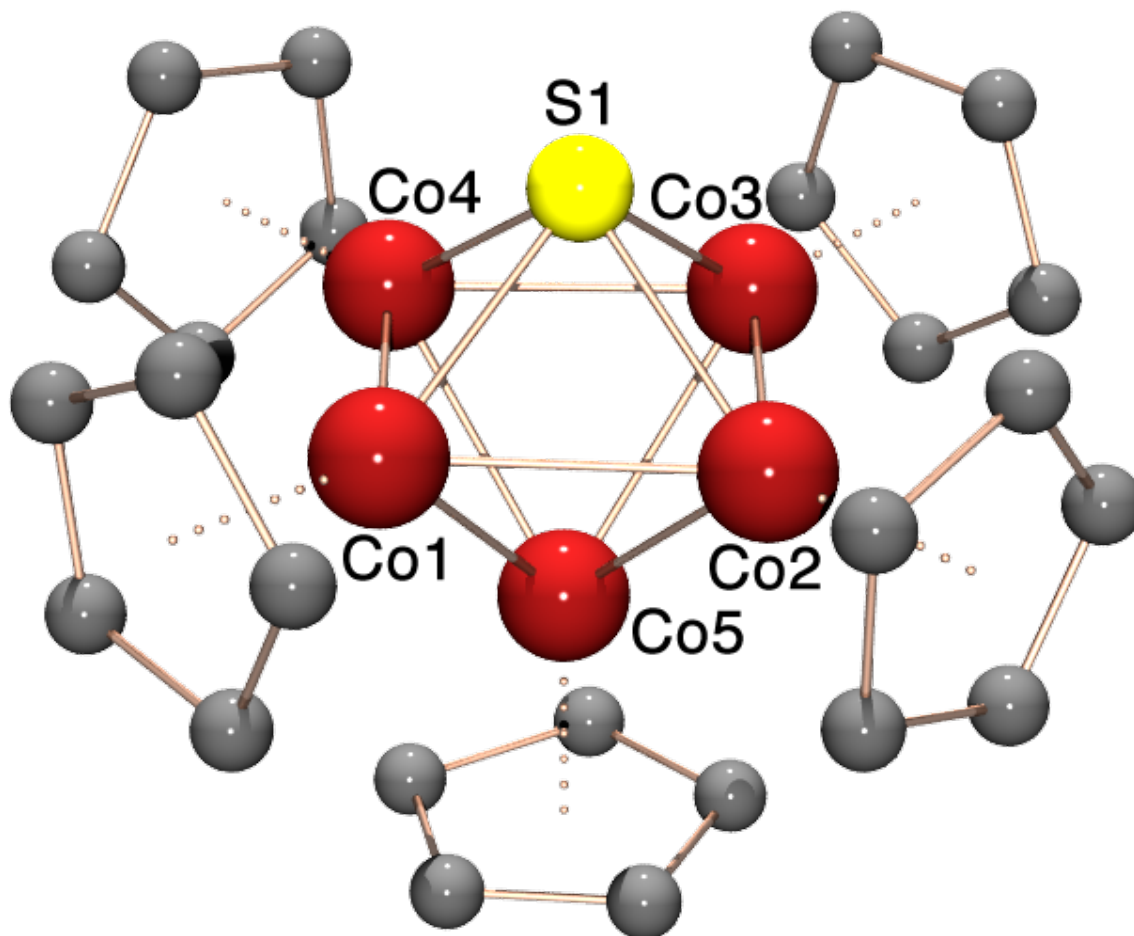


**Figure 4-1.** Solid-state structure of monoclinic cobalt cluster *closo*- $[(\eta^5\text{-C}_5\text{H}_5)\text{Co}]_5\text{S}$  (**1**). CCDC Number 710868; reocode VUKNIZ. R = 3.43%, Space Group  $P2_1/c$ .<sup>3</sup>

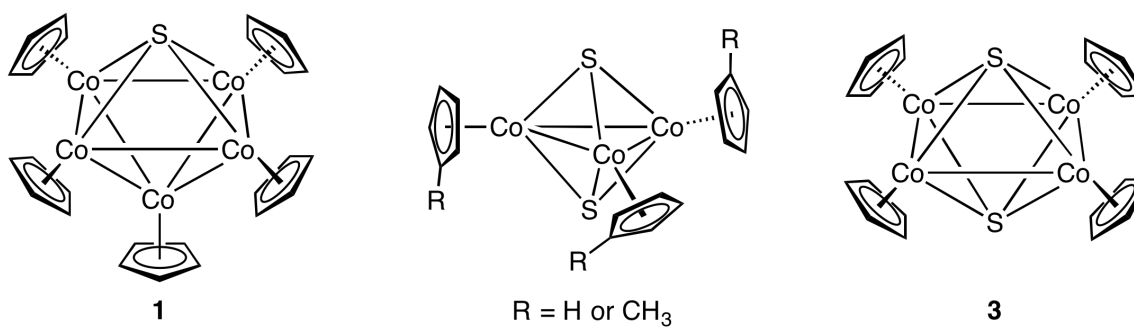


**Figure 4-2.** Crystallographically characterized  $[(\eta^5\text{-C}_5\text{H}_5)\text{Co}]_m\text{S}_n$  clusters.

The octahedral core of **1** is nearly perfect. The cluster-forming angles involving the ( $\eta^5$ -C<sub>5</sub>H<sub>5</sub>)Co units are all  $\pm 1.0^\circ$  of 60 and 90° and the  $\mu_4$ -S cap is very symmetrically placed. The narrow range of Co–S distances is 2.1665(10)–2.1885(10) Å. The average is 2.176(1) Å, which is identical to the Co–S average, 2.175(3) Å in  $[(\eta^5\text{-C}_5\text{H}_4\text{Me})\text{Co}]_3(\mu_3\text{-S})_2$ ,<sup>18</sup> and comparable to that found in  $[(\eta^5\text{-C}_5\text{H}_5)\text{Co}]_3(\mu_3\text{-S})_2$ ,<sup>19,20</sup> 2.168(4) Å. It is noteworthy that the average Co–S distance in the disulfur octahedral cluster **3**, 2.229(1) Å, is somewhat longer, which is in accord with the presence of two additional cluster-forming electrons, compared to **1**, and the prediction that these additional electrons will occupy a framework antibonding orbital.<sup>19</sup> Similarly, the distance between the capping sulfido and the plane formed by the equatorial cobalt atoms is shorter in **1** (1.326(1) Å) than in **3** (1.413(1) Å).

The average Co–Co distance in **1**, 2.429(1) Å, is only slightly shorter than in **3**, 2.438(1) Å. The greater bond length change found for adding two framework electrons on the Co–S bonds, compared to the Co–Co bonds, suggests that the lowest occupied antibonding levels have more Co–S than Co–Co character, in keeping with the greater electronegativity of sulfur compared to ( $\eta^5$ -C<sub>5</sub>H<sub>5</sub>)Co.<sup>14,21</sup>

**Table 4-1.** Selected bond distances [ $\text{\AA}$ ] and angles [ $^\circ$ ] for complex **1**.

<b>Cmpd No.:</b>		<i>closo</i> -[( $\eta^5$ -C <sub>5</sub> H <sub>5</sub> )Co] <sub>5</sub> S ( <b>1</b> )	
Co(1)-Co(2)	2.4334(7)	Co(2)-S	2.1681(10)
Co(1)-Co(4)	2.4476(7)	Co(3)-S	2.1810(11)
Co(2)-Co(3)	2.4281(7)	Co(4)-S	2.1665(10)
Co(3)-Co(4)	2.4514(7)	Co(5)-S	3.0200(11)
Co(1)-Co(5)	2.4014(7)	Cnt(1)-Co(1)	1.723(2)
Co(2)-Co(5)	2.4272(7)	Cnt(2)-Co(2)	1.716(2)
Co(3)-Co(5)	2.4097(7)	Cnt(3)-Co(3)	1.725(2)
Co(4)-Co(5)	2.4338(7)	Cnt(4)-Co(4)	1.730(2)
Co(1)-S	2.1885(10)	Cnt(5)-Co(5)	1.760(2)

**References.**

1. Housecroft, C. E. *Transition Metal-Main Group Cluster Compounds*; Fehlner, T. P., Ed. *Inorganometallic Chemistry*, Plenum, New York, **1992**.
2. González-Moraga, G. *Cluster Chemistry*, Springer-Verlag, Berlin, **1993**.
3. Portions of this chapter were previously communicated: Holland, R. L.; O'Connor, J. M.; Rheingold, A. L. *J. Clust. Sci.* **2009**, *20*, 261.
4. O'Connor, J. M.; Ji, H.; Iranpour, M.; and Rheingold, A. L. *J. Am. Chem. Soc.* **1993**, *115*, 1586.
5. Wakatsuki, Y.; Yamazaki, H.; Lindner, E.; and Bosamie, A. *(1,3-Butadiene-1,4-Diyl)( $\eta^5$ -cyclopentadienyl)-(Triphenylphosphine)Cobalt with Various Substituents*; Kaesz, H. D., Ed. *Inorganic Synthesis*, Wiley-Interscience, New York, **1989**.
6. O'Connor, J. M.; Ji, H.-L.; Rheingold, A. L. *J. Am. Chem. Soc.* **1993**, *115*, 9846.
7. O'Connor, J. M.; Fong, B. S.; Ji, H.-L.; Hiibner, K.; Rheingold, A. L. *J. Am. Chem. Soc.* **1995**, *117*, 8029.
8. O'Connor, J. M.; Chen, M.-C.; Frohn, M.; Rheingold, A. L.; Guzei, I. A. *Organometallics* **1997**, *16*, 5589.
9. O'Connor, J. M.; Chen, M.-C.; Rheingold, A. L. *Tetrahedron Lett.* **1997**, *38*, 5241.
10. Holland, R. L.; Bunker, K. D.; Chen, C. H.; DiPasquale, A. G.; Rheingold, A. L.; Baldrige, K. K.; O'Connor, J. M. *J. Am. Chem. Soc.* **2008**, *130*, 10093.
11. Mingos, D. M. P.; Wales, D. J. *Introduction to Cluster Chemistry*, Prentice Hall, Englewood Cliffs, **1990**.
12. Jiang, F.; Lei, X.; Huang, Z.; Hong, M.; Kang, B.; Wu, D.; Liu, H. *Chem. Commun.* **1990**, 1655.
13. Albano, V.; Chini, P.; Scatturin, V. *Chem. Commun.* **1968**, 163.
14. Corey, E. R.; Dahl, L. F.; Beck, W. *J. Am. Chem. Soc.* **1963**, *85*, 1202.
15. Garlaschelli, L.; Martinengo, S.; Bellon, P. L.; Demartin, F.; Manassero, M.; Chiang, M. Y.; Wei, C.-Y.; Bau, R. *J. Am. Chem. Soc.* **1984**, *106*, 6664.

16. Adams, R. D.; Babin, J. E.; Tasi, M. *Organometallics* **1988**, *7*, 503.
17. Adams, R. D.; Horvath, I. T.; Segmüller, B. E.; Yang, L.-W. *Organometallics* **1983**, *2*, 1301.
18. Pulliam, C. R.; Thoden, J. B.; Stacy, A. M.; Spencer, B.; Englert, M. H.; Dahl, L. F. *J. Am. Chem. Soc.* **1991**, *113*, 7398.
19. Frisch, P. D.; Dahl, L. F. *J. Am. Chem. Soc.* **1972**, *94*, 5082.
20. Kamijo, N. Watanabé, T. *Acta Crystallogr.* **1979** *B35*, 2537.
21. Halet, J.-F.; Hoffmann, R.; Saillard, J.-Y. *Inorg. Chem.* **1985**, *24*, 1695.

Chapter 4 is adapted from **R. L. Holland**, J. M. O'Connor, A. L. Rheingold "The Isolation of a Large Cyclopentadienylcobaltsulfide Cluster. The Synthesis and Crystal Structure of Octahedral *closo*-( $\eta^5$ -C<sub>5</sub>H<sub>5</sub>Co)<sub>5</sub>S" *J. Clust. Sci.*, **2009**, *20*, 261-265. Copyright 2009 The Author(s). Permission to use copyrighted images and data in the manuscript was obtained from J. M. O'Connor, and A. L. Rheingold. The dissertation author is the first author of this paper.

### **Experimental.**

**General Data.** All manipulations were performed under an atmosphere of dinitrogen, or in a Vacuum Atmospheres inert atmosphere glove box equipped with a Dri-Train MO 40-1 purifier. Toluene was distilled over sodium/benzophenone ketyl and rigorously degassed prior to use. Complex **2** and ( $\eta^5$ -C<sub>5</sub>H<sub>5</sub>)Co(PPh<sub>3</sub>)<sub>2</sub> were prepared by literature methods.<sup>4,5</sup>

***closo***-[( $\eta^5$ -C<sub>5</sub>H<sub>5</sub>)Co]<sub>5</sub>S (**1**). In the dry box, a 100-mL thick-walled reaction tube equipped with a threaded Teflon plug and O-ring was charged with the metallacyclobutene complex, ( $\eta^5$ -C<sub>5</sub>H<sub>5</sub>)Co(PPh<sub>3</sub>)[ $\kappa^2$ -C(SO<sub>2</sub>Ph)=C(TMS)CH(CO<sub>2</sub>Et)] (**2**; 356.4 mg, 0.50 mmol), ( $\eta^5$ -C<sub>5</sub>H<sub>5</sub>)Co(PPh<sub>3</sub>)<sub>2</sub> (524.2 mg, 0.81 mmol), and toluene (50 mL). The flask was sealed and the solution heated at 100 °C for 16 h. The reaction mixture was chromatographed on alumina in the dry box using 10% EtOAc/benzene as eluent. Two distinct brownish bands were observed. The bands were collected, the volatiles removed under vacuum, and the residue dissolved in methanol. Slow evaporation of methanol from the first of the fractions led to the formation of a small yield (< 1%) of narrow, blade-like black crystals of **1**. <sup>1</sup>H NMR spectroscopic analysis of the material that remained in the mother liquor suggested that a dicobalt complex had formed in addition to **1**. We have to date been unsuccessful in characterizing that product.

**Experimental for X-Ray Structure Determination.** Crystallographic data for **1** are summarized in Table 4-2. Data were collected using a Bruker D8 platform diffractometer equipped with an APEX CCD detector and a KryoFlex low-temperature apparatus. Crystals of *closo*-[ $\eta^5$ -C<sub>5</sub>H<sub>5</sub>)Co]<sub>5</sub>S (**1**) grew as very narrow black blades from MeOH and were mounted with mineral oil on a Nylon loop. The structure was solved by direct methods and refined by least squares on  $F^2$ . All non-hydrogen atoms were refined anisotropically and all hydrogen atoms were idealized. All software used in the data collection, solution, and refinement is contained in the APEX and SHELXTL libraries maintained by Bruker-AXS (Madison, WI).



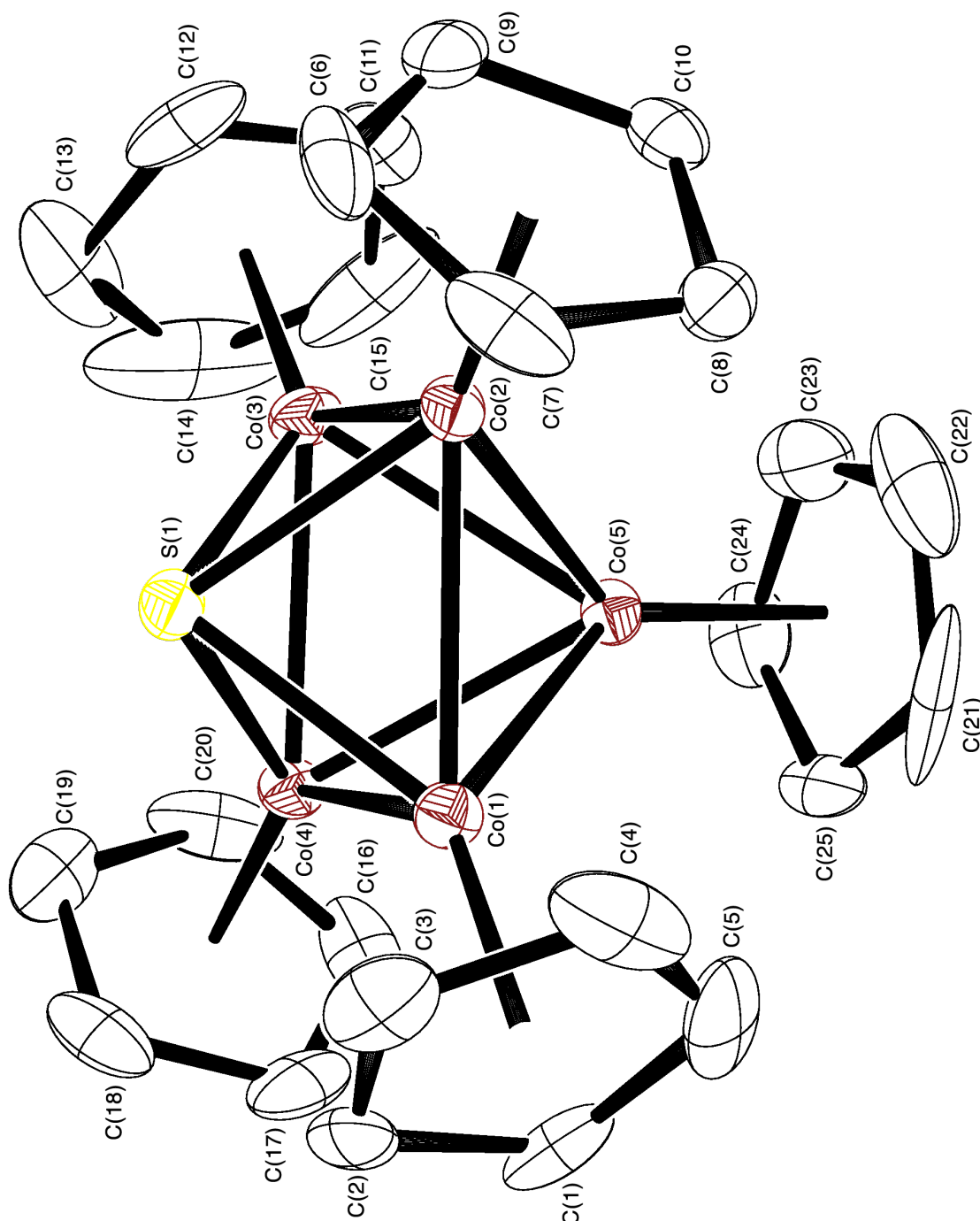


**Figure 4-3.** ORTEP of monoclinic  $closo-[(\eta^5-C_5H_5)Co]_5S$  (**1**). Ellipsoids shown at 30% probability. Hydrogens removed for clarity.

**Table 4-2.** Crystal data and structure refinement for **1**.

CCDC Refcode	VUKNIZ	
CCDC Deposition No.	710868	
Sample/notebook ID	rlh006	
Empirical formula	C <sub>25</sub> H <sub>25</sub> Co S	
Formula weight	652.16	
Temperature	100(2) K	
Wavelength	0.71073 Å	
Crystal system	Monoclinic	
Space group	<i>P</i> 2 <sub>1</sub> / <i>c</i>	
Unit cell dimensions	a = 9.3980(12) Å	$\alpha = 90^\circ$
	b = 17.011(2) Å	$\beta = 106.064(2)^\circ$
	c = 14.0890(18) Å	$\gamma = 90^\circ$
Volume	2164.5(5) Å <sup>3</sup>	
Z	4	
Density (calculated)	2.001 Mg/m <sup>3</sup>	
Absorption coefficient	3.860 mm <sup>-1</sup>	
F(000)	1304	
Crystal size	0.14 x 0.02 x 0.01 mm <sup>3</sup>	
Crystal color/habit	black blade	
Theta range for data collection	1.92 to 28.26°	
Index ranges	-12 ≤ h ≤ 12, -22 ≤ k ≤ 21, -18 ≤ l ≤ 18	
Reflections collected	18416	
Independent reflections	5015 [R(int) = 0.0849]	
Completeness to theta = 25.00°	99.9 %	
Absorption correction	Semi-empirical from equivalents	
Max. and min. transmission	0.9624 and 0.6141	
Refinement method	Full-matrix least-squares on F <sup>2</sup>	
Data / restraints / parameters	5015 / 0 / 280	
Goodness-of-fit on F <sup>2</sup>	0.780	
Final R indices [I > 2σ(I)]	R1 = 0.0343, wR2 = 0.0629	
R indices (all data)	R1 = 0.0604, wR2 = 0.0656	
Largest diff. peak and hole	0.782 and -0.615 e.Å <sup>3</sup>	